STUDIES OF MOLECULAR BONDING, INTERACTIONS AND DECOMPOSITION REACTIONS ON THE (001) SURFACE OF RUTHENIUM.

Thesis by
Brian H. Toby

In Partial Fulfillment of the Requirements
for the Degree of
Doctor of Philosophy

California Institute of Technology
Pasadena, California

1987

(Submitted October 2, 1986)

This thesis is dedicated to the memory of three inspirational people who did not live to see the completion of this work,

Violetta Adams, Mirra Breitman
and Stan Rogers.

Their presence is missed by many.

Acknowledgments

My years at Caltech have been extremely fruitful and I have grown considerably – if not in stature, at least in breadth. I have found myself to be part of a warm supportive community and have had the chance to fulfill a number of life-long dreams. To all those who have helped make this possible, I am very grateful. I wish to express my appreciation to all those people without whom I would never have arrived at Caltech or without whom I never would have stayed. But to attempt to mention everyone in a single page is futile. To all those whom I have not thanked explicitly, blame not my memory, rather the lack of space and time.

I am grateful to my research advisor, W. Henry Weinberg, for giving me the opportunity to follow my interests, both inside and outside the laboratory. I remember with appreciation everyone in the Weinberg group whose paths overlapped with mine. I particularly wish to thank Eric Hood, Ted Madey, Neil Avery and Udo Schwalke for their friendship, instruction and collaboration. My special thanks to my coworker Malina Hills; her help and friendship came to me at several dark times of true need. Thanks to ZAR (Dan Zirin) for a superbly run computer system.

Many members of the Rutgers School of Chemistry served as sources of advice and inspiration. Particular thanks go to Frina Toby, Sidney Toby, Harvey Schugar and Joseph Potenza.

I thank my supervisors at Union Carbide, Herb Hillery and Gordon Cagle, for doing so much over the last year to ease my path while working to complete this Thesis.

California may be a long way from my relatives, but I have never been short on family while here. I already miss the chance to see the Nimoys, the Josephs, the Manzano/Noor family and the Organ/Satz/Metz brouhaha. Without my adoptive families, life at Caltech could never have been as comfortable, secure, fun or fattening.

Caltech is not just a place to do science, but is an institution filled with active, motivated people. I had the great fortune to be involved in the Graduate Student Council, the Caltech Y, J. A. Profrock House (on-campus) and KPFK, the *LA Reader*, and the Democratic Club of Pasadena Foothills (off-campus). I also worked to found the the Caltech Folk Music Society and the Red Door Café. Best wishes to the folks who keep them running in my absence. My gratitude to the Caltech administration and staff for giving this student the latitude to follow his dreams.

I have gotten by with a little help from my friends Simon, Ronnie, Myra, Joanne, Roz and Howard. I have basked in the love of the closest friends that I have ever made, Kath, Bruce and Joanna. Words fail when I try to express the debt I feel. Thanks to you too Carole. Jackie, thanks for your patience and sagacious advice.

Abstract

The interactions of N_2, formic acid and acetone on the Ru(001) surface are studied using thermal desorption mass spectrometry (TDMS), electron energy loss spectroscopy (EELS), and computer modeling.

Low energy electron diffraction (LEED), EELS and TDMS were used to study chemisorption of N_2 on Ru(001). Adsorption at 75 K produces two desorption states. Adsorption at 95 K fills only the higher energy desorption state and produces a $(\sqrt{3} \times \sqrt{3})R30^\circ$ LEED pattern. EEL spectra indicate both desorption states are populated by N_2 molecules bonded "on-top" of Ru atoms.

Monte Carlo simulation results are presented on Ru(001) using a kinetic lattice gas model with precursor mediated adsorption, desorption and migration. The model gives good agreement with experimental data. The island growth rate was computed using the same model and is well fit by $R(t)^m - R(t_0)^m = At$, with m approximately 8. The island size was determined from the width of the superlattice diffraction feature.

The techniques, algorithms and computer programs used for simulations are documented. Coordinate schemes for indexing sites on a 2-D hexagonal lattice, programs for simulation of adsorption and desorption, techniques for analysis of ordering, and computer graphics routines are discussed.

The adsorption of formic acid on Ru(001) has been studied by EELS and TDMS. Large exposures produce a molecular multilayer species. A monodentate formate, bidentate formate, and a hydroxyl species are stable intermediates in formic acid decomposition. The monodentate formate species is converted to the bidentate species by heating. Formic acid decomposition products are CO_2, CO, H_2, H_2O and oxygen adatoms. The ratio of desorbed CO with respect to CO_2 increases both with slower heating rates and with lower coverages.

The existence of two different forms of adsorbed acetone, side-on, bonded through the oxygen and acyl carbon, and end-on, bonded through the oxygen, have been verified by EELS. On Pt(111), only the end-on species is observed.

On clean Ru(001) and p(2 × 2)O precovered Ru(001), both forms coexist. The side-on species is dominant on clean Ru(001), while O stabilizes the end-on form. The end-on form desorbs molecularly. Bonding geometry stability is explained by surface Lewis acidity and by comparison to organometallic coordination complexes.

Table of Contents

Section I.

Nitrogen on Ru(001): Local Surface Structure and its Effect on Adsorption and Desorption Kinetics

Chapter 1:

Introduction to Section I.

Nitrogen on Ru(001): Local Surface Structure and its Effect on Adsorption and Desorption Kinetics

The goals of scientific research are to observe and classify natural phenomena, and then to construct an interpretation within the context of theory that applies to a more broad range of systems. Where theory cannot be extended to agree with observation, new or more refined ideas must be developed. Theories are never proven and are rarely disproven. They gain acceptance when they are shown to be relevant to a wide range of problems. Conversely, a theory that is never disproven, but is very limited in scope, loses favor compared to a more utilizable theory.

The first section of this Thesis presents an example of this process in science. The initial experimental results presented here have several unusual features that require an unconventional interpretation. From the interpretation, a model for the system was developed. The model was first demonstrated to be consistent with the experimental results and finally it has been extended to predict results for experiments yet unmade.

The initial electron energy loss spectroscopy (EELS) and thermal desorption mass spectrometry (TDMS) and low energy electron diffraction (LEED) data are presented in Appendix A. Interpretation of data for adsorption of N_2 at 95 K is relatively straightforward. Nitrogen molecules adsorb in an end-on bonding configuration on on-top (six-fold) Ru sites in a $(\sqrt{3} \times \sqrt{3})R30°$ overlayer with a coverage of 1/3 monolayer, corresponding to adsorption at next-nearest-neighbor positions. These molecules desorb in a single thermal desorption peak. If adsorption is carried out at 75 K, additional molecules adsorb and a second, low temperature thermal desorption feature is observed. Yet, the nitrogen vibrational modes of the low temperature state molecules have approximately the same frequencies as the high temperature state molecules. Thus, the two states must both adsorb at the same sites.

Other unusual phenomena observed for N_2 adsorption, that are not reported here, are that if N_2 molecules are adsorbed at 100K and additional N_2 is allowed to adsorb after the surface has been cooled to 75 K, the number of molecules

desorbing in the high temperature state increases at the expense of the total saturation coverage on the surface [**1**]. If the two adsorption steps are repeated with different isotopes of N_2, most of the first isotope to be adsorbed desorbs in the high temperature state. Finally, the probability for N_2 molecules to adsorb to the surface rises with coverage, reaching a maximum of approximately thrice the initial value at approximately 10% of a monolayer coverage [**1,2**]. Only a few other cases had been noted in the literature, prior to this work, where the adsorption probability increases with coverage: oxygen on W(110) [**3**] and N_2 on several W surfaces [**4**].

A method of correlating the seemingly contradictory isotopic labeling results, which indicate two types of adsorption sites, the EELS results, which indicate only one type of N_2 bonding, and the annealing population results, which indicate that the high temperature state partially blocks the low temperature state, was initially suggested by N. R. Avery. He proposed that N_2 molecules form islands – small ordered $(\sqrt{3} \times \sqrt{3})R30°$ domains – which start from random nucleation points. When the islands grow with increased coverage, some islands will merge, but since there are three possible degenerate $(\sqrt{3} \times \sqrt{3})R30°$ lattices, related by a single Ru unit cell translation, out of phase islands will grow until they "run into" each other. The molecules that adsorb at antiphase domain boundaries are forced to adsorb on nearest-neighbor sites, which are relatively unfavorable in energy. These low energy sites will be the last to be filled and molecules which adsorb at these sites desorb at low temperatures even though there is no physical difference between them and the high temperature sites. Higher temperature adsorption encourages the formation of larger islands, which have a smaller ratio of edge sites to total sites and thus the number of high temperature sites is raised while the number of low temperature sites is lowered.

The explanation described above has a major failing. The saturation coverage for N_2 adsorption at 75 K is approximately 50% of a monolayer and

this is well beyond the range of coverages that can be accommodated by the additional sites created by antiphase boundaries. Nonetheless, it has served as a starting point for the development of the more detailed lattice gas model for N_2 adsorption and desorption which is presented in Chapter 2. It was found to be necessary to incorporate precursor-mediated adsorption into the model to give reasonable values for the probability of adsorption. The concept of a mobile precursor state has been discussed in the literature since the mid-1970's [**5**], but this is the first inclusion of a mobile precursor into a kinetic lattice gas model for simulation of both adsorption and desorption. The model was adapted into algorithms for Monte Carlo simulation of adsorption and thermal desorption, which are described in Appendix B, and FORTRAN implementations of the algorithms are given in Appendix C.

The results from the Monte Carlo simulations give excellent quantitative agreement with the experimental probability of adsorption data and the thermal desorption spectra. Simulations of isotope labeling duplicate the experimental results, which show that the last molecules to be adsorbed are primarily the first to be desorbed [**6**]. Saturation coverages are also in close agreement with experimental results. The mode by which adsorption occurs for coverages above approximately 40% of a monolayer was unanticipated. Islands do not stop growing after they "run into" the edges of neighboring islands. Rather, islands continue to grow by "overlapping" each other, creating thick antiphase domains. Adsorption continues in the antiphase domain regions at low rates until an equilibrium is established when the adsorption rate matches the desorption rate.

The model was then applied to the kinetics of ordering for islands of N_2 on Ru(001). The method for and results from these calculations are presented in Chapter 3. There is considerable current interest in the theory of order-disorder phenomena because of its relevance to the study of interactions between adspecies and diffusion [**7,8**]. Direct experimental measurements may be made for island growth rates but the level of analysis that can be accomplished will

depend on the extent to which the theory has been developed.

There have been many theoretical studies and Monte Carlo simulations made for island growth rates on surfaces [**9**]. Theoretical results predict that the average island radius, R, should increase as $R(t) \sim t^n$, where $n \simeq 1/2$, but the results from simulations have not all been in agreement. The model developed for N_2 on Ru(001) is ideal for computation of island growth, because all the parameters for adsorption and desorption have been determined to fit experimental data. The value of n determined from the N_2 on Ru(001) simulation is approximately $1/8$. The requirements for accurate experimental measurements in this system may be beyond the state of the art. While the reason that this result differs from theory could not be determined, it is hoped that this will spur additional investigation into the role of precursor mediated diffusion in island growth.

References

[1] A. B. Anton, N. R. Avery, T. E. Madey and W. H. Weinberg, J. Chem. Phys. Surface Sci. **85**, 507 (1986).

[2] P. Feulner and D. Menzel, Phys. Rev. B **25**, 4295 (1982); D. Menzel, H. Pfnür and P. Feulner, Surface Sci. **126**, 374 (1983).

[3] C. Wang and R. Gomer, Surface Sci. **84**. 329 (1979).

[4] M. Bowker and D. A. King, J. Chem. Soc. Faraday I, **75**, 2100 (1979).

[5] See references 3 and 4 in Chapter 2.

[6] E. H. Hood, B. H. Toby and W. H. Weinberg, in preparation.

[7] K. Binder, Ber. Bunsenges. Phys. Chem. **90**, 257 (1986).

[8] J. D. Gunton and K. Kaski, Surface Sci. **144**, 290 (1984); J. D. Gunton, M. San Miguel and P. S. Sahni, in *Phase Transitions and Critical Phenomena*, Vol. 8, edited by C. Domb and J. Lebowitz (Academic, New York, 1983).

[9] See references 7 and 11-27 in Chapter 3 of this Thesis.

Chapter 2:

Precursor-Mediated Molecular Chemisorption and Thermal Desorption: The Interrelationships among Energetics, Kinetics and Adsorbate Lattice Structures

VOLUME 55, NUMBER 22 PHYSICAL REVIEW LETTERS 25 NOVEMBER 1985

Precursor-Mediated Molecular Chemisorption and Thermal Desorption: The Interrelationships among Energetics, Kinetics, and Adsorbate Lattice Structure

Eric S. Hood, Brian H. Toby, and W. H. Weinberg

Division of Chemistry and Chemical Engineering, California Institute of Technology, Pasadena, California 91125

(Received 24 June 1985)

Precursor-mediated molecular chemisorption and thermal desorption are examined by means of a lattice-gas model using a combination of time-dependent Monte Carlo simulations and deterministic rate equations. Lateral interactions between coadsorbates are assumed to be both pairwise additive and limited in range to nearest and next-nearest neighbors. The interrelationships among kinetics, energetics, and adsorbate overlayer structures are analyzed in detail. The method is applied to the interaction of molecular nitrogen with the Ru(001) surface.

PACS numbers: 68.40.+e, 68.20.+t, 82.65.Dp

Although the concept of a physically adsorbed, "mobile precursor" state is not new,[1] much recent experimental effort has been directed toward the understanding of the phenomenon of precursor-mediated chemisorption.[2] Likewise, the influence of mobile precursor states on the kinetics of molecular chemisorption and desorption has been examined theoretically both by a reaction kinetics approach[3] and by statistical modeling.[4] In this Letter we introduce a theoretical modeling scheme for the study of precursor-mediated molecular chemisorption and thermal desorption, incorporating a combination of Monte Carlo simulations and deterministic rate equations with a stochastic formulation. The novelty of our approach lies in the simultaneous treatment of the various, competing elementary processes (physical adsorption, migration, chemisorption, and desorption) within a single, integrated model. In contrast to previous theoretical treatments, the microscopic detail inherent in our approach allows direct examination of the interrelationships among kinetics, energetics, and the formation and evolution of structure within the adsorbate overlayer. Numerical simulations provide a clear demonstration of the profound effects of island formation and growth.

Molecular chemisorption from a mobile precursor state is examined by use of a lattice gas model and time-dependent Monte Carlo (TDMC) simulations.[5] Molecules are placed sequentially on randomly chosen surface sites to simulate trapping from the gas phase into a physically adsorbed precursor state. Each precursor molecule migrates across the surface in single jumps to nearest-neighbor (nn) sites. This mobile intermediate state is occupied until either desorption or chemisorption occurs. The binding energy of the precursor is a function of the local molecular environment because of lateral interactions with previously chemisorbed molecules [assumed to be pairwise additive and limited in range to nn and nnn (next-nearest neighbor) adsorbates]. The binding energy of a molecule physically absorbed over an unoccupied lattice site (the intrinsic precursor state) is given by

$$\epsilon_p = \epsilon_0 - \sum_j n_j \epsilon_r + \sum_k n_k \epsilon_a, \tag{1}$$

where ϵ_0 is the binding energy of an isolated precursor to the surface, and ϵ_r and ϵ_a are the repulsive and attractive energies of interaction between the precursor and a neighboring *chemisorbed* molecule. The sums in Eq. (1) are performed over nn (j) and nnn (k) lattice sites, and n_j and n_k are occupation numbers. The binding energy (ϵ_a) of a molecule physically absorbed over a lattice site occupied by a chemisorbed molecule (the extrinsic precursor state) is assumed to have a constant value, 85% of ϵ_0.[6]

Each precursor molecule is temporarily confined to a particular lattice site by a periodic potential parallel to the surface, represented by adjacent, intersecting harmonic wells. The relative depths of neighboring potential-energy minima are computed according to Eq. (1). The activation barrier to precursor migration is given by the energy at the intersection point between adjacent harmonic potentials:

$$\epsilon_m = \epsilon_m^0 + \Delta\epsilon_p(i,j)/2 + [\Delta\epsilon_p(i,j)]^2/16\epsilon_m^0, \tag{2}$$

where ϵ_m^0 is the activation barrier to migration of an isolated intrinsic precursor molecule, and $\Delta\epsilon_p(i,j)$ is the difference in precursor binding energies between the ith and jth sites $[\Delta\epsilon_p(i,j) \equiv \epsilon_p(j) - \epsilon_p(i)]$. The probability for precursor migration from the ith to the neighboring jth lattice site is given by $P_m(i,j) = N\exp(-\epsilon_m/k_BT)$, where the constant N ensures unitarity. The probability for precursor desorption is given by $P_d = N\chi\exp(-\epsilon_p/k_BT)$, where the dynamical factor χ is the ratio between desorption and migration prefactors. The probability of molecular chemisorption is

$$P_c = [N\chi S_0 \exp(-\epsilon_0/k_BT)]/(1-S_0),$$

where S_0 is the initial (zero coverage) adsorption coef-

VOLUME 55, NUMBER 22 PHYSICAL REVIEW LETTERS 25 NOVEMBER 1985

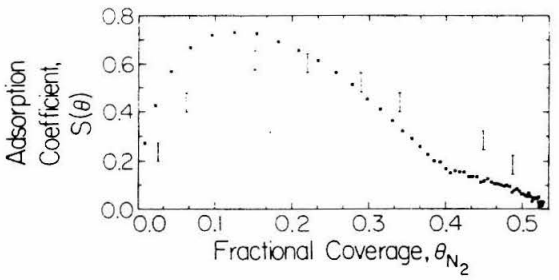

FIG. 1. Adsorption coefficient as a function of coverage for N_2 on Ru(001) at 77 K. Vertical bars represent experimental results (Ref. 9), while squares represent averages over eight TDMC simulations.

ficient. The relative probabilities of precursor desorption, migration to an adjacent site, or chemisorption are all functions of the local molecular environment. Maps displaying the locations of chemisorbed molecules can be constructed which detail the growth of adsorbate lattice structure as a function of coverage.

Thermal-desorption spectra (TDS) have been computed by use of a combination of deterministic rate equations with a Monte Carlo formalism.[5] Even though a single binding site and geometry are assumed, chemisorbed molecules can populate a number of energetically distinct binding states, characterized by different activation barriers to desorption $[\epsilon_b(i)]$ which are determined by the numbers and magnitudes of lateral interactions between the chemisorbed molecules, i.e.,

$$\epsilon_b(i) = \epsilon_b^0 - \sum_j n_j \bar{\epsilon}_r + \sum_k n_k \bar{\epsilon}_a. \quad (3)$$

In Eq. (3) ϵ_b^0 is the binding energy of an isolated chemisorbed molecule, and $\bar{\epsilon}_r$ and $\bar{\epsilon}_a$ are the repulsive and attractive energies of interaction between neighboring chemisorbed molecules. The rate of desorption from each chemisorption state is computed with use of a modified first-order Polanyi-Wigner equation with a coverage-dependent preexponential factor,[7]

$$d\sigma_i/dt = -\nu(\theta)\sigma_i \exp[-\epsilon_b(i)/k_B T], \quad (4)$$

with $\nu(\theta) \equiv \nu_0 \exp(\alpha\theta)$.[8] In Eq. (4) σ_i is the occupation number of the ith chemisorption state, and θ is the fractional coverage of chemisorbed molecules. The system of coupled differential equations describing desorption from all chemisorption states is solved numerically. During each computational cycle ($\Delta T \lesssim 0.5$ K), the appropriate number of molecules is selected from each chemisorption state according to Eq. (4) and removed from randomly chosen lattice sites to avoid the introduction of artificial correlation effects. The calculation is repeated until all molecules have desorbed.

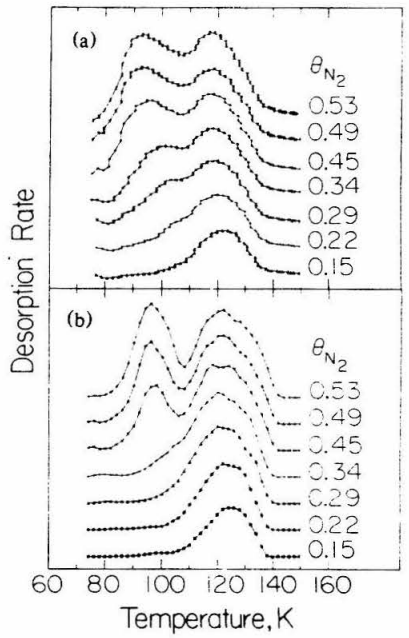

FIG. 2. Thermal-desorption spectra for N_2 on Ru(001) at various adsorbate coverages: (a) experimental results (Ref. 9), and (b) TDMC simulation and thermal-desorption modeling.

The interaction of N_2 with the Ru(001) surface has been examined by this methodology. The results of TDMC simulations are in good agreement with the experimentally measured adsorption coefficient[9,10] (cf. Fig. 1). Experimentally measured TDS are shown in Fig. 2(a). Although two peaks are observed at adsorbate coverages above 0.25, electron energy-loss spectra indicate that chemisorption of N_2 occurs only at atop sites.[10] Figure 2(b) shows TDS computed with the assumption of *a single binding geometry at atop sites.* Quantitative agreement between calculated and experimental thermal-desorption spectra is obtained for all adsorbate coverages.

TDMC simulations of N_2 adsorption on Ru(001) have been performed for a surface temperature of 77 K on a lattice composed of 9216 Ru atoms. Maps indicating the locations of chemisorbed N_2 molecules chart the growth of adsorbate lattice structure as a function of coverage (cf. Fig. 3). Because of the hexagonal geometry of Ru(001) and the nature and magnitude of adsorbate interactions, the energetically favored overlayer structure (as indicated by a well-developed LEED pattern[9] at 95 K) possesses $(\sqrt{3}\times\sqrt{3})R30°$ symmetry. However, three independent, degenerate adsorbate phases can exist on this hexagonal surface which are distinguishable by 120° rotations about a

VOLUME 55, NUMBER 22 PHYSICAL REVIEW LETTERS 25 NOVEMBER 1985

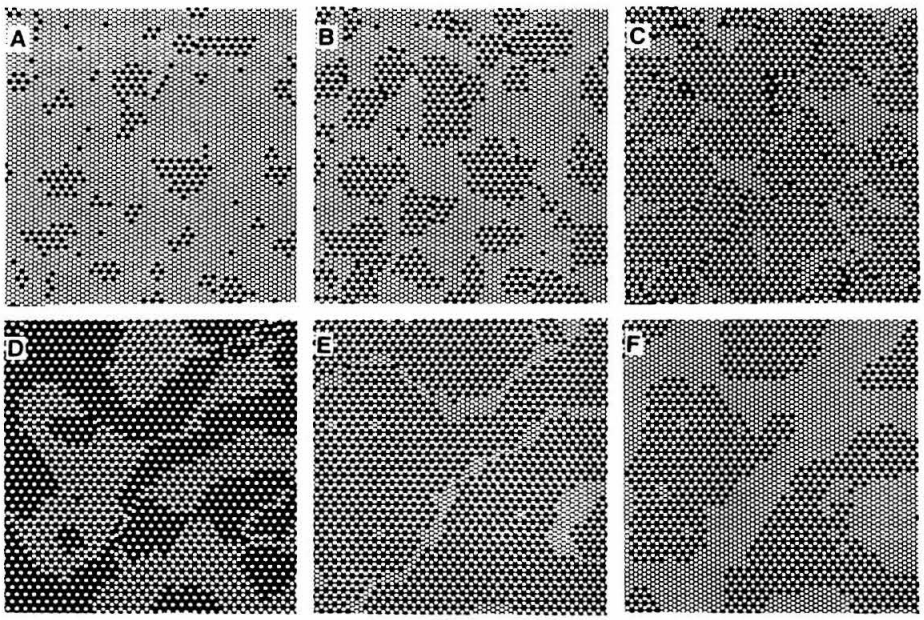

FIG. 3. Maps displaying the locations of N_2 chemisorbed on sections of the Ru(001) surface generated by (a)–(d) TDMC simulations of adsorption, and (e),(f) thermal-desorption modeling. Open circles represent surface Ru atoms, while dots represent N_2 chemisorbed atop Ru surface atoms. The solid lines represent the three degenerate phases characterizing this system. The fractional N_2 coverages are (a) 0.06, (b) 0.15, (c) 0.29, (d) 0.53, (e) 0.29, and (f) 0.15.

threefold axis centered within the triangle formed by three adjacent Ru atoms. Distinct adsorbate domains can be observed on a surface where two or more of these phases coexist.

An examination of both $S(\theta)$ and maps of the chemisorbed overlayer allows a detailed description of the adsorption process. Chemisorption at 77 K occurs in four distinct stages: (I) island nucleation, (II) growth of isolated island domains, (III) simulataneous growth of island domains and antiphase-domain boundaries, and (IV) growth of antiphase domains. The chemisorption of isolated molecules, acting as nucleation centers for the growth of numerous, small island domains, characterizes stage I [cf. Fig. 3(a)]. Cooperative behavior dominates stage II as $S(\theta)$ undergoes a threefold increase. Increasing order is observed in the chemisorbed overlayer as the edges of island domains serve as the most probable sites for chemisorption [cf. Fig. 3(b)]. The growth of isolated island domains continues up to a fractional coverage of approximately 0.22. "Crowding" between neighboring islands signals the onset of growth stage III [cf. Fig. 3(c)]. Adjacent domains of the same phase coalesce to form larger islands, while adjacent domains of differing phase develop grain boundaries. During stage III, $S(\theta)$ suffers a fivefold decrease as appreciable chemisorption occurs at grain boundaries in addition to the more energetically favorable island domains. The onset of stage IV is accompanied by a change in the slope of $S(\theta)$ at 0.4 monolayer (cf. Fig. 1). At adsorbate coverages above 0.4, chemisorption occurs in regions of antiphase domains. Saturation coverage occurs at approximately 0.55 because of a steady-state balance between the rate of precursor-mediated adsorption and the rate of desorption from the chemisorbed states [cf. Fig. 3(d)].

The influence of lateral interactions between coadsorbates on the kinetics and mechanism of molecular desorption can be evaluated by an examination of both the adsorbate lattice maps and the coverage-dependent TDS. For coverages below 0.25, the TDS consist of a single peak at a surface temperature of approximately 125 K. This peak is associated with desorption from the perimeters of isolated islands. The N_2 chemisorbed within isolated islands experience attractive lateral interactions which increase the activation barrier to desorption above that experienced by an isolated adsorbate. At adsorbate coverages above 0.3, a second peak at a surface temperature below 100 K appears in the TDS. This peak is associated with desorption from antiphase domains. Molecular N_2 chemisorbed within these antiphase domains experience

TABLE I. Kinetic and energetic parameters characterizing the interaction of molecular nitrogen with Ru(001) with energy in units of kcal/mole.

ϵ_0: Intrinsic precursor binding energy	1.6
ϵ_a: Extrinsic precursor binding energy	1.4
ϵ_b^0: Chemisorption state binding energy	5.8
ϵ_m^0: Precursor state migration barrier	0.3
$\epsilon_a, \tilde{\epsilon}_a$: Attractive next-nearest-neighbor interaction energy	0.45
$\epsilon_r, \tilde{\epsilon}_r$: Repulsive nearest-neighbor interaction energy	0.25
χ: Ratio of precursor preexponential factors of desorption to migration	500–1000
ν_0: Desorption preexponential factor (low coverage limit)	10^{12} s^{-1}
α: Desorption preexponential coverage dependence	17

repulsive lateral interactions which decrease the activation barrier to desorption. At saturation coverage, the number of molecules desorbing from antiphase domains and the number desorbing from isolated-island perimeters are nearly equal, as are the intensities of the two thermal desorption peaks. The value of this type of numerical simulation is clearly evident: By the relating of the adsorbate structure to kinetic measurements, the two peaks appearing in the "high"-coverage ($\theta \gtrsim 0.3$) TDS are shown to result solely from lateral interactions between molecules chemisorbed only at atop sites [cf. Figs. 3(d)–3(f)].

Numerical values of the parameters characterizing the system N_2 on Ru(001) (Table I) are obtained by minimization of the differences between the calculated and experimental coverage-dependent adsorption coefficients and TDS. Although precursor-state–chemisorption-state and chemisorption-state–chemisorption-state lateral interaction energies are treated as separate parameters, adsorption and desorption simulations yield nearly identical values for both. *This similarity in lateral interaction energetics is due primarily to the weak binding energy of chemisorbed molecular nitrogen on this surface.*

Examination of the maps of adsorbate positions as a function of coverage reveals obvious differences between the mechanisms of precursor-mediated molecular chemisorption and thermal desorption from the chemisorbed state. The absorption mechanism is dominated by kinetic trapping which results in the formation of numerous, small island domains [cf. Fig. 3(a)–3(d)]. Thermal desorption is dominated by relaxation (annealing), as evidenced by the formation of fewer, but much larger, island domains [cf. Figs. 3(e) and 3(f)]. The ability to disclose in microscopic detail the interrelationships among energetics, kinetics, and adsorbate overlayer structures demonstrates the value of this integrated approach to molecular chemisorption and thermal-desorption simulations.

This work was supported by the National Science Foundation under Grant No. CHE-8206487. One of us (E.S.H.) acknowledges receipt of a Bantrell Postdoctoral Fellowship.

[1]J. B. Taylor and I. Langmuir, Phys. Rev. **44**, 423 (1933).

[2]P. Alnot and D. A. King, Surf. Sci. **126**, 359 (1983); H. Pfnür and D. Menzel, J. Chem. Phys. **79**, 2400 (1983); M. Grunze, J. Fuhler, M. Neumann, C. Brundle, D. Auerbach, and J. Behm, Surf. Sci. **139**, 109 (1984); S. Tang, M. Lee, J. Beckerle, M. Hines, and S. Ceyer, J. Chem. Phys. **82**, 2826 (1985); M. Shayegan, E. D. Williams, R. E. Glover, and R. L. Park, Surf. Sci. **154**, L239 (1985).

[3]D. A. King and M. Wells, Proc. Roy. Soc. London, Ser. A **339**, 245 (1974); R. Gorte and L. Schmidt, Surf. Sci. **76**, 559 (1978); D. L. Freeman and J. D. Doll, J. Chem. Phys. **78**, 6002 (1983), and **79**, 2343 (1983).

[4]P. Kisliuk, J. Phys. Chem. Solids **3**, 95 (1957), and **5**, 78 (1958); D. A. King, Surf. Sci. **64**, 43 (1977); A. Cassuto and D. A. King, Surf. Sci. **102**, 388 (1981); J. E. Adams and J. D. Doll, Surf. Sci. **103**, 472 (1981), and **111**, 492 (1981).

[5]E. S. Hood, B. H. Toby, and W. H. Weinberg, unpublished.

[6]K. Christmann and J. Demuth, Surf. Sci. **120**, 291 (1982).

[7]P. Redhead, Vacuum **12**, 203 (1962); D. Adams, Surf. Sci. **42**, 12 (1974).

[8]A number of different functional forms for $\nu(\theta)$ have been tested, including the form presente by P. Feulner and D. Menzel, Phys. Rev. B **25**, 4295 (1982), and D. Menzel, H. Pfnür, and P. Feulner, Surf. Sci. **126**, 374 (1983). TDS computed with use of the exponential coverage dependence were in closest agreement with experimental results.

[9]Feulner and Menzel, Ref. 8; Menzel, Pfnür, and Feulner, Ref. 8.

[10]A. Anton, N. Avery, B. Toby, and W. H. Weinberg, J. Electron Spectrosc. Relat. Phenom. **29**, 181 (1983).

Chapter 3:

Simulation of N_2 Island Growth on Ru(001): Evidence for a New "Universality Class"

ABSTRACT

Monte Carlo simulation results are presented for N_2 island growth on the Ru(001) surface using a kinetic lattice gas model with precursor mediated adsorption, desorption and migration. The model has been previously demonstrated to give good agreement with experimental data. The observed growth rate is well fit by an growth law of $R(t)^m - R(t_0)^m = At$, with m approximately 8. The island size was determined from the width of the superlattice diffraction feature. Results from other recent theoretical and Monte Carlo studies of island ordering are also presented.

1. Introduction

The diffusion of adspecies on surfaces plays a major role in the kinetics of heterogenous chemical reactions. For example, in a surface-activated bimolecular chemical reaction, two reactant molecules must adsorb at or migrate to an active site before the reaction can be completed and the products must desorb or migrate away from the site before the site is again catalytically active. Despite the importance of the field, relatively little is known about surface-adspecies and adspecies-adspecies energetics. Nor have the mechanisms which govern molecular diffusion been well explored.

Experiments which directly probe surface-adspecies and adspecies-adspecies energetics are often difficult to design. Relatively few experiments can yield direct measurements of diffusion rates, either. However, information about both interaction energy and diffusion can be built into models for the kinetics of disorder-order transitions. Thus, the field of disorder-order kinetics provides a testing ground for the comparison of dynamical theory with experiment results.

When the state of a disordered system is changed to a set of conditions which favor greater order, local domains of higher order develop and grow in size with time until an equilibrium distribution of domain sizes is obtained. In two-dimensional systems, such as the aggregation of atoms or molecules on a surface, the local domains of order are called islands. Island growth has long been of major interest in surface science because it provides insight into the nature of adspecies interactions [**1**, **2**].

Understanding the growth of domains in three dimensions is central in the fields of metallurgy, mineralogy and materials science because of the importance of microcrystalline structure in the macroscopic properties of materials. Two dimensional models for domain growth are often chosen for study by workers in those fields because the lower dimensionality offers greater simplicity for both theory and calculations. It is widely accepted that growth laws in two and three dimensions are closely related [**3**].

Early theoretical work by Lifshitz [4], Allen and Cahn [5], resulted in a growth law for the average diameter, R, for islands (in two dimensions) and grains (in three dimensions) as a function of time, t, of

$$R(t) \sim t^{1/2}, \tag{1}$$

where the order parameter is not conserved. Equation (1) is known either as the Allen-Cahn or as the Lifshitz-Allen-Cahn (LAC) equation. Reduction in the curvature of domain walls is the driving force behind LAC growth. A second theory, governed by an "evaporation-condensation" growth mechanism predicts a $R(t) \sim t^{1/3}$ rate law for systems with a conserved order parameter (*e.g.*, the population of phases is time invariant, as would be found in alloy separation [6].) More recent theoretical work by Safran predicts that domain growth follows the rate equation:

$$R(t) \sim t^{n}, \tag{2}$$

for systems where the dimensionality (d) is less than the degeneracy (q) by one or more or the growth equation

$$R(t) \sim \ln(t), \tag{3}$$

for other systems where $d > q + 1$ [3]. These series of findings prompted the concept of "universality classes" – the growth law for a system is dependent on the number of degenerate phases, the dimensionality of the system; but the growth law is independent of the geometry of the lattice, the migration barrier or the adspecies-adspecies interaction energies. In a generalized Monte Carlo study in two dimensions, equation (2) was found to be valid for all q between 2 and 74. The value of n dropped linearly from 0.5 for the Ising ($q = 2$) model to 0.38 for systems with approximately 25 degenerate phases and did not change for systems with q values above 25 [7].

While static order-disorder measurements, such as definition of phase diagrams, have been made for a relatively large number of 2-D systems, very few

dynamic measurements of island growth rates have been made, attesting to the degree of experimental difficulty associated with these measurements. For adsorbate ordering on surfaces, the only low energy electron diffraction (LEED) measurements that have been reported are for the ordering of O adatoms on W(110) [**1**, **8**] and on W(112) [**9**].

In contrast, there has been a wealth of theoretical and Monte Carlo simulation studies in recent years of ordering growth rates in two dimensions [**10**, **11** – **27**]. While many of the studies have been made for generalized systems using arbitrarily chosen parameters and geometries, some specific systems that have been modeled using Monte Carlo techniques include: O on W(110) [**11**], H on Fe(110) [**12**] and N_2 on graphite [**13**,**14**]. Most of these studies are made using q-state Potts models (antiferromagnetic spin-flip and spin-exchange models), where the q degenerate phases on the surface are each assigned a unique spin state. In the case of a system where the degeneracy is two, the Potts model is equivalent to a Ising model. In the simulations of N_2 on graphite, the N_2 molecules are assumed to have their molecular axis parallel to the surface. The angle of molecular axis with respect to an arbitrary reference vector is allowed to take any value. Thus, this model is a ∞-state Potts model. Some Monte Carlo simulations have been done using more generalized, kinetic lattice gas models, which incorporate various extensions beyond the Potts model, such as more complex models for diffusion. A kinetic lattice gas model has also been used to study the effects of island growth on surface reaction kinetics [**15**]. This work will present the first reported growth law results for a lattice gas model incorporating precursor mediated adsorption, desorption and migration.

A large number of theoretical and Monte Carlo studies have been made where island growth obeyed the classical LAC law (algebraic growth with $n = 1/2$) [**16**-**22**]. However, several studies have been published where non-classical growth behavior is observed. These provide insight into factors which can change the universality class. Sadiq and Binder modeled growth rates for O adatoms on

W(110), using non-physical interaction energies and found that if surface density is conserved the growth exponent, n, is 0.35 for $q = 4$, while if the density is not conserved n has the classical value of $1/2$. This contrasts a similar system where $q = 2$ the value for n is $1/2$, with or without conservation of density [**11**]. Two studies by Mazenko and coworkers demonstrate that conservation of the order parameter also affects the growth law. In a theoretical Ginzburg-Landau model for systems with large q values, they found $n = 1/4$ if the order parameter is conserved, but $n = 1/2$ if not [**23**]. For a study with Monte Carlo Ising model, $n = 1/2$ (LAC) growth is observed for a non-conserved order parameter, but if Kawasaki spin-exchange dynamics, which conserve the order parameter, are used, a growth rate of $R(t) = \ln t$ is observed [**24**]. In their model for H on Fe(110), Viñals and Gunton determined that $n = 1/2$ for growth of a (2×1) overlayer, with $\theta = 0.5$, but the growth of the (3×1) overlayer, with $\theta = 0.667$, followed a more complex growth law that could be approximated by $0.15 < n < 0.25$ [**12**]. Systems have also been modeled where the growth behavior is too complex to express in terms of a simple law [**25**,**26**].

The most controversial studies in the current literature of island growth concern N_2 on graphite, often called the herringbone model because the N_2 molecules tend to align in alternating rows with perpendicular molecular axes, creating a herringbone pattern. Mouritsen, in his initial study, found growth could be fitted with $n = 0.4$ at early times and $n = 1/4$ at later times [**13**]. From this result he proposed a new universality class for systems with soft domain walls. For systems with small q, domain boundaries are sharply defined, meaning that all adspecies are members of clearly defined islands. In Mouritsen's nomenclature, such domain boundaries are deemed hard. In contrast, in the herringbone model, N_2 molecules may adopt any orientation and thus domain boundaries may be several layers thick. The domain boundary regions are populated by a disordered phase containing molecules unaligned with either surrounding phase. Kaski *et al.* have also modeled N_2 on graphite and reach

the conclusion that the growth obeys the LAC equation, if ordering at early times is ignored or an additional term is included in the growth law for this transient period [**14**]. Subsequent work by Mouritsen demonstrated $n = 1/4$ growth for a wide range in his "softness parameter" [**27**]. The debate over the role of soft domain walls in island growth has not been resolved in the literature.

This study presents recent Monte Carlo simulation results for island growth of N_2 molecules on the hexagonal Ru(001) surface using a kinetic lattice gas model with precursor mediated adsorption, desorption and migration. The model has previously been demonstrated to give excellent agreement with experimental thermal desorption, probability of adsorption and low energy electron energy loss data [**28**]. The model incorporates realistic microscopic detail in its treatment of molecular processes. Another significant advantage of this model is that its probabilistic formulations directly incorporate time as a parameter, thus eliminating the serious problem faced in other Monte Carlo simulations for correlating the Monte Carlo time scale to a real time scale. The growth rate observed in this study is well fit by an algebraic law with a growth order of approximately 1/8.

2. Methods Used for Calculations

Calculation of island growth is made in five steps:

(1) computation of a starting surface;

(2) simulation of the time evolution of the surface;

(3) calculation of a Fourier transform of surface maps;

(4) fitting of an intensity profile equation to the superlattice Fourier transform intensity feature;

(5) fitting of growth law parameters to the intensity profiles versus time.

The same simulation model was used for steps (1) and (2), but under different conditions. Each of these steps will be described in greater detail in this section.

2.1 Description of the Model

The model has been described elsewhere, but will be briefly recapitulated here [**28**,**29**]. A rectangular section of hexagonal lattice with either 96^2 or 132^2 sites was used for simulations. Cyclic boundary conditions were imposed. Absorption of molecules is simulated by computing a flux of incident molecules for the chosen pressure and it is assumed that all incident molecules enter the precursor state. Precursor molecules hop from lattice site to lattice site until they either desorb back into the gas phase or chemisorb. At periodic intervals, randomly selected chemisorbed molecules are either returned to the mobile precursor state or removed from the surface. All migration is via the precursor state.

A site energy, ϵ_j, is defined for each site on the lattice and is determined from the number of filled nearest neighbor sites (n_r) and the number of filled next nearest neighbor sites (n_a) by $\epsilon_j = \epsilon_0 - n_r E_r + n_a E_a$. If the site has already been filled, $\epsilon_j = E_n \epsilon_0$ (regardless of the number of filled neighbor sites.) The values used for ϵ_0, E_n, E_r and E_a are respectively 1.6, 0.86, 0.25 and 0.45 kcal/mole. These values yielded the best fit for the experimental data.

Precursor molecules may hop from their current site, i, to any of the six neighboring sites, j, where the probability for migration P_m^{ij}, depends on the

difference in site energy, $\Delta\epsilon_{ij} = \epsilon_j - \epsilon_i$.

$$P_m^{ij} = \begin{cases} N \exp\left[\dfrac{-E_m + \Delta\epsilon_{ij} + \Delta\epsilon_{ij}^2/(16E_m)}{kT}\right], & |\Delta\epsilon_{ij}| < 4E_m, \\ N \exp\left[\dfrac{-\Delta\epsilon_{ij}}{kT}\right], & \Delta\epsilon_{ij} \geq 4E_m, \\ N, & \Delta\epsilon_{ij} \leq -4E_m. \end{cases}$$

The probability for the precursor molecule to chemisorb, P_c^i, is given by

$$P_c^i = N\chi \exp\left[\frac{-\epsilon_0 + E_c}{kT}\right],$$

unless site i already occupied, in which case P_c^i is zero. The probability for the precursor molecule to desorb from site i is

$$P_d^i = N\chi \exp\left[\frac{-\epsilon_i}{kT}\right].$$

The values used for χ and E_m are 1000 s^{-1} and 0.284 kcal/mole, respectively, which yielded the best fit for the experimental data. The value for E_c, is calculated from $E_c = 77k\ln(1/S_0 - 1)$, where S_0, the clean-surface adsorption probability is 0.125 at 77 K. The normalization constant, N, is determined such that $P_d^i + P_c^i + \sum_{j=1}^{6} P_m^{ij} = 1$.

At periodic time intervals desorption scans are made and molecules may be removed from the surface or returned into the precursor phase. The total probability for a molecule to be excited out of the chemisorbed state either into the precursor or gas phase is P_t. The percentage of these excited molecules that return to the precursor phase versus those that desorb directly is P_p. While P_t is independent of the number of filled neighbor sites, P_p is a function of ϵ_i which is defined as $n_r E_r - n_a E_a$.

$$P_t = \nu(n_r, n_a)\Delta t \exp\left[\frac{-E_c + E_0}{kT}\right].$$

$$P_p = \begin{cases} 1 - \frac{1}{2}\exp\left[\dfrac{E_c + \epsilon_i}{kT}\right], & E_c + \epsilon_i < 0, \\ 0, & E_c + \epsilon_i \geq 0, \end{cases}$$

where $\nu(n_r, n_a)$ is the prefactor for site i, $\nu(n_r, n_a) = 10^{13} \exp(\nu_r n_r + \nu_a n_a)$, Δt is the time between desorption scans (in seconds), E_0 is the chemisorption well depth, 5.8 Kcal/mole, ν_r and ν_a were set at 1 and 0.35, respectively. Desorption scans were made at sufficiently frequent intervals so that the average number of molecules excited into the precursor phase was no more than 2% of the total coverage. Computation of desorption scans at more frequent intervals did not result in a significant change in the simulations.

2.2 Calculation of the Starting Surface

The previous model was used to compute a starting surface by simulating adsorption with conditions of a fixed temperature and pressure. Adsorption was terminated at $\theta = 0.15$ monolayer and a "map" or "snapshot" of the surface distribution of molecules was saved for use in future runs. The coverage of 15% was chosen because it corresponds at equilibrium to a surface that is approximately one-half covered by islands. Also, with higher coverages, islands develop "domain overlap" (antiphase domains several layers thick) at early times and this considerably complicates analysis.

2.3 Time Evolution of the Starting Surface

Time evolution of a populated surface was computed using the previous model. The density was constrained to be constant by allowing sufficient incident molecules to readsorb following each desorption scan to restore the coverage to the original level. The order parameter was not conserved. For one set of calculations, P_d^i and P_p were artificially constrained to be zero and one, respectively, allowing desorption into the precursor state but not allowing molecules to leave the surface.

At periodic intervals throughout the simulations, maps of the surface were stored for later analysis. Several sets of simulations were performed starting from the same surface, using identical parameters but a different sequence of random numbers. Computations were also performed at a number of different surface temperatures using the same starting surface.

2.4 Fourier Transform of the Surface Maps

A facile method for computation of a kinematical "diffraction pattern" was developed to utilize a fast Fourier transform (FFT) from a hexagonal surface. The usual 2-D FFT algorithm is restricted to coordinate systems with orthogonal axes. However, the N $\times$ N lattice site section of a hexagonal lattice can be reindexed in a 2N $\times$ N element rectangular coordinate system, where half of the array elements correspond to sites in the hexagonal lattice. Fourier transform intensities were then computed using standard IMSL 1-D FFT subroutines with time savings of several orders of magnitude over the direct computation of the Fourier transform, despite the doubled number of array elements.

Scattering from the Ru substrate atoms, the Bragg angular dependence of the scattering factor and the Debye-Waller factor are not relevant to the analysis applied to the FFT intensities and corrections for these factors were not applied.

2.5 Intensity Lineshape Analysis

It is possible to compute the distribution of island sizes from the the profile of the superlattice diffraction feature [**30**,**31**]. In this study no attempt was made to determine the distribution function. However, the approximation that $R^2 \propto 1/\Gamma$, where Γ is the full-width at half-maximum of the beam profile, was employed. It has been noted that the theoretical profile of a diffraction beam from a surface with an ensemble of islands is neither Gaussian nor Lorentzian, but has aspects of each [**30**]. The Voigt function, the convolution of a Gaussian and a Cauchy (Lorentz) function, is a logical choice for a profile function. However, the pseudo-Voigt is computationally much simpler to use and is a very good approximation of the Voigt [**32**,**33**]. A radially symmetric 2-D pseudo-Voigt intensity profile function, $I(M_i, N_i)$ gave good fits to the FFT intensity map of the superlattice ($\sqrt{3} \times \sqrt{3}$) diffraction feature with the mixing parameter, η,

typically between 0.2 and 1.

$$I(M_i, N_i) = \frac{2\kappa}{\Gamma}\left\{\frac{\eta}{1+\left(\frac{2\Delta r}{\Gamma}\right)^2} + (1-\eta)\sqrt{\frac{\ln 2}{\pi}}\exp\left[-\ln 2\left(\frac{2\Delta r}{\Gamma}\right)^2\right]\right\},$$

where $\Delta r^2 = \left(\frac{M_i - M_c}{M}\right)^2 + 3\left(\frac{N_i - N_c}{N}\right)^2$, $I(M_i, N_i)$ is the intensity of array element (M_i, N_i) and (M_c, N_c) corresponds to the beam center [at substrate reciprocal lattice coordinates $(\frac{2}{3}, \frac{1}{3})$]. The integrated beam intensity is $2\pi\kappa$. A least-squares refinement was used to determine the best values for the parameters η, κ and Γ.

2.6 Growth Law Fitting

The Sahni growth equation, (2), is derived from equation (4), below,

$$R(t)^m - R_0^m = \alpha t, \tag{4}$$

with $m = 1/n$ and making the assumption that R_0, which is defined as $R(t)$ at $t = 0$, is negligible compared to $R(t)$. This approximation is not necessary and indeed is invalid for this study. Substituting $\Gamma = \kappa/R^2$ into equation (4) yields

$$\Gamma(t) = \Gamma_0(\beta t + 1)^{-2/m}, \tag{5}$$

where $\beta = \alpha\Gamma^{m/2}\kappa^{-m}$. A least-squares refinement procedure is used to fit Γ_0, β and m using the fit values for Γ. When one than one set of runs is made from the same starting surface, the same value of Γ_0 is used for all runs and only β and m are refined.

3. Results

Maps of surfaces for use as starting points for the time evolution computations were prepared by simulated adsorption of N_2 at a pressure of 7.5×10^{-8} torr at 78 K on a 96 × 96 site surface and by adsorption on a 96 × 96 and on a 132 × 132 site surface at 120 K at 7.5×10^{-6} torr. Adsorption simulations were terminated when the surface coverage reached $\theta = 0.15$. Time evolution of these surfaces was then simulated at a number of temperatures between 75 and 100 K. For the 96 × 96 simulations, to improve statistics each run was repeated four times using a different set of random numbers for each run. The extensive amount of computer time needed (2 to 6 hours of CPU time per run on a VAX 11/780 computer) made additional averaging prohibitive. For the 132 × 132 simulations, the runs were repeated twice at each temperature.

During each simulation, 15 to 20 maps were stored at successive times. Typical maps showing the growth in island size are shown in Fig. 1. Fourier transforms were computed for each stored map and the intensities from equivalent maps at the same temperatures were averaged. Plots of the average FFT intensity array from four maps equivalent to the maps in Fig. 1 are shown in Fig. 2.

It was determined that the line-shape fitting program could not accurately determine half widths for both extremely broad and extremely narrow line shapes. In the case of very broad line widths, corresponding to islands with very small radii, the diffraction intensity is very small with respect to the random scatter in the intensity values. Greatly additional amounts of averaging would be necessary before the half width could be could be fit or even estimated by eye. For 96 × 96 site maps that are populated with several large islands, extremely narrow line-shapes are observed where only a few array elements have non-negligible intensity, This again leads to increased uncertainty in the width assignment. A 96 × 96 site map with a single round island at $\theta = 0.15$ yields Γ on the order of 0.01 rlu, of the same order as the pixel dimensions.

The uncertainty in fitting the line width for a surface with large radius islands can only be improved through calculations on a larger size map, which yields a greater density of points in reciprocal space. The method used here does yield good fits for Γ between 0.02 and 0.3 reciprocal lattice units (rlu) on a 96×96 site map. The estimated errors in the fit for Γ for the values presented in this work are typically on the order of a few percent.

The change in Γ with time is well fit by equation (5). However, the estimated error and the scatter in the fit growth parameter are relatively high. This result is not surprising because of the uncertainty is high when fitting an exponential function with a relatively small change in the observable parameter. Fig. 3 shows a sequence of runs with curves defined by the fitted values of m and β. A plot of m values from 19 sets of averaged runs is shown in Fig. 4. In contrast to the studies discussed previously where the growth order, n, is between 0.2 and 0.5, the values for m here are in the range of 8 ± 2, corresponding to $n \cong 1/8$.

Results are also plotted with fixed values of m to show that data are clearly not well fit by $m = 2$ or $m = 4$, while $m = 8$ does allow a good fit. In most Monte Carlo simulations in the literature, results are plotted as $R(t)$ versus t on logarithmic axes, yielding a straight line, where the slope is n. To incorporate a non-negligible R_0 term and still have a straight line, one must plot $R(t)$ against a reduced time, $\alpha t + 1$. This requires assumption of a value for m, to determine α. Plots of Γ versus time and Γ versus $\beta t + 1$, where β has been refined but m has been fixed at 8, 4 and 2, are shown in Figs. 5-7, respectively for the same data shown in Fig. 3.

An attempt was made to determine the sensitivity of m to parameters within the model. There exist two mechanisms for migration of a molecule from one site to another. Molecules may desorb from the surface into the gas phase and then reenter the precursor phase at a randomly chosen site, or they may desorb into the precursor phase and then hop from site to site until readsorbing. The effect of desorption into the gas phase on the growth order was investigated

by setting $P_d^i = 0$ and $P_p = 1$, thus "turning off" desorption. This had no affect on m, within the scatter of the fitted results. Relatively large changes were also made to the values of E_m, E_n, E_r, E_a, ν_r and ν_a, again with no affect on m, within the scatter of the fitted results.

4. Discussion and Conclusions

This study has demonstrated that a mobile precursor model for N_2 island growth on Ru(001) is well fit by the growth equation $R(t)^m - R_0^m = \alpha t$, where m is 8 ± 2. This value for m is much larger than that determined for other theoretical and Monte Carlo studies and is well outside the range for known universality classes. In practical terms, for a similar overall growth rate, a higher value for m translates to more rapid ordering at early times but slower ordering at later times. The question of why this unusual result is obtained cannot be answered within this study.

Experimental results for this system demonstrate two unusual features: two thermal desorption peaks from a single binding site and a probability for adsorption that rises with increasing coverage [**28**,**34**,**35**]. The model has several unusual features which allow the reproduction of the experimental results. The high value of the attractive interaction energy, E_a with respect to the repulsive interaction energy, E_r, the precursor binding energy, ϵ_0, and the chemisorption well binding energy, E_0, respectively, all increase the probability for adsorption of molecules which can attach themselves to island edges with respect to adsorption on the clean surface and decrease the probability for molecules in islands to desorb. The model incorporates both intrinsic and extrinsic precursor states, also necessary for good agreement with probability of adsorption versus coverage data. The model also features a prefactor formulation which depends on the number of attractive and repulsive interactions. This formula was chosen over the coverage-dependent prefactor, which was previously employed [**28**], because the former prefactor function is based on microscopic rather than macroscopic detail. However, either type of coverage dependence, local or global, is needed to insure that the high temperature thermal desorption peak does not rise with increased coverage, in agreement with experiment, but contrary to usual behavior for first-order desorption.

It might be suggested that the unusual parameter values chosen for this

model result in the atypical m value determined here. This conclusion seems unlikely given the result that neither changes in parameter values nor temperature had a significant effect on the growth order. This leads to the conclusion that $m = 8$ is characteristic of the model rather than the parameter values.

In the herringbone model for N_2 on graphite, m appears to have a value intermediate to the LAC theoretical value of 2 and the value determined here. The herringbone model and the Ru(001) model are quite different, despite use of the same adsorbate molecule and the identical symmetry of the surfaces, largely due to the difference in the assumed bonding geometry. There can be no soft domain walls in the model presented here because the phases are determined by lattice site rather than by rotational ordering.

Experimental measurement of the island growth rate for N_2 seems to be unlikely with the current level of LEED and vacuum technology. A factor of two change in the full-width of the superlattice beam, not allowing for experimental broadening, would require annealing for time periods in the range of hours, unless an annealing temperature close to the desorption temperature is chosen. The latter choice would require a relatively large backing pressure of N_2. In either the case of high pressure or long annealing times, adsorption of impurities would be likely. Coadsorption of CO and O_2 is known to have a major effect on N_2 thermal desorption [**36**] and could also be expected to affect ordering. In addition, very low electron beam currents would need to be utilized, as N_2 is subject to electron stimulated disordering [**37**].

It is unlikely that a non-precursor mediated model for N_2 on Ru(001) could be constructed that would yield close agreement with experimental results, so construction of a three-state Potts simulation for this system would not provide experimentally reasonable results. Further work will be necessary to determine if N_2 on Ru(001) is the first reported member of a new universality class, determined by factors that are now unclear, or if precursor mediation, when integrated into the models for other systems, results in higher values for m in

general.

Acknowledgment

This work was supported by the National Science Foundation under Grant Number CHE-8206487.

Figure 1. Maps displaying the locations of N_2 molecules on a 96×96 site Ru(001) lattice. The open circles represent Ru surface atoms, while the smaller closed circles represent N_2 molecules adsorbed on six-fold sites. The direction of the solid lines designates the three different degenerate phases for a $(\sqrt{3} \times \sqrt{3})R30^\circ$ overlayer. The maps demonstrate the increase in island size for a $\theta = 0.15$ monolayer surface adsorbed at 120 K with 7.5×10^{-6} torr N_2 down-quenched to 87.5 K for (a) 10, (b) 100, (c) 1000 and (d) 21500 seconds.

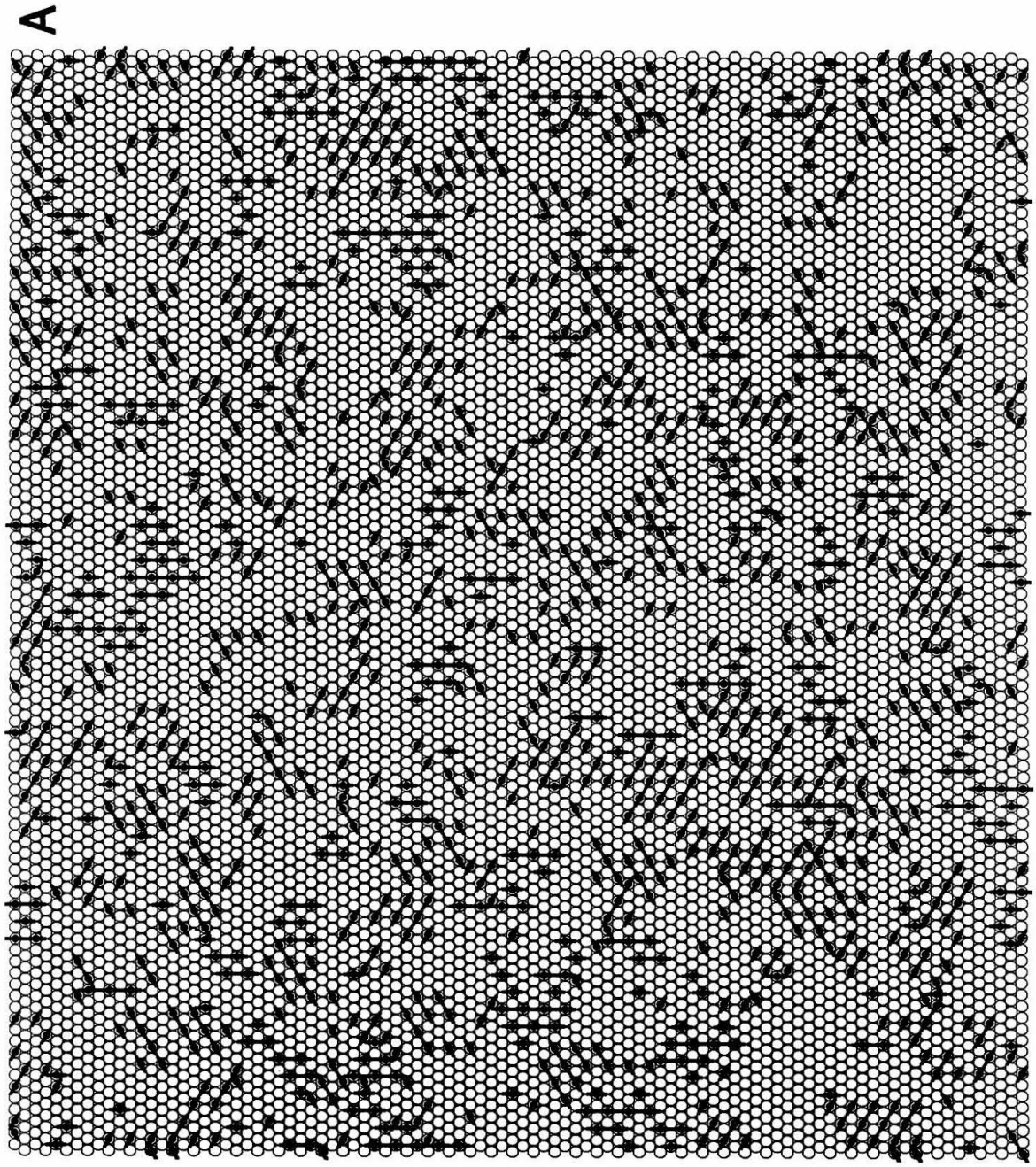
A

B

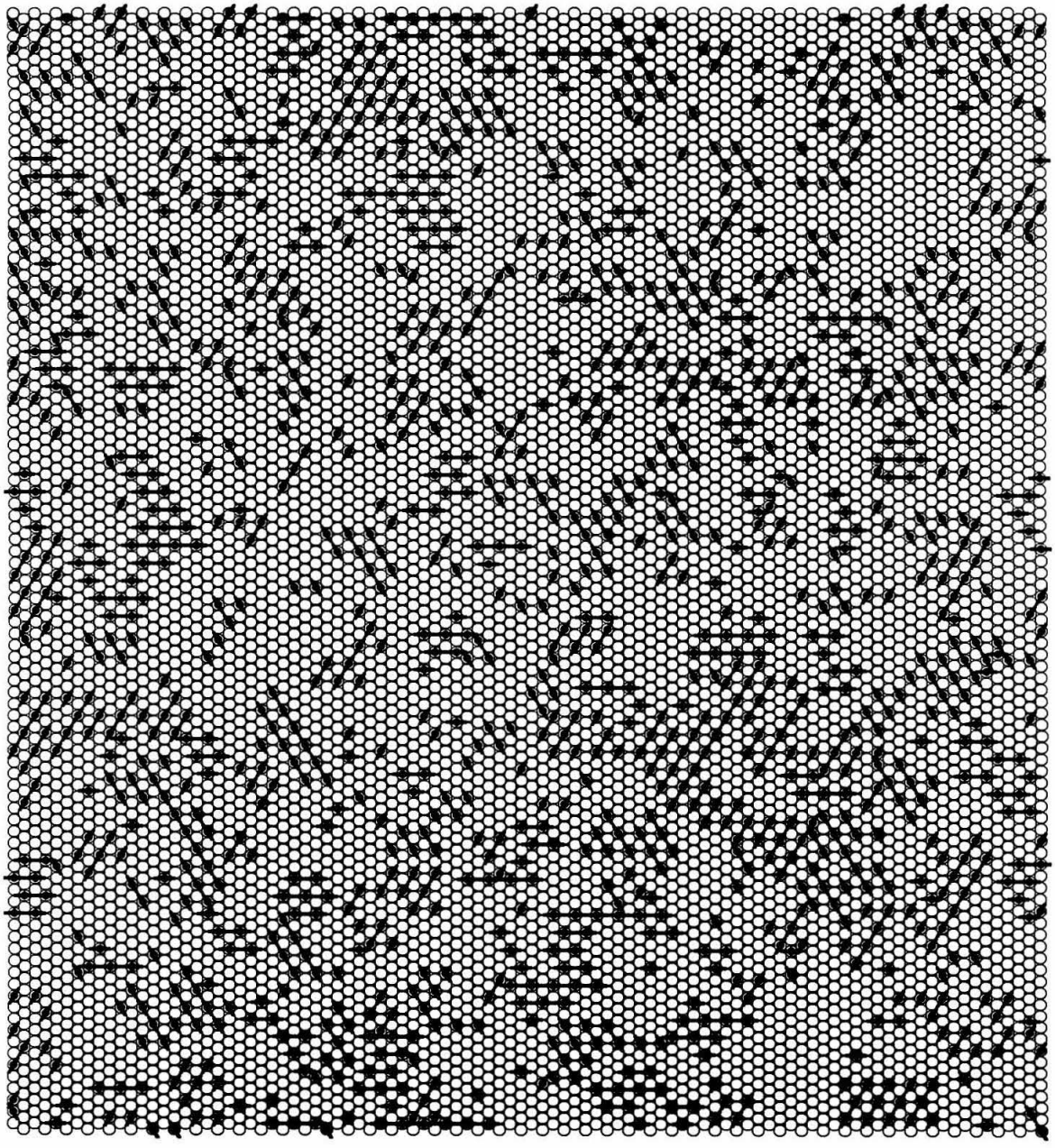

C

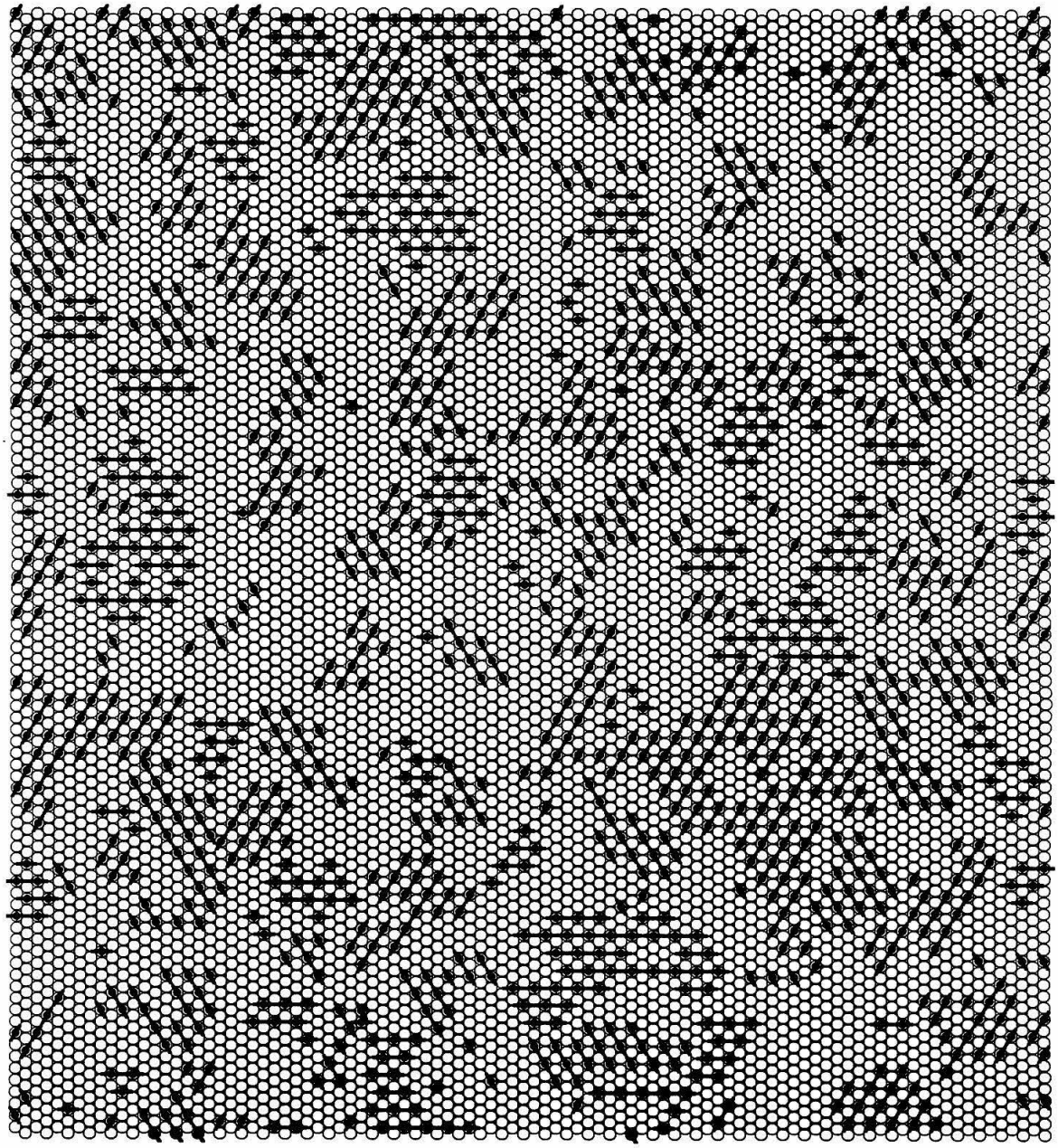

D

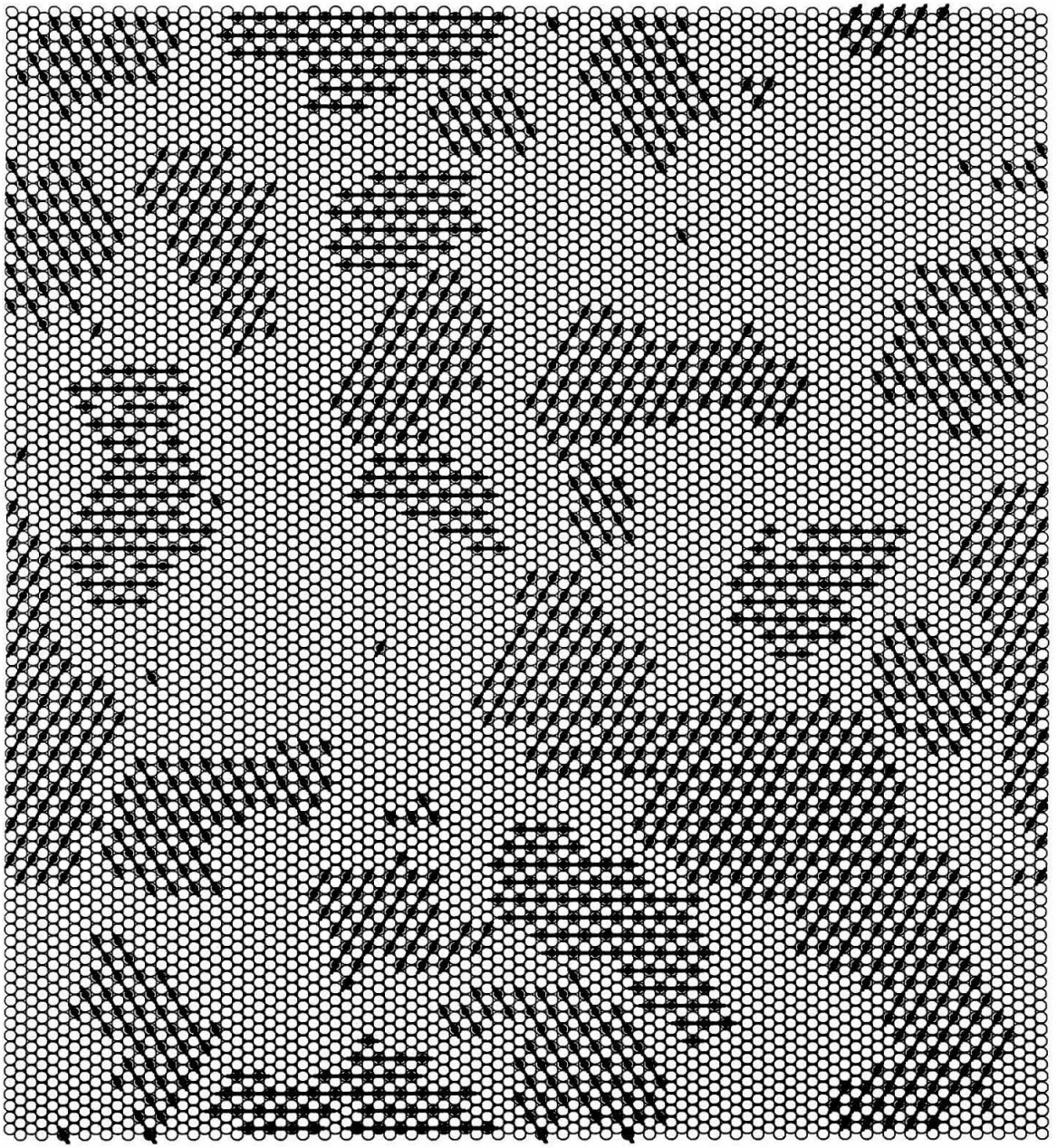

Figure 2. Plots of the Fourier transforms of the maps from Figure 1. The first order substrate diffraction maxima appear on the edges of the plot. The Fourier transform intensity is designated by the darkness of each pixel. The gray scale covers four orders of magnitude scaled to the maximum intensity pixel at (0,0). The plots demonstrate the decrease in width of the six symmetry related overlayer diffraction peaks for a $\theta = 0.15$ monolayer surface adsorbed at 120 K with 7.5×10^{-6} torr N_2 down-quenched to 87.5 K for (a) 10, (b) 100, (c) 1000 and (d) 21500 seconds.

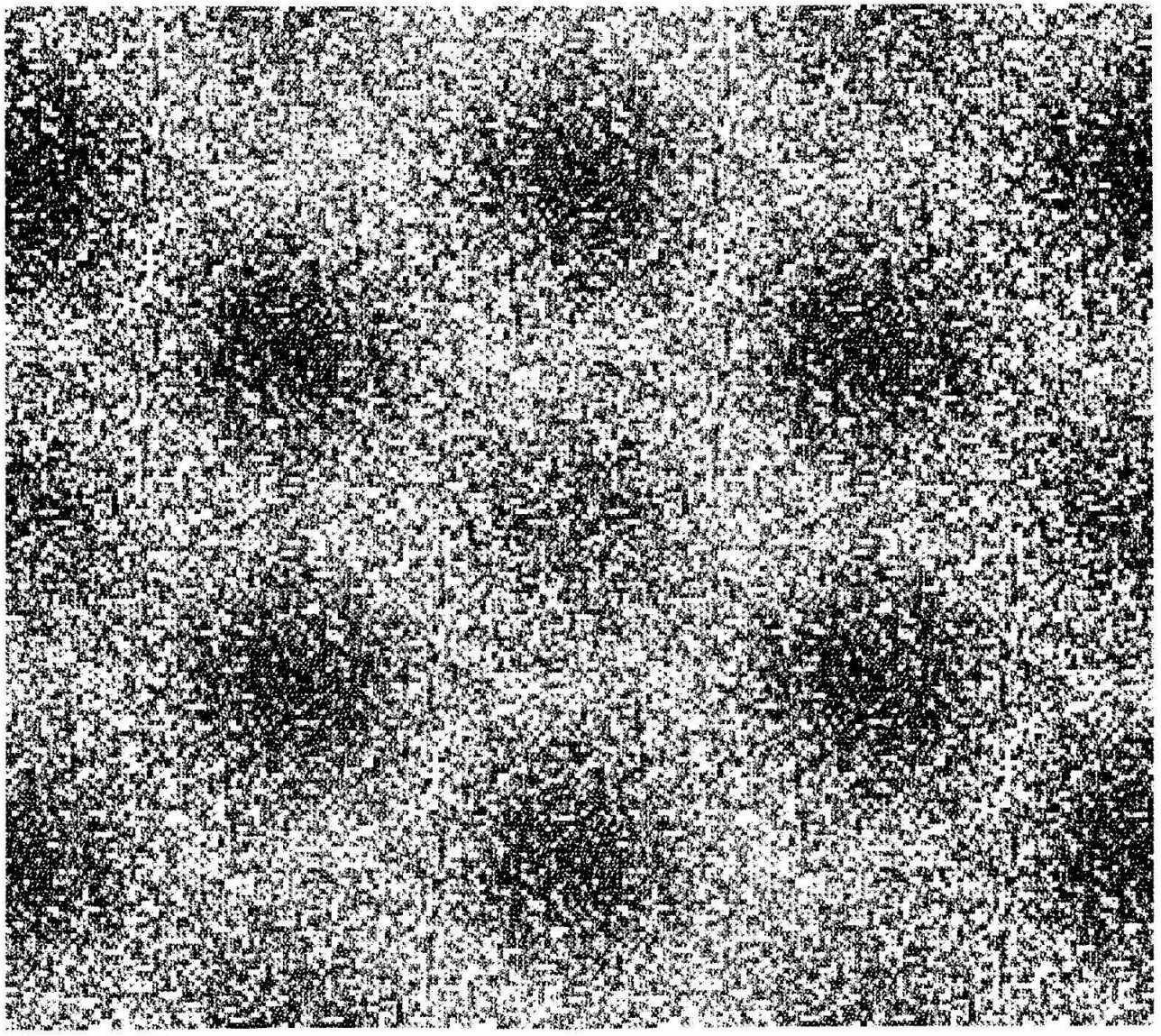
A
0.00010
0.00016
0.00025
0.00040
0.00063
0.00100
0.00158
0.00251
0.00398
0.00631
0.01000
0.01585
0.02512
0.03981
0.06310
0.10000
0.15849
0.25119
0.39811
0.63096
1.00000

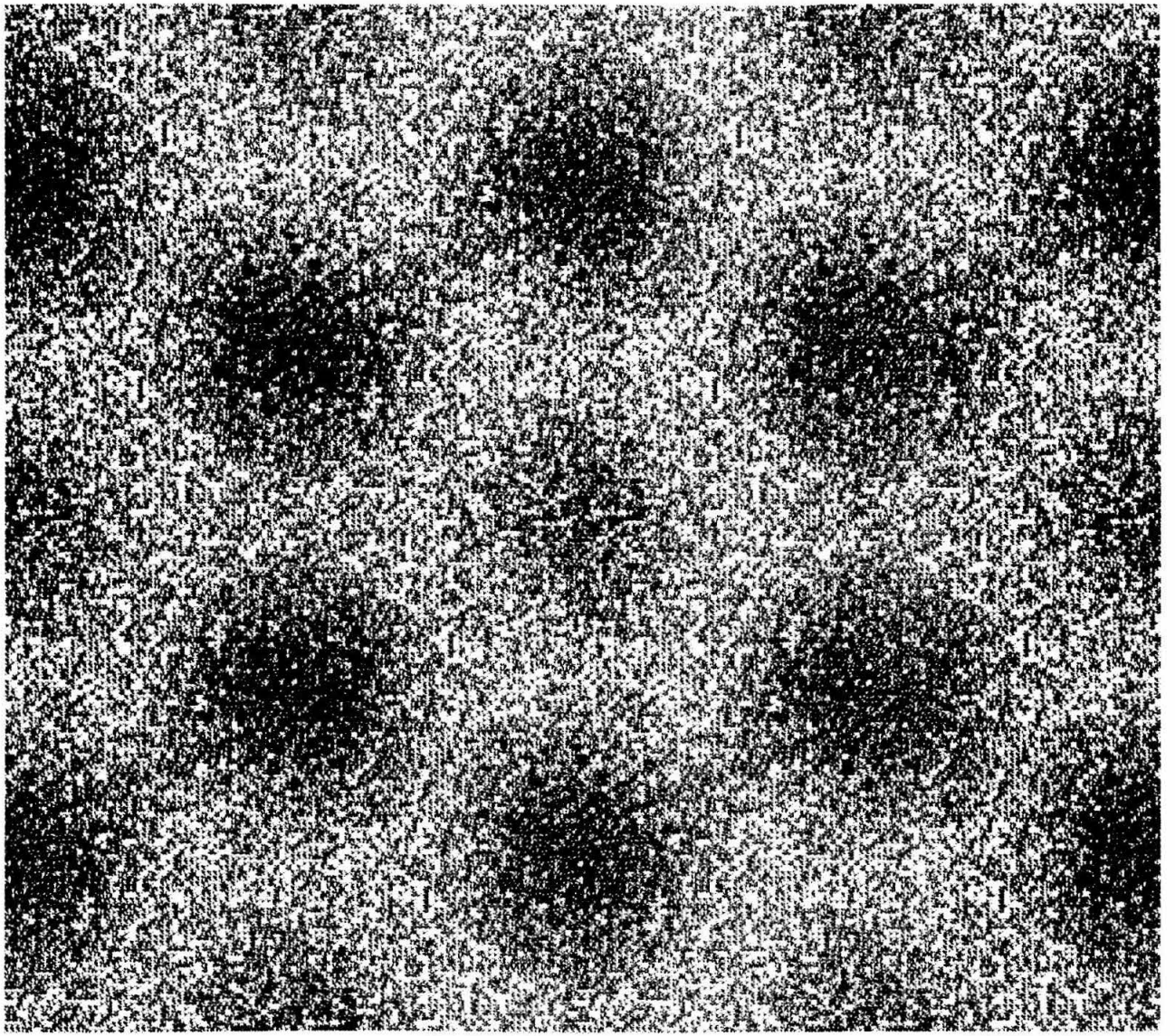
B
0.00010
0.00016
0.00025
0.00040
0.00063
0.00100
0.00158
0.00251
0.00398
0.00631
0.01000
0.01585
0.02512
0.03981
0.06310
0.10000
0.15849
0.25119
0.39811
0.63096
1.00000

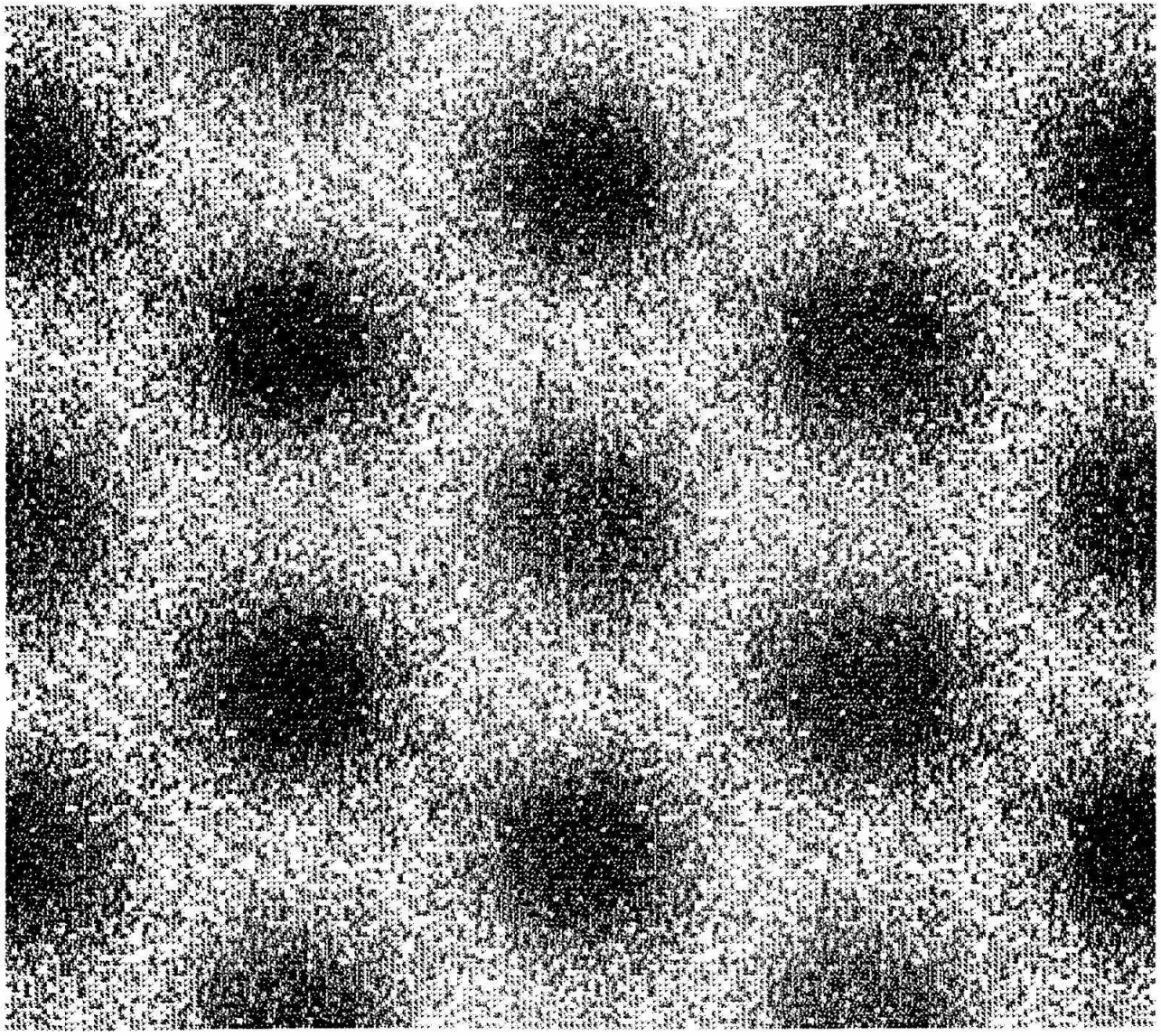
C
0.00010
0.00016
0.00025
0.00040
0.00063
0.00100
0.00158
0.00251
0.00398
0.00631
0.01000
0.01585
0.02512
0.03981
0.06310
0.10000
0.15849
0.25119
0.39811
0.63096
1.00000

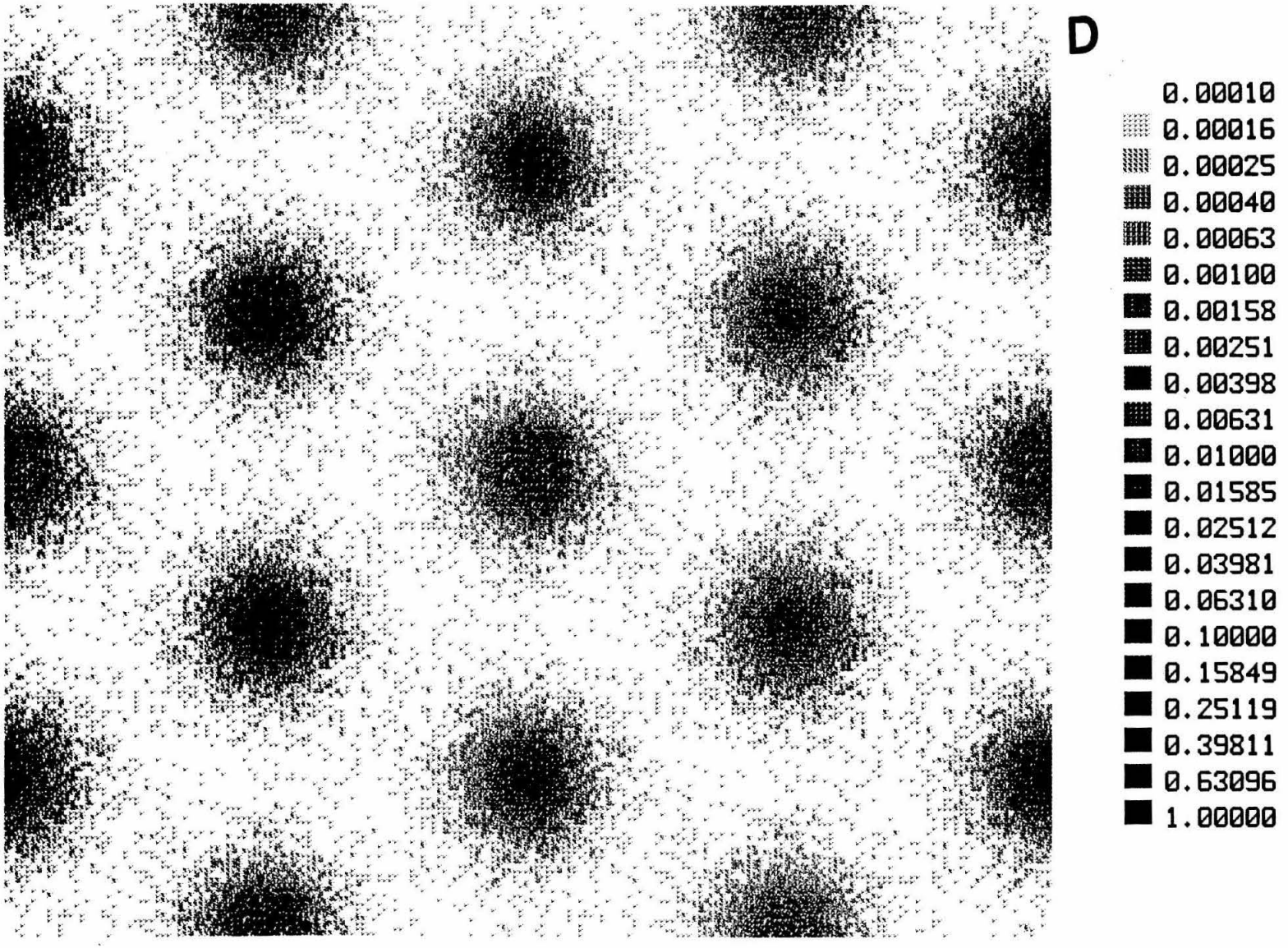
D
0.00010
0.00016
0.00025
0.00040
0.00063
0.00100
0.00158
0.00251
0.00398
0.00631
0.01000
0.01585
0.02512
0.03981
0.06310
0.10000
0.15849
0.25119
0.39811
0.63096
1.00000

Figure 3. A graph of Γ in reciprocal lattice units versus annealing time in seconds for a $\theta = 0.15$ monolayer, 96×96 site map where the starting surface was adsorbed at 120 K and 7.5×10^{-6} torr. The Γ values were fit from Fourier transform intensities that were were averaged for four runs with the same starting map. Annealing temperatures are 77.5, 82.5, 87.5 and 92.5 K, represented by triangles, squares, circles and crosses, respectively. The estimated error in the fit from the least-squares procedure is represented by the error bars; the actual error is likely to be larger. Lines have been drawn for growth equations with the best fit values for β and m.

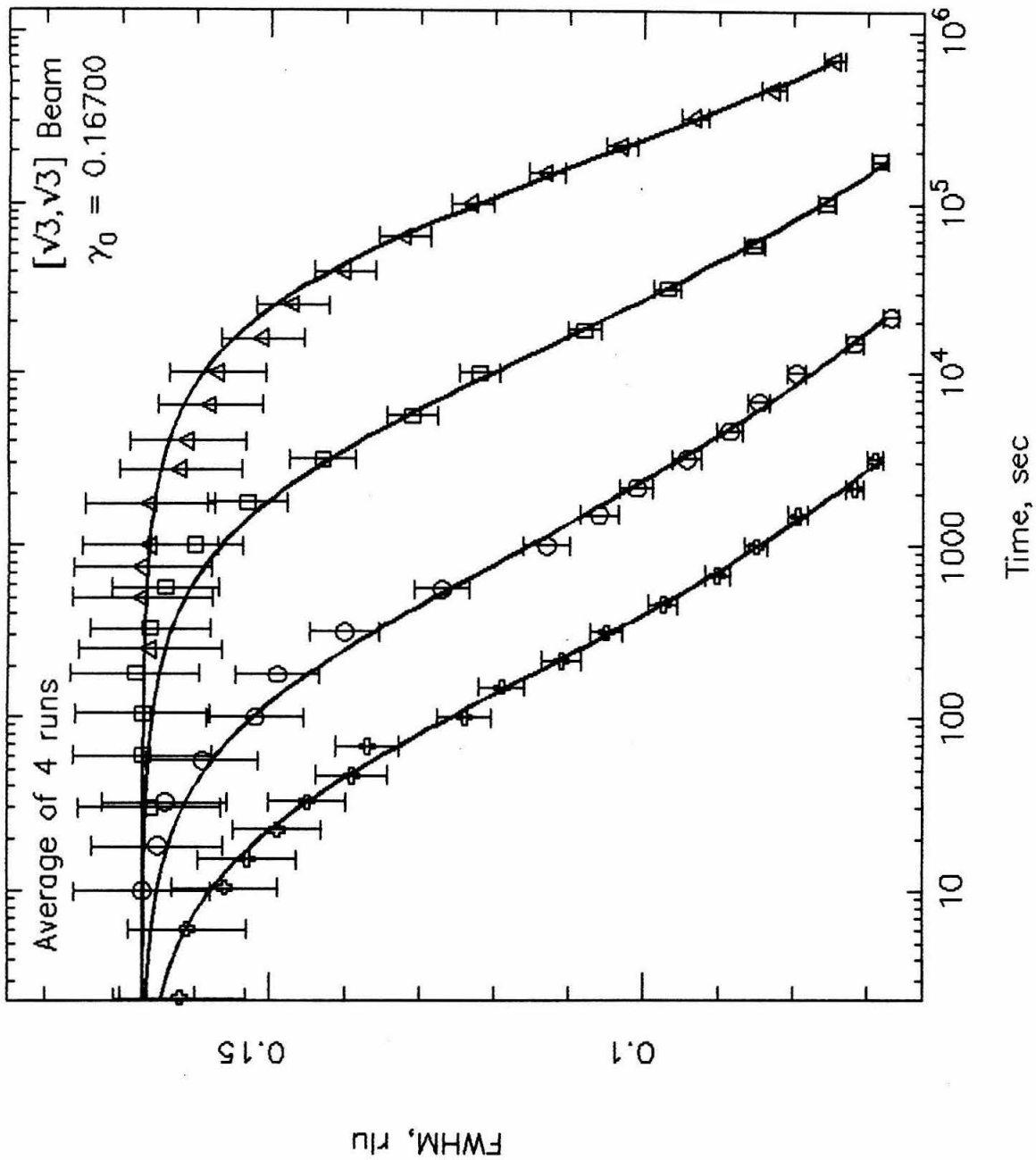
[√3,√3] Beam
γ_0 = 0.16700
Average of 4 runs
FWHM, rlu
0.15
0.1
10
100
1000
10^4
10^5
10^6
Time, sec

Figure 4. A graph of the fit values of m versus the annealing temperature. Circles represent runs from an "up-quenched," $\theta = 0.15$ monolayer, 96×96 site map where the starting surface was adsorbed at 78 K and 7.5×10^{-8} torr. Squares represent runs from a "down-quenched," $\theta = 0.15$ monolayer, 96×96 site map where the starting surface was adsorbed at 120 K and 7.5×10^{-6} torr. Crosses represent runs with the same starting map as was used for the runs designated with squares, however for these runs desorption was "turned off" (see text.) Triangles represent runs from a "down-quenched," $\theta = 0.15$ monolayer, 132×132 site map where the starting surface was adsorbed at 120 K and 7.5×10^{-6} torr. The four equivalent runs were averaged for the 96×96 site maps, and two runs were averaged for the 132×132 maps.

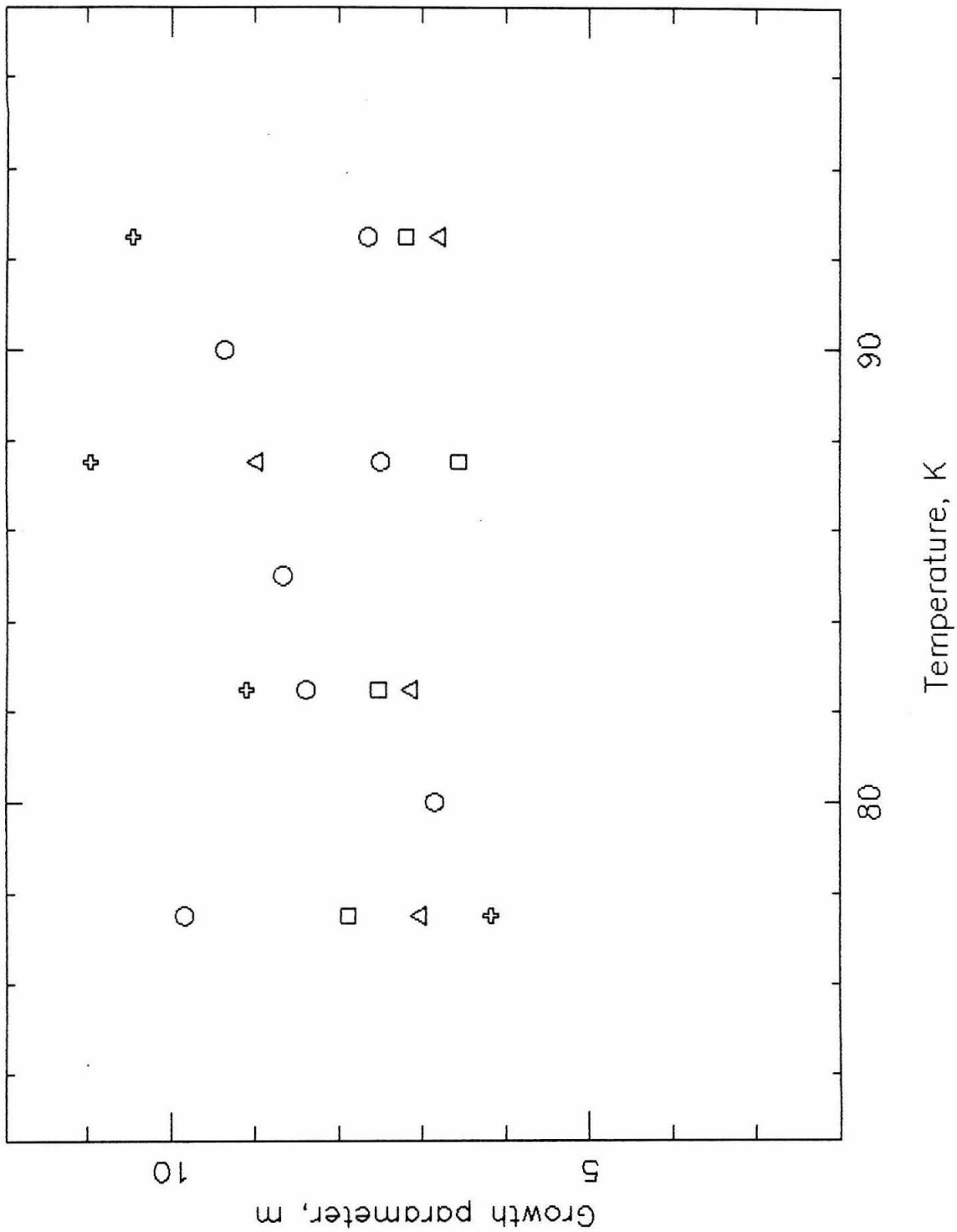
Growth parameter, m
10
5
80
90
Temperature, K

Figure 5. (a), A graph of Γ in reciprocal lattice units versus the annealing time in seconds for the same results presented in Figure 3, but where the lines represent best fits for β, where m has been fixed at 8. (b), A graph of Γ versus $\beta t + 1$ on a log-log scale. The line indicates the slope expected for $m = 8$. Note the good agreement between the measured values and the fitted lines.

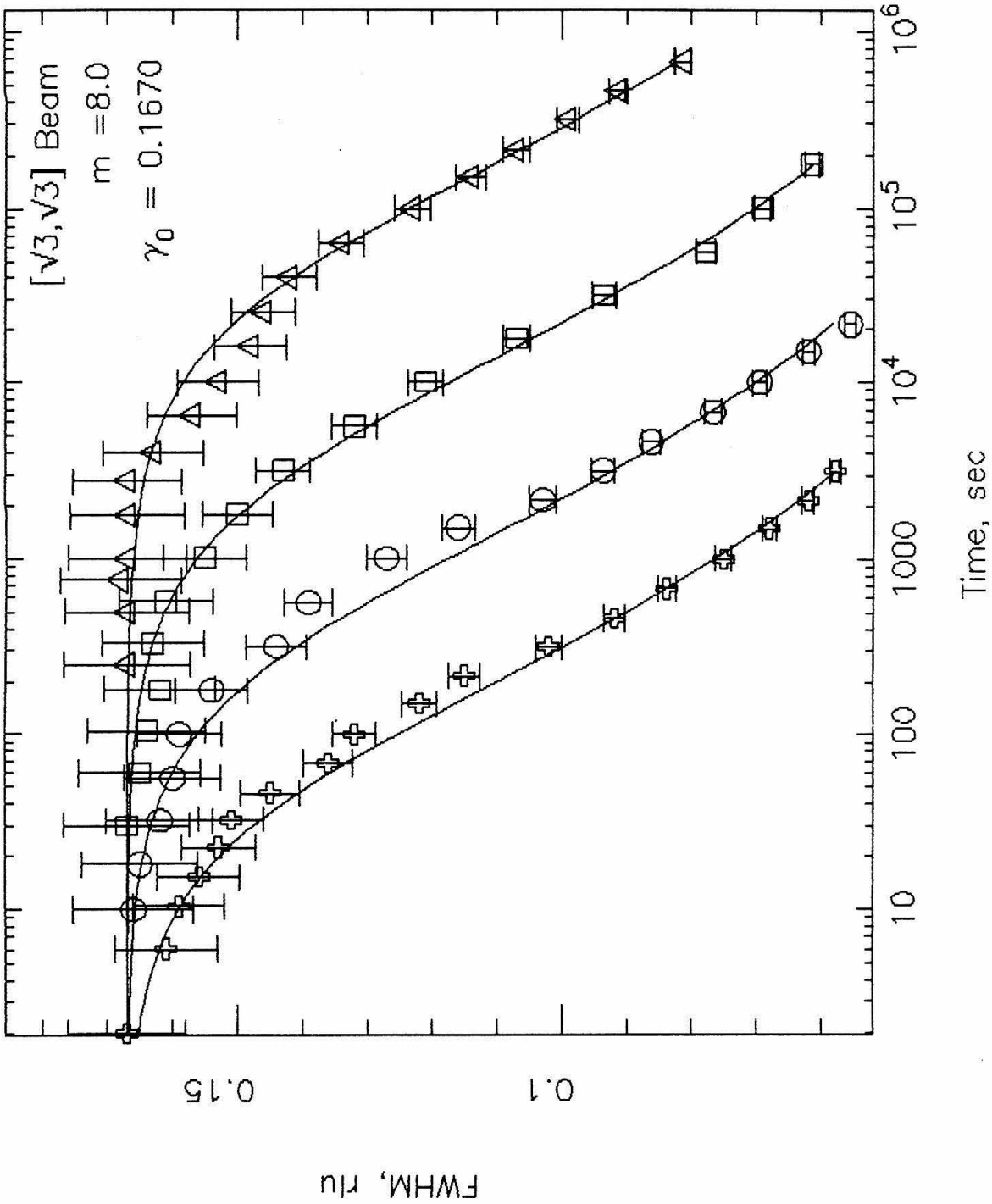
[√3,√3] Beam
m =8.0
γ_0 = 0.1670
FWHM, rlu
0.1
0.15
10
100
1000
10^4
10^5
10^6
Time, sec

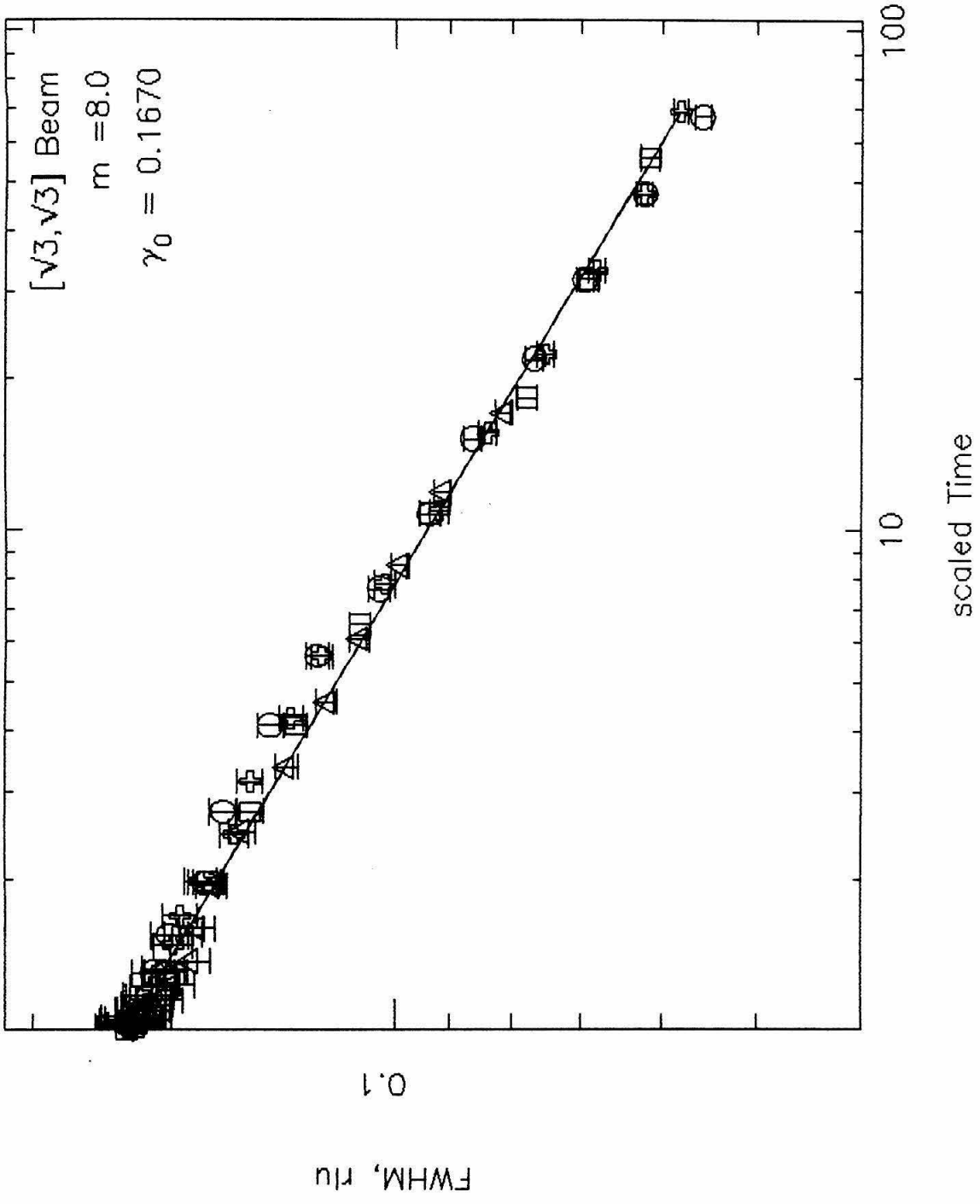
[√3,√3] Beam
m =8.0
γ_0 = 0.1670
FWHM, rlu
0.1
10
100
scaled Time

Figure 6. (a), A graph of Γ in reciprocal lattice units versus the annealing time in seconds for the same results presented in Figure 3, but where the lines represent best fits for β, where m has been fixed at 4. (b), A graph of Γ versus $\beta t + 1$ on a log-log scale. The line indicates the slope expected for $m = 4$. Note the relatively poor agreement between the measured values and the fitted lines in comparison to Figure 5.

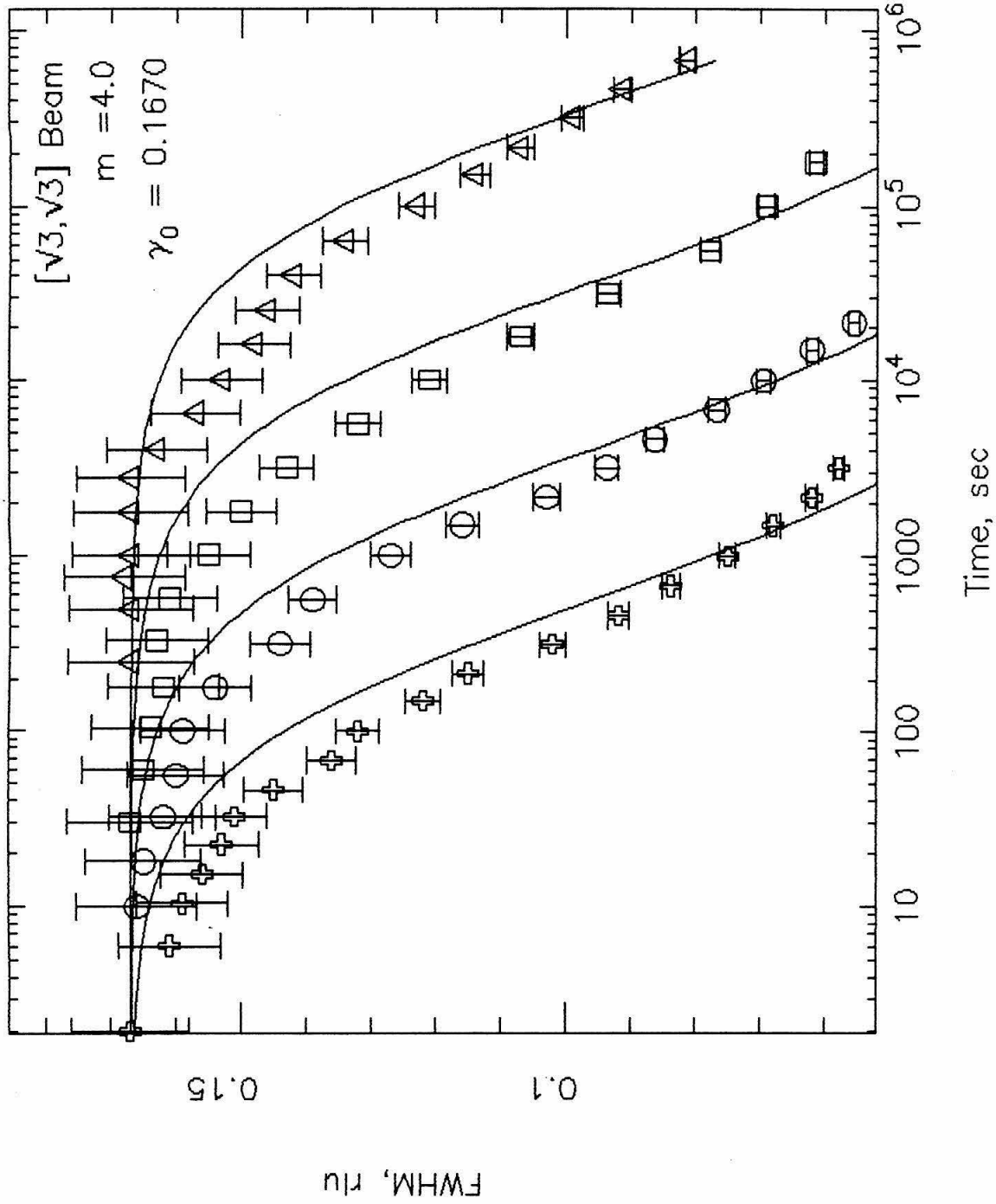
[√3,√3] Beam
m =4.0
γ_0 = 0.1670
FWHM, rlu
0.15
0.1
10
100
1000
10^4
10^5
10^6
Time, sec

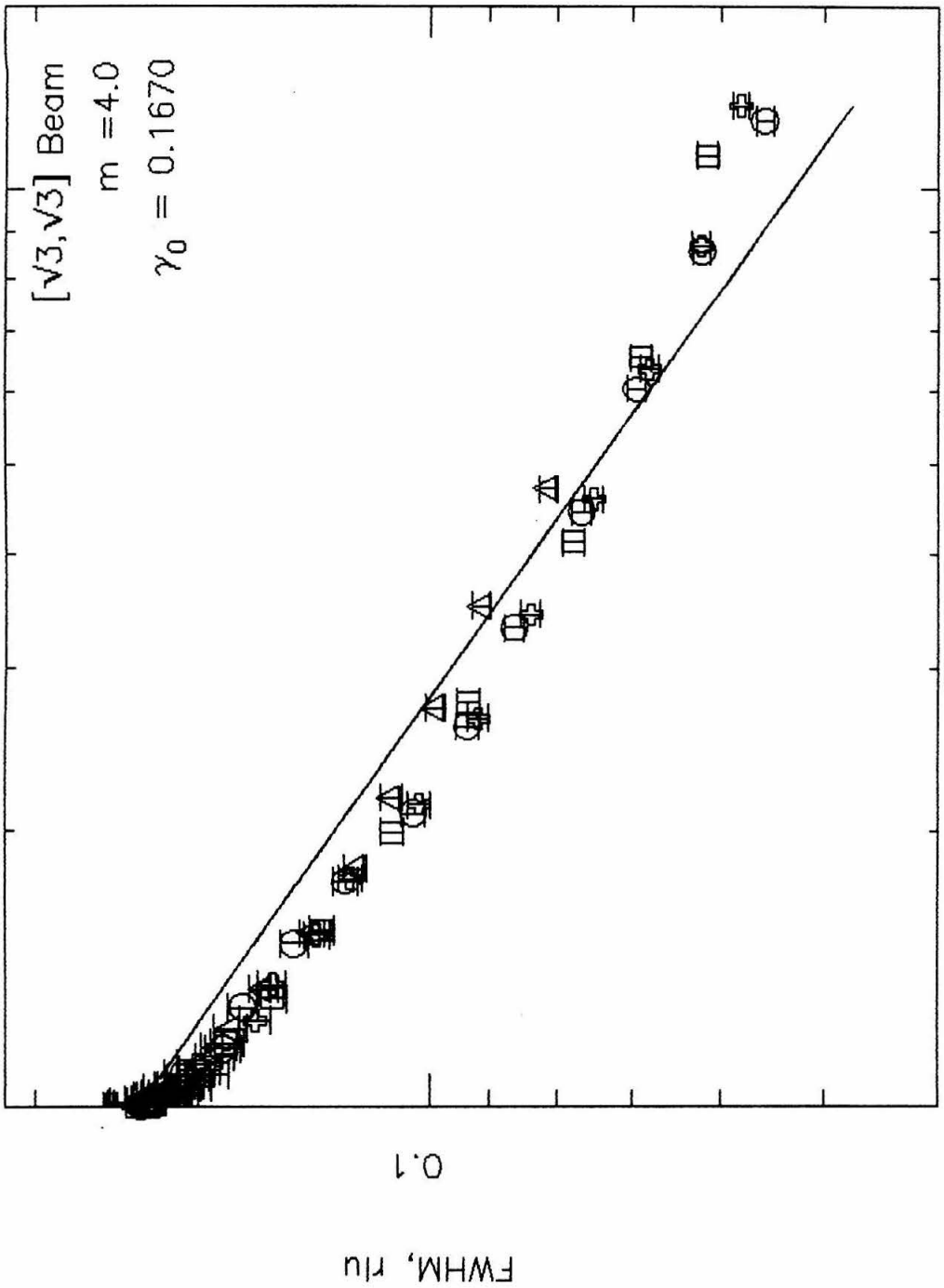
[√3,√3] Beam
m =4.0
γ_0 = 0.1670
FWHM, rlu
0.1
10
scaled Time

Figure 7. (a), A graph of Γ in reciprocal lattice units versus the annealing time in seconds for the same results presented in Figure 3, but where the lines represent best fits for β, where m has been fixed at 2. (b), A graph of Γ versus $\beta t + 1$ on a log-log scale. The line indicates the slope expected for $m = 2$. Note the relatively poor agreement between the measured values and the fitted lines in comparison to Figure 5.

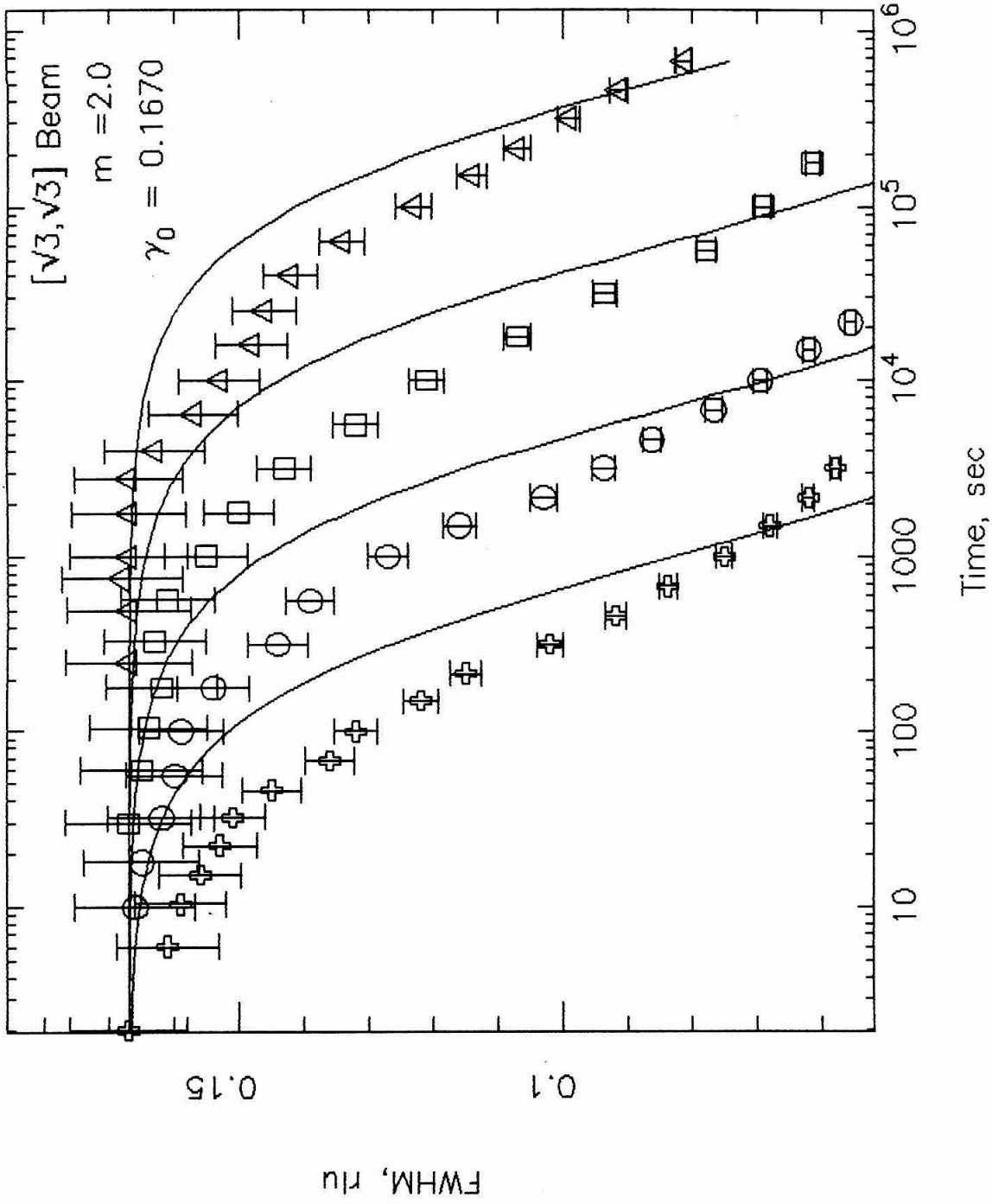
[√3,√3] Beam
m =2.0
γ_0 = 0.1670
FWHM, rlu
0.15
0.1
Time, sec
10
100
1000
10^4
10^5
10^6

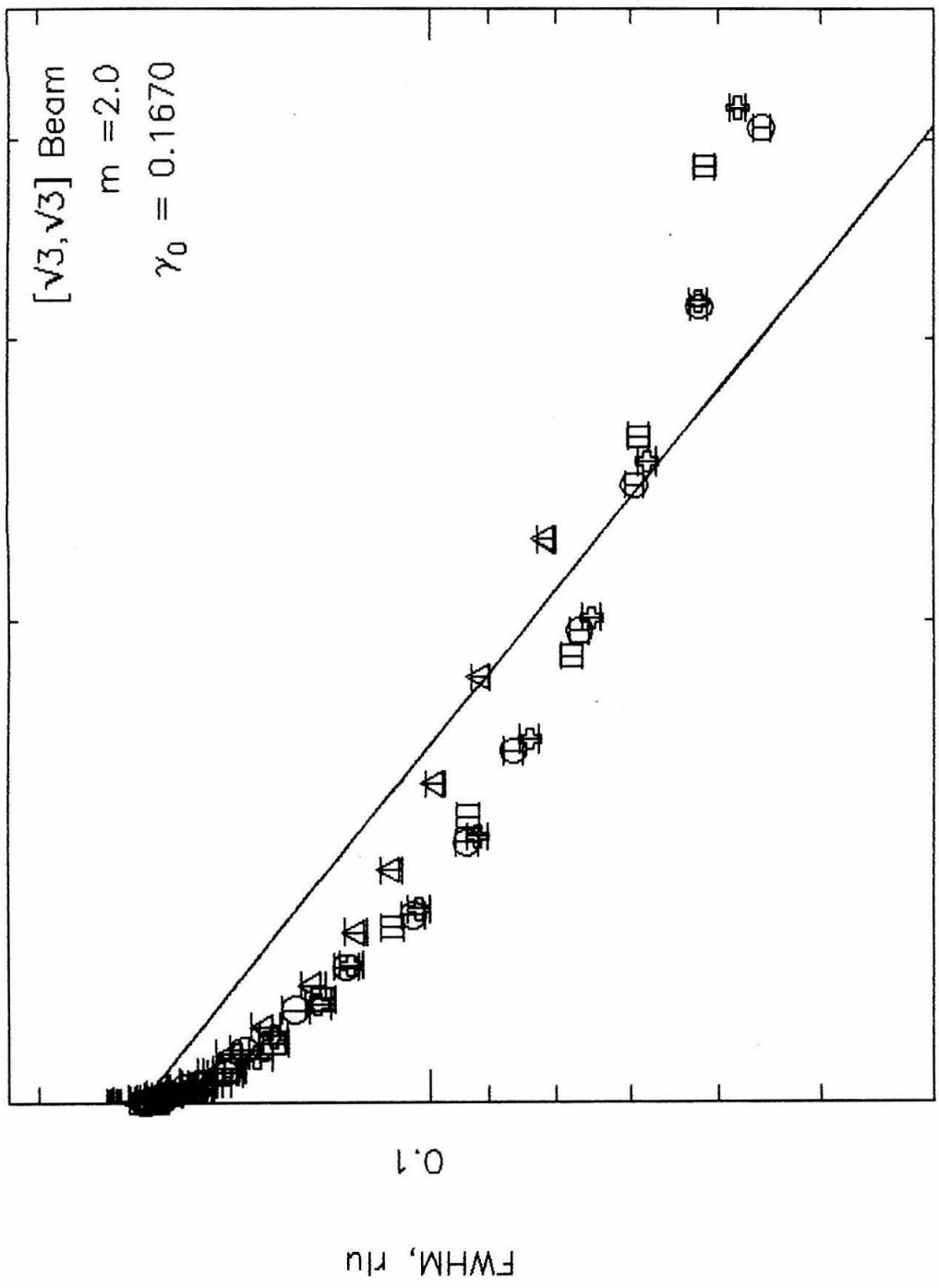
[√3,√3] Beam
m =2.0
γ_0 = 0.1670
0.1
FWHM, rlu
scaled Time

[1] M. G. Lagally, G.-C. Wang and T.-M. Lu, in *Chemistry and Physics of Solid Surfaces*, Vol. II, edited by R. Vanselow (CRC Press, Boca Raton, Florida, 1979).

[2] W. H. Weinberg, Ann. Rev. Phys. Chem. **34**, 217 (1983).

[3] S. A. Safran, Phys. Rev. Lett. **46**, 1581 (1981).

[4] I. M. Lifshitz, Zh. Eksp. Teor. Fiz. **42**, 1354 (1962) [Sov. Phys. JETP **15**, 939 (1962)].

[5] S. M. Allen and J. W. Cahn, Acta Metall. **27**, 1085 (1979).

[6] J. D. Gunton and M. Droz, in *Introduction to the Theory of Metastable and Unstable States*, Vol. 183 of *Lecture Notes in Physics*, edited by J. Zittarz, (Springer, Berlin, 1980).

[7] S. A. Safran, P. S. Sahni and G. S. Grest, Phys. Rev. B **28**, 2693 (1983); P. S. Sahni, D. J. Srolovitz, G. S. Grest, M. P. Anderson and S. A. Safran, Phys. Rev. B **28**, 2705 (1983); P. S. Sahni, G. S. Grest, M. P. Anderson and D. J. Srolovitz, Phys. Rev. Lett. **50**, 263 (1983); P. S. Sahni, G. S. Grest and S. A. Safran, Phys. Rev. Lett. **50**, 60 (1983).

[8] M. Tringides, P. K. Wu, W. Moritz and M. G. Lagally, Ber. Bunsenges. Phys. Chem. **90**, 277 (1986); P. K. Wu, J. H. Perepezko, J. T. McKinney and M. G. Lagally, Phys. Rev. Lett. **51**, 1577 (1983); J. C. Buchholtz and M. G. Lagally, Phys. Rev. Lett. **35**, 442 (1975).

[9] G.-C. Wang and T.-M. Lu, Phys. Rev. B **31**, 5918 (1985); G.-C. Wang and T.-M. Lu, Phys. Rev. Lett. **50**, 2014 (1983).

[10] For recent reviews see K. Binder, Ber. Bunsenges. Phys. Chem. **90**, 257 (1986); J. D. Gunton and K. Kaski, Surface Sci. **144**, 290 (1984); J. D. Gunton, M. San Miguel and P. S. Sahni, in *Phase Transitions and Critical Phenomena*, Vol. 8, edited by C. Domb and J. Lebowitz (Academic, New York, 1983).

[11] A. Sadiq and K. Binder, Phys. Rev. Lett. **51**, 674 (1983).

[12] J. Viñals and J. D. Gunton, Surface Sci. **157**, 473 (1985).

[13] O. G. Mouritsen, Phys. Rev. B **28**, 3150 (1983).

[14] K. Kaski, B. Kumar, J. D. Gunton and P. A. Rikvold, Surface Sci. **152/153**, 859 (1985); K. Kaski, B. Kumar, J. D. Gunton and P. A. Rikvold, Phys. Rev. B **29**, 4420 (1984).

[15] M. Silverberg, A. Ben-Shaul and F. Rebentrost, J. Chem. Phys. **83**, 6501 (1985).

[16] J. Viñals, M. Grant, M. San Miguel, J. D. Gunton and E. T. Gawlinski, Phys. Rev. Lett. **54**, 1264 (1985).

[17] K. Kaski, M. C. Yalabik, J. D. Gunton and S. A. Sahni, Phys. Rev. B **28**, 5263 (1983).

[18] K. Kaski, T. Ala-Nissilä and J. D. Gunton, Phys. Rev. B **31**, 310 (1985).

[19] M. Grant and J. D. Gunton, Phys. Rev. B **28**, 5496 (1983).

[21] T. Ala-Nissilä, J. D. Gunton and K. Kaski, Phys. Rev. B **33**, 7583 (1986).

[22] J. Viñals and J. D. Gunton, Phys. Rev. B **33**, 7795 (1986).

[23] G. F. Mazenko and M. C. Zannetti, Phys. Rev. B **32**, 4565 (1985).

[24] G. F. Mazenko, O. T. Valls and F. C. Zhang, Phys. Rev. B **31**, 4453 (1985).

[25] E. T. Gawlinski, S. Kumar, M. Grant, J. D. Gunton and K. Kaski, Phys. Rev. B **32**, 1575 (1985); E. T. Gawlinski, S. Kumar, M. Grant, and J. D. Gunton, Phys. Rev. Lett. **53**, 2266 (1984).

[26] K. Kaski, M. Grant and J. D. Gunton, Phys. Rev. B **31**, 3040 (1985).

[27] O. G. Mouritsen, Phys. Rev. Lett. **56**, 850 (1986); O. G. Mouritsen, Phys. Rev. B **31**, 2613 (1985).

[28] E. S. Hood, B. H. Toby and W. H. Weinberg, Phys. Rev. Lett. **55** 2437 (1985).

[29] See Appendices B and C for a description of the algorithms and computer programs.

[30] T.-M. Lu, G.-C. Wang and M. G. Lagally, Surface Sci. **108**, 494 (1981).

[31] D. Saloner, P. K. Wu and M. G. Lagally, J. Vac. Sci. Technol. A **3**, 1531 (1985).

[32] R. A. Young and D. B. Wiles, J. Appl. Cryst. **15** 430 (1982).

[33] J. B. Hastings, W. Thomlinson and D. E. Cox, J. Appl. Cryst. **17** 85 (1984).

[34] A. B. Anton, N. R. Avery, B. H. Toby and W. H. Weinberg, J. Electron Spectrosc. Relat. Phenom. **29**, 181 (1983).

[35] P. Feulner and D. Menzel, Phys. Rev. B **25**, 4295 (1982); D. Menzel, H. Pfnür and P. Feulner, Surface Sci. **126**, 374 (1983).

[36] A. B. Anton, N. R. Avery, T. E. Madey and W. H. Weinberg, J. Chem. Phys. Surface Sci. **85**, 507 (1986).

[37] T. E. Madey and W. H. Weinberg, unpublished communication.

Appendix A:

The Chemisorption of Nitrogen on the (001) Surface of Ruthenium

Journal of Electron Spectroscopy and Related Phenomena, 29 (1983) 181—186
Elsevier Scientific Publishing Company, Amsterdam — Printed in The Netherlands

THE CHEMISORPTION OF NITROGEN ON THE (001) SURFACE OF RUTHENIUM*

A.B. ANTON,[1] N.R. AVERY,[2] B.H. TOBY[1] and W.H. WEINBERG[1]

[1]Division of Chemistry and Chemical Engineering, California Institute of Technology, Pasadena, CA 91125 USA

[2]Division of Materials Science, CSIRO, University of Melbourne, Parkville, Australia 3052

ABSTRACT

High resolution electron energy loss spectroscopy (EELS), thermal desorption mass spectrometry (TDMS) and low energy electron diffraction (LEED) have been used to investigate the molecular chemisorption of N_2 on Ru(001) at 75 K and 95 K. Adsorption at 95 K produces a single chemisorbed state, and, at saturation, a $(\sqrt{3}\times\sqrt{3})R30^\circ$ LEED pattern is observed. Adsorption at 75 K produces an additional chemisorbed state of lower binding energy, and the probability of adsorption increases by a factor of two from its zero coverage value when the second chemisorbed state begins to populate. EEL spectra recorded for all coverages at 75 K show only two dipolar modes — $\nu(Ru-N_2)$ at 280-300 cm^{-1} and $\nu(N-N)$ at 2200-2250 cm^{-1} — indicating adsorption at on-top sites with the axis of the molecular standing perpendicular to the surface. The intensities of these loss features increase and $\nu(N-N)$ decreases with increasing surface coverage of both chemisorbed states.

INTRODUCTION

For years CO has served as the prototype for molecular chemisorption studies on well characterized surfaces (ref.1). Although the surface chemical bond in N_2 adsorption is fundamentally different from that of CO due to subtle differences in the electronic structure of the two molecules (ref.2), N_2 is isoelectronic with CO, making the investigation of N_2 adsorption and its comparison to CO a logical next step in understanding the surface chemical bond and interactions among chemisorbed molecules. With this goal in mind, the present investigation concerns the chemisorption of N_2 on the Ru(001) surface.

EXPERIMENTAL

The experiments described here were performed in two separate UHV systems, one equipped for LEED and Auger electron spectroscopy (AES) (ref.3), and the other for TDMS and EELS (ref.4). Ru(001) samples for both systems were prepared and cleaned by standard techniques (ref.5). Sample cooling allowed adsorption at 95 K in the LEED system and 75 K in the EELS system.

*Supported by the National Science Foundation under Grant No. CHE82-06487.

182

RESULTS AND DISCUSSION

Adsorption of N_2 at 95 K

Exposure of the Ru(001) surface to N_2 at 95 K gives a single, first order, TDMS feature, the binding energy of which shifts from 31.4 kJ/mole at low coverage to 29.4 kJ/mole at saturation (via the method of Redhead, ref.6). Saturation coverage at this temperature also produces a strong $(\sqrt{3}x\sqrt{3})R30^{\circ}$ LEED pattern (ref.7). Coverage estimates for these conditions, obtained by comparison of TDMS spectra to those obtained for desorption of a known coverage of CO, yield θ(sat. at 95 K)=0.35±0.10, implying formation of a complete $(\sqrt{3}x\sqrt{3})R30^{\circ}/\theta$ =0.33 overlayer.

EEL spectra recorded for adsorption at 95 K show only two dipolar modes — $\nu(Ru-N_2)$, appearing initially at 280 cm^{-1} and shifting upward with increasing coverage to 301 cm^{-1} at saturation; and $\nu(N-N)$, appearing initially at 2252 cm^{-1} and shifting downward to 2212 cm^{-1} at saturation. These frequencies are plotted as a function of exposure in Fig. 1.

The absence of bending modes in the EEL spectra indicates that the chemisorbed N_2 molecules have their axes perpendicular to the surface plane, and the frequency of $\nu(N-N)$ indicates that they are coordinated to single Ru atoms. The latter conclusion is substantiated by data for linear $Ru-N_2$ complexes which show $\nu(N-N)>2000$ cm^{-1} (ref.8).

As is the case for CO, the bonding of N_2 to a metal center is primarily via σ donation from the valence orbitals of N_2 to the metal (ref.2). The valence orbitals in N_2, $2\sigma_u$ and $3\sigma_g$, are shared equally between the two nitrogen atoms, and, although they mix upon interaction with a metal center to form two new σ orbitals with some lone pair character, the resulting donor bond is weak compared to that of CO, which bonds through its 5σ lone pair orbital, localized strongly on the carbon atom. Back-donation from the $d\pi$ levels of the metal to the $1\pi_g$ anti-bonding level of N_2 weakens the N-N bond, and changes in the amount of $d\pi$ back-donation with surface coverage can cause $\nu(N-N)$ to vary with coverage.

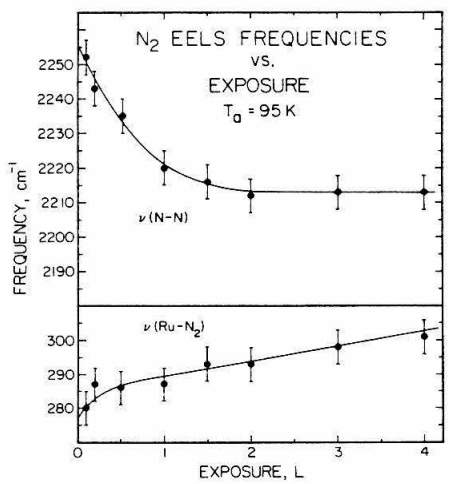

Fig. 1. EELS frequencies as a function of exposure for adsorption at 95 K.

Well-established theory (ref.9) which describes the interaction of an incident electron with an array of dipoles on a metal surface shows that the same properties of an adlayer which produce dipolar scattering also produce dipolar coupling in the adlayer, and this coupling interaction causes vibrational frequencies to increase monatonically with coverage. The intensity of the ν(N-N) mode seen in EELS is comparable to that seen for ν(C-O) at the same coverage (ref.10), indicating that N_2 is strongly polarized upon adsorption and has an induced dipolar moment approximately equal to that of CO. It follows that a 30-40 cm^{-1} upward shift of ν(N-N) from zero coverage to completion of a $(\sqrt{3}x\sqrt{3})R30^{\circ}/\theta=0.33$ overlayer occurs due to dipolar coupling (ref.10), as has been shown for CO on Ru(001) (refs.9,11). Then the data in Fig. 1 indicate that ν(N-N) shifts <u>downward</u> by <u>70-80 cm^{-1}</u> due to coverage dependent changes in the N-N bond.

Although negative frequency shifts with increasing surface coverage have been reported for CO adsorption on Cu(111) (ref.12) and on polycrystalline Au (ref.13) and for N_2 adsorption on Ni(110)(ref.14), the change in ν(C-O) and ν(N-N) observed in these investigations was less than $\sim$10 cm^{-1} and no detailed explanations of the change in the C-O or N-N bond with coverage were offered. A plausible explanation describes the decrease in ν(N-N) with increasing coverage as being due to formation of a $1\pi_g$ band with increasing coverage, broadening the $1\pi_g$ level and changing its population due to overlap with the fermi level of the substrate (ref.15).

If the energy of the $1\pi_g$ level for an isolated N_2 molecule chemisorbed on Ru(001) is above the fermi level of the metal, the $1\pi_g$ level is unpopulated and does not affect ν(N-N). Increasing the density of N_2 admolecules on the surface, however, could cause the $1\pi_g$ orbitals of adjacent molecules to overlap, forming a band and broadening the $1\pi_g$ level due to dispersion. Band formation at low coverage ($\theta<0.33$) is not unreasonable — the spatial extent of the $1\pi_g$ orbitals would be greater than the Van der Waals' diameter of N_2 ($\sim$5 Å), allowing significant overlap at the $\sqrt{3}$ intermolecular spacing of 4.6 Å. Island formation at low coverage, as is seen for CO adsorption on Ru(001) (ref.11), would enhance the effect. If the $1\pi_g$ level broadens sufficiently in energy to cross the fermi level, increasing population of this band would cause the N-N bond to weaken and decrease ν(N-N) for the adlayer. Broadening on the order of 1 eV due to dispersion is quite reasonable and has been reported for the 1π level of CO adsorbed on Ni(110) (ref.2).

<u>Adsorption of N_2 at 75 K</u>

Initial exposure of N_2 at 75 K produces the high temperature state seen for adsorption at 95 K. For exposures of 1.0 L or greater ($\theta/\theta_{max}>0.4$), however, a second feature appears with an initial binding energy of 24.4 kJ/mole, shifting to 21.3 kJ/mole at saturation. The probability of adsorption, $S(\theta)$, doubles

from its initial value of 0.4±0.2 when the low temperature state begins to populate, then gradually decreases as the surface coverage approaches saturation (ref.7). TDMS spectra recorded after a 2.0 L exposure of $^{15}N_2$ at 100 K, then a 2.0 L exposure of $^{14}N_2$ at 75 K (or vice versa), show only partial mixing of the two isotopes upon desorption, verifying the existence of two distinct binding states on the surface and ruling out the possibility of a compression structure at high coverage, as is seen for CO on Ru(001) (ref.3). Coverage estimates for saturation at 75 K yield θ=0.58±0.17 and indicate that the surface density (N_2/Ru surface atoms) in the low temperature state is approximately twice that in the high temperature state.

Although TDMS results show two distinct binding states, EELS results for adsorption at 75 K, illustrated in Fig. 2, again show only two modes, ν(Ru-N_2) and ν(N-N). Figure 3 shows the coverage dependence of the frequencies of these two modes. As was shown in Fig. 1 for adsorption at 95 K, ν(N-N) shifts downward with increasing coverage, a total shift of 49 cm^{-1} from 2247 cm^{-1} to 2198 cm^{-1} in this case, and ν(Ru-N_2) shifts upward from 278 cm^{-1} to 291 cm^{-1}.

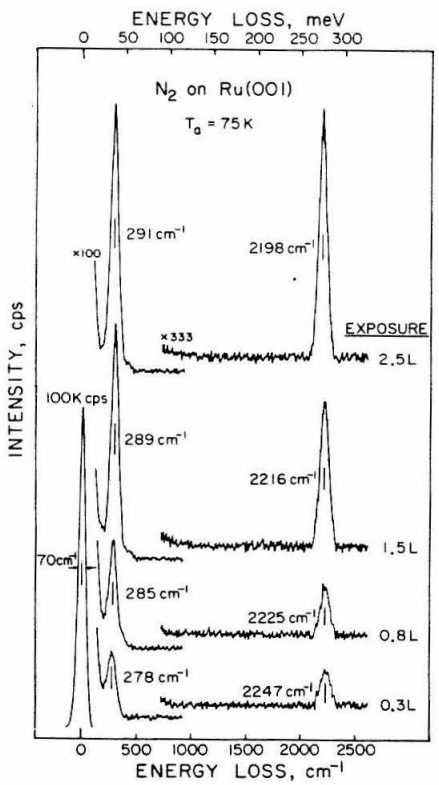

Fig. 2. Representative EEL spectra for adsorption at 75 K.

The addition of the second chemisorbed state, present only for adsorption at 75 K, contributes no new features to the specular EEL spectrum, causes no new features to appear in off-specular measurements, causes no abrupt changes in surface reflectivity, and causes no noticeable increase in the linewidth of either EELS band. Also, the intensities of both EELS bands, shown in Fig. 4, grow monotonically with total surface coverage of both chemisorbed states, exceeding the intensities of ν(Ru-N_2) and ν(N-N) seen for saturation at 95 K by 20% and 50%, respectively (ref.10). Although it has been shown that intensities of EELS bands are not absolute indicators of surface coverage (ref.9), the monatonic increase in the intensity of both modes with surface coverage and the absence of new features in the EEL spectra attributable to the other species does suggest that EELS is probing both chemisorbed states, i.e. the vibrational

spectra of the two states are identical within instrumental resolution. By these arguments, N_2 molecules in the low temperature state are also bonded with their molecular axes perpendicular to the surface, but, as was shown by TDMS coverage comparisons for adsorption at 95 K and 75 K, they are bonded in areas "crowded" with N_2 molecules, as surface density in the low temperature state is approximately twice that of the high temperature $\sqrt{3}$ state.

CONCLUSIONS

The conclusions of this work can be summarized as follows:

1. Adsorption of N_2 on Ru(001) at 95 K produces an ordered $(\sqrt{3}x\sqrt{3})R30^{\circ}/\theta = 0.33$ overlayer with the N_2 molecules at on-top sites, standing perpendicular to the surface plane. The binding energy of N_2 in this state is 31.4 kJ/mole at low coverage, shifting to 29.4 kJ/mole at saturation.

2. Adsorption at 75 K produces a second, distinct chemisorbed state, appearing for relative coverages (θ/θ_{max}) greater than 0.4 with an initial binding energy of 24.4 kJ/mole and shifting to 21.3 kJ/mole at saturation. This state is indistinguishable from the $\sqrt{3}$ state in EELS and is therefore also attributed to molecules standing upright on the surface.

3. Changes in the N-N bond with coverage, due presumably to changes in the relative amount of $1\pi_g$ backbonding, cause ν(N-N) to decrease with increasing coverage for adsorption at both 75 K and 95 K.

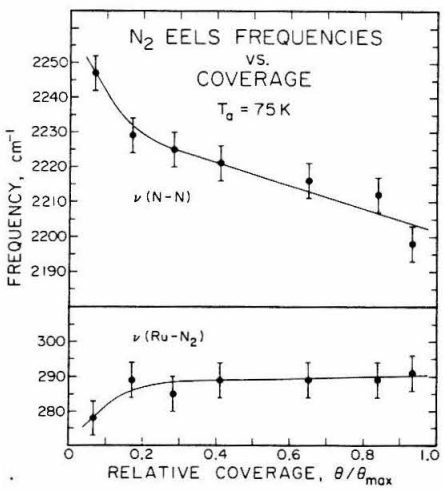

Fig. 3. EELS frequencies as a function of coverage for adsorption at 75 K.

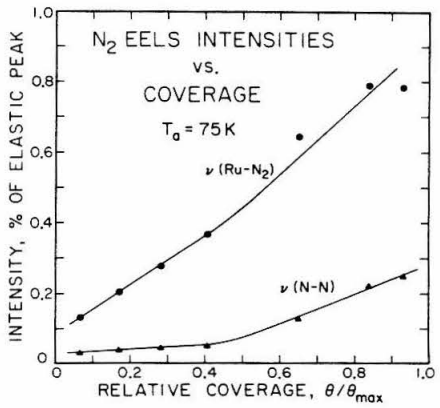

Fig. 4. EELS intensities as a function of coverage for adsorption at 75 K.

186

ACKNOWLEDGMENTS

We wish to acknowledge the assistance of Ted Madey in the collection and interpretation of data at the beginning of this project

REFERENCES

1 See, for example, Vibrational Spectroscopy of Adsorbates, R.F. Willis, ed., (Springer-Verlag, Berlin, 1980).
2 K. Horn, J. DiNardo, W. Eberhardt, H.-J. Freund and E.W. Plummer, Surface Sci. 118 (1982) 465.
3 E.D. Williams and W.H. Weinberg, Surface Sci. 82 (1979) 93.
4 G.E. Thomas and W.H. Weinberg, Rev. Sci. Instr. 50 (1979) 497.
5 G.E. Thomas and W.H. Weinberg, J. Chem. Phys. 69 (1978) 3611; 70 (1979) 954.
6 P.A. Redhead, Vacuum 12 (1979) 203.
7 P. Feulner and D. Menzel, Phys. Rev. B 25 (1982) 4295.
8 B. Folkesson, Acta. Chem. Scand. 26 (1972) 4008.
9 B.N.J. Persson and R. Ryberg, Phys. Rev. B 24 (1981) 6954, and references therein.
10 A.B. Anton, N.R. Avery, B.H. Toby and W.H. Weinberg, in preparation.
11 H. Pfnür, D. Menzel, F.M. Hoffmann, A. Ortega and A.M. Bradshaw, Surface. Sci. 93 (1980) 431.
12 P. Hollins and J. Pritchard, Surface Sci. 89 (1979) 486.
13 M.L. Kottke, R.G. Greenler and H.G. Tompkins, Surface Sci. 32 (1972) 231.
14 M Grunze, R.K. Driscoll, G.N. Burland, J.C.L. Cornish and J. Pritchard, Surface Sci. 89 (1979) 381.
15 A.M. Bradshaw, private communication.

Appendix B:

METHODOLOGY FOR N_2 SIMULATION CALCULATIONS

ABSTRACT

The algorithms and techniques used for a number of computer programs are documented. The first section details coordinate schemes developed for indexing sites on a 2-D hexagonal lattice. The second section covers a set of programs which simulate adsorption and desorption of N_2 molecules on the Ru(001) surface. The third section documents a set of programs used to analyze the ordering of N_2 molecules from the adsorption/desorption simulation results. The final section details several graphics programs and a graphics package written for plotting results from the previous programs.

Introduction

A series of programs have been developed for simulation of N_2 adsorption and desorption, for analyzing the island distributions from the simulation programs by computation of Fourier transforms of the "maps" which contain the locations of molecules on the simulated surface, and for graphic display of program results. This Appendix contains detailed descriptions of the most important of these programs. Less detailed descriptions are included for programs that are fairly straight forward to use. Listings of the programs discussed in this Appendix may be found in Appendix C.

This Appendix is written in four sections. The first section discusses methods used for indexing hexagonal coordinate systems. The second section discusses the adsorption and thermal desorption simulation programs. The third section discusses programs for computing Fourier transforms from maps, for fitting a line shape function to peaks in the FFT intensities and for fitting the widths of the line shapes to growth laws. The fourth section discusses programs used for plotting the results of the previous two programs.

The programs documented here were written to run on Digital Equipment Corporation VAX 11/780 and μVAX-II computers running the VAX/VMS operating system (Version 4.2) using FORTRAN 77 (Version 4.2). The larger programs were further adapted to run on a Floating Point Systems FPS-164 array processor (referred to hereafter as the AP), which uses an ANSI standard FORTRAN 77 cross compiler under the FPS Single Job Entry (SJE) system (both compiler and SJE are release G1). No attempt will be made to acquaint the reader with the details of the VAX/VMS or FPS operating systems or give detailed descriptions of VAX and SJE commands used for compiling, linking or running these programs, as minor reconfigurations of the computer systems would render this information obsolete and it can be guaranteed that these commands will need modification for other VAX systems. Nonetheless, for the adsorption and desorption programs, a sample input deck has been included, as

well as a command file to cross-compile and link the programs for the AP.

1. Indexing Hexagonal Surfaces

Positions of atoms in a hexagonal unit cell are normally indexed by fractional coordinates (x,y,z), which are interpreted to mean the atom is located by position vector $\vec{\mathbf{r}} = x\mathbf{a} + y\mathbf{b} + z\mathbf{c}$, where **a**, **b** and **c** are the unit cell vectors with **c** perpendicular to both **a** and **b**, and **a** is rotated 120° from **b**. On the (001) or basal plane of a hexagonal unit cell, all surface atoms have the same z value and only two coordinates, (x,y), need be used to specify a position. This coordinate system has some disadvantages when used for computer calculations and two alternate coordinate systems were developed for use in the simulation calculations. The adsorption and desorption programs use a coordinate system with a one-to-one mapping between atoms in a rectangular portion of a hexagonal lattice to elements in a two dimensional array. In this system, rows of atoms are placed one under another, but the even numbered rows are translated a half unit cell with respect to the odd rows, as diagrammed below.

$$\{1,1\} \quad \{1,2\} \quad \{1,3\} \quad \{1,4\}$$

$$\{2,1\} \quad \{2,2\} \quad \{2,3\} \quad \{2,4\}$$

$$\{3,1\} \quad \{3,2\} \quad \{3,3\} \quad \{3,4\}$$

$$\{4,1\} \quad \{4,2\} \quad \{4,3\} \quad \{4,4\}$$

This method of indexing will be referred to as the "pseudo-rectangular" coordinate scheme. Pseudo-rectangular coordinates, $\{m,n\}$, can be converted to Cartesian coordinates by the relationships:

$$\mathrm{x} = m\mathbf{a}\sin(60^\circ),$$

$$\mathrm{y} = \begin{cases} n\mathbf{a}, & m \text{ odd}, \\ (n-1/2)\mathbf{a}, & m \text{ even}, \end{cases}$$

where **a** is the the cell length. Note that the x-axis is vertical in this diagram.

The six nearest-neighbor sites and six next-nearest-neighbor sites to site $\{m,n\}$ are given by

	m odd	m even
Nearest-Neighbors	$\{m, n \pm 1\}$	$\{m, n \pm 1\}$
	$\{m \pm 1, n\}$	$\{m \pm 1, n\}$
	$\{m \pm 1, n+1\}$	$\{m \pm 1, n-1\}$
Next-Nearest-Neighbors	$\{m \pm 2, n\}$	$\{m \pm 2, n\}$
	$\{m \pm 1, n-1\}$	$\{m \pm 1, n+1\}$
	$\{m \pm 1, n+2\}$	$\{m \pm 1, n-2\}$.

For computation of a fast Fourier transform, it is necessary to use a coordinate system with two orthogonal axes. So, the "true-rectangular" coordinate scheme was developed. This is similar to the pseudo-rectangular system, but the density of lattice points in each row is doubled and the rows are no longer offset with respect to each other, as shown below. [Note that square brackets ([ ]) are used to indicate true-rectangular coordinates and braces ({ }) are used for pseudo-rectangular coordinates.]

[1,1] [1,2] [1,3] [1,4] [1,5] [1,6] [1,7] [1,8]

[2,1] [2,2] [2,3] [2,4] [2,5] [2,6] [2,7] [2,8]

[3,1] [3,2] [3,3] [3,4] [3,5] [3,6] [3,7] [3,8]

[4,1] [4,2] [4,3] [4,4] [4,5] [4,6] [4,7] [4,8]

For example, site $\{2,1\}$ maps to site [2,1] and site $\{1,1\}$ maps to site [1,2]. In general, site $\{m,n\}$ transforms to $[i,j]$ with $i = m$ and $j = 2m$ for m odd and $j = 2m - 1$ for m even. Thus, site $[i,j]$, where $i + j$ is even, does not correspond to an atomic position in the hexagonal lattice; such sites are

assigned a scattering amplitude of zero. While this transformation doubles the number of array elements to be processed, the greater speed of the fast Fourier transform algorithm often yields an order of magnitude better performance than direct Fourier transform of the pseudo-rectangular array. True-rectangular coordinates, $|i,j|$, can be converted to Cartesian coordinates by the relationships, $x = i\mathbf{a}\sin(60°)$ and $y = j\mathbf{a}/2$, where **a** is the the cell length.

2. Programs for N_2 Adsorption and Desorption

There exist three different versions of the system of programs for simulation of adsorption and desorption of N_2 on Ru(001) which are found in three directories, [BHT.N2.AP], [BHT.N2.NEW] and [BHT.N2.COV]. The programs found in [BHT.N2.COV] are an older modeling approach using a coverage-dependant prefactor and will not be discussed. The programs in the other two directories are largely similar, where the [BHT.N2.AP] programs are array processor versions, while the [BHT.N2.NEW] programs are VAX versions. The latest version of each of the programs discussed in the following sections is listed in Appendix C. The directory name will identify target computer.

The complete adsorption/desorption system consists of four programs. In addition there are also several graphics programs, which are discussed in Section 4 of this Appendix. The four programs are:

- ADS simulates adsorption and desorption of N_2 molecules from the Ru(001) surface during the adsorption process,
- DSB simulates thermal desorption spectra from maps produced by ADS,
- RAST creates a pseudo-random rastering list input to ADS and DSB,
- NU creates an input file and matrix of prefactor values for ADS and DSB.

A full list of the parameters required as input to these programs are listed in the Table at the end of this Appendix.

2.1 Programs ADS and DSB

Programs ADS and DSB are very similar and have been written to use the same COMMON blocks and the same subroutines. The unique portion of each program is contained in file ADS.FOR for ADS and file DSB.FOR for DSB. The COMMON blocks are found in files SIMCOMA.FOR, SIMCOMB.FOR, SIMCOMC.FOR, SIMCOMD.FOR and SIMCOME.FOR and the shared subroutines are found in files MIG.FOR and COMSUB.FOR; these files are listed in Appendix C. Since the programs use very similar algorithms, the two programs

will be described together, followed by more detailed descriptions of the shared subroutines.

Both ADS and DSB start by initializing variables and by reading input parameters from input files. Both programs require input of: (1) a rastering sequence file, written by program RAST, (2) an array of prefactor values, written by program NU, and (3) a number of input parameters. Program DSB also requires a map file, which is written by ADS. The map file also includes most of the parameter values input to ADS, so the same parameters do not need to be reinput to DSB. Optionally, ADS can read in a map as a starting point for the computation. However, if no map file is specified, the program starts with an empty lattice. Parameters are input in free format and after reading each group of parameters, the program skips the following card, so that comments may be included in the input deck.

2.1.1 Program ADS

Program ADS is written in two major sections. The first is used to adsorb molecules onto the surface. Computation of adsorption begins with selection of a random position on the lattice as a starting point for a precursor molecule. Subroutine MIGRATE is then used to allow that molecule to hop from site to site until the molecule either adsorbs or desorbs into the gas phase. At this point the exposure, coverage and time counters are updated. The adsorption/migration process then is repeated. At periodic intervals, statistical information is written to files and desorption scans are made. At points during the run, as selected by input parameters, maps may be written or new parameters may be read.

The second major section of ADS computes desorption. Subroutine DESORB scans the surface and, for each occupied site, computes the probability for the molecule at that site to desorb either into the gas phase or back into the precursor state, where again it migrates until it readsorbs or desorbs. The desorption probabilities are recomputed after MPASS desorption scans by subroutine DSBPROB. Variable DSBINT defines the interval in seconds between

successive desorption scans and should be specified so the excitation rate per scan (the number of molecules that desorb into the precursor state) is small, on the order of a few percent of the adsorbed molecules, but not too small, as that unnecessarily increases the time needed to run the program. The optimum value is established by successively lowering DSBINT until smaller values do not produce any change in the results.

The pressure parameter (PRES) is used to specify one of three different adsorption modes. If PRES is input as greater than zero, the value is the N_2 partial pressure in Torr and the value used to define the average time between collisions of N_2 molecules with the portion of the surface being modeled. In this approach, the time scale of the simulations is fixed by the number of molecules that have been placed onto the surface. At time intervals set by parameter DSBINT, desorption scans are made. The other two options are available for closed system calculations using prepopulated surfaces. With these options, the interval between desorption scans defines the time scale for the simulations. If PRES is input as less than zero, desorption and adsorption proceed as before, except that adsorption cycles are terminated and a desorption scan started, each time the coverage reaches its initial value. If PRES is input as zero, no molecules are allowed to adsorb from the gas phase or desorb into the gas phase. Thus, the adsorption section is not used and, while molecules are allowed to desorb into the precursor phase, they are not allowed to desorb into the gas phase. This will be explained in more detail in the descriptions of subroutines MIGRATE and DBSPROB.

The program can be set to change some of the input parameters at a prespecified point. Following each desorption scan, if the time counter (variable TIME) is greater than variable ANNEAL (assuming ANNEAL has been input non-zero), the program reads in a new set of parameters. Also, array CDESPL can be used to trigger reading of a new set of parameters. Arrays CDESPL and TDESPL contain input coverage and time values, respectively, which determine

when maps will be written to the map file. After writing a map, the program checks the next value of CDESPL. If the value is 1.0, the program stops. If it is 2.0, the program reads in a new parameter set. If the value of TIME or EXPOS (the exposure counter, in units of monolayers) exceeds TMAX or EXPMAX, respectively, the program will stop.

Variable DMPINT specifies the exposure interval (in monolayers) for printing statistical information and for computation of the average probability of adsorption (the increase in coverage divided by the increase in exposure). Most of these calculations are performed in subroutine DUMP. Also, the program can be set to stop or read in new parameters when the average probability of adsorption drops below a given threshold; if the sum of the previous four adsorption probability values drops below value input for variable STKMIN, the program will read in new parameter values (if ANNEAL is non-zero) or will write a map file and then stop (if ANNEAL is zero). Variable PLTINT specifies the exposure interval for writing exposure and coverage values to file.

2.1.2 Program DSB

Program DSB is a simplified version of program ADS, although original versions of DSB differed greatly from ADS. Program DSB computes desorption scan using the same subroutines as in ADS, but does not compute absorption cycles. The surface temperature is incremented following each desorption scan. The surface heating rate defines the simulation time scale.

The program begins by reading a map file written by a previous run of ADS. After reading the last map on the file, flag IFLG is set to one, which signals that maps will be written out at various coverages as molecules are desorbed, provided variable MAPN has been input as zero. The program then calculates the energy state distribution (the number of adsorbed molecules with each number of nearest- and next-nearest-neighbor molecules) and initializes a number of variables before starting the first desorption scan.

Desorption scans are made using subroutine DESORB and desorption

probabilities are computed in subroutine DSBPROB. To increase the speed of program DSB, desorption probabilities are computed at temperature intervals specified by variable DT (usually 0.5 K), but as many as 1000 desorption scans are made over this temperature interval, so that the excitation rate is kept at a reasonable level. The number of desorption scans to be made in temperature increment DT is stored in variable NPASS, which is computed so that the predicted excitation rate will does not exceed input parameter ATMAX. Prior to each desorption scan, a small correction term for the temperature change is applied to the desorption probabilities. To prevent roundoff errors in the temperature counter, the temperature is reset every time desorption probabilities are recomputed.

After the temperature has been incremented by NINT*DT, (NINT is usually 4, corresponding to a temperature change of 2 K), the distribution of molecules by energy state is recomputed and is output. Array DSBENG, containing the number of molecules that desorbed in the last increment, sorted by their energy state before desorption is also output. The next value for NPASS is set so that the estimated excitation rate does not exceed ATMAX and a number of counters are reset. At this point, if there are still molecules on the surface and the maximum temperature, TMAX, has not been reached, the program continues with more desorption scans. If the end of the scan has been reached and there are more maps to read, the program continues by reading the next map, otherwise the program stops.

2.1.3 Subroutine MIGRATE

Subroutine MIGRATE allows a single precursor molecule at a given lattice site to migrate until it either adsorbs and becomes chemisorbed or desorbs into the gas phase. Variables MX and NX are set to reflect the true distance the molecule has traveled from its original position, even if the molecule hops over an edge of the lattice, (cyclic boundary conditions are enforced). For each site the molecule hops to, starting with its initial site, the subroutine first calculates

the site energy for the current site, ϵ_0, and the six nearest-neighbor sites ϵ_j using

$$\epsilon_j = \begin{cases} n_r E_r - n_a E_a, & \text{Site } j \text{ empty,} \\ E_n, & \text{Site } j \text{ previously filled,} \end{cases}$$

where n_a is the number of attractive interactions (the number of filled next-nearest-neighbor sites) and n_r is the number of repulsive interactions (the number of filled nearest-neighbor sites). Energies E_a, E_r and E_n are input as variables EA, ER and EN, respectively. The relative probabilities for adsorption, P_a, desorption, P_d and migration from the current site to the jth site, P_m^j are then computed from:

$$P_a = \begin{cases} \chi \exp\left[\dfrac{-E_d + E_s}{kT}\right], & \text{current site is empty,} \\ 0, & \text{current site is filled;} \end{cases}$$

$$P_d = \begin{cases} \chi \exp\left[\dfrac{-E_d - \epsilon_0}{kT}\right], & \text{PRES} \neq 0, \\ 0 & \text{PRES} = 0; \end{cases}$$

$$P_m^j = \begin{cases} \exp\left[\dfrac{-E_m + \Delta\epsilon_j + \Delta\epsilon_j^2/(16E_m)}{kT}\right], & -4E_m < \Delta\epsilon_j < 4E_m, \\ \exp\left[\dfrac{-\Delta\epsilon_j}{kT}\right], & \Delta\epsilon_j \geq 4E_m, \\ 1, & -4E_m \geq \Delta\epsilon_j; \end{cases}$$

where $\Delta\epsilon_j = \epsilon_j - \epsilon_0$ and E_d, E_m and χ are input as ED, EM and CHI, respectively. The adsorption barrier, E_s, is calculated from $E_s = 77k\ln(1/S_0 - 1)$, where S_0 (input as variable S0) is the initial (zero coverage) probability of adsorption at 77 K. Where possible, probabilities are computed once and stored in COMMON blocks, to increase program speed.

After computing the eight probabilities, a normalization constant, PT, is determined such that $\text{PT} = P_d + P_a + \sum_{j=1}^{6} P_m^j$ and PT is multiplied by a random number, **r**, between 0 and 1. If $\mathbf{r}\text{PT} \leq P_d$, the molecule desorbs and the subroutine returns. If $P_d < \mathbf{r}\text{PT} \leq P_d + P_a$, the element in array HEX corresponding to the current site is set as non-zero, indicating a molecule has

adsorbed at that site. If $P_d + P_a < \mathrm{rPT} \leq P_d + P_a + \sum_{j=1}^{k} P_m^j$, the molecule hops to nearest-neighbor site k and the migration computations are restarted from the beginning, using site k as the current location.

2.1.4 Subroutine DSBPROB

Subroutine DSBPROB computes two arrays of probabilities: P_c, the total probability for a chemisorbed molecule to desorb from the surface either into the gas phase directly or into the precursor state; P_p, the probability for a desorbing molecule to return to the precursor state rather than desorbing directly into into the gas phase. Three different models are available for computing these two probabilities. If PREFLG is input as zero, all desorption is direct, and no molecules desorb via the precursor state. If PRES has been set to zero or PREFLG is input as less than zero, all desorbed molecules are placed into the precursor state. If PREFLG is input as greater than zero, P_p is a function of the site energy, ϵ_0, but P_c is site independant.

$$P_c = \begin{cases} \nu_{n_r,n_a} \Delta t \exp\left[\dfrac{-E_0 - \epsilon_0}{kT}\right], & \text{PREFLG} = 0, \\ \nu_{n_r,n_a} \Delta t \exp\left[\dfrac{-E_s + E_0}{kT}\right], & \text{PREFLG} \neq 0. \end{cases}$$

$$P_p = \begin{cases} 1 - \dfrac{1}{2}\exp\left[\dfrac{E_s + \epsilon_0}{kT}\right], & \text{PREFLG} > 0 \text{ and } E_s + \epsilon_0 < 0, \\ 0, & \text{PREFLG} > 0 \text{ and } E_s + \epsilon_0 \geq 0, \\ 0, & \text{PREFLG} = 0, \\ 1, & \text{PREFLG} < 0 \text{ or PRES} = 0, \end{cases}$$

where ν_{n_r,n_a} is the prefactor for the current site, which is determined by the number of nearest- and next-nearest-neighbors at that site (see the documentation for program NU, Section 2.2), Δt is the time between each desorption scan (in seconds), and E_0 is the chemisorption well depth. The three different options were included to determine the simulation sensitivity to the desorption model. Most computations are performed with the most reasonable model, that with PREFLG equal to zero.

2.1.5 Subroutine DESORB

Subroutine DESORB scans the surface, allowing molecules either to remain adsorbed at their current site, to desorb directly into the gas phase, or to desorb into the precursor state, where they hop from site to site until they either readsorb or desorb. The subroutine scans each site in a predetermined random order to minimize correlation between sequential desorption events that might occur if scans were done on a row-by-row basis. The same random sequence of sites is used for all scans in a given run. The random sequence is read from a file prepared using program RAST.

Desorption scans are made by selecting each occupied site in turn and determining the value of P_c for that site. A random number between zero and one is computed and then compared to the value of P_c. If the random number is less than or equal to P_c, a second random number is compared to P_p to determine if the molecule will desorb directly or into the precursor state. If the molecule does desorb into the precursor, subroutine MIGRATE is used. If the molecule desorbs (either directly or via the precursor), the element in array DSBENG corresponding to the site energy of the molecule when it was last adsorbed to the surface is incremented.

2.1.6 COMSUB Subroutines

There are six short utility subroutines in file COMSUB.FOR. Subroutine CYCLE is used to imposes cyclic boundary conditions, but it also updates variables MX and NX to reflect the position on an infinite lattice, so that migration distances can be computed. Function DIST is used to compute the actual distance between two sites. Functions NEAR and NEXT compute the number of filled nearest- and next-nearest-neighbor sites, respectively. Functions EREDHD and TREDHD use the method of Newtonian approximations to solve the Redhead equation $\nu \exp\left[-E/RT\right] = -\beta E/RT^2$ for E and T, respectively **(1)**. Function EREDHD is used to compute E_0 from the input ν values, and parameters that fix the low coverage temperature thermal desorption

peak, LCTP and NAAVG. Thus if the ν values are changed, a commensurate change will automatically be applied to E_0 and the thermal desorption peak temperature will remain unchanged. Function TREDHD is not currently used.

2.2 Programs RAST and NU

Two programs, RAST and NU, are used to prepare input files for DSB and ADS. Program RAST creates a rastering file which contains a list of all lattice sites, but listed in a random order. The only input this program requires is the size of the lattice and a starting point for the VAX/VMS random number generator. This number may be any value allowed for a INTEGER*4 variable, but it is recommended by DEC that this number be input as large and odd. Program RAST assigns a random number to each site and then uses an IMSL subroutine, VSRTP, to sort the array of random numbers by magnitude. The sorting sequence determines the order of the randomized rastering list. The lattice size used for ADS and DSB is determined by the lattice size read from the RAST file.

Program NU was originally separated from ADS and DSB to allow different models to be used for determining the prefactor. Changes could then be made to program NU, without having to modify and recompile the much larger ADS and DSB programs. Program NU reads the same input parameter file as ADS, as well as four additional parameters, IC, NU0, A and B, which determine the equation to be used for computing the prefactors. The equations used when IC is 1 or 3 have been demonstrated to be ineffective for N_2 simulations. Thus, the program should always be used with IC set to 2, which calculates the NU array using

$$\nu_{n_a,n_r} = \mathrm{NU0} \exp\left[n_a \mathrm{A} + n_r \mathrm{B}\right].$$

2.3 Sample Command Procedures

As an example of how the simulation programs are run, a set of sample commands with input to run RAST, NU, ADS and DSB has been included in

Appendix C. This is an input deck for a fairly complicated run. The procedure first assigns a DCL symbol, which defines the suffix to be used for file names of the output and intermediate files. The procedure then copies the input parameters to a file, where they are later read by programs NU and ADS. (Note the use of comment lines between input lines.) The programs RAST and NU are run. Processing is then started on the AP by using the SJE command and commands are given to the AP to start running program ADS. The ATTACH/WAIT command causes SJE to wait until the AP is available, if it is currently in use, and the SET/LIMIT=16000 sets a CPU time limit of 16,000 seconds (approximately four hours) for the running of *each* program. The next step is to copy the input files for program ADS from the VAX to the AP and then program ADS is executed. In this run, desorption is done at two different temperatures and different (isotopic) labels are used for the molecules adsorbed at each temperature. After ADS finishes, output files from ADS are copied to the VAX and then program DSB is run. After the final results are copied out of the AP, all the output files are renamed to share the common suffix. This suffix is then passed to command procedure PLT which plots the results.

Also included in Appendix C is a sample command file showing how programs ADS and DSB should be cross-complied and linked on the VAX to run on the AP. Note that the OPT= flag specifies to what level the compiler will attempt to optimize the program when compiling. Higher OPT levels may yield more efficient code, but may also introduce errors. The programs have been carefully tested at the current levels but higher levels have not been attempted. Following linking, the image file (the linked program) is then copied over to the AP and stored on the AP using SJE.

3. Programs for Fourier Transform Computations

Two programs perform most of the calculations used for computing Fourier transforms of surfaces. One is program FFT, which computes a fast Fourier transform from a map output by ADS or DSB and fits a Voigtian line shape to a peak in the Fourier transform intensities. The second program is EQFIT, which optimizes parameters for an island-growth expression to give the best fit to the full-widths at half-maximum Voigt function as computed by program FFT.

3.1 Program FFT

Program FFT reads maps from up to ten different map files and averages the FFT intensities computed from each map to improve the the signal-to-noise in the transform. If requested, FFT will also plot the Fourier transform intensity results and/or plot graphs of the radially averaged profile of the intensities and the fitted line shape.

The program first reads input values for the flags which determine what maps will be used and whether results will be plotted. Subroutine OPENIN reads a file name and reads the header on each file. Subroutine READIN reads in a map from each file. The dimensions of the lattice of each map should be divisible by two and all maps must be the same lattice size. The program then prepares to plot the intensity, if requested, by defining a set of pixels of different shades for use on the laser plotter.

Subroutine DIFFRACT is used to compute the Fourier transform intensity. The subroutine first expands the pseudo-rectangular array from the map file into a true-rectangular array, SCAT, using the coordinate transformations discussed in Section 1. Array elements corresponding to empty sites in the hexagonal lattice are assigned a scattering amplitude equal to variable RSCAT (usually 0); filled sites are assigned scattering amplitude equal to the sum of variables RSCAT and NSCAT (usually 1). The "extra" array elements, those not corresponding to a site in the hexagonal array, are always set to zero.

Subroutine DIFFRACT computes a two-dimensional fast Fourier transform by computing a one dimensional real-to-complex transform along the columns of SCAT, placing the results into a complex array, DPAT. Each row is then removed from array DPAT and is transformed using a one dimensional complex-to-complex fast Fourier to another complex vector, which is reinserted into the array DPAT. The fast Fourier transform routines used are both from the IMSL library, FFTRC for real-to-complex transforms and FFTCC for complex-to-complex transforms. The final section of DIFFRACT computes the magnitude (intensity) of each complex value in the DPAT matrix. Intensity values are summed into array INTEN and are later normalized to yield the intensity average values.

The intensity map is plotted by choosing one of twenty rectangular pixels for each array element, where the grey level of the pixel is chosen to match the scaled intensity. Intensity map plotting is done using the QUIC package (see Section 4.1). Function ARR is used to map any point in reciprocal space into a calculated intensity array element. Array element (M_i, N_i) are related to the reciprocal cell position vector $h\mathbf{a}^* + k\mathbf{b}^*$ by the equations

$$h = \frac{M_i}{M} - \frac{N_i}{N} \quad \text{and} \quad k = \frac{N_i}{N},$$

where the original dimensions of the map array are $(M, N/2)$.

The program calculates a profile for the $(\frac{2}{3}, \frac{1}{3})$ diffraction feature (also referred to as the $\sqrt{3}$ beam). Subroutine LSTFIT uses a least-squares refinement procedure to determine the best values for the parameters η, κ and Γ to fit the two dimensional pseudo-Voigt equation

$$I(M_i, N_i) = \frac{2\kappa}{\Gamma}\left\{\frac{\eta}{1+\left(\frac{2\Delta r}{\Gamma}\right)^2} + (1-\eta)\sqrt{\frac{\ln 2}{\pi}}\exp\left[-\ln 2\left(\frac{2\Delta r}{\Gamma}\right)^2\right]\right\},$$

where $\Delta r^2 = \left(\frac{M_i - M_c}{M}\right)^2 + 3\left(\frac{N_i - N_c}{N}\right)^2$, $I(M_i, N_i)$ is the Fourier transform intensity of array element (M_i, N_i) and (M_c, N_c) corresponds to the beam center.

The full-width at half-maximum of the beam profile is Γ and the integrated beam intensity is $2\pi\kappa$. The algorithm used in subroutine LSTFIT is discussed in more detail in Section 3.2, below. Program FFT uses subroutine TFIT to plot out the actual intensity points, radially averaged points and the fitted Voigtian function.

3.2 Program EQFIT

Program EQFIT uses a least-squares refinement procedure to determine the best values for parameters. The method of least-squares determines the best fit for a function $Y(x_i, p_1, p_2, \ldots, p_m)$ to a set of n data points x_i, y_i by minimizing the function

$$E = \sum_{i=1}^{n} w_i \left[Y(x_i, p_1, p_2, \ldots, p_m) - y_i\right]^2,$$

where $p_1, p_2, \ldots, p_m$ are the m parameters to be fit and w_i is the weight, usually $1/\sigma_i$, where σ_i is the estimated error in y_i **(2)**. The best fit then will be given when $\partial E/\partial P_j = 0$ for all j. Direct solution of this equation is not usually possible, but if function Y is approximated by a Taylor expansion of Y about values $a_1, a_2, \ldots, a_m$ for $p_1, p_2, \ldots, p_m$, where the non-linear terms [those of higher power than $(a_j - p_j)$] are neglected, then the problem can be solved using

$$Y \simeq Y' = Y(x_i, a_1, a_2, \ldots, a_m) + \sum_{k=1}^{m} \frac{\partial Y(x_i, a_1, a_2, \ldots, a_m)}{p_k} \Delta p_k,$$

where $\Delta p_k = p_k - a_k$. The m coupled $\partial E/\partial p_j = 0$ equations may then be written as

$$\begin{aligned} \frac{\partial E}{\partial p_j} &= 0 \\ &= \frac{\partial}{\partial p_j} \sum_{i=1}^{n} w_i \left(Y' - y_i\right)^2, \\ &= \sum_{i=1}^{n} w_i \left(Y' - y_i\right) \frac{\partial Y'}{\partial p_j}. \end{aligned}$$

Substitution for Y' and rearrangement yields

$$\sum_{i=1}^{n} w_i \left[y_i - Y(x_i, a_1, a_2, \ldots, a_m)\right] \frac{\partial Y(x_i, a_1, a_2, \ldots, a_m)}{p_j}$$

$$= \sum_{i=1}^{n} w_i \frac{\partial Y(x_i, a_1, a_2, \ldots, a_m)}{p_j} \sum_{k=1}^{m} \frac{\partial Y(x_i, a_1, a_2, \ldots, a_m)}{p_k} \Delta p_k.$$

Note that $\partial Y'/\partial p_j = \partial Y(x_i, a_1, a_2, \ldots, a_m)/p_j$. By defining two m element column vectors **B** and **P** and an m by m diagonally-symmetric matrix **A** such that

$$\mathbf{B}_j = \sum_{i=1}^{n} w_i \left[y_i - Y(x_i, a_1, a_2, \ldots, a_m)\right] \frac{\partial Y(x_i, a_1, a_2, \ldots, a_m)}{p_j},$$

$$\mathbf{A}_{j,k} = \sum_{i=1}^{n} w_i \frac{\partial Y(x_i, a_1, a_2, \ldots, a_m)}{p_j} \frac{\partial Y(x_i, a_1, a_2, \ldots, a_m)}{p_k}$$

and $\mathbf{P}_j = \Delta p_j = p_j - a_j$, the previous m coupled equations can be combined into one equation

$$\mathbf{B} = \mathbf{AP} \quad \text{or} \quad \mathbf{A}^{-1}\mathbf{B} = \mathbf{P}.$$

Thus, with a given set of starting values, $a_1, a_2, \ldots, a_m$, for the parameters $p_1, p_2, \ldots, p_m$, the correction terms to improve the fit of function $Y(x_i, p_1, p_2, \ldots, p_m)$ will be **P**, which can be computed by numerically evaluating the **B** and **A** elements and then inverting the m by m matrix. This procedure can be run iteratively until the correction terms become negligible.

Program EQFIT reads in the data to be fit, computes the starting values for the parameters, uses a least-squares refinement to improve the fit of the parameters and then plots the fitted equation and the data. Programs EQFIT and FFT both use subroutine LSTFIT to find the best fit to the equation coded in function DIRV. The version of LSTFIT in EQFIT is a better commented version of the routine, but the routine used in FFT is more efficient.

For equations that are difficult to fit – equations where the parameters are highly correlated – LSTFIT has a tendency to compute correction terms that are too large for the first few cycles, causing the refinement to diverge. For this reason a muting factor, SP, is applied. In the first cycle, correction terms are multiplied by this number (usually less than 0.5) and in subsequent cycles the muting factor is automatically raised to 1.0 before the last allowed

cycle, which is determined by variable NCYC. If the refinement cycles fail to show an improvement, as noted by negligible change in the goodness of fit, $\sqrt{\sum_{i=1,n} w_i \left[y_i - Y(x_i, a_1, a_2, \ldots, a_m)\right]^2/(n-m)}$, the refinement terminates.

Subroutine DIRV evaluates the function to be fit and the derivatives of the function with respect to all parameters that will be refined. The parameters are passed in array PAR and the independent variable in X. The array PI selects which derivative will be computed, *i.e.*, 0 to compute the function itself and 2 to compute the derivative with respect to PAR(2). While both LSTFIT and DIRV are dimensioned to fit a four-parameter equation, this number could be increased, if needed, with little effort.

4. Graphics Programs

Five graphics packages have been used in this thesis. The standard packages for the Versatec, Nicolet (Zeta) and Talaris plotters, VERSAPLOT, FPS and QMSPLOT, respectively, are documented both through manuals supplied by the vendors and through the XHMEIA on-line help facility (by typing HELP @USER GRAPHICS). Another package used, GRPPKG/PGPLOT, was written by Tim Pearson of the Caltech Astronomy Department. This fine package allows plotting of graphics on a number of devices including several types of computer terminals and the versatec plotter. Further information about the GRPPKG/PGPLOT package may be obtained through the XHMEIA on-line help facility, which will also give instructions for printing the manuals for the package, which are also stored on-line. A small graphics package, QUIC, was written by the author specifically for use in this thesis. This package, which will be described later in more detail, plot maps in high resolution on the laser plotter.

The graphics programs written for this thesis fall into three classes: programs for plotting numerical results from ADS and DSB (*e.g.*, probability of adsorption, thermal desorption intensity), programs for graphical display of maps, and three dimensional plotting programs for diagrams showing the number of molecules in selected energy states versus temperature and versus energy.

4.1 The QUIC package

The QUIC package was written for the Talaris laser plotter after it was discovered that the QMSPLOT package produced complex plots very slowly and inefficiently, because the QMSPLOT package fails to utilize most of the plotter's more advanced features. The QUIC package prepares a set of commands in the plotter's native command language, also called QUIC, which can then be sent directly to the plotter. Maps plotted using the specialized MAP program and the QUIC package plot approximately a factor of one hundred faster than a simpler program written to use QMSPLOT. The code for the package including

documentation and sample routines are listed in Appendix C.

4.2 Program MAP

Program MAP uses the QUIC package to create two fonts (collections of symbols): one font contains only two symbols, a filled circle and an open circle; the other font contains four symbols, one is blank and the other three are lines in three different directions. The program then reads in a map file and assembles a character string for each row in the map, using the letter A for an empty site and B for a filled site. The string is then written to disk where it can the be sent to the laser plotter. The laser plotter internally translates these characters to the previously defined circle symbols and constructs a diagram showing the empty sites as open circles and the filled sites as open circles with a filled closed circle inside.

The phase of each adsorbed atom, with respect to the three phases of $(\sqrt{3} \times \sqrt{3})$ domains, is indicated by the direction of the line drawn through the site. Three additional plots are superimposed on the plot showing filled and empty sites. In each of these plots, lines are drawn through all of the filled sites in each of the three phases.

4.3 Programs for State Analysis

It is informative to analyze, as a function of temperature, the number of molecules adsorbed in a given energy state and the number of molecules that desorb from a given energy state. The desorption program, DSB, writes two files containing information about the states of molecules. The FOR010 file contains, for each temperature, an array containing the numbers of molecules in all 49 adsorption states. The FOR015 file contains an array with the number of molecules that have desorbed from each of the 49 energy states in the previous temperature increment. A set of programs, 3A, 3D, 3DV and 3DR have been written to plot three dimensional representations of the number of molecules adsorbed or desorbed from a series of states versus both temperature and energy.

The only input to programs 3A and 3D are the names of the data files

to be averaged and a list of the energy states to be plotted (read from file STATE.DAT). Programs 3A and 3D read the FOR010 and FOR015 files, respectively, and create intermediate files with the numbers of adsorbed and desorbed molecules, respectively, for the subset of the 49 energy states which will be plotted.

The intermediate files are then plotted by program 3DV, which plots three dimensional diagrams on Versatec plotter using the VERSAPLOT package. The diagrams can also be plotted on a terminal using a similar program, 3DR which uses the GRPPKG/PGPLOT package. The only input to programs 3DR and 3DV is the name of the intermediate file, a flag to determine whether to use a file from program 3A or 3D, and two scaling parameters, THETA and R.

Programs 3DR and 3DV plot temperature along the vertical axis, the number of molecules along the horizontal axis and the energy of the state projected out of the page. The projected length and angle of the energy axis, with respect to the vertical and horizontal axes, is determined by the values of R and THETA. States are plotted in order of increasing energy, which is equivalent to plotting from front to back. For each energy state, a plot of the number of adsorbed (or desorbed) molecules versus temperature is projected onto the plane of the paper. The program maintains an array with the largest y value that has already been plotted at a given x value, in the plane of the paper. (The maximum y values are determined by interpolating the projected y values to each x value.) Each time the program plots a line, it checks to see if any section of the line is obscured "behind" a previously plotted line and if so, the section is not plotted or is plotted as dashed. This very simple algorithm is adequate to solve the "hidden line" problem for these plots.

4.4 Program SISO

Program SISO plots the probability of adsorption results from ADS and the thermal desorption intensities from DSB. The program computes smoothed derivatives in subroutine DERIV using the method of Savitzky and Golay **(3)**.

It can average results from up to ten different runs to reduce random noise. It can also be used to plot the desorption spectra of two differently labeled sets of molecules, if the "isotope" labeling option was used in ADS. The input to the program consists of a scaling factor, SCLFCT, which multiplies the thermal desorption spectra, the labeling selection flag, ISO, which selects the "isotope" type. A selection integer, IOMIT, is input for each thermal desorption spectrum. If IOMIT is one for any spectrum, that spectrum is not plotted.

Table. Input parameters for programs RAST, NU, ADS and DSB. Parameters are listed in the order they are normally input.

	Program RAST
SIZE^I	The lattice size to be used in RAST, ADS and DSB
IR^I	The starting point for the random number generator
	Programs ADS and NU
TITLE^C(72)	A title for the set of runs; the title will be stored on all files read or written by ADS, NU and DSB
ED^R	The precursor well depth or desorption energy, E_d
EM^R	The energy barrier to migration, E_m
EA^R	The attractive (next-nearest-neighbor) interaction energy, E_a
ER^R	The repulsive (nearest-neighbor) interaction energy, E_r
EN^R	The destabilization energy for filled sites, E_n
CHI^R	The ratio of prefactors for desorption and migration, χ
S0^R	The initial probability of adsorption at 77 K, S_0
TS^R	The surface temperature
EXPMAX^R	Maximum allowed exposure (in monolayer) before program ADS stops
TMAX^R	Maximum allowed time (in seconds) before program ADS stops
PRES^R	Pressure (in Torr)
DSBINT^R	Time interval between desorption scans (in seconds)
PLTINT^R	Exposure interval (in monolayer) between points written to the FOR008 file.
DMPINT^R	Exposure interval (in monolayer) between calls of subroutine DUMP
LCTP^R	Temperature assignment (in K) for the low coverage TDS peak; used to compute E_0
NAAVG^R	Number of attractive interactions assigned to the low coverage TDS peak; used to compute E_0; usually set to 1.5
BETA^R	TDS heating rate (in K/s)
DT^R	Temperature interval (in K) for program DSB

ANNEAL^R	Flag for parameter changes; when the time counter equals ANNEAL (for ANNEAL $\leq$ 0) new values will be read for TS, ISO, PRES, DSBINT, PLTINT, DMPINT, ANNEAL, STKMIN, NPASS
STKMIN^R	Minimum probability of adsorption, if the actual value is less than this threshold and ANNEAL $\leq$ 0, program ADS stops; if ANNEAL $>$ 0, new parameters are read (see ANNEAL)
PREFLG^I	Flag indicating method for desorption; PREFLG = 0 – normal; PREFLG $<$ 0 – all desorption is via precursor; PREFLG $>$ 0 – all desorption is direct.
NPASS^I	Number of desorption scans between each desorption probability calculation
CDESPL^R(20)	Array of coverages (in monolayers) where maps will be stored; if after storing a map, the next value is 1.0, the program stops; if it is 2.0, new parameters are read (see ANNEAL)
TDESPL^R(20)	Array of times (in seconds) where maps will be stored

Program NU

IC^I	Indicates the equation to be used for computing ν values, should always be input as 1
NU0^R	Desorption prefactor for an isolated molecule
A^R	Increase ν by exp(n_aA) for n_a attractive interactions
B^R	Increase ν by exp(n_rA) for n_r repulsive interactions

Program ADS

IR^I	The starting point for the random number generator

Program DSB

TMIN^I	Starting point for the TD scan (in K)
TMAX^I	Ending point for the TD scan (in K)
TINT^I	Specifies how often desorption statistics should be stored on file; information will be written following TINT desorption calculations (corresponding to DT*TINT degrees Kelvin)
CMIN^R	Minimum coverage (in monolayer) for TDS calculations; maps with lower coverages will be skipped.
IR^I	The starting point for the random number generator
MAPN^I	Flag for writing map files during desorption: 0 prevents writing of maps

PREFLG^I	Flag indicating the model for desorption; PREFLG = 0 normal; PREFLG < 0 – all desorption is via precursor; PREFLG > 0 – all desorption is direct.
ATMAX^R	Maximum number of precursor excitations allowed per desorption scan; program DSB will attempt to set NPASS so that this value is not exceeded
CDESPL^R(20)	Array of coverages (in monolayers) for which maps should be written.

Superscripts indicate the FORTRAN variable type. The types integer, real and character are indicated by superscripts *I*, *R* and *C*, respectively. A number in parenthesis following the variable name indicates the parameter has been dimensioned to that number of elements, or in the case of character variables, that number of characters.

References

[1] P. A. Redhead, Vacuum **12**, 203 (1962).

[2] G. H. Stout and L. H. Jenson, *X-ray Structure Determination,* Macmillan Publishing Co., Inc., New York, 1968.

[3] A. Savitzky and M. J. E. Golay, Anal. Chem **36**, 1627 (1964); J. Steinier, Y. Termonia, J. Deltour, Anal. Chem **44**, 1906 (1972).

Appendix C:

COMPUTER PROGRAM LISTINGS

1. Programs for N_2 Adsorption and Desorption
   - 1.1 Programs ADS and DSB
   - 1.2 Subroutines MIGRATE, DSBPROB and DESORB, COMSUB subroutines and COMMON blocks
   - 1.3 Programs RAST and NU
   - 1.4 Sample Command Procedures
2. Programs for FFT Computations
   - 2.1 Program FFT
   - 2.2 Subroutine LSTFIT
3. Graphics Programs
   - 3.1 The QUIC package
   - 3.2 Program MAP
   - 3.3 Programs for State Analysis: 3A, 3D, 3DR and 3DV
   - 3.4 Program SISO
   - 3.5 Program FFTMAP

Programs for N_2 Adsorption and Desorption

1.1 Programs ADS and DSB

[BHT.N2.AP]ADS.FOR

```
C*************************************************************************
C*************************************************************************
C****                                                                 *****
C****   PROGRAM TO MODEL N   ADSORPTION ON Ru(0001)                   *****
C****                     2                                           *****
C****                                                                 *****
C****   Using true Monte-Carlo type model                             *****
C****                                                                 *****
C****   BRIAN TOBY              12/83                                 *****
C****                                                                 *****
C****   ADAPTED FOR ARRAY PROCESSOR (BHT 6/84)                        *****
C****   Change isotope label during annealing (BHT 8/85)              *****
C****   Read in new parameters when time = ANNEAL (BHT 9/85)          *****
C****   Several changes:  (BHT 10/85)                                 *****
C****      CDESPL = 2.0 ==> treat as ANNEAL command                   *****
C****      PRES   = 0.0 ==> reset DT1MOL, branch around adsorption,   *****
C****           and disable desorption from precursor (set Pd to 0)   *****
C****      Print running sum of # of molecules desorbed after         *****
C****           adsorption, print info before probability computation *****
C****   Changed to allow "closed system" calculations: (BHT 5/86)     *****
C****      PRES   < 0.0 ==> adsorption only occurs until the coverage *****
C****           reaches the initial coverage.                         *****
C****      Map files may now be input to the program on file FOR022   *****
C****                                                                 *****
C****   Environment Dependant Prefactor Model                         *****
C****                                                                 *****
C*************************************************************************
C*************************************************************************
C**
C**   HEXAGONAL LATTICE IS STORED BY COORDINATES (m,n) WHICH ARE
C**   RELATED TO CARTESIAN COORDINATES (x,y) BY
C**
C**           x = m * A * sin(60)
C**           y = n * A                  (m ODD)
C**           y = n * A   -  A / 2       (m EVEN)
C**
C**    WHERE A IS THE LATTICE SPACING
C**
      BLOCK DATA
c      INCLUDE 'SIMCONA.FOR/list'       ! FOR VAX
$INSERT SIMCONA.FOR
c      INCLUDE 'SIMCONB.FOR/list'       ! FOR VAX
$INSERT SIMCONB.FOR
c      INCLUDE 'SIMCONC.FOR/list'       ! FOR VAX
$INSERT SIMCONC.FOR
c      INCLUDE 'SIMCOND.FOR/list'       ! FOR VAX
$INSERT SIMCOND.FOR
c      INCLUDE 'SIMCONE.FOR/list'       ! FOR VAX
$INSERT SIMCONE.FOR
C**
      DATA NEARM/-1,-1,0,0,1,1/
      DATA NEARN/0,1,-1,1,0,1,-1,0,-1,1,-1,0/
C** NEARM(i),NEARN(i,j) DESCRIBE THE NEAREST NEIGHBOR SITES RELATIVE TO
C**  THE CENTER SITE.  j IS 1 FOR m ODD;  2 FOR m EVEN.
C**
      DATA NEXTM/-2,-1,-1,1,1,2/
      DATA NEXTN/0,-1,2,-1,2,0,0,-2,1,-2,1,0/
C** NEXTM(i),NEXTN(i,j) DESCRIBE THE NEXT NEAREST NEIGHBOR SITES RELATIVE
C**  TO THE CENTER SITE.  j IS 1 FOR m ODD;  2 FOR m EVEN.
C**
      DATA HEX/10000*0/,SIZE/100/
C** SIZE IS THE DIMENSION OF THE [SQUARE] LATTICE
```

```
      DATA IR/256/
C** IR IS THE STARTING POINT FOR THE RANDOM NUMBER GENERATOR
      END
C!**
C*******************************************************************************
C*******************************************************************************
C**
c       INCLUDE 'SIMCOMA.FOR'     ! FOR VAX
$INSERT SIMCOMA.FOR
c       INCLUDE 'SIMCOMB.FOR'     ! FOR VAX
$INSERT SIMCOMB.FOR
c       INCLUDE 'SIMCOMC.FOR'     ! FOR VAX
$INSERT SIMCOMC.FOR
c       INCLUDE 'SIMCOMD.FOR'     ! FOR VAX
$INSERT SIMCOMD.FOR
c       INCLUDE 'SIMCOME.FOR'     ! FOR VAX
$INSERT SIMCOME.FOR
C**
C** LIST is the (decoded) random order rastering sequence
      INTEGER*2 LIST(2,10000)
      REAL E,T,NAAVG,LCTP
      REAL NRN,DSBINT
      CHARACTER*72 LINE,TITLE
      REAL CDESPL(20),time,dtim,tmax
      integer TDESPL(20)
      INTEGER DSBENG(49,2)
      real v1(49),v2(49)
      DATA DCDE0,DCDE1,DCDE2,DCDE3/4*1.0/
      DATA CDESPL/20*1.0/,TDESPL/20*-1/
      DATA time/0.0/,dtim/0.0/
C**AP TO VAX!*** COMMENT OUT FOLLOWING LINES
C**  Open output files
C UNIT=7 ==> :OUTPUT (by default) override to save VAX CPU:
      OPEN(UNIT=7, FILE=':S(XHMEIA):BHTOUT.ADS, FMT=F',
     1 ACCESS = 'SEQUENTIAL', RECL=132,  STATUS='unknown')
      OPEN(UNIT=8,FILE='FOR008.DAT, FMT=F', STATUS='unknown')
      OPEN(UNIT=9,FILE='FOR009.DAT, FMT=F', STATUS='unknown')
C       STATUS_CODE = SYS$GETTIME (CTIM, WTIM)
C       WRITE(7,108) CTIM,CTIM*0.0036,WTIM,WTIM*0.0036
  108 FORMAT(' CPU TIME =',F10.2,' ($',F7.2,')  REAL TIME = ',
     1 F10.2,' ($',F7.2,')')
C**
      IDESPL = 1
      JDESPL = 1
      N1 = 1
      N2 = 0
      IPLT = 1
      IDMP = 1
C** Exposure/coverage intervals for desorption, plot points, and interactions
c       DSBINT = 0.05
c       PLTINT = 0.02
c       DMPINT = 0.02
C**
      EXPMAX = 4.0
C** EXPMAX IS THE MAXIMUM EXPOSURE (IN MONOLAYER)
C**
      NEXP = 0
C** NEXP IS THE NUMBER OF MOLECULES "EXPOSED" TO THE SURFACE
C**
      NADS = 0
      MADS = 0
      NADSP = 0
      NADS1 = 1000
      NADStr = 0
C** NADS IS THE NUMBER OF MOLECULES "ADSORBED" ON THE SURFACE
C**
      NDES = 0
      DHOP = 0
      AHOP = 0
      ADIS = 0.0
```

```
      ADIS2 = 0.0
      DDIS = 0.0
      DDIS2 = 0.0
      SIZE = 40
C**
C*** PARAMETER DEFINITIONS:
C**
      ED = 1.6
C Desorption energy from clean surface (Kcal/mol)
      ER = 0.320
C Energy of a repulsive interaction (Kcal/mol)
      EA = 0.160
C Energy of an attractive interaction (Kcal/mol)
      EN = 0.8
C Energy difference for precursor on empty site vs. filled site (Kcal/mol)
      CURV = 0.1639041
C Curvature of well (in Kcal/A**2/mol)     CURV = Emig(0)*4/R**2
      CHI = 1.E3
C Controls number of hops
      RA = 2.7058
C Lattice spacing (in A)
      R = 1.9872
      K = 1.9872E-3
C UNITS: Kcal or cal/(K-mol)
      TS =  80.
C Temperature of surface (K)
      SO = .25
C initial sticking coefficient
      DT = 0.5
C UNITS: K / iteration
      PRES = 1.E-8
C PRESSURE: units of Torr
      NAAVG = 2.
C LOW COVERAGE PEAK TEMPERATURE
      LCTP = 130.
C ANNEAL: If non-zero change parameters at time = ANNEAL
      ANNEAL = 0.0
C NPASS: # of desorption scans/probability computation
      NPASS = 1
C
C*******************************************************************************
C**  Open/read rastering sequence array
C**AP TO VAX!*** COMMENT OUT FOLLOWING LINE
      OPEN(UNIT=20,FILE='RAST.DAT, FMT=F', STATUS='OLD')
      READ (20,202) SIZE,N2
  202 FORMAT(1X,2I6)
      siz2 = SIZE**2
      IF (N2 .NE. SIZ2) STOP '***WRONG RASTER LIST DIMENSION***'
      READ (20,212) (LIST(1,I),LIST(2,I),I=1,N2)
  212 FORMAT(1X,20I5)
      CLOSE(20)
C*******************************************************************************
C**  Open/read prefactor (NU) array
C**AP TO VAX!*** COMMENT OUT FOLLOWING LINE
      OPEN(UNIT=21,FILE='NU.DAT, FMT=F', STATUS='OLD')
      READ (21,222) (nu(i),i=1,49)
  222 FORMAT(1X,7E10.3)
      CLOSE(21)
C*******************************************************************************
C** Now open file/read in input parameters
C**AP TO VAX!*** COMMENT OUT FOLLOWING LINE
      OPEN(UNIT=4,FILE='ADS.DAT, FMT=F', STATUS='OLD')
      READ (4,9999) TITLE
      READ (4,9999) LINE
 9999 FORMAT(A72)
      READ (4,*,END=99) ED,EN,EA,ER,EN
      READ (4,9999) LINE
      READ (4,*,END=99) CHI,SO,TS
      READ (4,9999) LINE
C      READ (4,*,END=99) EXPMAX,Tmax,IR,PRES
```

```
      READ (4,*,END=99) EXPMAX,Tmax,PRES
      READ (4,9999) LINE
      READ (4,*,END=99) DSBINT,PLTINT,DMPINT
      READ (4,9999) LINE
      READ (4,*,END=99) LCTP,NAAVG,BETA,DT
      READ (4,9999,END=99) LINE
      READ (4,*,END=99) ANNEAL,STKMIN,PREFLG,NPASS
      READ (4,9999,END=99) LINE
      READ (4,*,END=99) (CDESPL(I),I=1,20)
      READ (4,9999,END=99) LINE
      READ (4,*,END=99) (TDESPL(I),I=1,20)
  99  CURV = EM *4./RA**2
      READ (5,*) IR
C** COMPUTE THE CHANGE IN TIME FOR EXPOSURE OF ONE MOLECULE
      IF (PRES .LE. 0) THEN
        DT1MOL = dsbint
      ELSE
        DT1MOL = 4.08E-6 / (siz2 * PRES)
      ENDIF
C*** PROBABILITIES ARE:
C Desorption = NRM * CHI * EXP( - (ED - EO) / KT)
C Migration  = NRM * EXP(- (EM + DE/2.) / KT)
C Sticking   = NRM * CHI * 1./(1./SO - 1.) * EXP( - ED / KT)
C (N.B. probability for sticking is site independant if site is not filled)
C    where EO = NRO*ER - NAO*EA or EO = EN (if site is filled)
C          Ei = NRI*ER - NAI*EA or Ei = EN (if Ith site is filled)
C          DE = Ei - EO
C  and NRO, NAO are # of repulsions/attractions for current site,
C      NRI, NAI are # of rep/att for migration to the Ith site (0<I<7),
C      NHOP is the number of hops the molecule has taken
C      NRM = 1./(Desorption + Migration + Sticking)
C*******************************************************************************
C***
      WRITE(7,29) TITLE,SIZE,SIZE,EXPMAX,EXPMAX*4.08,tmax,ED,EN,
     1 ER,EA,CURV,EM,SO,CHI,IR,TS
   29 FORMAT(' ',72('*'),/,1X,A72,/,1X,72('*'),//' LATTICE IS',I4,
     1  ' BY',I4,/,' MAXIMUM EXPOSURE: ',F6.3,' (monolayer) ',F6.2,
     a  ' (L.)',/,' MAXIMUM TIME: ',1pe10.3,' (Sec) ',/,
     b  ' DESORPTION ENERGY: ',OPF5.3,
     2 /,' DESTABILIZATION ENERGY FOR FILLED SITE:',F6.3,/,
     3 ' REPULSIVE INTERACTION ENERGY:',F6.3,/,
     4 ' ATTRACTIVE INTERACTIVE ENERGY:',F6.3,/,
     5 ' CURVATURE: ',F6.4,'    (EM: ',F7.4,')',/,
     6 ' INITIAL STICKING COEFFICIENT: ',F6.4,/,
     7 ' CHI = ',F12.5,'    SEED: ',I9,/,' TEMPERATURE:',F6.1,//)
      IF (ANNEAL .NE. 0.0) WRITE (7,*) 'EXPOSE FOR ',ANNEAL,
     1 'Sec, THEN CHANGE INPUT PARAMETERS'
      WRITE(7,228) DSBINT,NPASS,PLTINT,DMPINT,
     1 (CDESPL(I),I=1,20),(TDESPL(I),I=1,20),PRES,STKMIN/4
  228 FORMAT(/,' CALCULATE DESORPTION SCAN EVERY ',F6.2,
     a ' Sec -- RECALCULATE PROBABILITIES EVERY',I3,' SCANS',/,
     1 ' PLOT A POINT EVERY ',F6.3,' M (Exposure)',/,
     2 ' PRINT SUMMARY EVERY ',F6.3,' M (Exposure)',/,
     3 ' SAVE MAPS AT:',/,
     4 1x,5f5.2,10F6.2,5f7.2,' M (Cov)',/,
     5 1x,5I5,10i6,5i7,' S (Time)',/,
     6 ' Pressure is ',1P1E10.3,' Torr',/,
     7 ' Minimum average Sticking Coeffient =',0PF8.5,//)
      RATIO = ER / EA
      E = EREDHD(LCTP,BETA,NU(1),R,N)
      EO = E - EA * NAAVG
      WRITE(7,128) LCTP,E,NAAVG,EO,DT
  128 FORMAT(' TDS PEAK AT ',F5.0,'K (E = ',F6.3,
     2 ' Kcal) IS ASSIGNED TO ',f3.1,'*EA STATE',/,
     3 ' ISOLATED N2 MOLECULE - ENERGY IS ASSIGNED AS ',
     4  F6.3,' (Kcal)',/,' TEMPERATURE INCREMENT',F8.4,//)
C**
      WRITE (8,21) SIZE,ED,EN,EA,ER,EM,SO,CHI,TS,DSBINT,IR,TITLE,
     1 LCTP,E,EO,NAAVG,DT,BETA
```

```
      WRITE (9,21) SIZE,ED,EN,EA,ER,EM,SO,CHI,TS,DSBINT,IR,TITLE,
     1 LCTP,E,EO,NAAVG,DT,BETA
   21 FORMAT(I5,6F10.6,/,3F10.3,I12,/,A72,/,F10.1,2F10.6,F6.2,
     1 F6.4,15x,F6.1)
C**
C** CALCULATE ARRAY CONTENTS AT CURRENT TEMPERATURE
      KT = K * TS
C** If desorption into precursor is allowed (PREFLG <> 0)
      IF (PREFLG .NE. 0) THEN
         WRITE(7,*) 'Desorption via precursor state is allowed'
         IF (PREFLG .lt. 0)
     1    WRITE(7,*) 'No direct desorption is allowed'
      ELSE
         WRITE(7,*) 'Desorption is direct, not via precursor state'
      ENDIF
      ES = K * 77. * LOG(1./SO - 1.)
      PSO = CHI * EXP( - (ED + ES)/ KT)
      PMO = EXP(- EM / KT)
      IF (PRES .EQ. 0) THEN
        PDEN = 0.0
        PDO =  0.0
      ELSE
        PDEN = CHI * EXP((EN - ED) / KT)
        PDO = CHI * EXP( - ED / KT)
      ENDIF
      NRM = 1. / (PSO + 6.*PMO + PDO)
      DO 312 I = 1,7
      DO 312 J = 1,7
        L = I + (J-1)*7
        DSBENG(L,1) = 0
        DSBENG(L,2) = 0
        EI(L) =  (I-1.)*EA - (J-1.)*ER

C** This computes PDI (P=0, NO DESORPTION FROM PRECURSOR STATE)
        IF (PRES .EQ. 0) THEN
          PDI(L) = 0
        ELSE
          PDI(L) = CHI * EXP(- (ED + EI(L)) / KT)
        ENDIF

C** PROBABILITY FOR "DESORPTION" VIA PRECURSOR STATE vs. DIRECT DESORPTION
        IF (PREFLG .LT. 0 .or. pres .eq. 0.0) THEN
          PCPD(L) = 1.0
        elseIF (PREFLG .EQ. 0 .OR. EI(L) .LT. ES) THEN
          PCPD(L) = 0.0
        ELSE
          PCPD(L) = 1. - 0.5 * EXP((ES-EI(L))/KT)
        ENDIF
  312 CONTINUE

      WRITE(7,311) (J-1,J=1,7),(J-1,(EI(I+7*(J-1)),I=1,7),J=1,7)
  311 FORMAT(/,38X,'ENERGY OF MOLECULES BY INTERACTIONS (Kcal/mole)',
     1  /,45X,'NUMBER OF ATTRACTIVE INTERACTIONS',/
     2          20X,7I10,/,' NUMBER OF',/,
     3       ' REPULSIVE  ',I6,2X,7F10.4,6(/,12X,I6,2X,7F10.4),/)
      WRITE(7,313) (J-1,J=1,7),(J-1,(nu(I+7*(J-1)),I=1,7),J=1,7)
  313 FORMAT(/,40X,'PREFACTOR BY NUMBER OF INTERACTIONS (sec-1)',
     1  /,45X,'NUMBER OF ATTRACTIVE INTERACTIONS',/
     2          20X,7I10,/,' NUMBER OF',/,
     3       ' REPULSIVE  ',I6,2X,1P7E10.3,6(/,12X,I6,2X,7E10.3),/)
C**
      WRITE(7,772) TS,((PCPD(i+7*(j-1)),i=1,7),j=1,7)
  772 FORMAT(' PROBABILITY FOR DESORPTION TO PRECURSOR ',
     1 '(VS. DIRECT DESORPTION) AT T = ',F7.2,7(/,2X,7E13.4),//)
      WRITE(7,28) PSO,PSO*NRM,PDO,PDO*NRM,PMO,PMO*NRM
   28 FORMAT(' ZERO COVERAGE LIMIT: ',/,
     1 5X,'STICKING   PROBABILITY: ',F6.4,3X,F6.4,/,
     2 5X,'DESORPTION PROBABILITY: ',F6.4,3X,F6.4,/,
     3 5X,'MIGRATION  PROBABILITY: ',F6.4,3X,F6.4,/)
      IDSB = 1
```

```
      MDSB = 0
      MMOVE = 0
      MDSBP = 0
      MMOVEP = 0
      MATMP  = 0
      MATMPP = 0
      MDIR = 0
      NDSB = 0
      MPASS = 0
      ISO = 1
      dmpmin = 0.0
      pltmin = 0.0
      pltlvl = pltint
      dmplvl = dmpint
C*************************************************************************
C** Before getting started, is there a map to read from file?
      OPEN(UNIT=22,FILE='MAP.DAT, FMT=F', STATUS='OLD',err=1009)
      READ (22,221,end=1009,err=1009) m,line,cov,n
221   FORMAT(I5,//,A72,//,6x,f6.3,22x,i14)
      IF (M .ne. size) stop 'Incorrect Map size.'
      DO 224 I = 1, SIZE
        READ (22,911,end=1009,err=1009) (HEX(I,J),J=1,SIZE)
        do 224 j=1,size
          if (hex(i,j) .ne. 0) NADS = NADS + 1
224   continue
      write (7,223) line,cov,nads,n
223   format ('OMAP FILE READ ON UNIT 22: ',a72,/,' Coverage =',f5.3,
     1 '  NADS =',i7,' IR (on file) = ',i14,//)
      NADStr = nads
1009  IF (PRES .LE. 0 .and. NADS .LE. 0) stop 'Nothing to anneal.'
C*************************************************************************
C** MOLECULE "HITS" SURFACE
C*************************************************************************
 1000 IF (PRES .EQ. 0) goto 1001
C** Zero pressure ==> just go on to next scan
      NEXP = NEXP + 1
C*** NOW CALCULATE A STARTING SITE ON LATTICE
      M = 1. + SIZE * RAN(IR)
      N = 1. + SIZE * RAN(IR)
C MINT & NINT are molecule's initial position on lattice
      MINT = M
      NINT = N
C** NOW ALLOW MOLECULE TO MIGRATE ON SURFACE
      DSBFLG = 1
      CALL MIGRATE(ISO)
      D = DIST(MINT,NINT,M+MX,N+NX,RA)
      IF (DSBFLG .EQ. 0) THEN
C** Molecule was adsorbed:
         AHOP = AHOP + NHOP
         ADIS = ADIS + D
         ADIS2 = ADIS2 + D**2
         NADS = NADS + 1
      ELSE
C** Molecule was desorbed:
         NDES = NDES + 1
         DDIS = DDIS + D
         DDIS2 = DDIS2 + D**2
         DHOP = DHOP + NHOP
      ENDIF
C**
C** IF CURRENT COVERAGE IS LESS THAN INITIAL COVERAGE, CONTINUE ADSORBING
      if (nads .lt. nadstr .and. pres .lt. 0) goto 1000
C*************************************************************************
C** NOW CHECK IF THE SYSTEM "STATE" SHOULD BE DUMPED
C*************************************************************************
      EXPOS = NEXP / SIZ2
1001  COV = NADS / SIZ2
      DTIM = DTIM + DT1MOL
C*************************************************************************
C**DESORPTION INTERVAL: (Time)
```

```
      IF (DTIM .LT. DSBINT) GOTO 901
C*************************************************************************
C*** NOW DESORB MOLECULES FROM SURFACE
C*************************************************************************
C** SHOULD WE RECALCULATE THE DESORBTION PROBABILITIES ON THIS PASS?
      IF (MOD(MPASS,NPASS) .EQ. 0) THEN
C** COMPUTE THE DESORPTION PROBABILITIES
        CALL DSBPROB(DTIM)
        WRITE(7,324) TIME,NEXP,NADS,MMOVE,MMOVE-MMOVEP,
     1  mdsb,mdsb-mdsbP,(MATMP-MATMPP)/(1.*NPASS)
  324   FORMAT(' DESORBED AT ',1PG10.3,' S, (',I6,I6,' Mol) Move:',
     1  I7,'(',I3,'), Dsb:',i7,'(',i3,'), Excit/scan',1PG10.3)
c        WRITE(7,313) (J-1,J=1,7),(J-1,(PCTD(I+7*(J-1)),I=1,7),J=1,7)
        MMOVEP = MMOVE
        MDSBP  = MDSB
        MATMPP = MATMP
      ENDIF
      NATMP = 0
      NDIR = 0
      NDSB = 0
      IMOVE = 0
      CALL DESORB(NDIR,NATMP,LIST,NPASS,1.,DSBENG,IMOVE)
      MPASS = MPASS + 1
      MMOVE = MMOVE + IMOVE
      MDIR = MDIR + NDIR
      MDSB = MDSB + NDSB
      MATMP = MATMP + NATMP
      TIME = TIME + DTIM
      DTIM = 0
c      WRITE(7,323) TIME,NEXP,NATMP,NDIR,NDSB,IMOVE
c  323 FORMAT(' DESORBED AT ',F9.1,' S,  (',I6,' Mol):',4I4
c     1 ,' Molecule(s)')
C*************************************************************************
C** CHECK EXPOSURE AGAINST CUTOFF ONLY AFTER DOING A DESORPTION SCAN
      IF (TIME .LT. ANNEAL .OR. ANNEAL .EQ. 0.0) GOTO 901
C** NOW CHANGE THE SURFACE TEMPERATURE
      WRITE (7,*) '***CHANGE OF PARAMETERS AT ',time,'Sec ('
     1  ,EXPOS*4.08,'L)'
908   dmplvl = DMPINT * IDMP
      dmpmin = dmplvl
      IDMP = 0
      pltlvl = pltINT * Iplt
      pltmin = pltlvl
      Iplt = 0
      read (4,9999,end=2000) LINE
      READ (4,*,END=2000) TS,ISO,PRES
      read (4,9999,end=2000) LINE
      READ (4,*,END=99) DSBINT,PLTINT,DMPINT
      read (4,9999,end=2000) LINE
      READ (4,*,END=2000) ANNEAL,STKMIN,NPASS
      WRITE(7,729) ISO,TS
  729 FORMAT(' ISOTOPE:',I2,' ADSORPTION TEMPERATURE:',F6.1)
      IF (ANNEAL .NE. 0.0) WRITE (7,*) 'EXPOSE FOR ',ANNEAL,
     1 'Sec, THEN CHANGE INPUT PARAMETERS (AGAIN)'
      WRITE(7,228) DSBINT,NPASS,PLTINT,DMPINT,
     1 (CDESPL(I),I=1,20),(TDESPL(I),I=1,20),PRES,STKMIN/4
C** COMPUTE THE CHANGE IN TIME FOR EXPOSURE OF ONE MOLECULE
C** (or per scan if PRES <= 0)
      IF (PRES .LE. 0) THEN
        DT1MOL = dsbint
      ELSE
        DT1MOL = 4.08E-6 / (siz2 * PRES)
      ENDIF
C** FORCE NEW DSBPROB CALCULATION AT START OF NEXT SCAN
      MPASS = 0
      KT = K * TS

C** CALCULATE ARRAY CONTENTS AT CURRENT TEMPERATURE
      IF (PRES .EQ. 0) THEN
C** AP!: This computes PDI (P=0, NO DESORPTION FROM PRECURSOR STATE)
```

```
        CALL VCLR(pdi,1,49)
C** VAX!: This computes PDI (P=0, NO DESORPTION FROM PRECURSOR STATE)
c         DO 414 L = 1,49
c           PDI(L) = 0            ! replace above for VAX
c414      CONTINUE
        PDEN = 0.0
        PDO =  0.0
      ELSE
C** AP!: This computes PDI (DESORPTION PROBABILITIES FROM PRECURSOR STATE)
        call zvsmsa(ei,1,-1./kt,-ed/kt,v1,1,49)
        call vexp(v1,1,v2,1,49)
        call zvsmul(v2,1,chi,pdi,1,49)
C** VAX!: This computes PDI (DESORPTION PROBABILITIES FROM PRECURSOR STATE)
c         DO 413 L = 1,49
c           PDI(L) = CHI * EXP(- (ED + EI(L)) / KT) ! replace above for VAX
c413      CONTINUE
        PDEN = CHI * EXP((EN - ED) / KT)
        PDO = CHI * EXP( - ED / KT)
      ENDIF

C** PROBABILITY FOR "DESORPTION" VIA PRECURSOR STATE vs. DIRECT DESORPTION
      DO 412 L = 1,49
      IF (PREFLG .LT. 0 .or. pres .eq. 0.0) THEN
        PCPD(L) = 1.0
      else IF (PREFLG .EQ. 0 .OR. EI(L) .LT. ES) THEN
        PCPD(L) = 0.0
      ELSE
        PCPD(L) = 1. - 0.5 * EXP((ES-EI(L))/KT)
      ENDIF
  412 CONTINUE

      PSO = CHI * EXP( - (ED + ES)/ KT)
      PMO = EXP(- EM / KT)
      WRITE (7,772) TS,((PCPD(i+7*(j-1)),i=1,7),j=1,7)
C*** WAIT A FEW ADSORPTION CYCLES AT NEW TEMPERATURE BEFORE STOPPING
      DCDE1 = 1.0
C*************************************************************************
C** MAP INTERVAL: (coverage)
  901 IF (COV .GE. CDESPL(IDESPL)) THEN
C**    NOW WRITE OUT HEX MATRIX
        WRITE (9,912) 1,cov,expos,time+dtim,ir
912     FORMAT(1X,I5,f6.3,f11.3,f11.1,i14)
        DO 3000 I = 1, SIZE
         WRITE (9,911) (HEX(I,J),J=1,SIZE)
911      FORMAT(1X,100I1)
3000    CONTINUE
        if (idespl .lt. 20) then
          IDESPL = IDESPL + 1
        else
          CDESPL(IDESPL) = 100.
        endif
        IF (CDESPL(IDESPL) .EQ. 2.0) THEN
          IDESPL = IDESPL + 1
          WRITE (7,*) '***CHANGE OF PARAMETERS AT ',time,'Sec (COV='
     1  ,COV,'%)'
          GOTO 908
        ENDIF
        IF (CDESPL(IDESPL) .EQ. 1.0) GOTO 2000
      ENDIF
C*************************************************************************
C** MAP INTERVAL: (TIME)
      IF (time+dtim .GE. TDESPL(JDESPL)) THEN
C**    NOW WRITE OUT HEX MATRIX
        WRITE (9,912) 1,cov,expos,time+dtim,ir
        DO 3001 I = 1, SIZE
         WRITE (9,911) (HEX(I,J),J=1,SIZE)
3001    CONTINUE
        if (jdespl .lt. 20) then
          JDESPL = JDESPL + 1
        else
```

```
          tDESPL(jDESPL) = 99999999
        endif
      ENDIF
C*************************************************************************
      IF (EXPOS .GE. EXPMAX .or. time .GE. tmax) GOTO 2000
      IF (EXPOS .LT. dmplvl) GOTO 903
C** CHECK FOR SATURATION COVERAGE
      IF (DCDEO + DCDE1 + DCDE2 + DCDE3 .LE. STKMIN) GOTO 2005
      DCDE3 = DCDE2
      DCDE2 = DCDE1
      DCDE1 = DCDEO
      CALL DDUMP(DCDEO,MDSB,MADS,time+dtim)
C**AP TO VAX!*** COMMENT OUT FOLLOWING LINES
      STATUS_CODE = SYS$GETTIME (CTIM, WTIM)
      WRITE(6,108) CTIM,CTIM*0.0036,WTIM,WTIM*0.0036
      IDMP = IDMP + 1
      dmplvl = dmpmin + dmpINT * Idmp
C*************************************************************************
  903 IF (EXPOS .GE. pltlvl) THEN
        WRITE (8,23) NEXP,NADS,TIME+DTIM
23        FORMAT(1X,2I7,f11.1)
        IPLT = IPLT + 1
        pltlvl = pltmin + PLTINT * IPLT
      ENDIF
C** CONSTANT COV SYSTEM? DON'T ADSORB MORE IF COV IS ABOVE INITIAL VALUE.
      if (nads .GE. nadstr .and. pres .lt. 0) goto 1001
      GOTO 1000
C*************************************************************************
C HAVE WE HAVE HIT SATURATION AT FIRST PARAMETER SET? IF SO CHANGE AND RESUME
C*************************************************************************
 2005 IF (ANNEAL .NE. 0.0) THEN
      WRITE (7,*) '***CHANGE OF PARAMETERS AT ',time+dtim,'Sec ('
     1  ,EXPOS*4.08,'L)  (SATURATION REACHED)'
      GOTO 908
      ENDIF
C** NOW WRITE OUT HEX MATRIX
      WRITE (9,912) 1,cov,expos,time+dtim,ir
      DO 3005 I = 1, SIZE
        WRITE (9,911) (HEX(I,J),J=1,SIZE)
 3005 CONTINUE

 2000 CALL DDUMP(DCDEO,MDSB,MADS,time+dtim)
      CLOSE(8)
c** write flag - no more maps follow
      WRITE (9,912) 0
      CLOSE(9)
      WRITE (7,325) MDIR,MDSB
  325 FORMAT(//,1X,'Total Desorbed:',I5,' (DIRECT),  ',I5,
     1 ' (TOTAL)')
C**AP TO VAX!*** COMMENT OUT FOLLOWING LINES
      STATUS_CODE = SYS$GETTIME (CTIM, WTIM)
      WRITE(6,108) CTIM,CTIM*0.0036,WTIM,WTIM*0.0036
      WRITE(7,108) CTIM,CTIM*0.0036,WTIM,WTIM*0.0036
      CLOSE(7)
      STOP
      END
C!**
C*************************************************************************
C**
C** SUBROUTINE TO DUMP INFO ABOUT THE STATE OF THE SYSTEM
C**
C*************************************************************************
C**
      SUBROUTINE DDUMP(DCDE,MDSB,MADS,time)
c       INCLUDE 'SINCONA.FOR'     ! FOR VAX
$INSERT SINCONA.FOR
c       INCLUDE 'SINCONB.FOR'     ! FOR VAX
$INSERT SINCONB.FOR
c       INCLUDE 'SINCONC.FOR'     ! FOR VAX
$INSERT SINCONC.FOR
```

```
C**
      INTEGER ODD
      SAVE EXPPRV,COVPRV
      DATA EXPPRV/0.0/,COVPRV/0.0/
C**
C       DO 5 L=1,49       ! For AP:
C     5 INT(L) = 0        ! Replace with VCLR
      CALL VCLR(INT,1,49)
      DCOV = COV - COVPRV
      DEXP = EXPOS - EXPPRV
      COVPRV = COV
      EXPPRV = EXPOS
      if (DEXP .eq. 0) then
        DCDE = 0.0
      else
        DCDE = DCOV / DEXP
      endif
      tmp = NADS + MDSB - MADS
      if (tmp .eq. 0) then
        AVGAD2 = 0.
        ASIG = 0.
        ADIS = 0.
        TAHOP = 0.
      else
        AVGAD2 = ADIS2/tmp
        ASIG = SQRT(AVGAD2 - (ADIS/tmp)**2)
        ADIS = ADIS/tmp
        TAHOP = AHOP/tmp
      endif
      if (NDES .eq. 0) then
        DDIS = 0.
        TDHOP = 0.
        AVGDD2 = 0.
        DSIG = 0.
      else
        DDIS = DDIS/NDES
        TDHOP = DHOP/(1.*NDES)
        AVGDD2 = DDIS2/NDES
        DSIG = SQRT(AVGDD2 - (DDIS/NDES)**2)
      endif
      WRITE(6,11) EXPOS*4.08,NEXP,COV,NADS,DCDE,time
   11 FORMAT(' EXP:',F6.3,'L (',I6,') ',
     2       ' COV:',F6.3,'M (',I6,') ',
     3 ' STK CO:',F5.2,' TIME:',1pe10.3)
      WRITE(7,10) EXPOS,NEXP,EXPOS*4.08,COV,NADS,DCDE,TAHOP,
     1 ADIS,SQRT(AVGAD2),ASIG,TDHOP,DDIS,SQRT(AVGDD2),DSIG
   10 FORMAT(/,'             EXPOSURE:',F6.3,' M (',I6,' MOLECULES) ',
     1 F6.2,' (LANGMUIR)',/,
     2       ' FRACTIONAL COVERAGE: ',F6.4,'  (',I6,' MOLECULES)',/,
     3 ' DIFFERENTIAL STICKING COEFFICIENT: ',
     4 F10.5,/,' AVERAGES: (ABSORBED)',F6.2,' (HOPS)',F6.2,' (NET)',
     5 F6.2,' (RMS)',' SIGMA = ',F6.3,/,
     6 ' AVERAGES: (DESORBED)',F6.2,' (HOPS)',F6.2,' (NET)',
     7 F6.2,' (RMS)',' SIGMA = ',F6.3,/)
      MADS = NADS + MDSB
      DHOP = 0
      AHOP = 0
      ADIS = 0.0
      ADIS2 = 0.0
      DDIS = 0.0
      DDIS2 = 0.0
      DO 100 M=1,SIZE
      ODD = 2 - MOD(M,2)
      DO 101 N=1,SIZE
      IF (HEX(M,N) .EQ. 0) GOTO 101
      NREP = NEAR(M,N,ODD)
      NATT = NEXT(M,N,ODD)
      INT(NATT+1+7*NREP) = INT(NATT+1+7*NREP) + 1
  101 CONTINUE
  100 CONTINUE
```

```
      DO 6 J1=1,7
      J = 7*(J1-1) + 1
      INTS(J1) = INT(J) + INT(1+J) + INT(2+J) + INT(3+J) + INT(4+J) +
     1 INT(5+J) + INT(6+J)
    6 CONTINUE
      WRITE(7,30) (I-1,I=1,7),0,(INT(I),I=1,7),INTS(1)
   30 FORMAT(/,17X,'BREAKDOWN OF MOLECULES BY INTERACTIONS',
     1          //,20X,'NUMBER OF ATTRACTIVE INTERACTIONS',/
     2          20X,7I6,' TOTAL',/,' NUMBER OF',/,
     3       ' REPULSIVE  ',I6,2X,8I6)
   33 FORMAT(12X,I6,2X,8I6)
      DO 32 J=2,7
      IF (INTS(J).NE. 0) WRITE(7,33) J-1,(INT((J-1)*7+I),I=1,7),INTS(J)
   32 CONTINUE
C Now print a blank line for better readability
      WRITE(7,33)
      RETURN
      END
```

[BHT.N2.AP]DSB.FOR

```
C*************************************************************************
C*************************************************************************
C****                                                                 *****
C****   PROGRAM TO MODEL N   DESORPTION ON Ru(0001)                   *****
C****                     2                                           *****
C****   Using Monte-Carlo type model                                  *****
C****                                                                 *****
C****   BRIAN TOBY             12/83                                  *****
C****                                                                 *****
C****   ADAPTED FOR ARRAY PROCESSOR (BHT 6/84)                        *****
C****   Change isotope label during annealing (BHT 8/85)              *****
C****   Environment Dependant Prefactor Model                         *****
C****                                                                 *****
C*************************************************************************
C*************************************************************************
C**
C**   HEXAGONAL LATTICE IS STORED BY COORDINATES (m,n) WHICH ARE
C**   RELATED TO CARTESIAN COORDINATES (x,y) BY
C**
C**           x = m * A * sin(60)
C**           y = n * A                  (m ODD)
C**           y = n * A   -  A / 2       (m EVEN)
C**
C**    WHERE A IS THE LATTICE SPACING
C**
      BLOCK DATA
C      INCLUDE 'SIMCOMA.FOR'    ! FOR VAX
$INSERT SIMCOMA.FOR
C      INCLUDE 'SIMCOMB.FOR'    ! FOR VAX
$INSERT SIMCOMB.FOR
C      INCLUDE 'SIMCOMC.FOR'    ! FOR VAX
$INSERT SIMCOMC.FOR
C      INCLUDE 'SIMCOMD.FOR'    ! FOR VAX
$INSERT SIMCOMD.FOR
C      INCLUDE 'SIMCOME.FOR'    ! FOR VAX
$INSERT SIMCOME.FOR
C**
      DATA NEARN/-1,-1,0,0,1,1/
      DATA NEARN/0,1,-1,1,0,1,-1,0,-1,1,-1,0/
C** NEARN(i),NEARN(i,j) DESCRIBE THE NEAREST NEIGHBOR SITES RELATIVE TO
C**  THE CENTER SITE.  j IS 1 FOR m ODD;  2 FOR m EVEN.
C**
      DATA NEXTN/-2,-1,-1,1,1,2/
      DATA NEXTN/0,-1,2,-1,2,0,0,-2,1,-2,1,0/
C** NEXTN(i),NEXTN(i,j) DESCRIBE THE NEXT NEAREST NEIGHBOR SITES RELATIVE
C**  TO THE CENTER SITE.  j IS 1 FOR m ODD;  2 FOR m EVEN.
C**
C** SIZE IS THE DIMENSION OF THE [SQUARE] LATTICE
```

```
      DATA HEX/10000*0/,SIZE/100/
      END
C!**
C*****************************************************************************
C*****************************************************************************
C**
C       INCLUDE 'SIMCOMA.FOR'     ! FOR VAX
$INSERT SIMCOMA.FOR
C       INCLUDE 'SIMCOMB.FOR'     ! FOR VAX
$INSERT SIMCOMB.FOR
C       INCLUDE 'SIMCOMC.FOR'     ! FOR VAX
$INSERT SIMCOMC.FOR
C       INCLUDE 'SIMCOMD.FOR'     ! FOR VAX
$INSERT SIMCOMD.FOR
C       INCLUDE 'SIMCOME.FOR'     ! FOR VAX
$INSERT SIMCOME.FOR
C**
C** LIST is the (decoded) random order rastering sequence
      INTEGER*2 LIST(2,10000)
      INTEGER ODD
      REAL COVI(49),COVIP(49)
      REAL TEMP(200)
      INTEGER TMIN,TMAX,TINT
      REAL BETA,E,T,NAAVG,LCTP
      REAL CDESPL(20)
      INTEGER DSBENG(49,2)
      CHARACTER*72 LINE,TITLE
C** IR IS THE STARTING POINT FOR THE RANDOM NUMBER GENERATOR
C**
      DATA CDESPL/20*-1./
      DATA IR/256/
C**AP TO VAX!*** COMMENT OUT FOLLOWING LINES
C**  Open output files
      OPEN(UNIT=10,FILE='FOR010.DAT, FMT=F', STATUS='NEW')
      OPEN(UNIT=14,FILE='FOR014.DAT, FMT=F', STATUS='NEW')
      OPEN(UNIT=15,FILE='FOR015.DAT, FMT=F', STATUS='NEW')
C UNIT=6 ==> :OUTPUT (by default) override to save VAX CPU:
      OPEN(UNIT=7, FILE=':S(XHMEIA):BHTOUT.DSB, FMT=F',
     1 ACCESS = 'SEQUENTIAL', RECL=132,  STATUS='unknown')
      STATUS_CODE = SYS$GETTIME (CTIM, WTIM)
      WRITE(7,108) CTIM,CTIM*0.0036,WTIM,WTIM*0.0036
C**
C*** PARAMETER DEFINITIONS:
C**
      R = 1.9872
      K = 1.9872E-3
C UNITS: Kcal or cal/(K-mol)
      BETA = 6.
C UNITS: K/sec
      CVINT = 0.05
      DT = 0.5
C UNITS: K / iteration
      NAAVG = 2.
C LOW COVERAGE PEAK TEMPERATURE:
      LCTP = 130.
      RA = 2.7058
C Lattice spacing (in A)
C**
      ED = 1.6
C Desorption energy from clean surface (Kcal/mol)
      ER = 0.320
C Energy of a repulsive interaction (Kcal/mol)
      EA = 0.160
C Energy of an attractive interaction (Kcal/mol)
      EN = 0.8
C Energy difference for precursor on empty site vs. filled site (Kcal/mol)
      CHI = 1.E3
C Controls number of hops
      TS =  80.
C Temperature of surface during adsorption (K)
```

```
      SO = .25
C initial sticking coefficient
C
      READ (5,9999) LINE
 9999 FORMAT(A72)
      READ (5,*,END=99) TMIN,TMAX,TINT,CMIN
      READ (5,9999) LINE
      READ (5,*,END=99) IR,MAPN,PREFLG,ATMAX
      READ (5,9999) LINE
      READ (5,*,END=99) (CDESPL(I),I=1,20)
C*******************************************************************************
C**  Open/read rastering sequence array
C**AP TO VAX!*** COMMENT OUT FOLLOWING LINE
      OPEN(UNIT=20,FILE='RAST.DAT, FMT=F', STATUS='OLD')
C** Now read in rastering sequence array
      READ (20,202) N,N2
  202 FORMAT(1X,2I6)
      READ (20,212) (LIST(1,I),LIST(2,I),I=1,N2)
  212 FORMAT(1X,20I5)
      CLOSE(20)
C*******************************************************************************
C**  Open/read prefactor (NU) array
C**AP TO VAX!*** COMMENT OUT FOLLOWING LINE
      OPEN(UNIT=20,FILE='NU.DAT, FMT=F', STATUS='OLD')
      READ (20,222) (nu(i),i=1,49)
  222 FORMAT(1X,7E10.3)
      CLOSE(20)
C*******************************************************************************
C**  Open/read adsorption program results
C**AP TO VAX!*** COMMENT OUT FOLLOWING LINE
      OPEN(UNIT=9,FILE='FOR009.DAT, FMT=F', STATUS='OLD')
   99 READ (9,21) SIZE,ED,EN,EA,ER,EM,SO,CHI,TS,DSBINT,IP,TITLE,
     1 LCTP,E,EO,NAAVG,DT,BETA
   21 FORMAT(I5,6F10.6,/,3F10.3,I12,/,A72,/,F10.1,2F10.6,F6.2,
     1 F6.4,15x,F6.1)
      IF (N2 .NE. SIZE**2) STOP '***WRONG RASTER LIST DIMENSION***'
      WRITE (10,21) SIZE,ED,EN,EA,ER,EM,SO,CHI,TS,DSBINT,IR,TITLE,
     1 LCTP,E,EO,NAAVG,DT,BETA
      WRITE (15,21) SIZE,ED,EN,EA,ER,EM,SO,CHI,TS,DSBINT,IR,TITLE,
     1 LCTP,E,EO,NAAVG,DT,BETA
      WRITE (14,21) SIZE,-ED,EN,EA,ER,EM,SO,CHI,TS,DSBINT,IR,TITLE,
     1 LCTP,E,EO,NAAVG,DT,BETA
      RATIO = ER / EA
      WRITE(7,29) TITLE,SIZE,SIZE,ED,EN,ER,EA,RATIO
     1 ,EM,SO,CHI,IR,TS
   29 FORMAT('0',72('*'),/,1X,A72,/,1X,72('*'),//' LATTICE IS',I4,
     1   ' BY',I4,/,' DESORPTION ENERGY: ',
     2 F5.3,/,' DESTABILIZATION ENERGY FOR FILLED SITE:',F6.3,/,
     3 ' REPULSIVE INTERACTION ENERGY:',F6.3,/,
     4 ' ATTRACTIVE INTERACTIVE ENERGY:',F6.3,/,
     5 ' ER / EA: ',F5.3,/,' MIGRATION ENERGY: ',F7.4,/,
     6 ' INITIAL STICKING COEFFICIENT: ',F6.4,/,' CHI = ',F12.5,
     7 '    SEED: ',I9,/,' ADSORPTION TEMPERATURE:',F6.1,//)
      WRITE(7,128) LCTP,E,NAAVG,EO,DT,ATMAX*100.
  128 FORMAT(' TDS PEAK AT ',F5.0,'K (E = ',F6.3,
     2 ' Kcal) IS ASSIGNED TO ',f3.1,'*EA STATE',/,
     3 ' ISOLATED N2 MOLECULE - ENERGY IS ASSIGNED AS ',
     4  F6.3,' (Kcal)',/,' TEMPERATURE INCREMENT',F8.4,/,
     5 ' EXCITE NO MORE THAN',F5.0,
     6 '% OF SURFACE DURING EACH INCREMENT',//)
      WRITE(7,228) (CDESPL(I),I=1,20)
  228 FORMAT(' SAVE MAPS AT:',20F5.2,' M (Coverage)',//)
C**
C** Print if desorption into precursor is allowed (PREFLG <> 0)
      IF (PREFLG .NE. 0) THEN
         WRITE(7,*) 'Desorption via precursor state is allowed'
         IF (PREFLG .lt. 0)
     1    WRITE(7,*) 'No direct desorption is allowed'
      ELSE
         WRITE(7,*) 'Desorption is direct, not via precursor state'
```

```
      ENDIF
      DO 312 I = 1,7
      DO 312 J = 1,7
      L = I + (J-1)*7
      EI(L) =  (I-1.)*EA - (J-1.)*ER
  312 CONTINUE
      WRITE(7,311) (J-1,J=1,7),(J-1,(EI(I+7*(J-1)),I=1,7),J=1,7)
  311 FORMAT(38X,'ENERGY OF MOLECULES BY INTERACTIONS (Kcal/mole)',
     1  /,45X,'NUMBER OF ATTRACTIVE INTERACTIONS',/
     2          20X,7I10,/,' NUMBER OF',/,
     3       ' REPULSIVE  ',I6,2X,7F10.4,6(/,12X,I6,2X,7F10.4),//)
      WRITE(7,321) (J-1,J=1,7),(J-1,(NU(I+7*(J-1)),I=1,7),J=1,7)
  321 FORMAT(/,40X,'PREFACTOR BY NUMBER OF INTERACTIONS (sec-1)',
     1  /,45X,'NUMBER OF ATTRACTIVE INTERACTIONS',/
     2          20X,7I10,/,' NUMBER OF',/,
     3       ' REPULSIVE  ',I6,2X,1P7E10.3,6(/,12X,I6,2X,7E10.3),/)
      ES = K * 77. * LOG(1./SO - 1.)
C*******************************************************************************
C*******************************************************************************
C** NOW READ IN MATRIX
C***
      READ (9,912,END=999) imore
      NPLT = 0
 1000 DO 3000 I = 1, SIZE
      READ (9,911,END=999) (HEX(I,J),J=1,SIZE)
  911 FORMAT(1X,100I1)
 3000 CONTINUE
c** Is there another map on the file?
      imore = 0
      READ (9,912,END=913) imore
  912 FORMAT(1X,I5,f6.3)
C**
  913 IF (imore .EQ. 0 .and. mapn .ne. 0) then
        IFLG = 1
      else
        IFLG = 0
      endif
      N1 = 0
C** NOW SCAN LATTICE FOR DISTRIBUTION BY # OF INTERACTIONS
      NADS = 0
C      DO 5 L=1,49       ! For AP:
C      PCPD(L) = 0.0     ! Replace with VCLR (below)
C      DSBENG(L,1) = 0   ! Replace with VCLR (below)
C      DSBENG(L,2) = 0   ! Replace with VCLR (below)
C    5 INT(L) = 0        ! Replace with VCLR (below)
      CALL VCLR(INT,1,49)
      CALL VCLR(DSBENG,1,98)
      CALL VCLR(PCPD,1,49)
      DO 100 M=1,SIZE
      ODD = 2 - MOD(M,2)
      DO 101 N=1,SIZE
      IF (HEX(M,N) .EQ. 0) GOTO 101
      NADS = NADS + 1
      NREP = NEAR(M,N,ODD)
      NATT = NEXT(M,N,ODD)
      INT(NATT+1+7*NREP) = INT(NATT+1+7*NREP) + 1
  101 CONTINUE
  100 CONTINUE
      DO 6 J1=1,7
      J = 7*(J1-1) + 1
      INTS(J1) = INT(J) + INT(1+J) + INT(2+J) + INT(3+J) + INT(4+J) +
     1 INT(5+J) + INT(6+J)
    6 CONTINUE
      COVO = (1.*NADS)/SIZE**2
      IF (COVO .LT. CMIN) GOTO 1000
C Don't try to store maps which are lower coverage than the initial coverage
      DO 313 I=1,20
      MAP = I
      IF (CDESPL(MAP) .LT. COVO) GOTO 314
  313 CONTINUE
```

```
  314 NADSO = NADS
      WRITE(7,34) NADSO,COVO
      WRITE(6,34) NADSO,COVO
   34 FORMAT(//,3X,'NADS = ',I5,'    COVERAGE = ',F6.3)
      WRITE(7,30) 'ADSORBED',(I-1,I=1,7),0,(INT(I),I=1,7),INTS(1)
   30 FORMAT(/,23X,'BREAKDOWN OF ',A8,' MOLECULES BY INTERACTIONS',
     1         /,30X,'NUMBER OF ATTRACTIVE INTERACTIONS',/
     2          20X,7I6,' TOTAL',/,' NUMBER OF',/,
     3       ' REPULSIVE  ',I6,2X,8I6)
   33 FORMAT(12X,I6,2X,8I6)
      DO 32 J=2,7
      IF (INTS(J).NE. 0) WRITE(7,33) J-1,(INT((J-1)*7+I),I=1,7),INTS(J)
   32 CONTINUE
      STATUS_CODE = SYS$GETTIME (CTIM, WTIM)
      WRITE(6,108) CTIM,CTIM*0.0036,WTIM,WTIM*0.0036
C*******************************************************************************
C*******************************************************************************
C** PREPARE FOR START OF TDS SCAN
C
C STARTING TEMPERATURE FOR SCAN
      T = TMIN
      TEMP(1) = T
      N = (TMAX-TMIN)/(TINT*DT) + 1
      WRITE (10,125) N,COVO,NADSO
  125 FORMAT(I5,F8.4,I7)
      WRITE (10,24) TEMP(1)
      WRITE (10,26) (INT(I),I=1,49)
      WRITE (15,125) N,COVO,NADSO
      WRITE (15,24) TEMP(1)
  126 FORMAT(7I6,3x,7I6)
      WRITE (15,126) (((DSBENG(I,ik),I=J,j+6),ik=1,2),j=1,43,7)
      NT = 2
      MDSB = 0
      NDSB = 0
      imove = 0
      NDIR = 0
      NATMP = 0
C NPASS: # of desorption scans/probability computation
      NPASS = 2
      NADSP = NADSO
      MPASS = NPASS + 1
      NINT = 0
C
C*******************************************************************************
C*******************************************************************************
C** NOW START DESORPTION PROCESS
   35 COV = (1.*NADS) / SIZE**2
C CHECK TO WRITE DESORPTION MAP FILE
      IF (COV .GT. CDESPL(MAP) .OR. IFLG .EQ. 0) GOTO 315
      IF (MAP .LT. 20) MAP = MAP + 1
      WRITE (14,912) 1,cov
      DO 3009 I = 1, SIZE
      WRITE (14,911) (HEX(I,J),J=1,SIZE)
 3009 CONTINUE
C**
C** SHOULD WE RECALCULATE THE DESORBTION PROBABILITIES ON THIS PASS?
315   IF (MPASS .GE. NPASS) THEN
        T = TMIN + NINT * DT
        KT = T * K
        NINT = NINT + 1
        MPASS = 0
        DTT = DT / NPASS
C** COMPUTE THE CHANGE IN TIME FOR CURRENT DTT
        DTIM = DTT / BETA
C** CALCULATE DESORPTION PROBABILITIES ONLY IF MIGRATION WILL BE NEEDED
        IF (PREFLG .NE. 0) THEN
           DO 316 L = 1,49
             PDI(L) = CHI * EXP(- (ED + EI(L)) / KT)
C**   PROBABILITY FOR "DESORPTION" VIA PRECURSOR STATE vs. DIRECT DESORPTION
        IF (PREFLG .LT. 0) THEN
          PCPD(L) = 1.0
```

```
        else IF (EI(L) .LT. ES) THEN
            PCPD(L) = 0.0
          ELSE
            PCPD(L) = 1. - 0.5 * EXP((ES-EI(L))/KT)
        ENDIF
  316   CONTINUE
           PSO = CHI * EXP( - (ED + ES)/ KT)
           PDO = CHI * EXP( - ED / KT)
           PDEN = CHI * EXP((EN - ED) / KT)
           PMO = EXP(- EN / KT)
        ENDIF
C** COMPUTE THE DESORPTION PROBABILITIES
        CALL DSBPROB(DTIM)
        TCALC = T
        TCORR = 1.0
      ELSE
        T = T + DTT
        KT = T * K
C**  CALCULATE THE PROBABILITY INCREASE/DECREASE FROM THE CHANGE IN T
        IF (PREFLG .NE. 0) THEN
           TCORR = EXP((EO + ES)*(T-TCALC) / (KT*T))
        ELSE
           TCORR = EXP( EO*(T-TCALC) / (KT*T))
        ENDIF
      ENDIF
      CALL DESORB(NDIR,NATMP,LIST,NPASS,TCORR,DSBENG,imove)
      MPASS = MPASS + 1
      IF (MPASS .LT. NPASS .OR. MOD(NINT,TINT) .NE. 0) GOTO 35
C*******************************************************************************
C** IT IS NOW TIME TO WRITE SURFACE COVERAGE INFO TO DISK
      Y = (NDSB*2.0)/(1.*DT*TINT*SIZE**2)
      TEMP(NT) = TMIN + (NINT-TINT/2.) * DT
      WRITE (15,24) TEMP(NT),NATMP,NDIR,IMOVE,NDSB
      WRITE (15,126) (((DSBENG(I,ik),I=J,j+6),ik=1,2),j=1,43,7)
C** NOW SCAN LATTICE FOR DISTRIBUTION BY # OF INTERACTIONS
      NADS = 0
C      DO 15 I=1,49      ! For AP:
C      DSBENG(I,1) = 0   ! Replace with VCLR
C      DSBENG(I,2) = 0   ! Replace with VCLR
C   15 INT(I) = 0        ! Replace with VCLR
      CALL VCLR(DSBENG,1,98)
      CALL VCLR(INT,1,49)
      DO 1100 M=1,SIZE
      ODD = 2 - MOD(M,2)
      DO 1100 N=1,SIZE
      IF (HEX(M,N) .NE. 0) THEN
         NADS = NADS + 1
         NREP = NEAR(M,N,ODD)
         NATT = NEXT(M,N,ODD)
         INT(NATT+1+7*NREP) = INT(NATT+1+7*NREP) + 1
      ENDIF
 1100 CONTINUE
      WRITE (10,24) TEMP(NT)
   24 FORMAT(F6.2,i8,3i4)
      WRITE (10,26) (INT(I),I=1,49)
   26 FORMAT(7I6)
c      IF (NDSB.GT.0)
      WRITE(7,323) TEMP(NT),NATMP,NDIR,NDSB,imove,Y,NPASS,NADS
  323 FORMAT(1X,F6.2,4I7,F8.5,2I7)
C** COMPUTE NEXT NUMBER OF DESORPTION SCANS PER DT
      NPASS = NATMP*2.0/((NADSP+NADS)*TINT*ATMAX) + 1.
      NADSP = NADS
      MPASS = NPASS + 1
      DTT = DT / NPASS
      imove = 0
      NDIR = 0
      NATMP = 0
      MDSB = MDSB + NDSB
      NDSB = 0
      NT = NT + 1
```

```
      IF (TEMP(NT-1) .GE. TMAX) GOTO 441
      IF (NADS .GT. 0) GOTO 35
C*************************************************************************
C*************************************************************************
C** NO N2 LEFT ON SURFACE -- WRITE OUT ZERO ARRAYS
C       J = TEMP(NT-1) + TINT*DT
C       I = TINT*DT
C       DO 442 I=J,TMAX,I
C       TEMP(NT) = I
C       WRITE (10,24) TEMP(NT)
C       WRITE (10,26) (INT(J1),J1=1,49)
C       NT = NT + 1
C  442 CONTINUE
  441 NT = NT - 1
C** write negative T to indicate last entry in file
      WRITE (10,24) -1.
      WRITE (15,24) -1.
      WRITE(7,325) COVO,MDSB,NADS
  325 FORMAT(1X,F8.5,' TOTAL DESORBED = ',I5,' FINAL COVERAGE',I3)
      if (imore .ne. 0) GOTO 1000
  999 CLOSE(9)
      CLOSE(10)
      CLOSE(15)
c** write flag - no more maps follow
      WRITE (14,912) 0
      CLOSE(14)
C**AP TO VAX!*** COMMENT OUT FOLLOWING LINES
      STATUS_CODE = SYS$GETTIME (CTIN, WTIN)
      WRITE(7,108) CTIN,CTIN*0.0036,WTIN,WTIN*0.0036
  108 FORMAT(' CPU TIME =',F10.2,' ($',F7.2,')  REAL TIME = ',
     1 F10.2,' ($',F7.2,')')
      CLOSE(7)
      STOP
      END
```

1.2 Subroutines MIGRATE, DSBPROB and DESORB, COMSUB subroutines and COMMON blocks

[BHT.N2.AP]MIG.FOR

```
C*************************************************************************
C*************************************************************************
C****   Environment Dependant Prefactor Model                          *****
C****   Change isotope label during annealing (BHT 8/85)               *****
C**
      SUBROUTINE MIGRATE(ISO)
c       INCLUDE 'SIMCOMA.FOR'     ! FOR VAX
$INSERT SIMCOMA.FOR
c       INCLUDE 'SIMCOMB.FOR'     ! FOR VAX
$INSERT SIMCOMB.FOR
c       INCLUDE 'SIMCOMC.FOR'     ! FOR VAX
$INSERT SIMCOMC.FOR
c       INCLUDE 'SIMCOMD.FOR'     ! FOR VAX
$INSERT SIMCOMD.FOR
c       INCLUDE 'SIMCOME.FOR'     ! FOR VAX
$INSERT SIMCOME.FOR
C**
      INTEGER ODD,ODDI
      REAL P(6),PC,PT,PS,PD
C**
      NHOP = 0
C MX & NX Define the quadrant
      MX = 0
      NX = 0
C**
C** CALCULATE MIGRATION & DESORPTION PROBABILITIES
```

```
C**
  500 ODD = 2 - MOD(M,2)
C** COMPUTE SITE ENERGY - current site
C** Is site filled?
      IF (HEX(M,N) .NE. 0) THEN
C      Site is filled, so prevent sticking
        PS = 0
C      Calculate site energy level (independant of the number of interactions)
        EIO = EN
C      Desorption probability: (independant of the number of interactions)
        PD = PDEN
      ELSE
C      Site is not filled, so allow sticking
        PS = PSO
        NRO = NEAR(M,N,ODD)
        NAO = NEXT(M,N,ODD)
C      Desorption probability: (depends on number of interactions)
        PD = PDI(NAO+1+7*NRO)
C      Calculate energy level of current site (EIO)
        EIO = NRO*ER - NAO*EA
      ENDIF
C** COMPUTE # OF ATTRACTIVE & REPULSIVE INTERACTIONS - for each neighbor site
      DO 100 I = 1,6
      MI = M + NEARM(I)
      NI = N + NEARN(I,ODD)
      IF (MI .LE. 0) THEN
        MI = MI + SIZE
        ELSE IF (MI .GT. SIZE) THEN
          MI = MI - SIZE
      ENDIF
      IF (NI .LE. 0) THEN
        NI = NI + SIZE
        ELSE IF (NI .GT. SIZE) THEN
          NI = NI - SIZE
      ENDIF
      EJ = EN
      IF (HEX(MI,NI) .NE. 0) GOTO 105
      ODDI = 2 - MOD(MI,2)
C** CALCULATE ENERGY LEVEL OF NEIGHBOR SITE (EJ)
      NRI = NEAR(MI,NI,ODDI)
      NAI = NEXT(MI,NI,ODDI)
      EJ = NRI*ER - NAI*EA
  105 DE = EJ - EIO
C Migration probability:
      IF (DE .EQ. 0) THEN
        P(I) = PMO
      ELSE if (de .le. -4.*EM) then
          p(i) = 1
        else if (de .ge. 4*EM) then
            P(I) = EXP(- DE / KT)
          else
            P(I) = EXP(- (EM + DE/2. + DE**2/(16.*EM)) / KT)
      ENDIF
  100 CONTINUE
C Total probability (before normalizing):
      PT = PD + P(1) + P(2) + P(3) + P(4) + P(5) + P(6) + PS
  101 PC = PT * RAN(IR)
C Should we desorb?
      IF (PC .LE. PD) RETURN
C Should we migrate?
      PT = PD
      DO 110 I = 1,6
      PT = PT + P(I)
      IM = I
C Is random number in range for Ith site? If true, migrate to that site
      IF (PC .LE. PT) GOTO 250
  110 CONTINUE
C Should we stick at current site?
      IF (PC .LE. PT+PS) GOTO 300
C** No migration or desorption -- What are we doing here?!
```

```
      WRITE(6,*) '**** ERROR - MOLECULE DIDN''T DO ANYTHING ****'
      GOTO 101
C** Migrate:
  250 NHOP = NHOP + 1
      M = M + NEARM(IM)
      N = N + NEARN(IM,ODD)
      CALL CYCLE(M,MX,N,NX,SIZE)
      GOTO 500
  300 IF (HEX(M,N) .NE. 0) WRITE(6,*)
     1 '**** ERROR - ADSORPTION ON FILLED SITE ****',M,N
      HEX(M,N) = ISO
      DSBFLG = 0
      RETURN
      END
C!**
C*************************************************************************
C*************************************************************************
C****   Environment Dependant Prefactor Model                          *****
C****   Change isotope label during annealing (BHT 8/85)               *****
C**
      SUBROUTINE DSBPROB(DTIM)
c      INCLUDE 'SIMCOMA.FOR'    ! FOR VAX
$INSERT SIMCOMA.FOR
c      INCLUDE 'SIMCOMB.FOR'    ! FOR VAX
$INSERT SIMCOMB.FOR
c      INCLUDE 'SIMCOMC.FOR'    ! FOR VAX
$INSERT SIMCOMC.FOR
c      INCLUDE 'SIMCOMD.FOR'    ! FOR VAX
$INSERT SIMCOMD.FOR
c      INCLUDE 'SIMCOME.FOR'    ! FOR VAX
$INSERT SIMCOME.FOR
C**
      REAL PCT
      INTEGER ODD
C** Next is needed for AP only!
      REAL V1(49),V2(49)
C*************************************************************************
      IF (PREFLG .EQ. 0) THEN
C** This block computes desorption probabilities for non-precursor desorption
C*************************************************************************
C**    AP!: The following 4 lines compute PCTD
        call zvsmsa(ei,1,-1./kt,-e0/kt,v1,1,49)
        call vexp(v1,1,v2,1,49)
        CALL ZVSMUL(V2,1,dtim,v1,1,49)
        call zvmul(v1,1,nu,1,pctd,1,49)
C**    VAX!: The following do loop (up to 300) computes PCTD
c         DO 300 L = 1,49
c           PCTD(L) = NU(L) * DTIM * EXP(-(E0 + EI(L))/KT)
c  300    CONTINUE
C*************************************************************************
      ELSE
C** This block computes desorption probabilities for precursor desorption
C*************************************************************************
        PCT = EXP(-(ES + E0)/KT) * DTIM
C**    AP!: The following line computes PCTD
        CALL ZVSMUL(NU,1,PCT,PCTD,1,49)
C**    VAX!: The following do loop (up to 305) computes PCTD
c         DO 305 L = 1,49
c           PCTD(L) = NU(L) * PCT
c  305    CONTINUE
C*************************************************************************
      ENDIF
      RETURN
      END
C!**
C*************************************************************************
C*************************************************************************
C****   Environment Dependant Prefactor Model                          *****
C****   Change isotope label during annealing (BHT 8/85)               *****
C**
```

```
      SUBROUTINE DESORB(NDIR,NATMP,LIST,NPASS,TCORR,DSBENG,imove)
c       INCLUDE 'SIMCOMA.FOR'     ! FOR VAX
$INSERT SIMCOMA.FOR
c       INCLUDE 'SIMCOMB.FOR'     ! FOR VAX
$INSERT SIMCOMB.FOR
c       INCLUDE 'SIMCOMC.FOR'     ! FOR VAX
$INSERT SIMCOMC.FOR
c       INCLUDE 'SIMCOMD.FOR'     ! FOR VAX
$INSERT SIMCOMD.FOR
c       INCLUDE 'SIMCOME.FOR'     ! FOR VAX
$INSERT SIMCOME.FOR
C**
C** LIST is the (decoded) random order rastering sequence
      INTEGER*2 LIST(2,10000)
      INTEGER ODD
      REAL TCORR,PCT(49)
      INTEGER DSBENG(49,2)
      MDSB = 0
C** APPLY ERROR CORRECTION TERM TO PCTD
C** AP!: The following statement computes PCT
      CALL ZVSMUL(pctd,1,Tcorr,pct,1,49)
C** VAX!: The following do loop computes PCT
c       DO 50 L=1,49
c         PCT(L) = PCTD(L)*TCORR
c   50 CONTINUE
C** SCAN LATTICE IN RANDOM SEQUENCE
      DO 100 I=1,SIZE**2
C** NOW DETERMINE LOCATION OF SITE TO BE TESTED
        M = LIST(1,I)
        N = LIST(2,I)
C** IS THERE A MOLECULE AT THAT SITE?
        IF (HEX(M,N) .EQ. 0) GOTO 100
C** SITE IS OCCUPIED -- FIND NUMBER OF INTERACTIONS
        ODD = 2 - MOD(M,2)
        NREP = NEAR(M,N,ODD)
        NATT = NEXT(M,N,ODD)
        L = NATT+1+7*NREP
C** NOW WE KNOW WHAT THE MOLECULE'S ENERGY STATE IS
C** SHOULD IT BE REMOVED FROM THE CHEMISORPTION WELL?
C** Total probability for chemisorbed species to desorb to precursor or
C**   gas phase in time interval DTIM is PCT(L) = PCTD(NATT+7*NREP+1)*TCORR
        IF (RAN(IR) .GT. PCT(L)) GOTO 100
C** MOLECULE WILL DESORB.  SHOULD IT DESORB DIRECTLY TO GAS PHASE?
C** NATMP is total # of molecules which leave chemisorbed state (some reabsorb)
        NATMP = NATMP + 1
        ISO = HEX(M,N)
        HEX(M,N) =  0
C** Probability for desorbing species to enter precursor state
C**   is PCPD(NATT+7*NREP+1)
        IF (PREFLG .EQ. 0 .OR. PCPD(L) .EQ. 0.0) THEN
C**       DESORPTION IS DIRECT FOR THIS STATE
C NDIR is # of molecules which desorb directly (from chemisorbed state to gas)
          NDIR = NDIR + 1
C MDSB is total # of molecules which have desorbed (in this scan only)
          MDSB = MDSB + 1
C Now update desorption energy array
          DSBENG(L,iso) = DSBENG(L,iso) + 1
        ELSEIF (RAN(IR) .GT. PCPD(L)) THEN
C** DESORPTION IS DIRECT ANYWAY
          NDIR = NDIR + 1
          MDSB = MDSB + 1
C Now update desorption energy array
          DSBENG(L,iso) = DSBENG(L,iso) + 1
        ELSE
C** OH BOY, BACK INTO THE PRECURSOR STATE AGAIN
          DSBFLG = 1
          MINT = M
          NINT = N
          CALL MIGRATE(ISO)
          IF (DSBFLG .EQ. 0) THEN
```

```
C** Molecule was adsorbed: did it move?
            IF (MINT .NE. M+MX .OR. NINT .NE. N+NX) IMOVE=IMOVE+1
          ELSE
C** Molecule was desorbed:
C**       If the flag is still 1, the molecule has desorbed
            MDSB = MDSB + 1
C         Now update desorption energy array
            DSBENG(L,iso) = DSBENG(L,iso) + 1
          ENDIF
        ENDIF
  100 CONTINUE
      NADS = NADS - MDSB
      NDSB = NDSB + MDSB
      RETURN
      END
```

[BHT.N2.AP]COMSUB.FOR

```
C!**
C*************************************************************************
C**
C**  SUBROUTINE TO IMPOSE CYCLIC BOUNDARIES
C**
C*************************************************************************
C**
      SUBROUTINE CYCLE(M,MX,N,NX,ISIZE)
      IF (M .GT. 0) GOTO 1
      M = M + ISIZE
      MX = MX - ISIZE
      GOTO 2
    1 IF (M .LE. ISIZE) GOTO 2
      M = M - ISIZE
      MX = MX + ISIZE
    2 IF (N .GT. 0) GOTO 3
      N = N + ISIZE
      NX = NX - ISIZE
      RETURN
    3 IF (N .LE. ISIZE) RETURN
      N = N - ISIZE
      NX = NX + ISIZE
      RETURN
      END
C!**
C*************************************************************************
C**
C** SUBROUTINE TO DETERMINE HOW MANY NEAREST NEIGHBORS A MOLECULE HAS
C**
C*************************************************************************
C**
      INTEGER FUNCTION NEAR(MO,NO,ODD)
C      INCLUDE 'SIMCOMA.FOR'     ! FOR VAX
$INSERT SIMCOMA.FOR
C      INCLUDE 'SIMCOMC.FOR'     ! FOR VAX
$INSERT SIMCOMC.FOR
      INTEGER ODD
      NEAR = 0
      DO 100 I = 1,6
      M = MO + NEARM(I)
      N = NO + NEARN(I,ODD)
      IF (M .LE. 0) M = M + SIZE
      IF (M .GT. SIZE) M = M - SIZE
      IF (N .LE. 0) N = N + SIZE
      IF (N .GT. SIZE) N = N - SIZE
      IF (HEX(M,N) .NE. 0) NEAR = NEAR + 1
  100 CONTINUE
      RETURN
      END
C!**
C*************************************************************************
```

```
C**
C** SUBROUTINE TO DETERMINE HOW MANY NEXT NEAREST NEIGHBORS A MOLECULE HAS
C**
C*************************************************************************
C**
      INTEGER FUNCTION NEXT(MO,NO,ODD)
C      INCLUDE 'SIMCOMA.FOR'     ! FOR VAX
$INSERT SIMCOMA.FOR
C      INCLUDE 'SIMCOMC.FOR'     ! FOR VAX
$INSERT SIMCOMC.FOR
      INTEGER ODD
      NEXT = 0
      DO 100 I = 1,6
      M = MO + NEXTM(I)
      N = NO + NEXTN(I,ODD)
      IF (M .LE. 0) M = M + SIZE
      IF (M .GT. SIZE) M = M - SIZE
      IF (N .LE. 0) N = N + SIZE
      IF (N .GT. SIZE) N = N - SIZE
      IF (HEX(M,N) .NE. 0) NEXT = NEXT + 1
  100 CONTINUE
      RETURN
      END
C!**
C*************************************************************************
C**
C** SUBROUTINE TO SOLVE REDHEAD EQUATION FOR E KNOWING T
C**
C*************************************************************************
C**
      FUNCTION EREDHD(T,BETA,NU,R,N)
      REAL BETA,NU,E,R,T
      F(E) = (NU / BETA ) * EXP(-E/(R*T)) - E/(R*T**2)
      FP(E) = (-1/(R*T)) * (1./T + (NU / BETA ) * EXP(-E/(R*T)))
C INITIAL GUESS: E = T * 30000. / 500.
      E = 30000. * T / 500.
      N = 0
   10 CORR = F(E) / FP(E)
      N = N + 1
      E = E - CORR
      IF (ABS(CORR/E) .GT. 0.001 .AND. N .LE. 25) GOTO 10
      EREDHD = E/1000.
C cal ==> Kcal
      RETURN
      END
C!**
C*************************************************************************
C**
C** SUBROUTINE TO SOLVE REDHEAD EQUATION FOR T KNOWING E
C**
C*************************************************************************
C**
      FUNCTION TREDHD(ET,BETA,NU,R,N)
      REAL BETA,NU,E,ET,R,T
      F(T) = (BETA / NU) * EXP(E/(R*T)) - R*T**2/E
      FP(T) = -(BETA * E / (T**2 * NU)) * EXP(E/(R*T)) - 2.*R*T/E
      E = ET*1000.
C Kcal ==> cal
C INITIAL GUESS: T = 500. * E / 30000.
      T = 500. * E / 30000.
      N = 0
   10 CORR = F(T) / FP(T)
      N = N + 1
      T = T - CORR
      IF (ABS(CORR/T) .GT. 0.001 .AND. N .LE. 25) GOTO 10
      TREDHD = T
      RETURN
      END
C!**
C*************************************************************************
C**
```

```
C** SUBROUTINE TO CALCULATE DISTANCES
C**
C*************************************************************************
C**
      FUNCTION DIST(M1,N1,M2,N2,R)
      X(M) = M * 0.866025403
      Y(M,N) = N + 0.5*ABS(1.*MOD(M,2))
      DIST = R * SQRT((Y(M1,N1)-Y(M2,N2))**2 + (X(M1)-X(M2))**2)
      RETURN
      END
```

[BHT.N2.AP]SIMCOMA.FOR

```
      COMMON /A/ NEARM,NEARN,NEXTM,NEXTN,NADS,NEXP,NDES,COV,DHOP
     1 ,AHOP,ADIS,ADIS2,DDIS,DDIS2,EXPOS
      INTEGER NEARM(6),NEARN(6,2),NEXTM(6),NEXTN(6,2)
      INTEGER NADS,NEXP,NDES,AHOP,DHOP
      REAL COV,ADIS,ADIS2,DDIS,DDIS2,EXPOS
C**
```

[BHT.N2.AP]SIMCOMB.FOR

```
      COMMON /B/ EI,NU,EA,ER,EO,EN,ED,NDSB,IR,K,KT,CHI,EM,ES
     1  ,INT,INTS
      INTEGER NDSB,IR,INT(49),INTS(7)
      REAL EI(49),NU(49),EA,ER,EO,EN,ED,K,KT,CHI,EM,ES
C**
```

[BHT.N2.AP]SIMCOMC.FOR

```
      COMMON /C/ SIZE,HEX
      INTEGER*2 HEX(100,100)
      INTEGER SIZE
C**
```

[BHT.N2.AP]SIMCOMD.FOR

```
      COMMON /D/ PMO,PDO,PSO,PDEN,PDI,PCPD,PCTD
      REAL PMO,PDO,PSO,PDEN,PDI(49),PCPD(49),PCTD(49)
C**
```

[BHT.N2.AP]SIMCOME.FOR

```
      COMMON /E/ M,N,NHOP,DSBFLG,MX,NX,PREFLG
      INTEGER M,N,NHOP,DSBFLG,MX,NX,PREFLG
C**
```

1.3 Programs RAST and NU

[BHT.N2.NEW]RAST.FOR

```
C** PROGRAM TO DEVELOP A RANDOM ORDERED RASTER LIST FOR A n BY n ARRAY
C**
      INTEGER RAS(10000),LIST(2,10000)
      REAL RN(10000)
      TYPE *,'Input N, IR'
      ACCEPT *,N,IR
      DO 10 I = 1,N
      DO 10 J = 1,N
      K = J + (I-1)*N
      RAS(K) = I*10000 + J
      RN(K) = RAN(IR)
   10 CONTINUE
      CALL VSRTP(RN,K,RAS)
      DO 30 I=1,K
      LIST(1,I) = RAS(I) / 10000
      LIST(2,I) = RAS(I) - 10000 * LIST(1,I)
   30 CONTINUE
      WRITE (20,20) N,K
   20 FORMAT(1X,2I6)
      WRITE (20,212) (LIST(1,I),LIST(2,I),I=1,K)
  212 FORMAT(1X,2OI5)
      STOP
      END
```

[BHT.N2.NEW]NU.FOR

```
C*************************************************************************
C*************************************************************************
C****                                                                 *****
C****   PROGRAM TO MODEL N   ADSORPTION ON Ru(0001)                   *****
C****                        2                                        *****
C****   Compute Prefactor                                             *****
C*************************************************************************
C*************************************************************************
      INCLUDE 'AP:SIMCOMA.FOR'  ! FOR VAX
      INCLUDE 'AP:SIMCOMB.FOR'  ! FOR VAX
      INCLUDE 'AP:SIMCOMC.FOR'  ! FOR VAX
      INCLUDE 'AP:SIMCOMD.FOR'  ! FOR VAX
      INCLUDE 'AP:SIMCOME.FOR'  ! FOR VAX
C**
      REAL E,T,NAAVG,LCTP
      REAL NRN,DSBINT,nu0,a
      CHARACTER*72 LINE,TITLE
      REAL CDESPL(20)

        accept *,ic,nu0,A,B
C*************************************************************************
C** Now open file/read in input parameters
      READ (1,9999) TITLE
      READ (1,9999) LINE
 9999 FORMAT(A72)
      READ (1,*,END=99) ED,EM,EA,ER,EN
      READ (1,9999) LINE
      READ (1,*,END=99) CHI,SO,TS
      READ (1,9999) LINE
      READ (1,*,END=99) EXPMAX,IR,PRES
      READ (1,9999) LINE
      READ (1,*,END=99) DSBINT,PLTINT,DMPINT
      READ (1,9999) LINE
      READ (1,*,END=99) LCTP,NAAVG,BETA,DT
      T2 = TS
      READ (1,9999,END=99) LINE
      READ (1,*,END=99) ANNEAL,T2,PREFLG,NPASS
      READ (1,9999,END=99) LINE
```

```
      READ (1,*,END=99) (CDESPL(I),I=1,20)
C***
  99  WRITE(6,29) TITLE,ED,EN,ER,EA,EM,SO,CHI,IR,TS
   29 FORMAT('1',72('*'),/,1X,A72,/,1X,72('*'),//
     1  ,' DESORPTION ENERGY: ',
     2 F5.3,/,' DESTABILIZATION ENERGY FOR FILLED SITE:',F6.3,/,
     3 ' REPULSIVE INTERACTION ENERGY:',F6.3,/,
     4 ' ATTRACTIVE INTERACTIVE ENERGY:',F6.3,/,
     5 ' MIGRATION ACTIVATION BARRIER: ',F7.4,/,
     6 ' INITIAL STICKING COEFFICIENT: ',F6.4,/,
     7 ' CHI = ',F12.5,'    SEED: ',I9,/,' TEMPERATURE:',F6.1,//)
        if (ic .lt. 0)  type *,
        1       'NU(L) = ',nu0,'E(L) >',B,' ELSE  NU = ',A*NUO
        if (ic .gt. 0)  type *,
        1       'NU(L) = ',nu0,'*exp((',B,' - EI(L))*',A,')'
        if (ic .eq. 0)  type *,
        1       'NU(L) = ',nu0,'*exp(NR(L)*',A,' + NA(L)*',B,')'
       DO 312 NA = 1,7
       DO 312 NR = 1,7
       L = NA + (NR-1)*7
       EI(L) =  (NA-1.)*EA - (NR-1.)*ER
         if (ic) 501,502,503
501      if (EI(L) .LE. B) then
                NU(L) = A*NUO
         else
                NU(L) = NUO
         endif
         goto 312
502      NU(L) = nu0*exp((NR-1)*A + (NA-1)*B)
         goto 312
503      NU(L) = NUO*exp((B - EI(L))*A)
  312 CONTINUE
C*******************************************************************************
C**  Open/write prefactor (NU) array
C       OPEN(UNIT=20, FILE='NU.DAT', STATUS='NEW')
       write (20,222) (nu(i),i=1,49)
  222 FORMAT(1X,1P7E10.3)
       CLOSE(20)
       WRITE (6,311) (J-1,J=1,7),(J-1,(EI(I+7*(J-1)),I=1,7),J=1,7)
  311 FORMAT(/,38X,'ENERGY OF MOLECULES BY INTERACTIONS (Kcal/mole)',
     1  /,45X,'NUMBER OF ATTRACTIVE INTERACTIONS',/
     2          20X,7I10,/,' NUMBER OF',/,
     3       ' REPULSIVE  ',I6,2X,7F10.4,6(/,12X,I6,2X,7F10.4),/)
       WRITE (6,313) (J-1,J=1,7),(J-1,(nu(I+7*(J-1)),I=1,7),J=1,7)
  313 FORMAT(/,40X,'PREFACTOR BY NUMBER OF INTERACTIONS (sec-1)',
     1  /,45X,'NUMBER OF ATTRACTIVE INTERACTIONS',/
     2          20X,7I10,/,' NUMBER OF',/,
     3       ' REPULSIVE  ',I6,2X,1P7E10.3,6(/,12X,I6,2X,7E10.3),/)
C**
       STOP
       END
```

1.4 Sample Command Procedures

[BHT.N2.AP]FM1.COM

```
$ SETNAME "N2 Simulation"
$ SET DEF [BHT.N2.AP]
$ queue :=b4                          ! Queue for plotting
$ temp :==scr01:[s.bht]               ! location for output files
$ ASSIGN 'TEMP' TEMP:
$ delete TEMP:ads.out;*,dsb.out;*,ADS.DAT;*/NOLOG
$ ass TEMP:rast.dat FOR020
$ RUN [BHT.N2.NEW]RAST
96,100001                             ! Lattice size, random number
$ name :=FM1                          ! Run name
$ copy SYS$COMMAND TEMP:ads.dat/L       ! input to ADS and NU follows
FM1 (A2) -- 95K FOR 4.0 L (P=7.5E-8), THEN 78K (P=7.5E-8),
ED,  EM,    EA,      ER,   EN,
1.6, 0.284, 0.45, 0.275, 0.22
CHI,       SO,    TS
1000., 0.125,    85
EXPMAX,  TMAX,   PRES
2.0,     106.7, 7.5E-8
DSBINT, PLTINT, DMPINT
0.1,       0.02,    0.1
LCTP,  <NA>, BETA, DT
115.0,  1.5,  6.0, .5
ANNEAL,  STKMIN, PREFLG, NPASS
53.333,   0.00,      1,    10
ARRAY OF 20 MAP INTERVALS (COVERAGE):
0.336,0.412,0.443,0.483,0.530,1.0,1,1,1,1,1,1
1.0,1.0,1.0,1.0,1.0,1.0,1.0,1.0,1.0
ARRAY OF 20 MAP INTERVALS (TIME):
53.333,10000,10000,10000,10000,10000,10000,10000,10000,10000,10000
10000,10000,10000,10000,10000,10000,10000,10000,10000,10000
New Parms: T, ISO,   PRES
          78,   2,   7.5E-8
DSBINT, PLTINT, DMPINT
0.4,       0.02,    0.1
ANNEAL, STKMIN, NPASS
   0.0,  -0.1,    10
$ ass TEMP:ads.dat for001
$ ASS TEMP:NU.DAT FOR020
$ run [BHT.N2.new]nu
0,1.e13,1.,0.35
$ SJE
attach/wait
set/limit=16000
copyin TEMP:nu.dat, nu.dat
copyin TEMP:ads.dat, ads.dat
copyin TEMP:rast.dat, rast.dat
:s(xhmeia):bht:ads.img
100001
copyout/CC :s(xhmeia):bhtout.ads, TEMP:ads.out
copyout for008.dat, TEMP:for008.
copyout for009.dat, TEMP:for009.
del :s(xhmeia):bhtout.ads
:s(xhmeia):bht:dsb.img
TMIN,TMAX,TINT, CMIN
75,  160,    4, 0.14
IR,   MAPN, PREFLG, ATMAX
100001,  1,      1,    .25
ARRAY OF 20 MAP INTERVALS:
0.483,0.443,0.411,0.336,0.279,0.210,0.138,0.068,0.027,-1.0
-1.0,-1.0,-1.0,-1.0,-1.0,-1.0,-1.0,-1.0,-1.0,-1.0
copyout/CC :s(xhmeia):bhtout.dsb, TEMP:dsb.out
copyout for010.dat, TEMP:for010.
copyout for015.dat, TEMP:for015.
copyout for014.dat, TEMP:for014.
del :s(xhmeia):bhtout.dsb
```

```
detach
quit
$ rename TEMP:rast.dat,NU.DAT,for0%%.,%%%.OUT  .'name'/l
$ @[bht]chkque 'queue'
$ 'queue'/PAR=('NAME','TEMP',"","",'queue')/NAME='NAME'PLT/LOG='temp'PLT
$ nextjob ARRAY
```

[BHT.N2.AP]COMPCPY.COM

```
$ SET DEF [BHT.N2.AP]
$ apftn64/LIN/LIST/OPT=2/onetrip ADS
$ apftn64/LIN/LIST/OPT=2/onetrip DSB
$ apftn64/LIN/LIST/OPT=2/onetrip MIG
$ apftn64/LIN/LIST/OPT=3/onetrip COMSUB
$ PURGE *.LIS,*.AOB
$ aplink64 ads,mig,comsub
$ aplink64 dsb,mig,comsub
$ DEL ADS.AOB;,DSB.AOB;
$ PURGE *.img,*.AOB
$ sje
attach/wait/PRIORITY=1
copyin/binary ads.img, :s(xhemia):bht:ads.img
copyin/binary dsb.img, :s(xhemia):bht:dsb.img
detach
quit
$ nextjob array
```

Programs for FFT Computations

2.1 Program FFT

[BHT.N2.LEED]FFT.FOR

```
C*******************************************************************************
C*******************************************************************************
C**
C**     PROGRAM TO COMPUTE DIFFRACTION PATTERNS FROM A HEXAGONAL SURFACE
C**
C**  This program computes a 2-D FFT using a 1-D real to complex FFT and then
C**  a 1-D complex to complex FFT.  This gives matrix INTEN which gives
C**  intensities for one half of reciprocal space.  All reciprocal space is
C**  then mapped into this matrix by subroutine ARR.  Subroutine LSTFIT uses
C**  a least-squares iteration to determine the width, height and center of
C**  the root 3 spot.
C**
C**              Brian H. Toby  12/84
C**
C*******************************************************************************
C*******************************************************************************
      COMMON /A/ INTEN,M,N
      COMMON /B/ MO2P1,COV,COVT,IALL,NSCAT,RSCAT
      COMMON /pgplt/ NC,NC,K,GAM,ERRS,covS,exposS,timeS,eta
      character*72 TITLE
      REAL INTEN(129,256),INTNP(129,256)
      REAL SCAT(128,256)
      COMPLEX DPAT(129,256)
      INTEGER SIZE,TSIZE,PRVSZ,NSCAT,RSCAT
      INTEGER NA(20),nsel(4),siza(10),NSEG/20/
      REAL BETA,NU,NUO,E,T,NAAVG,LCTP,CHI,ERRS(4)
      REAL*8 DATSTR(2)
      REAL IMAX,MC,NC,K,GAM,R
      REAL XC(4),YC(4),YL1/0.0/,YL2/0.2/
      REAL ALIN(20),DLIN(20),XLIN(202),YLIN(202)
      REAL CDESPL(20),EDESPL(20),TDESPL(20)
      byte ch,ty(132)
      INTEGER fta,hofg,cnum,wofg,bhi,bwi,orient
      Data fta/9999/,orient/1/,nplt/0/,siza/10*0/
      DATA CDESPL/20*-1./,EDESPL/20*-1./,TDESPL/20*-1./
      DATA icd,ied,itd/3*1/
      D(I,J,MC,NC) = SQRT(((I-mc)/M)**2 + 3.*((j-nc)/N)**2)
      R3 = SQRT(3.)
c** ILOG   0 ==> linear intensity scaling
c** ILOG > 0 ==> log intensity scaling
c** ILOG < 0 ==> no versatec plot
!       TYPE *,'Enter 0 for a linear intensity scale; 1 for logarithmic'
!       TYPE *,'Enter -1 for no diffraction map'
!       ACCEPT *,ILOG
C
        nscat = 1
        rscat = 0
!       TYPE *,'Enter Scattering power of N2, Ru'
!       READ (5,*) NSCAT,RSCAT
       WRITE (6,913) NSCAT,RSCAT
  913 FORMAT(' N2 SCATTERING POWER IS',I3,/,
     1 ' Ru SCATTERING POWER IS',I3,/)
C
        type *,'Enter  0 for plotting on LA50 printer'
        type *,'Enter  1 for plotting on VT125 terminal'
        type *,'Enter  2 for plotting on Tektronix 4010 terminal'
        type *,'Enter -1 for no plotting'
        accept *,iplot
C
c       type *,'Enter  0 for unit weights'
c       type *,'Enter  1 for radial weighting'
c       type *,'Enter -1 for intensity weighting'
```

```
c       accept *,iweigh
c       IF (IWEIGH) 1,2,3
c1     type *,'Using intensity weighting'
c      goto 901
c2     type *,'Using unit weights'
c      goto 901
c3     type *,'Using radial weighting'
C*******************************************************************************
901    type *,'Enter 0 to process all spectra, 1 to select by coverage'
       ACCEPT *,iall
C
       IPASS1 = 0
!       iwr = 1          ! IWR is a flag -- 0 ==> Write intensity data on file
       IF (IALL .EQ. 0) THEN
           WRITE (6,914)
914        FORMAT(' PROCESS ALL MAPS',/)
       ELSE
         write (6,*) 'Enter map coverages'
         READ (5,*,END=199) (CDESPL(I),I=1,20)
199      write (6,*) 'Enter map exposures'
         READ (5,*,END=299) (EDESPL(I),I=1,20)
299      write (6,*) 'Enter map times'
         READ (5,*,END=399) (TDESPL(I),I=1,20)
       ENDIF
399      continue
C
       if (iplot .eq. 0) then
         CALL pgbegin(1,'tmp:printronix.rast/pri',1,1)
         CALL PGPAPER(10.,0.8,0.)
       elseif (iplot .eq. 1) then
         CALL pgbegin(1,'/vt',1,1)
       elseif (iplot .eq. 2) then
         CALL pgbegin(1,'/tek',1,1)
       endif
C*******************************************************************************
C** FILE DEFINITIONS
!       LUNQ = 1          ! QUIC FILE
       LUNo = 9
       LUNM = 10
       LUN = LUNM
!       IF(IWR .eq. 0) then
!         IWRT = 0               ! Open output file & write header now
!       else
!         IWRT = 1
!       endif
C*******************************************************************************
       DO 210 J=1,10
       CALL OPENIN(LUN,LUNo,NSCAT,RSCAT,TSIZE,IWRT,TITLE,ts)
!C** don't open file again
!       IWRT = 1
       SIZA(J) = TSIZE
       IF (TSIZE .LE. 0) GOTO 919
C**   NOW REDUCE TSIZE SO THAT SIZE = 2*N
       SIZE = 2 * IFIX(TSIZE / 2.)
       IF (SIZE .NE. TSIZE) WRITE (6,902) TSIZE,SIZE
  902  FORMAT(' REDUCING LATTICE SIZE FROM',I3,' TO',I3,/)
       IF (J .EQ. 1) PRVSZ = size
       IF (PRVSZ .NE. size) then
         WRITE(6,903) PRVSZ,SIZE
903      FORMAT(' ***ERROR*** UNEQUAL LATTICE SIZES',I3,'<>',I3)
         goto 998
       endif
       LUN = LUN + 1
  210 CONTINUE
C*******************************************************************************
C*******************************************************************************
  919 IF (LUN .EQ. LUNM) GOTO 998
       LUN = LUN - 1
       M = SIZE
```

```
      N = 2 * SIZE
      MO2P1 = SIZE / 2 + 1
C** Write results on file
922   format(a72)
      write (8,922) title
      write (8,923) M,N,NSCAT,RSCAT,ts
923   format(4i12,f8.2)
C*************************************************************************
!       INCLUDE 'QPLOT1.FOR'
C*************************************************************************
C** NOW READ IN MAPS
C*************************************************************************
1000  SUMSIZE = 0
      WRITE (6,33)
   33 FORMAT('0',75('*'))
C** IADD = 0 ==> Zero INTEN array before computing FFT intensity
      IADD = 0
      covS = 0.0
      exposS = 0.0
      timeS = 0.0
      imap = 0
      DO 220 L=LUNM,LUN
C SKIP OVER FILE IF IT HAS ENDED ALREADY
      tsize = SIZA(1+L-LUNM)
      IF (tsize .EQ. 0) GOTO 220
      CALL READIN(L,tsize,cov0,expos,time)
      IF (cov0 .LE. 0) THEN
C**     END OF FILE -- SKIP OVER FILE NEXT TIME
        SIZA(1+L-LUNM) = 0
        CLOSE(L)
        GOTO 220
      endif
      covS = covS + cov0*tsize*tsize
      exposS = exposS + expos*tsize*tsize
      timeS = timeS + time
      imap = imap + 1
C**   SHOULD WE DIFFRACT THIS MAP?
      IF (IALL .EQ. 0 .OR. IADD .NE. 0) THEN
        IFLAG = 1
      ELSE
        IFLAG = 0
        IF (ABS(COV0 - CDESPL(ICD)) .le. 0.011) THEN
           IFLAG = 1
           ICD = ICD + 1
        endif
        IF (ABS(expos/eDESPL(IeD)-1) .le. 0.05) THEN
          IFLAG = 1
          IeD = IeD + 1
        endif
        IF (ABS(time/tDESPL(ItD)-1.) .le. 0.05) THEN
          IFLAG = 1
          ItD = ItD + 1
        endif
      endif
      IF (IFLAG .EQ. 1) then
C**    Calculate the FFT
        CALL DIFFRACT(SCAT,DPAT,IADD)
        IADD = IADD + 1 ! Number of averaged FFTs
C**     IADD >= 1 ==> Add to INTEN array next time
      endif
      SUMSIZE = SUMSIZE + SIZA(1+L-LUNM)**2
      WRITE (6,34) L,COV0,expos,time,IFLAG
34    FORMAT(' File #',i3,' COVERAGE = ',F6.3,
     1  'N, EXPOS =',f7.2,'N, TIME =',f13.1,' Sec  (',I1,')')
  220 CONTINUE
C*************************************************************************
C IF SUMSIZE IS ZERO THEN ALL FILES ARE NOW EMPTY
      IF (SUMSIZE .LE. 0) goto 999
      covS = covS/sumsize
      exposS = 4.08*exposS/sumsize
```

```
      timeS = timeS/imap
      avgSIZE = SQRT(SUMSIZE)
      WRITE (6,35) covS,exposS,timeS
35    FORMAT(' Averages: COVERAGE = ',F6.3,
     1   'M, EXPOS =',f7.2,'L, TIME =',f13.1,' Sec',/,' ',75('*'))
      IF (IFLAG .NE. 1) goto 1000
c** Adjust intensities to reflect number of averaged maps
      IF (IADD .gt. 1) THEN
        DO 205 I=1,MO2P1
        DO 205 J=1,N
          INTEN(I,J) = INTEN(I,J) / iadd
205     CONTINUE
      ENDIF
C*******************************************************************************
C** Write results on file
      write (8,912) 0,covS,exposS,timeS,iadd
912     FORMAT(1X,I5,f6.3,f11.3,f11.1,i5)
C** Write out file?
C       IF (IWR .eq. 0) THEN
C         Write (luno,912) imore,covS,exposS,timeS
C         DO 206 J=1,N
C           write (luno,207) (INTEN(I,J),I=1,MO2P1)
C206      CONTINUE
C207      format(1x,1P12E10.3)
C       ENDIF
C*******************************************************************************
!       INCLUDE 'QPLOT2.FOR'
C*******************************************************************************
C**  Find the root 3 spot beam profile
 2000 NC = 0
      NC = N/3.
! start with small radius
      r = .10
      GAM = .02
!      ETA = 1.          ! Lorentzian
      ETA = 0.5
C** find approximate peak area as starting point for K
      NCPR = NC + R * M + 0.5
      NCMR = NC - R * M - 0.5
      K = 0
      DO 5 I=NCMR,NCPR
      K = K + ARR(I,J)
   5  CONTINUE
C refine K and GAMMA
      nsel(1) = 1
      nsel(2) = 0
      nsel(3) = 1
      CALL LSTFIT(R,nsel,.4,7)
C refine K, GAMMA and Eta
      nsel(1) = 1
      nsel(2) = 1
      nsel(3) = 1
C increase the size of the radius to 0.25 rlu
      r = 0.25
      CALL LSTFIT(R,nsel,.6,8)
      CALL tfit(iplot,nplt,r,1,title)
C** Write results on file
      write (8,908) K,ERRS(1),ETA,ERRS(2),GAM,ERRS(3)
      write (7,909) K,ERRS(1),ETA,ERRS(2),GAM,ERRS(3)
  908 FORMAT(1P8G10.3)
  909 FORMAT(' K = ',G10.3,' + or - (',G10.4,')',/,
     2 '  Eta = ',1PG10.3,' + or - (',G10.3,')',/,
     2 '  Gamma (FWHM) = ',1PG10.3,' + or - (',G10.3,')')

2500    continue
!       include '00fit.for'
 3000 CONTINUE
C       IF (IALL .NE. 0) then
C         type *,'Enter coverage'
```

```
C         READ (5,*,end=999) COVT
C       endif
        GOTO 1000
c* Delete font, close files
999     CONTINUE
!         IF (ILOG .ge. 0) then
!          call qfnt(-1,fta,orient)
!          CALL qini(1)
!       endif
        IF (Iplot .ge. 0) CALL pgend
!       IF (IWR .eq. 0) CLOSE(LUNo)
  998 STOP
        END
C!*****************************************************************************
        FUNCTION ARR(I,J)
        COMMON /A/ INTEN,M,N
        REAL INTEN(129,256)
        IP = MOD(I,M) + 1
        IF (IP .LE. 0) IP = IP + M
        JP = MOD(J,N) + 1
        IF (JP .LE. 0) JP = JP + N
        IF (IP .GT. M/2+1 .AND. JP .EQ. 1) THEN
          ARR = INTEN(M+2-IP,1)
        ELSE IF (IP .GT. M/2+1) THEN
          ARR = INTEN(M+2-IP,N+2-JP)
        ELSE
          ARR = INTEN(IP,JP)
        ENDIF
        RETURN
        END
```

[BHT.N2.LEED]DIFFRACT.FOR

```
C!*****************************************************************************
        SUBROUTINE DIFFRACT(SCAT,DPAT,IADD)
        COMMON /A/ INTEN,M,N
        COMMON /B/ MO2P1,COV,COVT,IALL,NSCAT,RSCAT
        COMMON /C/ SIZE,HEX
C**
        REAL SCAT(M,N),WK(1486)
        COMPLEX DPAT(MO2P1,N),CVEC(256)
        REAL INTEN(129,256)
        INTEGER HEX(128,128)
        INTEGER SIZE,TSIZE,NSCAT,RSCAT
C*****************************************************************************
C**  Lets start by expanding the "Quasi-rectangular" HEX matrix into the
C       "True Rectangular" matrix SCAT
        DO 1000 J = 1,N
        NJ = (J + 1)/2
        DO 1000 I = 1,M
        SCAT(I,J) = 0
        IF (MOD(I+J,2) .EQ. 0) GOTO 1000
        SCAT(I,J) = NSCAT * HEX(I,NJ) + RSCAT
 1000 CONTINUE
C*****************************************************************************
C**  Now compute the FFT of the matrix
C*****************************************************************************
C** COMPUTE THE FFT ALONG THE FIRST AXIS
        DO 240 J=1,N
        CALL FFTRC(SCAT(1,J),M,DPAT(1,J),WK,WK)
  240 CONTINUE
C** COMPUTE THE FFT ALONG THE SECOND AXIS
        DO 250 I=1,MO2P1
C** REMOVE ROW FROM MATRIX
        DO 251 J = 1,N
        CVEC(J) = DPAT(I,J)
  251 CONTINUE
C** NOW TRANSFORM THE VECTOR
        CALL FFTCC(CVEC,N,WK,WK)
```

```
C** PUT ROW BACK INTO MATRIX
      DO 252 J = 1,N
      DPAT(I,J) = CVEC(J)
  252 CONTINUE
  250 CONTINUE
C*******************************************************************************
C** Now calculate intensity (magnitude **2) from complex matrix
      IF (IADD .eq. 0) THEN
        DO 205 I=1,MO2P1
        DO 205 J=1,N
          INTEN(I,J) = 4.*(CABS(DPAT(I,J)) / (M*N))**2
c** the 4 adjusts the intensities to reflect that the SCAT array is half zeros
205     CONTINUE
      ELSE
        DO 206 I=1,MO2P1
        DO 206 J=1,N
          INTEN(I,J) = INTEN(I,J) + 4.*(CABS(DPAT(I,J)) / (M*N))**2
c** the 4 adjusts the intensities to reflect that the SCAT array is half zeros
206     CONTINUE
      ENDIF
C*******************************************************************************
      RETURN
      END
```

[BHT.N2.LEED]OPENIN.FOR

```
C!*******************************************************************************
      SUBROUTINE OPENIN(LUN,LUNo,NSCAT,RSCAT,TSIZE,IWR,TITLE,ts)
      COMMON /pgplt/ MC,NC,K,GAM,ERRS,covS,exposS,timeS
      REAL ERRS(4)
      character*72 TITLE
      character*50 fnam
      INTEGER LUN,LUNo,NSCAT,RSCAT,TSIZE,IWR
      REAL BETA,NU,NUO,E,T,NAAVG,LCTP,CHI
C*******************************************************************************
      WRITE (6,*) 'Enter filename'
      read (5,935,end=998) fnam
935   format(A50)
      open (unit=lun, file=fnam, status='old', err=998)
C*******************************************************************************
      READ (LUN,21,ERR=998,END=998) TSIZE,ED,EN,EA,ER,EM,SO,CHI,TS,
     1 DSBINT,IR,TITLE,LCTP,E,EO,NAAVG,DT,A,NUO,BETA
   21 FORMAT(I5,6F10.6,/,3F10.3,I12,/,A72,/,F10.1,2F10.6,F6.2,
     1 F6.4,F6.2,E9.2,F6.1)
      RATIO = ER / EA
  211 WRITE(6,29) TITLE,TSIZE,TSIZE,ABS(ED),EN,ER,EA,
     1 RATIO,EM,SO,CHI,TS,IR
   29 FORMAT('O',72('*'),/,1X,A72,/,1X,72('*'),//' LATTICE IS',I4,
     1  ' BY',I4,/,' DESORPTION ENERGY: ',
     2 F5.3,/,' DESTABILIZATION ENERGY FOR FILLED SITE:',F7.3,/,
     3 ' REPULSIVE INTERACTION ENERGY:',F6.3,/,
     4 ' ATTRACTIVE INTERACTIVE ENERGY:',F6.3,/,
     5 ' ER / EA: ',F5.3,/,' MIGRATION ENERGY: ',F7.4,/,
     6 ' INITIAL STICKING COEFFICIENT: ',F6.4,/,' CHI = ',F12.5,
     7 /,' ADSORPTION TEMPERATURE:',F6.1,/,
     8 ' RANDOM STARTING POINT:',I10,//)
C*******************************************************************************
!       IF (IWR .ne. 0) RETURN
C*******************************************************************************
!       Write (LUNo,21) SIZE,ED,EN,EA,ER,EM,SO,CHI,TS,
!      1 DSBINT,IR,TITLE,LCTP,E,EO,NAAVG,DT,A,NUO,BETA
!       Write (LUNo,*) NSCAT,RSCAT
      RETURN
C** return to main program - Unexpected end of file or other error
998   TSIZE  = -1
      RETURN
      END
```

[BHT.N2.LEED]READIN.FOR

```
C!*****************************************************************************
      SUBROUTINE READIN(LUN,tsize,cov0,expos,time)
      COMMON /C/ SIZE,HEX
C**
      INTEGER HEX(128,128)
      INTEGER SIZE,TSIZE
C*****************************************************************************
C** readin preface of map
      READ (LUN,912,END=999) imore,cov0,expos,time
912     FORMAT(1X,I5,f6.3,f11.3,f11.1)
      if (imore .eq. 0) goto 999
C*****************************************************************************
C** NOW READ IN MAP (HEX MATRIX)
C*****************************************************************************
 1000 ICOV = 0
      DO 1003 I = 1, TSIZE
      READ (lun,911,END=998) (HEX(I,J),J=1,TSIZE)
  911 FORMAT(1X,100I1)
C** now compute actual coverage on surface
c       DO 1003 J = 1, TSIZE
c       IF (HEX(I,J) .NE. 0) ICOV = ICOV + 1
 1003 CONTINUE
c       COV = ICOV / (1.*TSIZE **2)
C*****************************************************************************
C** return to main program - readin successful
      RETURN
C** return to main program - no more maps on file
999   COVO =  0.0
      RETURN
C** return to main program - Unexpected end of file or other error
998   COVO =  -1.0
      RETURN
      END
```

[BHT.N2.LEED]TFIT.FOR

```
C!*****************************************************************************
      SUBROUTINE tfit(iplot,nplt,Rp,itype,title)
      COMMON /A/ INTEN,M,N
      COMMON /pgplt/ MC,NC,K,GAM,ERRS,covS,exposS,timeS,eta
      character*72 TITLE
C**
      REAL INTEN(129,256)
      INTEGER NA(20),NSEG/20/
      Character*36 ty
      Character*40 ty1
      REAL ERRS(4),par(4)
      REAL ALIN(20),DLIN(20),R,Rp,XLIN(202),YLIN(202),MC,NC,K,GAM
      integer zero(4)/4*0/
      D(I,J,MC,NC) = SQRT(((I-mc)/M)**2 + 3.*((j-nc)/N)**2)
      R3 = SQRT(3.)
!       R = 2.*gam
        R = Rp
C** Now compute the radially averaged beam profile
      PAR(1) = K
      PAR(2) = ETA
      PAR(3) = GAM
      AMAX = DI(0.,PAR,zero)
      MCPR = MC + R * M + 0.5
      MCMR = MC - R * M - 0.5
      NCPR = NC + R * N / R3 + 0.5
      NCMR = NC - R * N / R3 - 0.5
      DO 220 I=1,NSEG
      ALIN(I) = 0.
      DLIN(I) = 0.
      NA(I) = 0
```

```
  220 CONTINUE
      DO 230 I=MCMR,MCPR
      DO 230 J=NCMR,NCPR
      if (i .eq. 0 .and. j .eq. 0) goto 230     ! omit center spot
      ID = NSEG * D(I,J,MC,NC) / R + 1
      IF (ID .GT. NSEG) GOTO 230
      A = ARR(I,J)
      ALIN(ID) = ALIN(ID) + A
      DLIN(ID) = DLIN(ID) + D(I,J,MC,NC)
      NA(ID) = NA(ID) + 1
  230 CONTINUE
      Write (7,242) (NA(I),I=1,NSEG)
  242 FORMAT(1X,20I6)
  241 FORMAT(1X,20F6.3)
      Write (7,241) (ALIN(I)/(AMAX*MAX(NA(I),1)),I=1,NSEG)
        if (iplot .lt. 0) return
c       if (nplt .ge. 0) CALL PGADVANCE
        nplt = nplt + 1
        CALL pgsetc(1.2)
        CALL pgenv(-r,r,0.,1.,0,0)
          encode (40,701,ty1) covs,exposs,times
701     format('Cov:',F4.2,', Exp:',F5.1,'L, Time =',1PG10.3,' s')
        if (itype .eq. 0) then
          CALL pglabel('Distance from [0,0] Beam (rlu)'
        1 ,'Scaled Intensity',ty1)
        else
          CALL pglabel('Distance from [\(2255)3,\(2255)3] Beam (rlu)'
        1 ,'Scaled Intensity',ty1)
        endif
        call pgMtext('R',1.5,0.5,0.5,title)
        if (iplot .lt. 0) then
           CALL pgsetc(.8)
           cspa = 0.025
        else
           CALL pgsetc(1.4)
           cspa = 0.06
        endif
        encode (36,703,ty) gam,errs(3)
703     format('FWHM (\gG): ',1pe9.3,'\(2233)',1pe8.2)
      xt = -.96 * R
      yt = 0.95
      call pgtext(xt,yt,ty)
        encode (36,704,ty) K,errs(1)
704     format('k: ',1pe9.3,'\(2233)',1pe8.2,2x)
      yt = yt - cspa
      call pgtext(xt,yt,ty)
        encode (36,705,ty) Eta,errs(2)
705     format('\gy: ',1pe9.3,'\(2233)',1pe8.2)
      yt = yt - cspa
      call pgtext(xt,yt,ty)
C** Now calculate and plot the fit beam profile
      J1 = 0
      DO 420 J=NSEG,1,-1
      IF (NA(J) .LE. 0) GOTO 420
      J1 = J1 + 1
      YLIN(J1) = ALIN(J)/(AMax*NA(J))
      XLIN(J1) = - DLIN(j)/NA(j)
  420 CONTINUE
C       if (iplot .eq. 0) then
C          CALL GRSETLW(3)                ! darker points
C       else
C         CALL GRSETCOL(2)                ! red
C       endif
      call pgpoint(j1,xlin,ylin,2)        ! plot points
      J1 = 0
      CALL GRSETCOL(3)                    ! green
      DO 430 I=MCMR,MCPR
      DO 430 J=NCMR,NCPR
```

```
      if (i .eq. 0 .and. j .eq. 0) goto 430     ! omit center spot
      Dt = D(I,J,MC,NC)
      IF (Dt .GT. r) GOTO 430
      if (j1 .ge. 200) then
        call pgpoint(j1,xlin,ylin,-1)   ! plot points
        J1 = 0
      endif
      J1 = J1 + 1
      yLIN(j1) = ARR(I,J)/amax
      xLIN(j1) = Dt
  430 CONTINUE
        call pgpoint(j1,xlin,ylin,-1)   ! plot points
C       if (iplot .eq. 0) then
C          CALL GRSETLW(1)              ! back to normal
C       else
C          CALL GRSETCOL(1)             ! white
C       endif
      J1 = 0
      DO 530 J=0,100
      J1 = J1 + 1
      XLIN(J1) = -J * R / 100.
      YLIN(J1) = DI(XLIN(J1),PAR,zero)/amax
  530 CONTINUE
        call pgline(j1,xlin,ylin)       ! draw connected line
      J1 = 0
      DO 540 J=0,100
      J1 = J1 + 1
      XLIN(J1) = J * R / 100.
      YLIN(J1) = DI(XLIN(J1),PAR,zero)/amax
  540 CONTINUE
        call pgline(j1,xlin,ylin)       ! draw connected line
        CALL PGADVANCE
999     RETURN
        END
```

2.2 Subroutine EQFIT

[BHT.N2.LEED]LSTFIT.FOR

```
C!*****************************************************************************
C** This subroutine calculates the best fit parameters for the n parameter
C** equation DI using a least squares iteration.
C**
C** NOTE: DI(...,NSEL,DERIV) returns the function and DERIV contains the
C** derivatives with respect to the parameters for which NSEL is non-zero
C**
C*****************************************************************************
      SUBROUTINE LSTFIT(R,Nsel,SP,NCYC)
      COMMON /A/ INTEN,M,N
      COMMON /pgplt/ MC,NC,K,GAM,ERRS,covS,exposS,timeS,eta
      REAL INTEN(129,256),ERRS(4)
      REAL DI,MC,NC,K,eta,GAM,DP(4),IMAX,PAR(4),TPAR(4),SFT,deriv(4)
      INTEGER PI,PJ,M,N,MI,NI,nsel(4),ipar(4),npar,zero(4)
      REAL*8 A(4,4),B(4)
      REAL*8 D1/-1.0/,D2,WK(8)
      data zero/4*0/
C* set up variables before starting
      R3 = SQRT(3.)
      SFT = SP
      PAR(1) = K
      PAR(2) = ETA
      PAR(3) = GAM
      MCPR = MC + R * M + 0.5
      MCMR = MC - R * M - 0.5
      NCPR = NC + R * N / R3 + 0.5
      NCMR = NC - R * N / R3 - 0.5
      RFACP = 0.
      GOFP = 0.
      SUMARR = 1.E-20
      SUMWA2 = 1.E-20
      NP = 0
      NPAR = 0
C** Select parameters to be varied
      DO 101 I=1,3
        iPAR(I) = 0
        ERRS(I) = 0.0
        if (nsel(I) .ne. 0) then
          npar = npar + 1
          iPAR(npar) = i
        endif
  101 CONTINUE
C** Compute initial R factor and Goodness of fit
C**
      DO 130 I=MCMR,MCPR
      DO 130 J=NCMR,NCPR
      D = SQRT(((I-MC)/M)**2 + 3.*((J-NC)/N)**2)
      if (D .eq. 0) goto 130    ! omit center spot
C      if (i .eq. 0 .and. j .eq. 0) goto 130    ! omit center spot
      NP = NP + 1
      SUMARR = SUMARR + ARR(I,J)
      SUMWA2 = SUMWA2 + ARR(I,J)**2
      ERR = ARR(I,J) - DI(D,PAR,zero,deriv)
      RFACP = RFACP + ABS(ERR)
      GOFP = GOFP + ERR**2
  130 CONTINUE
      GOFP = SQRT(GOFP/(NP - NPAR))
      WRFACP = SQRT(GOFP/SUMWA2)
      RFACP = RFACP/SUMARR
      ICNT = 0
C** create working copy of parameters (TPAR), zero matrix and vector terms
   10 DO 100 PI=1,4
      TPAR(PI) = PAR(PI)
      B(PI) = 0.0
      DO 100 PJ=1,4
```

```
      A(PI,PJ) = 0.0
  100 CONTINUE
      ICNT = ICNT + 1
C** Compute variance - covariance matrix
      DO 230 I=MCMR,MCPR
      DO 230 J=NCMR,NCPR
c      if (i .eq. 0 .and. j .eq. 0) goto 230    ! omit center spot
        D = SQRT(((I-MC)/M)**2 + 3.*((J-NC)/N)**2)
        if (D .eq. 0) goto 230  ! omit center spot
        ERR = ARR(I,J) - DI(D,PAR,NSEL,deriv)
        DO 240 PI=1,NPAR
          DP(PI) = deriv(ipar(PI))
          B(PI) = B(PI) + ERR * DP(PI)
240     CONTINUE
        DO 250 PI=1,NPAR
        DO 250 PJ=1,NPAR
          A(PI,PJ) = A(PI,PJ) + (DP(PI) * DP(PJ))
250     CONTINUE
230   CONTINUE
C** Solve matrix equation
      if (npar .ne. 2) then
        CALL LINV3F(A,B,3,NPAR,4,D1,D2,WK,IERR)
        IF (IERR .NE. 0) THEN
          TYPE *,'MATRIX INVERSION PROBLEM, CYCLE =',ICNT
          GOTO 999
        ENDIF
      elseif (A(1,2) .ne. A(2,1)) Then
C** non-symmetric matrix
        write (6,*) 'non-symmetric matrix:',A(1,2),A(2,1)
          GOTO 999
      else
C** Invert 2x2 matrix A
        AFC = A(1,1)*A(2,2) - A(1,2)**2
        AT = A(1,1)
        A(1,1) = A(2,2)/AFC
        A(2,2) = AT/AFC
        A(1,2) = -1.*A(1,2)/AFC
        A(2,1) = A(1,2)
C** multiply 2x2 matrix A**-1 times B
        B1 = A(1,1) * B(1) + A(1,2) * B(2)
        B(2) = A(1,2) * B(1) + A(2,2) * B(2)
        B(1) = B1
      endif
      DO 444 I=1,NPAR
        IF (A(I,I) .GT. 0.0) ERRS(ipar(I)) = GOFP*SQRT(A(I,I))
        TPAR(ipar(I)) = PAR(ipar(I)) + SFT*B(I)
444   continue
      RFAC = 0.
      GOF = 0.
C** Recompute R factor and Goodness of fit
      DO 330 I=MCMR,MCPR
      DO 330 J=NCMR,NCPR
c      if (i .eq. 0 .and. j .eq. 0) goto 330    ! omit center spot
      D = SQRT(((I-MC)/M)**2 + 3.*((J-NC)/N)**2)
      if (D .eq. 0) goto 330    ! omit center spot
      ERR = ARR(I,J) - DI(D,TPAR,zero,deriv)
      RFAC = RFAC + ABS(ERR)
      GOF = GOF + ERR**2
  330 CONTINUE
      GOF = SQRT(GOF/(NP - NPAR))
      WRFAC = SQRT(GOF/SUMWA2)
      RFAC = RFAC/SUMARR
C** Has refinement diverged?
      IF (GOF .GE. GOFP) then
C* Yes, use refinement results from previous cycle
        DO 445 I=1,NPAR
          TPAR(ipar(I)) = PAR(ipar(I))
445     continue
C** Has refinement converged?
```

```
      elseIF (GOF*1.000001 .LT. GOFP .and. ICNT .LE. NCYC) then
C* No, use refinement results as starting point for next cycle
        SFT = AMIN1(1.,SFT + (1. - SP)/(NCYC - 2.))
        RFACP = RFAC
        WRFACP = WRFAC
        GOFP = GOF
        DO 446 I=1,4
446     PAR(I) = TPAR(I)
        GOTO 10
      endif
999   K   = TPAR(1)
      ETA = TPAR(2)
      GAM = TPAR(3)
!      WRITE (7,*)
!      WRITE (7,*)'CYCLE ',ICNT
!      WRITE (7,*)'         R factor = ',RFAC,' FROM (',RFACP,')'
!      WRITE (7,*)'Weighted R factor = ',WRFAC,' FROM (',WRFACP,')'
!      WRITE (7,*)'   Goodness of fit= ',GOF,' FROM (',GOFP,')'
!      WRITE (7,*)'Shifts muted by factor of',SFT
!      WRITE (7,*)'K  =   ',PAR(1),TPAR(1),errs(1)
!      WRITE (7,*)'Eta =  ',PAR(2),TPAR(2),errs(2)
!      WRITE (7,*)'GAMMA =',PAR(3),TPAR(3),errs(3)
!      WRITE (7,*)'CORRELATION COEF. MATRIX:'
!      write (7,4) ((A(I,J)/SQRT(A(I,I)*A(J,J)),J=1,NPAR),I=1,NPAR)
    4 FORMAT(4(1X,1P<NPAR>G13.6,/))
      RETURN
      END
C!*****************************************************************************
C** This subroutine calculates the Pseudo-Voigt intensity function in two space
C** and its derivatives with respect to each parameter
C*****************************************************************************
      FUNCTION DI(D,PAR,nsel,deriv)
      COMMON /A/ INTEN,M,N
      REAL INTEN(129,256)
      REAL G,L,c1,y1,X,X2,D,DI,PAR(4),Pi,DERIV(4)
      INTEGER NSEL(4)
      data C4Ln2,C8Ln2/2.7725887,5.5451774/,Pi/3.14159265/
      data S1n2Pi/0.4697186/
C       PAR(1) ==> K -- integrated intensity
C       PAR(2) ==> eta -- 0 -> Gaussian; 1 -> Lorentzian
C       PAR(3) ==> gamma -- Full Width at Half maximum (FWHM)
C*****************************************************************************
C** Compute needed intermediates (in hopes of saving time)
      X = D / PAR(3)
      X2 = X*X
C Gaussian
      G = EXP(-C4ln2*X2)
C Lorentzian
      L = 1./(1.+4.*X2)
C weighted Lorentzian + Gaussian
      y1 = (PAR(2)*L/Pi + (1.-PAR(2))*G*S1n2Pi)
C coefficient
      c1 = 2. * PAR(1) / PAR(3)
C*****************************************************************************
C** ALWAYS -- CALCULATE INTENSITY FUNCTION
C*****************************************************************************
      DI = c1 * Y1
C*****************************************************************************
C** NSEL(1) Non-zero -- CALCULATE DERIVATIVE W/R TO PAR(1)
C*****************************************************************************
      if (NSEL(1) .ne. 0) DERIV(1) = 2. * y1 / PAR(3)
C*****************************************************************************
C** NSEL(2) Non-zero -- CALCULATE DERIVATIVE W/R TO PAR(2)
C*****************************************************************************
      if (NSEL(2) .ne. 0) DERIV(2) = c1 * (L/Pi - G*S1n2Pi)
C*****************************************************************************
C** NSEL(3) Non-zero -- CALCULATE DERIVATIVE W/R TO PAR(3)
C*****************************************************************************
      if (NSEL(3) .ne. 0) then
        DL = 2./(PAR(3)*(.5/X + 2.*X)**2)
```

```
      DG = G * C8ln2 * X2 / PAR(3)
      DERIV(3) =
1       c1 * ((PAR(2)*DL/Pi + (1.-PAR(2))*DG*Sln2Pi) - y1 / PAR(3))
 endif
 RETURN
 END
```

Graphics Programs

3.1 The QUIC package

[BHT.LASER]QUIC.DOC

```
QUIC -- Graphics for the QMS/Talaris Laser Plotter
==================================================

Yet another package for doing graphics on XHMEIA is available. The laser
plotter has a very powerful graphics language, called QUIC which has
capabilities for shading, automatic generation of circles, sophisticated
lettering, user definable fonts and numerous other features.  Users who
wish to use simple, error-resistant, graphics routines for the laser plotter,
will be better off using the QMSPLOT package, which does not make use of many
of QUIC features (for example it does lettering by drawing the letters with
vectors!). However, for more demanding applications the loss of versatility
and speed from QMSPLOT may be intolerable. Or, the size of the "qms" files
produced by QMSPLOT may be much larger than acceptable.

As an alternative to use of QMSPLOT a library for functions, QUIC has been
prepared to allow simple use of many QUIC features.  Alas, the two packages
cannot be used together (mostly because QMSPLOT is very badly designed).
The QUIC routines are very fast, but require that the user know something
about the quic language (see the QMS QUIC Programming Manual, next to the
plotter).  As an example of it's power, a fairly complex graphics program
for the Versatec was relinked to QMSPLOT and produced "qms" files averaging
greater than 10,000 blocks per page and took 20 minutes (or more) per page to
print. The program was redesigned around the QUIC package using specially
designed fonts, the resulting "qms" files were reduced to 60 blocks/page and
print in well under a minute.

The QUIC routines do not perform any error checking.  It is the users
responsibility to feed them meaningful parameters and to be sure that commands
are given in the proper sequences (e.g. do not do vector plotting before
turning vector mode on). Nor do the routines currently allow access to all QMS
features. Additions of more routines to the library is strongly encouraged.

All output is buffered, to optimize the number of characters per line sent to
the plotter.  Brief descriptions of the routines follow; for more detail look
as the library source code and consult the QUIC manual.

Subroutine QINI(ini,LUNI,orient,fname)
        Used to start and stop plotting and to start a new page.

Subroutine QARC(x,y,r,ia1,ia2,iw)
        Used to generate an arc or circle

Subroutine QLBL(x,y,r,n,arr,id)
        Used to generate labels of adjustable sized lettering.

Subroutine QTONE(x,y,ip)
        Used to fill an enclosed area with a fill pattern

Subroutine QVEC(in,ipen)
        Used to enter/leave vector plotting mode

Subroutine QVMOV(x,y,in,im)
        Used to move/draw/erase while in vector mode

Subroutine QAPOS(r,im)
        Used for absolute positioning when not in vector mode

Subroutine QBUFF(NCHR,ENTRY,iclear)
        Used to buffer output from the above routines

Subroutine QFNT(iact,ftno,orient,ver,fnam,glyh,bas)
```

```
        Used to select/delete and define fonts

Subroutine QFDEF(iact,char,qlyw,bitmh,bitmw,voff,hoff)
        Used to prepare plotter to receive bit maps defining
        characters when loading fonts into the plotter.


Two sample programs which demonstrate the usage of these routines:

QDEMO   - QUIC graphics demonstration.
FONTDEM - Demonstration of simple font design and printing.


Comments and questions are welcome, suggestions for improvments will be
are also welcome, provided the person suggesting is willing to make the
appropriate changes himself/herself.

                                        Brian Toby (XHMEIA::BHT)
                                        6/15/85
```

[BHT.LASER]QUIC.FOR

```
C*************************************************************************
C                                                                        *
C   Routines to create QUIC commands for a TALARIS 800 Laser Printer     *
C                                                                        *
C       Brian Toby  June 1985                                            *
C                                                                        *
C!************************************************************************
        SUBROUTINE QTONE(x,y,ip)
C
C  Subroutine to generate a QUIC command to fill an area with a pattern
C    on Talaris Laser Printer. (x,y) may be any point inside the area
C    to be filled.
C
C  Parameters:
C       x  = interior point measured from left margin
C       y  = interior point measured from top margin
c       ip = fill pattern number (integer between 0 and 24)
C
C All of the above parameters are REAL, except ip which is INTEGER
C************************************************************************
        include 'quic.cmn'
        ix = (1000. * x) + 0.5
        iy = (1000. * y) + 0.5
        encode (18,701,buff) ix,iy,ip
701     format ('^LAF',2I5.5,i2.2,'^G')
      CALL qbuff(18,buff,0)
        return
        end
C!************************************************************************
        SUBROUTINE QARC(x,y,r,ia1,ia2,iw)
C
C  Subroutine to generate a QUIC command to draw an arc on the
C    Talaris Laser Printer. (x,y) will be the focus of the arc (which
C    need not lie on the page.) To draw a circle set ia1 = ia2
C
C  Parameters:
C       x   = arc center measured from left margin (inches)
C       y   = arc center measured from top margin (inches)
C       r   = radius of arc center (inches)
c       ia1 = starting angle for arc (degrees from x axis)
c       ia2 = ending angle for arc (degrees from x axis)
c       iw  = width of arc in dots (odd integer between 3 and 31)
C
C
C x,y,r are REAL, ia1,ia2,iw are INTEGER
```

```
C*************************************************************************
        include 'quic.cmn'
        ix = (1000. * x) + 0.5
        iy = (1000. * y) + 0.5
        ir = (1000. * r) + 0.5
        encode (28,701,buff) ix,iy,ir,ia1,ia2,iw
      CALL qbuff(28,buff,0)
701     format ('^LA',3I5.5,2i3.3,i2.2,'^G')
        return
        end
C!*************************************************************************
        SUBROUTINE QLBL(x,y,r,n,arr,id)
C
C  Subroutine to generate QUIC labeling
C
C  Parameters:
C       x   = height of letters (inches)
C       y   = width of letters (inches)
C       r   = distance from previous pass (inches)
c       n   = number of characters to be printed
c       arr = BYTE array of characters
C       id  = direction
C                1 for horizontal
C                2 for vertical - right
C                3 for vertical - left
C                4 for horizontal - upside down
C            if id is negative, decenders are turned off
C
C x,y,r are REAL, n,id are INTEGER
C*************************************************************************
        include 'quic.cmn'
        byte arr(1),dir(4)
        data dir/'M','V','E','U'/
        ix = (100. * x) + 0.5
        iy = (100. * y) + 0.5
        ir = (1000. * r) + 0.5
        encode (13,701,buff) dir(abs(id)),ix,iy,ir
      CALL qbuff(13,buff,0)
701     format('^',a1,2i3.3,i5.5)
        if (id .gt. 0) CALL qbuff(3,'^DL',0)
      CALL qbuff(n,arr,0)
c      CALL qbuff(2,'^-',0)
        return
        end
C!*************************************************************************
        SUBROUTINE QVEC(in,ipen)
C
C  Subroutine to enter/leave vector mode
C
C  Parameters:
C       in    =  0 vector mode on
C             <> 0 vector mode off
c       ipen  =  width of 'pen' in dots (odd integer between 3 and 31)
C
C in,ipen are INTEGER
C*************************************************************************
        include 'quic.cmn'
      if (in .eq. 0) then
c Vector mode on; pen up; define pen width
      CALL qbuff(6,'^IGV^U',0)
        encode (5,701,buff) ipen
701     format ('^PW',i2.2)
      CALL qbuff(5,buff,0)
      else
c Vector mode off
      CALL qbuff(4,'^IGE',0)
      endif
        return
```

```
        end
C!*****************************************************************************
        SUBROUTINE QVMOV(x,y,in,im)
C
C  Subroutine to move/draw vectors (in vector mode)
C
C  Parameters:
c       X     =  X coordinate value or array (measured from left margin)
c       Y     =  Y coordinate value or array (measured from top margin)
c       in    =  number of (x,y) points
C       im    =  0 move to first number, draw to remaining numbers
C             >  0 draw to first number, draw to remaining numbers
C             <  0 move to first number, erase to remaining numbers
C
C x,y are REAL, in,im are INTEGER
C*****************************************************************************
        include 'quic.cmn'
        REAL X(1),Y(1)
        if (im .le. 0) then
      CALL qbuff(3,'^U ',0)
        else
      CALL qbuff(3,'^D ',0)
        endif
        DO 100 i = 1,in
        if (i .eq. 2 .and. im .lt. 0) CALL qbuff(3,'^E ',0)
        if (i .eq. 2 .and. im .eq. 0) CALL qbuff(3,'^D ',0)
        ix = (1000. * x(i)) + 0.5
        iy = (1000. * y(i)) + 0.5
        encode (12,701,buff) ix,iy
701     format (i5.5,':',i5.5,' ')
      CALL qbuff(12,buff,0)
  100   Continue
        return
        end
C!*****************************************************************************
        SUBROUTINE QAPOS(r,im)
C
C  Subroutine for absolute positioning (non-vector mode)
C
C  Parameters:
c       r  =  absolute distance (inches)
C       im =  1 ==> r is vertical distance measured from top of page
C          =  2 ==> r is horizontal distance measured from left edge of page
C
C r is REAL, im is INTEGER
C*****************************************************************************
        include 'quic.cmn'
        byte char(2)
        data char/'V','H'/
        ir = (1000. * r) + 0.5
        encode (8,701,buff) char(im),ir
701     format ('^I',a1,i5.5)
      CALL qbuff(8,buff,0)
        return
        end
C!*****************************************************************************
        Subroutine QINI(ini,LUNI,orient,fname)
C
C  Subroutine to initialize/close plotting file
C
C  Parameters:
C       ini     = 0 if file is to be opened
C               > 0 if file is to be closed
C               < 0 to start new page
C       LUNI    = Logical unit number for plotting file
c       orient  = orientation of page: 1 = landscape; 2 = portrait
c       fname   = output file name
C
C All of the above parameters are INTEGER, except fname which is BYTE
```

```
C*************************************************************************
        include 'quic.cmn'
        byte char(2),fname(1)
        byte reset(15)
        integer orient
        data char/'L','P'/
        data reset/'R','e','S','e','T','r','E','s','E','t'
        1         ,'R','e','S','e','T'/
      if (ini) 3,1,2
C** Open file and initialize Laser printer
1       LUN = luni
        open(unit=LUN,status='new',carriagecontrol='list',
        1       name=fname)
        loc = 0
        call QBUFF(15,reset,1)
        call QBUFF(5,'^PY^-',1)
        call QBUFF(10,'^DFEA^G^I0',0)
        call QBUFF(1,char(orient),0)
        call QBUFF(38,'^ISYNTAX00000^IFXX0X^IJ00000^IT00000^F',1)
        return
C** Terminate plot and close file
2       call QBUFF(30,'^IT00^IJ00^I0L^IS1217^IFXX0X^0',1)
        call QBUFF(7,'^-^PN^-',1)
        close (LUN)
        return
C** Start new page
3       call QBUFF(4,'^-^,',1)
        return
        end
C!*************************************************************************
        SUBROUTINE QBUFF(NCHR,ENTRY,iclear)
C  Subroutine to buffer output
C
C  Parameters:
c       nchr    = number of characters to be added to buffer (must be < 132)
c               = 0 do not add any characters, write out buffer
c
C       entry   = BYTE array of characters
c
C       iclear  = 0 save array in buffer, empty buffer first, if needed
C               <> 0 as above, plus write out buffer after adding array
C
C All of the above parameters are INTEGER, except entry which is BYTE
C*************************************************************************
        include 'quic.cmn'
        BYTE ENTRY(1)
        INTEGER iclear,nchr
        if (nchr .eq. 0) goto 120
c** will current line fit in buffer?
100     IF (loc+NCHR .LE. 132) GO TO 102
c no: empty the buffer
        write (LUN,701) (line(i),i=1,loc)
701     format (132A1)
        loc = 0
c yes: line will fit
102     L2=loc+NCHR
        J=0
        DO 110 I=loc+1,L2
          J=J+1
          line(I)=ENTRY(J)
110     CONTINUE
        Loc=L2
c Should we clear the buffer before exiting?
        if (iclear .eq. 0) return       ! (no)
c yes: empty the buffer
120     write (LUN,701) (line(i),i=1,loc)
        loc = 0
        return
        END
```

```
C!*****************************************************************************
      SUBROUTINE QFNT(iact,ftno,orient,ver,fnam,glyh,bas)
C
C  Subroutine to select/delete/start definition of a font
C
C  Parameters:
C       iact    = action to take:
C                       1 define font
C                       0 select font as default
C                      -1 delete font
C       ftno    = Font number
C       orient  = orientation of page: 1 = landscape; 2 = portrait
c       ver     = version number (0-9)
c       fnam    = font name (4 characters)
c       glyh    = height of glyph (in dots, 300 dots/inch)
C       bas     = baseline height (in dots)
C
C All of the above parameters are INTEGER, except fnam which is BYTE
C*****************************************************************************
      include 'quic.cmn'
      byte fnam(1),dir(2)
      integer iact,ftno,orient,ver,glyh,bas
      data dir/'Y','X'/
      if (iact) 900,100,400
c** Select font as default
100   encode (8,101,buff) ftno
101   format('^IS',i5.5)
      call qbuff(8,buff,0)
      return
c** Define font
400   encode (20,401,buff) ftno,dir(orient),ver,fnam,glyh,bas
401   format('^DF',i5.5,a1,i1,a4,2i3.3)
      call qbuff(20,buff,0)
      return
c** Delete font
900   encode (11,901,buff) ftno,dir(orient)
901   format('^DF',i5.5,a1,'^G')
      call qbuff(11,buff,0)
      return
      end
C!*****************************************************************************
      SUBROUTINE QFDEF(iact,char,qlyw,bitmh,bitmw,voff,hoff)
C
C  Subroutine to define characters by of a font
C
C  Parameters:
C       iact    = action to take:
C                       0 define character in font
C                      -1 end font definition
C       char    = character to be defined (BYTE)
c       glyw    = width of glyph (in dots, 300 dots/inch)
C       bitmh   = height of bit map (in dots)
C       bitmw   = width of bit map (in dots)
C       voff    = vertical offset (in dots)
C       hoff    = horizontal offset (in dots)
C
C All of the above parameters are INTEGER, except char which is BYTE
C*****************************************************************************
      include 'quic.cmn'
      byte char
      integer iact,qlyw,bitmh,bitmw,voff,hoff
      if (iact .ge. 0) goto 900
c** close font definition
      call qbuff(2,'^G',0)
      return
c** Define font
900   encode (19,901,buff) char,qlyw,bitmh,bitmw,voff,hoff
901   format(', ',z2.2,5i3.3)
      call qbuff(19,buff,0)
```

```
        return
        end
```

[BHT.LASER]QUIC.CMN

```
        COMMON /QUIC/ LOC,LUN,LINE,BUFF
        BYTE LINE(132),BUFF(132)
        INTEGER LOC,LUN
```

[BHT.LASER]FONTDEM.FOR

```
      INTEGER SIZE,NC(4)
      INTEGER fta,ftb,hofg,cnum,wofg,bhi,bwi,orient/1/
        logical*1 ty(100),tyn(4)
        data tyn/'A','B','C','D'/
      Data fta/9999/,ftb/9998/
      DATA SIZE/100/
      SIN60 = SIN(3.14159/3.)
        LUN = 30
C** START Plot -- landscape mode
        call qini(0,LUN,orient,'font.qms')
c** define the glyph heigth and width
        Hofg = 8.5 * 300. / 70. ! Font size in dots (300 dots/inch)
        wofg = hofg      ! square font: glyph height is same as width
        bhi = hofg       ! height of bit map (in dots)
        bwi = hofg       ! width of bit map (in dots)
c** define the diameter of a circle in inches
        SCL = hofg / 300.
C*************************************************************************
C*NOW DEFINE THE FONT SET
        call qfnt(1,fta,orient,0,'bht1',wofg,0)
C* CHAR 41 (A) -- An open circle
        call qfdef(0,'A',hofg,bwi,bhi,0,0)
      CALL font(LUN,bhi,bwi,1,2)
C* CHAR 42 (B) -- An open circle and a concentric filled circle
        call qfdef(0,'B',hofg,bwi,bhi,0,0)
      CALL font(LUN,bhi,bwi,3,5)
c** End font definition
        call qfdef(-1)
C*************************************************************************
c** Fill page with circles
        call qfnt(0,fta)
      DO 100 M=1,15
      ODD = 2 - MOD(M,2)
      X = (1. - (ODD - 1.)/2.) * scl + 3.
      Y = M * SIN60 * scl + 3.
        do 110 n=1,15
      if (MOD(n,3) + odd .ne. 3) then
        ty(n) = tyn(1)  ! Empty Site - Open circle
      else
        ty(n) = tyn(2)  ! Filled Site - Two circles
      endif
110     continue
        call qapos(x,2) ! x coordinate
        call qapos(y,1) ! y coordinate
      CALL qbuff(size,ty,0)
      CALL qbuff(2,'^-',0)
  100 CONTINUE
        call qfnt(-1,fta,orient)
      CALL qini(1)
      STOP
      END
C!*************************************************************************
      subroutine font(LUN,nr,nc,ntyp,w)
C**** Program to create PIXEL Array for LASER PRINTER
```

```
C* nc is number of columns (bits per row);
C* nr is number of rows (bits per column);
        integer w
        byte pixel(50),ca(16),lpixel(200)
        data ca/'0','1','2','3','4','5','6','7','8','9',
        1       'A','B','C','D','E','F'/
        ncp = (nc + 15.)/16.
        nch = 4*ncp
        ncp = 16*ncp
C* ncp is nc after padding to a multiple of 16
C* nch is number of characters per row
!       type *,nc,nr,ncp,nch
c** Now for the "rule" to determine the pattern
        cnc = (nc+1.)/2.
        cnr = (nr+1.)/2.
        do 100 j=1,nr
        do 200 i=1,ncp
        lpixel(i) = 0
        if (i .gt. nc) goto 200
        r = sqrt((i-cnc)**2 + (j-cnr)**2)
C* -- An open circle
        if (ntyp .lt. 4 .and. r .le. cnc .and. r .gt. cnc-2)
        1       lpixel(i) = 1
c** Now for the "rule" to determine the pattern
        goto (200,92,93,94,95,96,200) ntyp
        goto 200
C* Cross
92      if (abs(i-cnc) .le. w .or. abs(j-cnr) .le. w) lpixel(i) = 1
        goto 200
C* Concentric circles
93      if (r .le. (nc*w/20.))  lpixel(i) = 1
        goto 200
C* A horizontal line
94      if (abs(j-cnr) .le. w*.5)       lpixel(i) = 1
        goto 200
C* A upward line
95      if (abs(j-cnr) .gt. (nr+3.)/4. .or. abs(i-cnc) .gt. (nr+5.)/6.)
        1       goto 200
        yc = (1./sqrt(3.))*j + 1.
        if (abs(yc-i) .le. w*.58)       lpixel(i) = 1
        goto 200
C* A downward line
96      if (abs(j-cnr) .gt. (nr+3.)/4. .or. abs(i-cnc) .gt. (nr+5.)/6.)
        1       goto 200
        yc = nc - (1./sqrt(3.))*j
        if (abs(yc-i) .le. w*.58)       lpixel(i) = 1
200     continue
!       type 1,(lpixel(i),i=1,ncp)
1       format(1x,100i1)

        do 400 i=1,ncp,4
        num = 1 + lpixel(i)*8 + lpixel(i+1)*4 + lpixel(i+2)*2
        1 + lpixel(i+3)
        pixel((i-1)/4+1) = ca(num)
400     continue
      CALL qbuff(nch,pixel,0)
!       type 2,(pixel(i),i=1,nch)
2       format(1x,20a1)

100     continue
        return
        end
```

[BHT.LASER]QDEMO.FOR

```
c*******************************************************************************
c  QUIC demo program              Brian Toby, June 1985
c*******************************************************************************
        integer orient/1/
        real x1(5)/6.,6.,7.5,7.5,6./,y1(5)/1.,2.5,2.5,1.,1./
        real x2(3)/9.,8.,10./,y2(3)/1.,2.5,2.5/
        real x3(2)/4.5,5.5/,y3(4)/1.5,2.5,2.5,1.5/
        real x4(2)/2.75,4.5/,y4(2)/2.,2./
        LUN = 30        ! Logical device # for plot file
C** START Plot -- landscape mode (Xmax>Ymax)
        call qini(0,LUN,orient,'qdemo.qms')
C** Draw two overlapping circles
        call qarc(2.,2.,1.,0,0,3)       ! thin border
        call qarc(3.5,2.,1.,0,0,17)     ! thicker border
C** Shade area where circles overlap
        call qtone(2.75,2.,24)  ! (any point in region, pattern #24)
C** Shade area of second circle
        call qtone(3.75,2.2,19) ! (any point in region, pattern #19)
c** Move to (1.,4.) and label with QUIC letters
        call qapos(1.,2)        ! x coordinate
        call qapos(4.,1)        ! y coordinate
        call qlbl(0.25,0.4,0.,22,'This is QUIC lettering',1)
C** Now draw some things in vector mode
        call qvec(0,5)  ! enter vector mode - thin line
        call qvmov(x1,y1,5,0)   ! draw a square - move first
        call qvec(0,15) ! enter vector mode - thicker line
C** "Erase" a line partly through the overlapping cicrles
        call qvmov(x4,y4,2,-1)
        call qvmov(x2(3),y2(3),1,0)     ! draw a triangle - move to last point
        call qvmov(x2,y2,3,1)   ! draw a triangle - draw only
C** The following is an example of how to enter a QUIC command which does
C** not have a subroutine defined for it
      CALL QBUFF(3,'^V5',0)     ! SET LINE PATTERN TO TYPE #5
        call qvmov(x3,y3,2,0)   ! draw an X piece #1
        call qvmov(x3,y3(3),2,0)        ! draw an X piece #2
        call qvec(1)    ! exit vector mode
c** Move to (1.,8.) and label with QUIC letters
        call qapos(1.25,2)      ! x coordinate
        call qapos(6.5,1)       ! y coordinate
C** More QUIC lettering, no decenders this time
        call qlbl(1.5,.7,0.,12,'QDEMO sample',-1)
C** END Plot
      CALL qini(1,LUN)
      STOP
      END
```

3.2 Program MAP

[BHT.N2.LASER]MAP.FOR

```
C*************************************************************************
C*************************************************************************
C****                                                                 *****
C****   PROGRAM TO MODEL N    DESORPTION ON Ru(0001)                 *****
C****                     2                                           *****
C****                                                                 *****
C****   Program to plot maps on Laser Plotter -- Brian Toby 6/85      *****
C****                                                                 *****
C*************************************************************************
C*************************************************************************
C**
      INTEGER*2 HEX(100,100)
      INTEGER SIZE,ODD,INT(8,7),NC(4)
c      INTEGER NEARM(6),NEARN(6,2),NEXTM(6),NEXTN(6,2)
      REAL BETA,NU,NUO,E,R,T,NAAVG,LCTP,CHI
      REAL CDESPL(20),EDESPL(20),TDESPL(20)
      byte TITLE(72)
      INTEGER fta,ftb,hofg,cnum,wofg,bhi,bwi,orient/1/
        logical*1 ty(100),tyn(4)
        data tyn/'A','B','C','D'/
      Data fta/9999/,ftb/9998/
      DATA HEX/10000*0/,SIZE/100/
c      DATA NEARM/-1,-1,0,0,1,1/
c      DATA NEARN/0,1,-1,1,0,1,-1,0,-1,1,-1,0/
c      DATA NEXTM/-2,-1,-1,1,1,2/
c      DATA NEXTN/0,-1,2,-1,2,0,0,-2,1,-2,1,0/
      DATA CDESPL/20*-1./,EDESPL/20*-1./,TDESPL/20*-1./
      DATA icd,ied,itd/3*1/
      R302 = SQRT(3.)/2.
      SIN60 = SIN(3.14159/3.)
        LUN = 30
C** START Plot -- landscape mode
        call qini(0,LUN,orient,'map.qms')
      READ (9,21,ERR=211) SIZE,ED,EN,EA,ER,EM,SO,CHI,TS,
     1 DSBINT,IR,(TITLE(i),i=1,72),LCTP,E,EO,NAAVG,DT,A,NUO,BETA
   21 FORMAT(I5,6F10.6,/,3F10.3,I12,/,72A1,/,F10.1,2F10.6,F6.2,
     1 F6.4,F6.2,1PE9.2,F6.1)
C***
211   RATIO = ER / min(EA,1.)
      WRITE(6,29) (TITLE(i),i=1,72),SIZE,SIZE,abs(ED),EN,ER,EA
     1 ,RATIO,EN,SO,CHI,TS,IR
   29 FORMAT(/,1X,72('*'),/,1X,72A1,/,1X,72('*'),//' LATTICE IS',I4,
     1  ' BY',I4,/,' DESORPTION ENERGY: ',
     2 F5.3,/,' DESTABILIZATION ENERGY FOR FILLED SITE:',F6.3,/,
     3 ' REPULSIVE INTERACTION ENERGY:',F6.3,/,
     4 ' ATTRACTIVE INTERACTIVE ENERGY:',F6.3,/,
     5 ' ER / EA: ',F5.3,/,' MIGRATION ENERGY: ',F7.4,/,
     6 ' INITIAL STICKING COEFFICIENT: ',F6.4,/,' CHI = ',F12.5,
     7 /,' ADSORPTION TEMPERATURE:',F6.1,/,
     8 ' RANDOM STARTING POINT:',I10,//)
      NPLT = -1
        icir = 7
        ilin = 8
!      READ (5,*) icir,ilin
      type *,'Enter 0 to process all spectra, 1 to select by coverage'
      READ (5,*) iall
      IF (IALL .EQ. 0) THEN
        WRITE (6,914)
  914   FORMAT(' PLOT ALL MAPS',/)
      ELSE
        write (6,*) 'Enter map coverages'
        READ (5,*,END=199) (CDESPL(I),I=1,20)
199     write (6,*) 'Enter map exposures'
        READ (5,*,END=299) (EDESPL(I),I=1,20)
299     write (6,*) 'Enter map times'
```

```
        READ (5,*,END=399) (TDESPL(I),I=1,20)
      ENDIF
399     continue
c** define the glyph heigth and width in terms of the number of sites
        Hofg = 8.5 * 300. / size ! Font size in dots (300 dots/inch)
        wofg = hofg      ! square font: glyph height is same as width
        bhi = hofg       ! height of bit map (in dots)
        bwi = hofg       ! width of bit map (in dots)
c** define the diameter of a circle in inches
        SCL = hofg / 300.
C*************************************************************************
C*NOW DEFINE THE FONT SET
        call qfnt(1,fta,orient,0,'bht1',wofg,0)
C* CHAR 41 (A) -- An open circle
        call qfdef(0,'A',hofg,bwi,bhi,0,0)
      CALL font(LUN,bhi,bwi,1,2)
C* CHAR 42 (B) -- An open circle and a concentric filled circle
        call qfdef(0,'B',hofg,bwi,bhi,0,0)
      CALL font(LUN,bhi,bwi,3,icir)
c** End font definition
        call qfdef(-1)
C*************************************************************************
c** define the glyph heigth and width in terms of the number of sites
        Hofg = 2.*sin60*hofg ! Font size in dots (300 dots/inch)
        wofg = 3*wofg    ! glyph width is three times height
        bhi = hofg       ! height of bit map (in dots)
        bwi = wofg       ! width of bit map (in dots)
c** define the width of the connecting line through filled sites:
        iwidth = ilin * 100. / size
C*************************************************************************
C*NOW DEFINE THE FONT SET
        call qfnt(1,ftb,orient,0,'bht2',hofg,0)
C* CHAR 41 (A) -- A blank
        call qfdef(0,'A',wofg,bwi,bhi,0,0)
      CALL font(LUN,bwi,bhi,7,0)
C* CHAR 42 (B) -- An horizontal line
        call qfdef(0,'B',wofg,bwi,bhi,0,0)
      CALL font(LUN,bwi,bhi,4,iwidth)
C* CHAR 43 (C) -- An upward sloping line
        call qfdef(0,'C',wofg,bwi,bhi,0,0)
      CALL font(LUN,bwi,bhi,5,iwidth)
C* CHAR 44 (D) -- An downward sloping line
        call qfdef(0,'D',wofg,bwi,bhi,0,0)
      CALL font(LUN,bwi,bhi,6,iwidth)
c** End font definition
        call qfdef(-1)
C*************************************************************************
C***
!       IF (IALL .ne. 0) then
!         TYPE *,'Enter COVT'
!         READ (5,*,END=999) COVT
!       endif
C*************************************************************************
C** NOW READ IN MATRIX
1000  if (CDESPL(ICD) .eq. -1 .and. eDESPL(IeD) .eq. -1 .and.
     1       tDESPL(ItD).eq. -1 .and. iall .ne. 0) goto 999
      READ (9,912,END=999) imore,cov,expos,time
      if (imore .eq. 0) goto 999
912   FORMAT(1X,I5,f6.3,f11.3,f11.1)

      DO 3000 I = 1, SIZE
      READ (9,911,END=999) (HEX(I,J),J=1,SIZE)
  911 FORMAT(1X,100I1)
 3000 CONTINUE
C**
      NPLT = NPLT + 1
      NADS = 0
      DO 1102 N=1,SIZE
```

```
      DO 1102 N=1,SIZE
      IF (HEX(M,N) .NE. 0) NADS = NADS + 1
 1102 CONTINUE
      COV = (1.*NADS)/SIZE**2
 1103 WRITE (6,34) COV,expos,time
   34 FORMAT(//,' COVERAGE = ',F6.3,', EXPOSURE = ',F10.2,
     1 ', TIME = ',F11.1)
      IF (IALL .EQ. 0) THEN
        IFLAG = 1
      ELSE
        IFLAG = 0
        IF (ABS(COV - CDESPL(ICD)) .le. 0.011) THEN
          IFLAG = 1
          ICD = ICD + 1
        endif
        IF (ABS(expos/eDESPL(IeD)-1) .le. 0.05) THEN
          IFLAG = 1
          IeD = IeD + 1
        endif
        IF (ABS(time/tDESPL(ItD)-1.) .le. 0.05) THEN
          IFLAG = 1
          ItD = ItD + 1
        endif
      endif
      IF (IFLAG .NE. 1) goto 1000

        write (6,*) 'PLOTTING MAP'
        call qapos(9.75,2)       ! x coordinate
      IF (ED .GT. -1) then
        encode (59,731,ty) cov,expos,time
731     format('ADSORBED TO',F5.2,', EXPOSURE =',F5.1,'L, TIME =',
        1       1PG11.4,' Sec' )
        call qapos(.5,1)         ! y coordinate
        call qlbl(0.12,0.12,0.,59,ty,3)
      ELSE
        call qapos(6.,1)         ! y coordinate
        encode (16,701,ty) 'DESORBED TO',cov
701     format(A,F5.2)
        call qlbl(0.15,0.15,0.,16,ty,3)
      ENDIF
c** Fill page with circles
        call qfnt(0,fta)
      DO 100 M=1,SIZE
      ODD = 2 - MOD(M,2)
      X = (1. - (ODD - 1.)/2.) * scl + 0.5
      Y = M * SIN60 * scl + 0.25
        do 110 n=1,size
      IF (HEX(M,N) .EQ. 0) then
        ty(n) = tyn(1)  ! Empty Site - Open circle
      else
        ty(n) = tyn(2)  ! Filled Site - Two circles
      endif
110     continue
        call qapos(x,2) ! x coordinate
        call qapos(y,1) ! y coordinate
      CALL qbuff(size,ty,0)
      CALL qbuff(2,'^-',0)
  100 CONTINUE
        call qapos(3.,1)         ! y coordinate
        call qapos(10.25,2)      ! x coordinate
        call qlbl(0.1,0.1,10.5,72,title,3)

c** Fill page with horizontal lines
        call qfnt(0,ftb)
      DO 200 M=1,SIZE
      ODD = 2 - MOD(M,2)
      n0 = 1
      if (odd .eq. 2) n0 = 3
      X = (n0 - 1. - (ODD - 1.)/2.) * scl + 0.5
```

```
      Y = N * SIN60 * scl - (SIN60-0.5) * scl + 0.25
        ip = 0
        do 210 n=n0,size,3
        ip = ip + 1
      IF (HEX(M,N) .EQ. 0) then
        ty(ip) = tyn(1) ! Empty Site - no line
      else
        ty(ip) = tyn(2) ! Filled Site - line
      endif
210     continue
        call qapos(x,2) ! x coordinate
        call qapos(y,1) ! y coordinate
      CALL qbuff(ip,ty,0)
      CALL qbuff(2,'^-',0)

c** Fill page with upward lines
      n0 = 2
      if (odd .eq. 2) n0 = 1
      X = (n0 - 1. - (ODD - 1.)/2.) * scl + 0.5
        ip = 0
        do 220 n=n0,size,3
        ip = ip + 1
      IF (HEX(M,N) .EQ. 0) then
        ty(ip) = tyn(1) ! Empty Site - no line
      else
        ty(ip) = tyn(3) ! Filled Site - line
      endif
220     continue
        call qapos(x,2) ! x coordinate
        call qapos(y,1) ! y coordinate
      CALL qbuff(ip,ty,0)
      CALL qbuff(2,'^-',0)

c** Fill page with downward lines
      n0 = 3
      if (odd .eq. 2) n0 = 2
      X = (n0 - 1. - (ODD - 1.)/2.) * scl + 0.5
        ip = 0
        do 230 n=n0,size,3
        ip = ip + 1
      IF (HEX(M,N) .EQ. 0) then
        ty(ip) = tyn(1) ! Empty Site - no line
      else
        ty(ip) = tyn(4) ! Filled Site - line
      endif
230     continue
        call qapos(x,2) ! x coordinate
        call qapos(y,1) ! y coordinate
      CALL qbuff(ip,ty,0)
      CALL qbuff(2,'^-',0)
  200 CONTINUE

!      IF (IALL .NE. 0) then
!        type *,'Enter coverage'
!        READ (5,*,end=999) COVT
!      endif
C** START NEW PAGE
      CALL qini(-1)
      GOTO 1000
c* Delete font
999     call qfnt(-1,fta,orient)
        call qfnt(-1,ftb,orient)
      CALL qini(1)
  913 STOP
      END
C!*****************************************************************************
      subroutine font(LUN,nr,nc,ntyp,w)
C**** Program to create PIXEL Array for LASER PRINTER
```

```
C* nc is number of columns (bits per row);
C* nr is number of rows (bits per column);
        integer w
        byte pixel(50),ca(16),lpixel(200)
        data ca/'0','1','2','3','4','5','6','7','8','9',
        1       'A','B','C','D','E','F'/
        ncp = (nc + 15.)/16.
        nch = 4*ncp
        ncp = 16*ncp
C* ncp is nc after padding to a multiple of 16
C* nch is number of characters per row
!       type *,nc,nr,ncp,nch
c** Now for the "rule" to determine the pattern
        cnc = (nc+1.)/2.
        cnr = (nr+1.)/2.
        do 100 j=1,nr
        do 200 i=1,ncp
        lpixel(i) = 0
        if (i .gt. nc) goto 200
        r = sqrt((i-cnc)**2 + (j-cnr)**2)
C* -- An open circle
        if (ntyp .lt. 4 .and. r .le. cnc .and. r .gt. cnc-2)
        1       lpixel(i) = 1
c** Now for the "rule" to determine the pattern
        goto (200,92,93,94,95,96,200) ntyp
        goto 200
C* Cross
92      if (abs(i-cnc) .le. w .or. abs(j-cnr) .le. w) lpixel(i) = 1
        goto 200
C* Concentric circles
93      if (r .le. (nc*w/20.))  lpixel(i) = 1
        goto 200
C* A horizontal line
94      if (abs(j-cnr) .le. w*.5)       lpixel(i) = 1
        goto 200
C* A upward line
95      if (abs(j-cnr) .gt. (nr+3.)/4. .or. abs(i-cnc) .gt. (nr+5.)/6.)
        1       goto 200
        yc = (1./sqrt(3.))*j + 1.
        if (abs(yc-i) .le. w*.58)       lpixel(i) = 1
        goto 200
C* A downward line
96      if (abs(j-cnr) .gt. (nr+3.)/4. .or. abs(i-cnc) .gt. (nr+5.)/6.)
        1       goto 200
        yc = nc - (1./sqrt(3.))*j
        if (abs(yc-i) .le. w*.58)       lpixel(i) = 1
200     continue
!       type 1,(lpixel(i),i=1,ncp)
1       format(1x,100i1)

        do 400 i=1,ncp,4
        num = 1 + lpixel(i)*8 + lpixel(i+1)*4 + lpixel(i+2)*2
        1 + lpixel(i+3)
        pixel((i-1)/4+1) = ca(num)
400     continue
      CALL qbuff(nch,pixel,0)
!       type 2,(pixel(i),i=1,nch)
2       format(1x,20a1)

100     continue
        return
        end
```

3.3 Programs 3A, 3D, 3DR and 3DV

[BHT.N2.AVG]3A.FOR

```
C*************************************************************************
C*************************************************************************
C****                                                                 *****
C****   PROGRAM TO MODEL N   ADSORPTION ON Ru(0001)                   *****
C****                    2                                            *****
C****                                                                 *****
C****   Using true Monte-Carlo type model                             *****
C****                                                                 *****
C****   BRIAN TOBY 6/85                                               *****
C****                                                                 *****
C****   Plot results from array processor program                     *****
C****   State analysis of adsorbed molecules as a function of T       *****
C*************************************************************************
C*************************************************************************
C**
      INTEGER SIZE,SIZA(10),NP(10),int(7),ndm(7,7),ndmt(7,7)
      INTEGER nr(49),na(49)
      REAL TEMP(100)
      INTEGER NI(7,7),TMIN,TMAX,nd(7,7,100),ndt(100)
      REAL BETA,E,R,TS,NAAVG,LCTP,CHI,nu0
        BYTE NAM(3),FNAM(50),TITLE(72)
        INTEGER TYP
C**
      LUNM = 10
      LUN = LUNM
      SUMSIZE = 0
        TYP = 10
C*************************************************************************
      DO 410 J=1,10
        type *,'Enter File:'
        READ (5,701,END=959) NAM
701     FORMAT(3A1)
        ENCODE(15,702,FNAM) TYP,NAM
702     FORMAT('INP:FOR',I3.3,'.',3A1,1X)
        OPEN(UNIT=LUN,ERR=959,FILE=FNAM,TYPE='OLD')
      READ(LUN,121,END=959,ERR=959) SIZE,ED,EN,EA,ER,EM,SO,CHI,
     1 TS,DSBINT,IR,TITLE,LCTP,E,EO,NAAVG,DT,A,NUO,
     2 BETA
  121 FORMAT(I5,6F10.6,/,3F10.3,I12/,72A1,/,F10.1,2F10.6,3F6.2,
     1 1PE9.2,F6.1)
      SIZA(J) = SIZE
      SUMSIZE = SUMSIZE + SIZA(J)**2
   29 FORMAT(/,' File #',I3,' = ',15A1
     A  ,/,' ',72('*'),/,1X,72A1,/,1X,72('*')
     1  ,/' LATTICE IS',I4,' BY',I4,/,' DESORPTION ENERGY: ',
     2 F5.3,/,' DESTABILIZATION ENERGY FOR FILLED SITE:',F6.3,/,
     3 ' REPULSIVE INTERACTION ENERGY:',F6.3,/,
     4 ' ATTRACTIVE INTERACTIVE ENERGY:',F6.3,/,
     5 ' MIGRATION ENERGY: ',F7.4,')',/,
     6 ' INITIAL STICKING COEFFICIENT: ',F6.4,/,
     7 ' CHI = ',F12.5,/,' ADSORPTION TEMPERATURE:',F6.1,/
     8 ' RANDOM STARTING POINT:',I10,//)
      TYPE 29,LUN,(FNAM(I),I=1,15),TITLE,SIZE,SIZE
     1 ,ABS(ED),EN,ER,EA,EM,SO,CHI,TS,IR
      LUN = LUN + 1
      WRITE (6,128) EO,DT,NUO,A,BETA
  128 FORMAT(' ISOLATED N2 ATTRACTION IS E = ',
     3  F6.3,' (Kcal)',/,' TEMPERATURE INCREMENT',F8.4,/,1X,
     4 'PREFACTOR:',1P1E9.2,' * EXP(',0PF5.2,
     5 ' * COV)',/,' BETA:',F5.1,//)
  410 CONTINUE
  959 IF (LUN .EQ. LUNM) GOTO 2999
      LUN = LUN - 1
C*************************************************************************
C**  NOW READ IN STATES TO BE TRACKED FROM FILE 4
```

```
      NSTATE = 0
      OPEN(UNIT=4,ERR=3999,FILE='state.dat',TYPE='OLD')
      DO 382 K=1,30
        read (4,*,end=381) NA(K),NR(K)
        nstate = nstate + 1
  382 CONTINUE
C** REORDER STATES BY INCREASING ENERGY
381   DO 380 K=1,nstate
      DO 380 J=K+1,nstate
        if (NA(K)*EA - NR(K)*ER .LE. NA(J)*EA - NR(J)*ER) GOTO 380
        I = NA(K)
        NA(K) = NA(J)
        NA(J) = I
        I = NR(K)
        NR(K) = NR(J)
        NR(J) = I
  380 CONTINUE
C*******************************************************************************
C**  NOW READ IN POINTS FROM FILE
 1100 N2 = 0
      COVP = 0.0
      SUMSIZE = 0
      TP = 0.0

      DO 420 L=LUNM,LUN
C SKIP OVER FILE IF IT HAS ENDED ALREADY
      IF (SIZA(1+L-LUNM) .EQ. 0) GOTO 420
      READ (L,125,END=969) NP(1+L-LUNM),COVO,nads0
C       TYPE *,l,np(1+l-lunm),' COVERAGE',COVO
  125 FORMAT(I5,F8.4,I7)
      N2 = max(N2,NP(1+L-LUNM))

      IF (L .NE. LUNM .AND. ABS(COVO-COVP) .GT. 0.02) THEN
        TYPE *,'ERROR WRONG COVERAGE',L,COVO,COVP
        STOP
      ELSE
        COVP = COVO
      ENDIF
      SUMSIZE = SUMSIZE + SIZA(1+L-LUNM)**2
      GOTO 420

C END OF FILE -- SKIP OVER FILE NEXT TIME
  969 SIZA(1+L-LUNM) = 0
      CLOSE(L)
  420 CONTINUE

C IF SUMSIZE IS ZERO THEN ALL FILES ARE NOW EMPTY
      IF (SUMSIZE .EQ. 0) goto 1999
      NPLT = NPLT + 1
      mdes = 0

        ICOV = 100 * COVO
      NDSB = 0

C*******************************************************************************
C*** NOW READ IN T AND DESORPTION STATE DATA
       DO 400 K=1,N2
      if (k .gt. 3) TEMP(K) = 2.*TEMP(K-1) - TEMP(K-2)
      NDT(k) = 0          ! clear total per T increment
      DO 201 I=1,7
      DO 201 J=1,7
      ND(i,j,k) = 0       ! clear state counter
  201 CONTINUE

      DO 202 L=LUNM,LUN
C SKIP OVER FILE IF IT HAS ENDED ALREADY OR IF WE HAVE READ ALL
C       POINTS FROM THIS TDS SCAN
        IF (SIZA(1+L-LUNM) .EQ. 0 .or. NP(1+L-LUNM) .EQ. 0) GOTO 202
        READ (L,124) TP
124     FORMAT(F6.2)
```

```
c** Is this T < 0
      IF (TP .lt. 0.) THEN
        NP(1+L-LUNM) = 0        ! prevent reading more points from current file
        goto 202
      ENDIF
      IF (L .NE. LUNM .AND. ABS(TEMP(K)-TP) .GT. 0.1) THEN
          TYPE *,'ERROR WRONG TEMPERATURE',K,L,TEMP(K),TP
          STOP
      ENDIF
        TEMP(K) = TP
        READ (L,126) ((NI(I,J),I=1,7),J=1,7)
126     FORMAT(7I6)
        DO 202 I=1,7
        DO 202 J=1,7
            ndt(k) = ndt(k) + NI(I,J)           ! desorbed per T increment
            nd(i,j,k) = nd(i,j,k) + NI(I,J)     ! desorbed by state
202     CONTINUE
        ndsb = ndsb + ndt(k)
  400 CONTINUE

      nads = ndt(1) ! total adsorbed
      type 770,nads/sumsize,nads
770   format('0averaged coverage:',f7.3,',  total adsorbed:',i6,/)

      DO 302 I=1,7
      DO 302 J=1,7
        ndm(i,j) = nd(i,j,1)
  302 CONTINUE
      n1 = 0
      DO 205 K=2,N2
      ndtrk = 0
      DO 350 j=1,nstate
        ndtrk = ndtrk + ND(NA(j)+1,NR(j)+1,k)
  350 CONTINUE
        if (ndt(k) .ne. 0.) type 771,
     1  temp(k),ndtrk,ndt(k),ndt(k)/sumsize,(100.*ndtrk)/ndt(k)
771   format(1x,f4.0,2i7,2f7.2)
      DO 205 I=1,7
      DO 205 J=1,7
        ndm(i,j) = max(nd(i,j,k),ndm(i,j))
  205 CONTINUE

      DO 6 J=1,7
      INT(J) = ndm(1,J) + ndm(2,J) + ndm(3,J) + ndm(4,J) + ndm(5,J) +
     1 ndm(6,J) + ndm(7,J)
    6 CONTINUE
      WRITE (6,30) 'Maximum number',(I-1,I=1,7),0
     1       ,(ndm(I,1),I=1,7),int(1)
   30 FORMAT(/,23X,a,' of molecules by interactions',
     1         /,30X,'NUMBER OF ATTRACTIVE INTERACTIONS',/
     2          20X,7I6,' TOTAL',/,' NUMBER OF',/,
     3       ' REPULSIVE  ',I6,2X,8I6)
   33 FORMAT(12X,I6,2X,8I6)
      DO 32 J=2,7
      IF (INT(J) .NE. 0) WRITE (6,33) J-1,(ndm(I,J),I=1,7),int(j)
   32 CONTINUE
      DO 7 J=1,7
      INT(J) = nd(1,J,1) + nd(2,J,1) + nd(3,J,1) + nd(4,J,1) +
     1 nd(5,J,1) + nd(6,J,1) + nd(7,J,1)
    7 CONTINUE
      WRITE (6,30) '# (at start)',(I-1,I=1,7),0,
     1       (nd(I,1,1),I=1,7),int(1)
      DO 34 J=2,7
      IF (INT(J) .NE. 0) WRITE (6,33) J-1,(nd(I,J,1),I=1,7),int(j)
   34 CONTINUE

        type 322,'Natt',(NA(k),k=1,nstate)
        type 320,'Nrep',(Nr(k),k=1,nstate)
        type 320,'Dsta',(ND(NA(k)+1,NR(k)+1,1),k=1,nstate)
```

```
        type 320,'Dmax',(NDM(NA(k)+1,NR(k)+1),k=1,nstate)
        type 321,'E',(NA(K)*EA - NR(k)*ER,k=1,nstate)
322     format(//,1x,a4,1x,20i5,:,/,3x,20i5)
320     format(1x,a4,1x,20i5,:,/,3x,20i5)
321     format(1x,a4,1x,20f5.2,/,:,3x,20f5.2)

C** NOW OPEN FILE 2 -- T VS. Ndsb for selected states
        ENCODE(15,704,FNAM) NAM,ICOV,'DAT'
704     FORMAT('OUT:',3A1,'A',I2.2,'.',A3,1X)
        OPEN(UNIT=2,FILE=FNAM,TYPE='NEW',FORM='FORMATTED')
        nsize = sqrt(sumsize)
        write (2,323) nstate,nsize
        write (2,323) (NA(k),k=1,nstate)
        write (2,323) (Nr(k),k=1,nstate)
        write (2,323) (ND(NA(k)+1,NR(k)+1,1),k=1,nstate)
        write (2,323) (NDM(NA(k)+1,NR(k)+1),k=1,nstate)
        write (2,324) (NA(K)*EA - NR(k)*ER,k=1,nstate)
323     format(30i5)
324     format(30f5.2)

      DO 330 K=1,N2
        write (2,341) temp(k),(ND(NA(i)+1,NR(i)+1,k),i=1,nstate)
        if (ndt(k) .ne. 0)
        1       type 340,temp(k),(ND(NA(i)+1,NR(i)+1,k),i=1,nstate)
c       type 340,temp(k),(ND(NA(i)+1,NR(i)+1,k),i=1,nstate)
340     format(1x,f5.0,20i5,:,/,3x,20i5)
341     format(f5.0,20i5)
  330 CONTINUE
        close (2)
      GOTO 1100
1999    continue
2999    continue
3999    STOP
      END
```

[BHT.N2.AVG]3D.FOR

```
C*************************************************************************
C*************************************************************************
C****                                                                 *****
C****   PROGRAM TO MODEL N   ADSORPTION ON Ru(0001)                   *****
C****                     2                                           *****
C****                                                                 *****
C****   Using true Monte-Carlo type model                             *****
C****                                                                 *****
C****   BRIAN TOBY 6/85                                               *****
C****                                                                 *****
C****   Plot results from array processor program  (BHT 6/84)         *****
C****   State analysis of adsorbed molecules as a function of T       *****
C*************************************************************************
C*************************************************************************
C**
      INTEGER SIZE,SIZA(10),NP(10),int(7),ndm(7,7),ndmt(7,7),ndtot(7,7)
      INTEGER nr(49),na(49)
      REAL TEMP(100),cov(100)
      INTEGER NI(7,7),TMIN,TMAX,nd(7,7,100),ndt(100)
      REAL BETA,E,R,TS,NAAVG,LCTP,CHI,nu0
        BYTE NAM(3),FNAM(50),TITLE(72)
        INTEGER TYP
C**
c      CALL PLOTS(0,2,0)
      LUNM = 15
      LUN = LUNM
      SUMSIZE = 0
        TYP = 15
C       READ (5,*) TYP
C*************************************************************************
      DO 410 K=1,10
```

```
        type *,'Enter File:'
        READ (5,701,END=959) NAM
701     FORMAT(3A1)
        ENCODE(15,702,FNAM) TYP,NAM
702     FORMAT('INP:FOR',I3.3,'.',3A1,1X)
        OPEN(UNIT=LUN,ERR=959,FILE=FNAM,TYPE='OLD')
      READ(LUN,121,END=959,ERR=959) SIZE,ED,EN,EA,ER,EM,SO,CHI,
     1 TS,DSBINT,IR,TITLE,LCTP,E,EO,NAAVG,DT,A,NUO,
     2 BETA
  121 FORMAT(I5,6F10.6,/,3F10.3,I12/,72A1,/,F10.1,2F10.6,3F6.2,
     1 1PE9.2,F6.1)
      SIZA(K) = SIZE
      SUMSIZE = SUMSIZE + SIZA(K)**2
   29 FORMAT(/,' File #',I3,' = ',15A1
     A  ,/,' ',72('*'),/,1X,72A1,/,1X,72('*')
     1  ,/' LATTICE IS',I4,' BY',I4,/,' DESORPTION ENERGY: ',
     2 F5.3,/,' DESTABILIZATION ENERGY FOR FILLED SITE:',F6.3,/,
     3 ' REPULSIVE INTERACTION ENERGY:',F6.3,/,
     4 ' ATTRACTIVE INTERACTIVE ENERGY:',F6.3,/,
     5 ' MIGRATION ENERGY: ',F7.4,')',/,
     6 ' INITIAL STICKING COEFFICIENT: ',F6.4,/,
     7 ' CHI = ',F12.5,/,' ADSORPTION TEMPERATURE:',F6.1,/
     8 ' RANDOM STARTING POINT:',I10,//)
      TYPE 29,LUN,(FNAM(I),I=1,15),TITLE,SIZE,SIZE
     1 ,ABS(ED),EN,ER,EA,EM,SO,CHI,TS,IR
960     LUN = LUN + 1
      WRITE (6,128) EO,DT,NUO,A,BETA
  128 FORMAT(' ISOLATED N2 ATTRACTION IS E = ',
     3  F6.3,' (Kcal)',/,' TEMPERATURE INCREMENT',F8.4,/,1X,
     4 'PREFACTOR:',1P1E9.2,' * EXP(',OPF5.2,
     5 ' * COV)',/,' BETA:',F5.1,//)
  410 CONTINUE
  959 IF (LUN .EQ. LUNM) GOTO 2999
      LUN = LUN - 1
C*******************************************************************************
C**  NOW READ IN STATES TO BE TRACKED FROM FILE 4
      NSTATE = 0
      OPEN(UNIT=4,ERR=3999,FILE='state.dat',TYPE='OLD')
      DO 382 K=1,30
        read (4,*,end=381) NA(K),NR(K)
        nstate = nstate + 1
  382 CONTINUE
C** REORDER STATES BY INCREASING ENERGY
381   DO 380 K=1,nstate
      DO 380 J=K+1,nstate
        if (NA(K)*EA - NR(K)*ER .LE. NA(J)*EA - NR(J)*ER) GOTO 380
        I = NA(K)
        NA(K) = NA(J)
        NA(J) = I
        I = NR(K)
        NR(K) = NR(J)
        NR(J) = I
  380 CONTINUE
C*******************************************************************************
C**  NOW READ IN POINTS FROM FILE
 1100 N2 = 0
      COVP = 0.0
      SUMSIZE = 0
      TP = 0.0

      DO 420 L=LUNM,LUN
        IF (SIZA(1+L-LUNM) .EQ. 0) GOTO 420     ! Has file ended already?
        READ (L,125,END=969) NP(1+L-LUNM),COVO,nads0
        TYPE *,l,np(1+l-lunm),' COVERAGE',COVO
125     FORMAT(I5,F8.4,I7)
        N2 = max(N2,NP(1+L-LUNM))

      IF (L .NE. LUNM .AND. ABS(COVO-COVP) .GT. 0.02) THEN
        TYPE *,'ERROR WRONG COVERAGE',L,COVO,COVP
        STOP
```

```
      ELSE
        COVP = COVO
      ENDIF
        SUMSIZE = SUMSIZE + SIZA(1+L-LUNM)**2
        GOTO 420

969     SIZA(1+L-LUNM) = 0      ! END OF FILE -- SKIP OVER FILE NEXT TIME
        CLOSE(L)
  420 CONTINUE

      IF (SUMSIZE .EQ. 0) goto 1999     ! IF ZERO -- ALL FILES ARE NOW EMPTY
      ICOV = 100 * COVO
C Clear total and max arrays before starting
      DO 302 I=1,7
      DO 302 J=1,7
        ndm(i,j) = 0
        ndtot(i,j) = 0
  302 CONTINUE
      NDSB = 0
C*******************************************************************************
C*** NOW READ IN T AND DESORPTION STATE DATA
       DO 400 K=1,N2
      if (k .gt. 3) TEMP(K) = 2.*TEMP(K-1) - TEMP(K-2)
      NDT(k) = 0          ! clear total per T increment
      DO 201 I=1,7
      DO 201 J=1,7
      ND(i,j,k) = 0       ! clear state counter
  201 CONTINUE

      DO 202 L=LUNM,LUN
C SKIP OVER FILE IF IT HAS ENDED ALREADY OR IF WE HAVE READ ALL
C       POINTS FROM THIS TDS SCAN
        IF (SIZA(1+L-LUNM) .EQ. 0 .or. NP(1+L-LUNM) .EQ. 0) GOTO 202
        READ (L,124) TP
124     FORMAT(F6.2)
c** Is this T < 0
      IF (TP .lt. 0.) THEN
        NP(1+L-LUNM) = 0          ! prevent reading more points from current file
        goto 202
      ENDIF
      IF (L .NE. LUNM .AND. ABS(TEMP(K)-TP) .GT. 0.1) THEN
          TYPE *,'ERROR WRONG TEMPERATURE',K,L,TEMP(K),TP
          STOP
      ENDIF
        TEMP(K) = TP
        READ (L,126) ((NI(I,J),I=1,7),J=1,7)
126     FORMAT(7I6)
        DO 202 I=1,7
        DO 202 J=1,7
            ndt(k) = ndt(k) + NI(I,J)           ! desorbed per T increment
            ndtot(i,j) = ndtot(i,j) + NI(I,J)   ! total per T increment
            nd(i,j,k) = nd(i,j,k) + NI(I,J)     ! desorbed by state
202     CONTINUE
        ndsb = ndsb + ndt(k)
  400 CONTINUE
      nads = ndsb ! total adsorbed
      ndtrk = 0
      DO 350 K=1,nstate
        ndtrk = ndtrk + NDtot(NA(k)+1,NR(k)+1)
  350 CONTINUE
      type 770,nads/sumsize,nads,ndtrk,(100.*ndtrk)/nads
770   format('0averaged coverage:',f7.3,',  total adsorbed:',i6,
       1 /,' desorbed from tracked states:',i6,' (',f7.3,'%)',/)
      n1 = 0
      DO 206 K=1,N2
        ndsb = ndsb - ndt(k)
        cov(k) = ndsb/sumsize
      DO 205 I=1,7
      DO 205 J=1,7
        ndm(i,j) = max(nd(i,j,k),ndm(i,j))   ! maximum desorbed for each state
```

```
  205 CONTINUE
c      if (ndt(k) .ne. 0) type *,temp(k),cov(k),ndt(k)
  206 CONTINUE
        close (1)
      DO 6 J=1,7
      INT(J) = ndm(1,J) + ndm(2,J) + ndm(3,J) + ndm(4,J) + ndm(5,J) +
     1 ndm(6,J) + ndm(7,J)
    6 CONTINUE
      WRITE (6,30) 'Maximum',(I-1,I=1,7),0,(ndm(I,1),I=1,7),int(1)
   30 FORMAT(/,23X,a,' desorbed molecules by interactions',
     1         /,30X,'NUMBER OF ATTRACTIVE INTERACTIONS',/
     2          20X,7I6,' TOTAL',/,' NUMBER OF',/,
     3       ' REPULSIVE  ',I6,2X,8I6)
   33 FORMAT(12X,I6,2X,8I6)
      DO 32 J=2,7
      IF (INT(J) .NE. 0) WRITE (6,33) J-1,(ndm(I,J),I=1,7),int(j)
   32 CONTINUE
      DO 7 J=1,7
      INT(J) = ndtot(1,J) + ndtot(2,J) + ndtot(3,J) + ndtot(4,J) +
     1 ndtot(5,J) + ndtot(6,J) + ndtot(7,J)
    7 CONTINUE
      WRITE (6,30) 'Total',(I-1,I=1,7),0,(ndtot(I,1),I=1,7),int(1)
      DO 34 J=2,7
      IF (INT(J) .NE. 0) WRITE (6,33) J-1,(ndtot(I,J),I=1,7),int(j)
   34 CONTINUE
c** Find Top ten desorbing states by total desorbed
c      DO 300 K=1,10
c      IMAX = -1
c      DO 310 I=1,7
c      DO 310 J=1,7
c      IF (K .EQ. 1) NDMT(I,J) = NDTOT(I,J)
c      IF (IMAX .LT. NDMT(I,J)) THEN
c       NA(K) = I - 1
c       NR(K) = J - 1
c       IMAX = NDMT(I,J)
c      ENDIF
c  310 CONTINUE
c      NDMT(NA(k)+1,NR(k)+1) = 0
c  300 CONTINUE
       type 322,'Natt',(NA(k),k=1,nstate)
       type 320,'Nrep',(Nr(k),k=1,nstate)
       type 320,'Dtot',(NDtot(NA(k)+1,NR(k)+1),k=1,nstate)
       type 320,'Dmax',(NDM(NA(k)+1,NR(k)+1),k=1,nstate)
       type 321,'E',(NA(K)*EA - NR(k)*ER,k=1,nstate)
322    format(//,1x,a4,1x,20i5,:,/,3x,20i5)
320    format(1x,a4,1x,20i5,:,/,3x,20i5)
321    format(1x,a4,1x,20f5.2,/,:,3x,20f5.2)
C** NOW OPEN FILE 2 -- T VS. Ndsb for selected states
       ENCODE(15,704,FNAM) NAM,ICOV,'DAT'
704    FORMAT('OUT:',3A1,'D',I2.2,'.',A3,1X)
       OPEN(UNIT=2,FILE=FNAM,TYPE='NEW',FORM='FORMATTED')
       nsize = sqrt(sumsize)
       write (2,323) nstate,nsize
       write (2,323) (NA(k),k=1,nstate)
       write (2,323) (Nr(k),k=1,nstate)
       write (2,323) (NDtot(NA(k)+1,NR(k)+1),k=1,nstate)
       write (2,323) (NDM(NA(k)+1,NR(k)+1),k=1,nstate)
       write (2,324) (NA(K)*EA - NR(k)*ER,k=1,nstate)
323    format(30i5)
324    format(30f5.2)
      DO 330 K=1,N2
       write (2,341) temp(k),(ND(NA(i)+1,NR(i)+1,k),i=1,nstate)
       if (ndt(k) .ne. 0)
       1       type 340,temp(k),(ND(NA(i)+1,NR(i)+1,k),i=1,nstate)
340    format(1x,f5.0,20i5,:,/,3x,20i5)
341    format(f5.0,20i5)
  330 CONTINUE
       close (2)
      GOTO 1100
```

```
1999    continue
2999    continue
3999    STOP
      END
```

[BHT.N2.AVG]3DR.FOR

```
C*************************************************************************
C*************************************************************************
C****                                                                  *****
C****   PROGRAM TO MODEL N    ADSORPTION ON Ru(0001)                  *****
C****                     2                                          *****
C****                                                                  *****
C****   Using true Monte-Carlo type model                              *****
C****                                                                  *****
C****   BRIAN TOBY 6/85                                                *****
C****                                                                  *****
C****   Plot results from array processor program  (BHT 6/84)          *****
C****   State analysis of adsorbed molecules as a function of T        *****
C*************************************************************************
C*************************************************************************
C**
      INTEGER nr(49),na(49),ndm(49)
      REAL TEMP(100),es(49),x(200),y(200)
      REAL ym(200),yz(200),xf(400),yf(400)
      REAL x1(102),y1(102)
      INTEGER nd(49,100),ndtot(49)
        BYTE NAM(3),PNAM(50),FNAM(50),Q,TITLE(72)

C**
C** NOW OPEN FILE 2 -- T VS. Ndsb for selected states
1       TYPE *,'ENTER FILE PREFIX'
        READ (5,701,END=959) NAM
701     FORMAT(3A1)
        TYPE *,'ENTER FILE TYPE (A - Adsorbed / D - Desorbed)'
        READ (5,701,END=959) Q
2       TYPE *,'ENTER COVERAGE'
c       cov = 0.53
        READ (5,*,END=1) COV
        ICOV = 100.*COV + 0.5
        ENCODE(14,704,FNAM) NAM,Q,ICOV,'DAT'
704     FORMAT('INP:',4A1,I2.2,'.',A3)
        OPEN(UNIT=2,FILE=FNAM,TYPE='OLD',FORM='FORMATTED',ERR=2)
!       OPEN(UNIT=2,FILE=FNAM,TYPE='OLD',FORM='FORMATTED',ERR=1)
        read (2,323) nstate
        read (2,323) (NA(k),k=1,nstate)
        read (2,323) (Nr(k),k=1,nstate)
        read (2,323) (NDtot(k),k=1,nstate)
        read (2,323) (NDM(k),k=1,nstate)
        read (2,324) (ES(K),k=1,nstate)
323     format(30i5)
324     format(30f5.2)
        n = 0
        Tmax = -9.E9
        Tmin =  9.E9
      DO 330 K=1,100
        read (2,340,end=350) temp(k),(ND(i,k),i=1,nstate)
340     format(f5.0,20i5)
        if (temp(k) .gt. Tmax) Tmax = temp(k)
        if (temp(k) .lt. Tmin) Tmin = temp(k)
        n = n + 1
  330 CONTINUE
350     close (2)

        ndmax = ndm(1)
      DO 311 K=2,nstate
        if (ndm(k) .gt. ndmax) ndmax = ndm(k)
  311 CONTINUE
```

```
3       type *,'enter theta, R,inum'
        READ (5,*,END=2),theta,R,inum
        mpower = 4
        nseg = 7
        io = 1
        navg = 3
        dx = tmax - tmin
        dy = ndmax
        zm = (es(nstate)-ES(1))/r
        cost = cos(theta*3.14159/180.)*dx
        sint = sin(theta*3.14159/180.)*dy
        xmax = tmax + zm*cost
        Dmax = NDmax + zm*sint
      CALL pgbegin(1,'/vt',1,1)
c       CALL GRSCR(IC,RED,G,B)
        CALL GRSCR(3,0.0,0.5,0.0)

9      CALL pgenv(tmin,xmax,0.,dmax,0,0)
c Draw lines in Z direction
        y(1) = 0.0
        y(2) = zm*sint
        do 530 j=80,160,20
          x(1) = j
          x(2) = j + zm*cost
          call pgline(2,x,y)
530     continue

c!      CALL pglabel('Temperature','Number Desorbed',' ')
      CALL pglabel('T','N',' ')
      DO 501 i=1,nstate
        z = (es(I)-ES(1))/r
        cosz = z*cost
        sinz = z*sint
      DO 500 K=1,N
        x(k) = temp(k) + cosz
        y(k) = nd(i,k) + sinz
        x1(k) = temp(k)
        y1(k) = nd(i,k)
  500 CONTINUE
        CALL GRSETCOL(1)
      if (inum .ne. 0) call pgpoint(n,x,y,47+i)
        j = 1
        ivis = 2
        j1 = 0
        DO 502 K=1,200
        if (i .eq. 1) ym(k) = -1.
        xt = tmin + (xmax-tmin)*(k-1)/200.
        xtz = xt - cosz
        if (xtz .le. temp(1) .or. xtz .ge. temp(n)) goto 502
        if (xtz .gt. temp(j)) then
          x0 = x1(j)
          y0 = y1(j)
          j = j + 1
        endif
        yt = y0 + (xtz - x0)*(y1(j) - y0)/(x1(j) - x0)
        j1 = j1 + 1
        x(j1) = xt
        y(j1) = yt + sinz
        yz(j1) = max(sinz,ym(k))
        if (ym(k) .le. yt + sinz) then
c line is visible
c       draw previous invisible line first if last point was invisible
          if (ivis .eq. 1) then
            CALL GRSETCOL(2)            ! red
            call pgpoint(j1,x,y,-1)     ! plot points
            j1 = 1
            x(1) = xt
```

```
            y(1) = yt + sinz
            yz(1) = max(sinz,ym(k))
          endif
          ym(k) = yt + sinz
          ivis = 0
        else
c line is invisible
c       draw previous visible line first, if last point was visible
          if (ivis .eq. 0) then
            is = 0
            j4 = 0
          do 541 j2 = 1,j1
            if (y(j2) .le. yz(j2) .or. j2 .eq. j1) goto 542
            is = 1
            j4 = j4 + 1
            xf(j4) = x(j2)
            yf(j4) = y(j2)
            goto 541
c       start/end of fill area:
542         if (is .eq. 0) then          !line not started - use as first point
              xf(1) = x(j2)
              yf(1) = y(j2)
              j4 = 1
            else
            j4 = j4 + 1
            xf(j4) = x(j2)
            yf(j4) = y(j2)
              do 543 j3 = 1,j4-1         ! now load in last n points
                xf(j4+j3) = x(j2-j3)
                yf(j4+j3) = yz(j2-j3)
  543         CONTINUE
              CALL GRSETCOL(3)           ! green
              call pgpoly(2*j4-1,xf,yf)
              is = 0
            endif
  541     CONTINUE
!           CALL GRSETCOL(1)             ! white
            CALL GRSETCOL(2)             ! red
            call pgline(j1,x,yz)
            CALL GRSETCOL(2)             ! red
            call pgline(j1,x,y)
            j1 = 1
            x(1) = xt
            y(1) = yt + sinz
            yz(1) = max(sinz,ym(k))
          endif
          ivis = 1
        endif
  502   CONTINUE
        if (ivis .eq. 0) then
            is = 0
            j4 = 0
          do 551 j2 = 1,j1
            if (y(j2) .le. yz(j2) .or. j2 .eq. j1) goto 552
            is = 1
            j4 = j4 + 1
            xf(j4) = x(j2)
            yf(j4) = y(j2)
            goto 551
c       start/end of fill area:
552         if (is .eq. 0) then          !line not started - use as first point
              xf(1) = x(j2)
              yf(1) = y(j2)
              j4 = 1
            else
            j4 = j4 + 1
            xf(j4) = x(j2)
```

```
            yf(j4) = y(j2)
              do 553 j3 = 1,j4-1          ! now load in last n points
                xf(j4+j3) = x(j2-j3)
                yf(j4+j3) = yz(j2-j3)
  553         CONTINUE
              CALL GRSETCOL(3)            ! green
              call pgpoly(2*j4-1,xf,yf)
              is = 0
            endif
  551     CONTINUE
!           CALL GRSETCOL(1)              ! white
            CALL GRSETCOL(2)              ! red
            call pgline(j1,x,yz)
            CALL GRSETCOL(2)              ! red
            call pgline(j1,x,y)
          else
            CALL GRSETCOL(2)              ! red
            call pgpoint(j1,x,y,-1)       ! plot points
          endif
  501   CONTINUE
        CALL pgend
          READ (5,701,END=959) NTMP
          GOTO 3
959       STOP
        END
```

[BHT.N2.AVG]3DV.FOR

```
C*************************************************************************
C*************************************************************************
C****                                                                 *****
C****   PROGRAM TO MODEL N    ADSORPTION ON Ru(0001)                 *****
C****                     2                                           *****
C****                                                                 *****
C****   Using true Monte-Carlo type model                             *****
C****                                                                 *****
C****   BRIAN TOBY 6/85                                               *****
C****                                                                 *****
C****   Plot results from array processor program  (BHT 6/84)         *****
C****   State analysis of adsorbed molecules as a function of T       *****
C*************************************************************************
C*************************************************************************
C**
      REAL TEMP(100),es(49),x(402),y(402)
      REAL ym(402),yz(402),xf(800),yf(800)
      INTEGER nr(49),na(49),ndm(49),ipat(16)
      INTEGER nd(49,100),ndtot(49)
        BYTE NAM(3),PNAM(50),FNAM(50),Q,TITLE(72)
        data ipat/Z0001,Z0002,Z0004,Z0008,
        1       Z0010,Z0020,Z0040,Z0080,
        2       Z0100,Z0200,Z0400,Z0800,
        3       Z1000,Z2000,Z4000,Z8000/
C**
C** NOW OPEN FILE 2 -- T VS. Ndsb for selected states
1       TYPE *,'ENTER FILE PREFIX'
        READ (5,701,END=959) NAM
701     FORMAT(3A1)
        TYPE *,'ENTER FILE TYPE (A - Adsorbed / D - Desorbed)'
        READ (5,701,END=959) Q
2       TYPE *,'ENTER COVERAGE'
        READ (5,*,END=1) COV
        ICOV = 100.*COV + 0.5
        ENCODE(14,704,FNAM) NAM,Q,ICOV,'DAT'
704     FORMAT('INP:',4A1,I2.2,'.',A3)
        OPEN(UNIT=2,FILE=FNAM,TYPE='OLD',FORM='FORMATTED',ERR=2)
!       OPEN(UNIT=2,FILE=FNAM,TYPE='OLD',FORM='FORMATTED',ERR=1)
        read (2,323) nstate,nsize
```

```
        read (2,323) (NA(k),k=1,nstate)
        read (2,323) (Nr(k),k=1,nstate)
        read (2,323) (NDtot(k),k=1,nstate)
        read (2,323) (NDM(k),k=1,nstate)
        read (2,324) (ES(K),k=1,nstate)
323     format(30i5)
324     format(30f5.2)
        n = 0
        Tmax = -9.E9
        Tmin =  9.E9
      DO 330 K=1,100
        read (2,340,end=350) temp(k),(ND(i,k),i=1,nstate)
340     format(f5.0,20i5)
        if (temp(k) .gt. Tmax) Tmax = temp(k)
        if (temp(k) .lt. Tmin) Tmin = temp(k)
        n = n + 1
  330 CONTINUE
350     close (2)

        ndmax = ndm(1)
      DO 311 K=2,nstate
        if (ndm(k) .gt. ndmax) ndmax = ndm(k)
  311 CONTINUE

        type *,'Energy range:',es(1),es(nstate)
!       type *,'Enter plotting limits:'
        EMIN = 0.
        EMAX = 3.001
!       accept *,emin,emax
        THETA = 45
!       R = 2.0
!       type *,'enter theta, R'
        type *,'enter R'
        READ (5,*,END=2) R

        dx = tmax - tmin        ! temperature range of spectra
        dy = ndmax              ! maximum state dsb rate
        npoint = 300
        zm = (emax - emin)/r    ! energy range of Z axis
        cost = cos(theta*3.14159/180.)*dx
        sint = sin(theta*3.14159/180.)*dy
        xmax = tmax + zm*cost           ! maximum X point on plot
        Dmax = NDmax + zm*sint          ! maximum Y point on plot
        xlen = 6.0              ! length of T scale (x axis)
        xmin = 80.              ! start labeling X axis at 80K
        xscale = 80.0/xlen      ! axis runs to 160 K
        xlbl = 79.95/xscale     ! length of drawn axis -- almost to 160 K
        ylen = 4.               ! length of highest peak (y axis)
        yscale = Ndmax/ylen     ! scale Y axis
        zlen = zm*sqrt((cost/xscale)**2 + (sint/yscale)**2)
        zinc = (emax-emin)/zlen
        ang = atand((sint*xscale)/(cost*yscale))
        type *,'Maximum page dimensions: X=',(xmax-xmin)/xscale,
        1       ' Y=',dmax/yscale,' Z=',zlen
        type *,'Actual Z axis angle:',ang
        x(1) = (160 - xmin)/xscale
        if (nam(1) .ge. 97) nam(1) = nam(1) - 32
        if (nam(2) .ge. 97) nam(2) = nam(2) - 32
        if (nam(3) .ge. 97) nam(3) = nam(3) - 32
      CALL PLOTS(0,2,0)
      CALL PLOT(.5,.75,-3)
      CALL SYMBOL(.5,2.,.15,'FILE: ',90.,+6)
      CALL SYMBOL(999.,999.,.15,nam,90.,+3)
      CALL SYMBOL(999.,999.,.15,', COVERAGE: ',90.,+12)
      CALL NUMBER(999.,999.,.15,COV,90.,+3)
      CALL SYMBOL(999.,999.,.15,', EQV. SIZE: ',90.,+13)
      CALL NUMBER(999.,999.,.15,1.*nsize,90.,-1)
      CALL SYMBOL(.8,2.,.1,'Y SCALE: 1 INCH = ',90.,+18)
```

```
      CALL NUMBER(999.,999.,.1,yscale,90.,+1)
      CALL SYMBOL(999.,999.,.1,' MOLECULES',90.,+10)
        CALL TONE(0.,0.,ipat,-16)
      CALL NAXIS(0.,0.,'TEMPERATURE',-11,xlbl,0.,xmin,xscale
     1 ,2./xscale,5,0.,0.,-1,0.,0.)
!       CALL NAXIS(0.,0.,'NUMBER DESORBED',15,6.,90.,0.,yscale
!     1 ,0.,0,0.,0.,-1,0.,0.)
      CALL NAXIS(x(i),0.,'RELATIVE ENERGY',-15,zlen,ang,emin,zinc
     1 ,.1/zinc,5,0.,0.,1,0.,0.)

c Draw lines in Z direction
        y(1) = 0.0
        y(2) = zm*sint/yscale
        do 530 j=80,150,10
          x(1) = (j - xmin)/xscale
          x(2) = (j + zm*cost - xmin)/xscale
          CALL DASHLN(X,Y,2,.1,.1)
530     continue
      DO 501 i=1,nstate
        z = (es(I)-emin)/r
        cosz = z*cost
        sinz = z*sint
c       DO 500 K=1,N
c       x(k) = temp(k) + cosz
c       y(k) = nd(i,k) + sinz
c  500 CONTINUE
c       x(N+1) = xmin
c       x(N+2) = xscale
c       y(N+1) = 0.0
c       y(N+2) = yscale
c       if (inum .ne. 0) CALL LINE(X,Y,N,1,-1,I)
c*****************************************************************************
c** Draw a dashed baseline -- the visible parts will be covered by a filled
c** line
        CALL NEWPEN(3)
        x(1) = temp(1)  + cosz
        x(2) = temp(N) + cosz
        y(1) = sinz
        y(2) = sinz
        x(3) = xmin
        x(4) = xscale
        y(3) = 0.0
        y(4) = yscale
            CALL CURVE(X,Y,-2,-0.02)
c*****************************************************************************
        j = 1
        ivis = 2
        j1 = 0
        DO 502 K=1,npoint
        if (i .eq. 1) ym(k) = -1.
        xt = tmin + (xmax-tmin)*(k-1)/(1.*npoint)
        xtz = xt - cosz
        if (xtz .le. temp(1) .or. xtz .ge. temp(n)) goto 502
        if (xtz .gt. temp(j)) then
          x0 = temp(j)
          y0 = nd(i,j)
          j = j + 1
        endif
        yt = y0 + (xtz - x0)*(nd(i,j) - y0)/(temp(j) - x0)
        j1 = j1 + 1
        x(j1) = xt
        y(j1) = yt + sinz
        yz(j1) = max(sinz,ym(k))
        if (ym(k) .le. yt + sinz) then
c line is visible
c       draw previous invisible line first if last point was invisible
          if (ivis .eq. 1) then
```

```
            CALL NEWPEN(3)
            x(j1+1) = xmin
            x(j1+2) = xscale
            y(j1+1) = 0.0
            y(j1+2) = yscale
            CALL CURVE(X,Y,-J1,-0.02)
            j1 = 1
            x(1) = xt
            y(1) = yt + sinz
            yz(1) = max(sinz,ym(k))
          endif
          ym(k) = yt + sinz
          ivis = 0
        else
c line is invisible
c       draw previous visible line first, if last point was visible
          if (ivis .eq. 0) then
            x(j1+1) = xmin
            x(j1+2) = xscale
            y(j1+1) = 0.0
            y(j1+2) = yscale
            yz(j1+1) = 0.0
            yz(j1+2) = yscale
            CALL NEWPEN(4)
            CALL LINE(X,YZ,J1,1,0,0)
!           CALL NEWPEN(5)
            CALL LINE(X,Y,J1,1,0,0)
            is = 0
            j4 = 0
          do 541 j2 = 1,j1
            if (y(j2) .le. yz(j2) .or. j2 .eq. j1) goto 542
            is = 1
            j4 = j4 + 1
            xf(j4) = (x(j2) - xmin)/xscale
            yf(j4) = y(j2)/yscale
            goto 541
c       start/end of fill area:
542         if (is .eq. 0) then          !line not started - use as first point
              xf(1) = (x(j2) - xmin)/xscale
              yf(1) = yz(j2)/yscale
              j4 = 1
            else
            j4 = j4 + 1
            xf(j4) = (x(j2) - xmin)/xscale
            yf(j4) = yz(j2)/yscale
              do 543 j3 = 1,j4-1         ! now load in last n points
                xf(j4+j3) = (x(j2-j3) - xmin)/xscale
                yf(j4+j3) = yz(j2-j3)/yscale
  543         CONTINUE
              CALL TONE(XF,YF,2*J4-1,1)
              is = 0
            endif
  541     CONTINUE
            j1 = 1
            x(1) = xt
            y(1) = yt + sinz
            yz(1) = max(sinz,ym(k))
          endif
          ivis = 1
        endif
  502   CONTINUE
        x(j1+1) = xmin
        x(j1+2) = xscale
        y(j1+1) = 0.0
        y(j1+2) = yscale
        if (ivis .eq. 0) then
```

```
            yz(j1+1) = 0.0
            yz(j1+2) = yscale
            CALL NEWPEN(4)
            CALL LINE(X,YZ,J1,1,0,0)
!           CALL NEWPEN(5)
            CALL LINE(X,Y,J1,1,0,0)
            is = 0
            j4 = 0
          do 551 j2 = 1,j1
            if (y(j2) .le. yz(j2) .or. j2 .eq. j1) goto 552
            is = 1
            j4 = j4 + 1
            xf(j4) = (x(j2) - xmin)/xscale
            yf(j4) = y(j2)/yscale
            goto 551
c       start/end of fill area:
552         if (is .eq. 0) then          !line not started - use as first point
              xf(1) = (x(j2) - xmin)/xscale
              yf(1) = y(j2)/yscale
              j4 = 1
            else
            j4 = j4 + 1
            xf(j4) = (x(j2) - xmin)/xscale
            yf(j4) = y(j2)/yscale
              do 553 j3 = 1,j4-1         ! now load in last n points
                xf(j4+j3) = (x(j2-j3) - xmin)/xscale
                yf(j4+j3) = yz(j2-j3)/yscale
  553         CONTINUE
              CALL TONE(XF,YF,2*J4-1,1)
              is = 0
            endif
  551     CONTINUE
        else
            CALL NEWPEN(3)
            CALL CURVE(X,Y,-J1,-0.02)
        endif
  501 CONTINUE
      CALL PLOT(0.,0.,999)
c       READ (5,701,END=959) NTMP
959     STOP
      END
```

3.4 Program SISO

[BHT.N2.LASER]SISO.FOR

```
C*************************************************************************
C*************************************************************************
C****                                                                 *****
C****   PROGRAM TO MODEL N   ADSORPTION ON Ru(0001)                   *****
C****                     2                                           *****
C****                                                                 *****
C****   Using true Monte-Carlo type model                             *****
C****                                                                 *****
C****   BRIAN TOBY, ERIC HOOD  12/83                                  *****
C****                                                                 *****
C****   Plot results from array processor program  (BHT 6/84)         *****
C****     Compute smoothed derivatives (BHT 11/85)                    *****
C****                                                                 *****
C*************************************************************************
C*************************************************************************
C**
      INTEGER SIZE,SIZA(10),NP(10),NDSB1(200),NDSB2(200)
      REAL*8 TITLE(9),DATSTR(2)
      DIMENSION X1(504),Y1(504),X2(504),Y2(504),c(20),s(20)
      REAL TEMP(200),COVI(7,7),COVIP(7,7),EI(7,7),TINT
      INTEGER NI(7,7,2),TMIN,TMAX
      REAL BETA,NU,NUO,E,R,T,NAAVG,LCTP,CHI
        BYTE BUFF(110)
C**
      CALL PLOTS(0,0,0)
      CALL DATE(DATSTR)
      N1 = 0
      SUMSIZE = 0
      LUNM = 10
      LUN = LUNM
        specspc = 1.0
        sclfct = 1.0
        type *,'enter scale factor, spacing between spectra'
        read (5,*,end=222) sclfct,specspc
222     DO 210 J=1,10
      READ(LUN,121,END=919,ERR=919) SIZE,ED,EN,EA,ER,EM,SO,CHI,
     1 TS,DSBINT,IR,(TITLE(I),I=1,9),LCTP,E,EO,NAAVG,DT,
     2 BETA
  121 FORMAT(I5,6F10.6,/,3F10.3,I12/,9A8,/,3F10.3,2F6.2,15x,f6.3)
      SIZA(J) = SIZE
      SUMSIZE = SUMSIZE + SIZA(J)**2
      TYPE 29,LUN,(TITLE(I),I=1,9),SIZE,SIZE,ED,EN,ER,EA,
     1 EN,SO,CHI,TS,IR
   29 FORMAT(/,' File #',I3,/,' ',72('*'),/,1X,9A8,/,1X,72('*')
     1   ,/' LATTICE IS',I4,' BY',I4,/,' DESORPTION ENERGY: ',
     2 F5.3,/,' DESTABILIZATION ENERGY FOR FILLED SITE:',F6.3,/,
     3 ' REPULSIVE INTERACTION ENERGY:',F6.3,/,
     4 ' ATTRACTIVE INTERACTIVE ENERGY:',F6.3,/,
     5 ' MIGRATION ENERGY: ',F7.4,')',/,
     6 ' INITIAL STICKING COEFFICIENT: ',F6.4,/,
     7 ' CHI = ',F12.5,/,' ADSORPTION TEMPERATURE:',F6.1,/
     8 ' RANDOM STARTING POINT:',I10,//)
      LUN = LUN + 1
  210 CONTINUE
  919 IF (LUN .EQ. LUNM) GOTO 929
      LUN = LUN - 1
      avgSIZE = SQRT(SUMSIZE)
C***
      X1(1) = 0        ! EXPOSURE (in L.)
      Y1(1) = 0        ! COVERAGE
      N1 = 1
C**  NOW READ IN POINTS FROM FILE
  100 NADSS = 0
      NEXPS = 0
      SUMSIZE = 0
```

```
      DO 220 L=LUNM,LUN
C SKIP OVER FILE IF IT HAS ENDED ALREADY
      IF (SIZA(1+L-LUNM) .EQ. 0) GOTO 220
      READ (L,22,END=939) NEXP,NADS
   22 FORMAT(1X,2I7)
      NADSS = NADSS + NADS
      NEXPS = NEXPS + NEXP
      SUMSIZE = SUMSIZE + SIZA(1+L-LUNM)**2
      GOTO 220
C END OF FILE -- SKIP OVER FILE NEXT TIME
  939 SIZA(1+L-LUNM) = 0
      CLOSE(L)
  220 CONTINUE
C IF SUMSIZE IS ZERO THEN ALL FILES ARE NOW EMPTY
      IF (SUMSIZE .EQ. 0) goto 949
      COV = NADSS / SUMSIZE
      EXPOS = NEXPS / SUMSIZE
C** NOTE EXPOSURE FROM FILE IS IN "MONOLAYERS" AND MUST BE CONVERTED
C**       TO LANGMUIR (L) USING THE RELATION:
C**    Flux = 4.08 L / MONOLAYER
C**       From Dushman p. 14, and B. Anton (private comm.) using:
C**          Flux = 3.513E22 P * (MOL. WT. * T)**-0.5 / cm**2 * sec
C**          T = 295 K
C**          MONOLAYER DENSITY = 1.58E15 Ru Atoms/cm**2
C**
C** NOW SET UP ARRAYS FOR PLOTTING
C**
      N1 = N1 + 1
      X1(N1) = EXPOS * 4.08
      Y1(N1) = COV
      GOTO 100
C** Now compute d(coverage)/d(exposure)
 949  N2 = 0
        ipol = 3
        ncnv = 11
!       type *,'Sticking Coef: polynomial size, convolute size'
!       read (5,*,end=223) ipol,ncnv
C      X2(0) = 0        ! COVERAGE
C      Y2(0) = Sinit    ! d(coverage)/d(exposure)
223     continue
      TYPE *,(X1(I),I=1,N1)
      TYPE *,(Y1(I),I=1,N1)
      DX = (X1(11) - X1(1))/40.8
!      TYPE *,'DX = ',DX
        call SDRV(y1,y2,n1,ncnv,ndrop,ipol)
      N2 = 0
C now drop points on ends
      DO 200 I=ndrop,N1-ndrop-1,2
      N2 = N2 + 1
      X2(N2) = (Y1(I)+Y1(I+1))/2.                ! COVERAGE
      Y2(N2) = (Y2(I)+Y2(I+1))/(DX*2.)           ! dC/dE
  200 CONTINUE
!      TYPE *,(X2(I),I=1,N2)
!      TYPE *,(Y2(I),I=1,N2)
C*** NOW START PLOTTING
c      CALL FACTOR(0.5)
c      CALL PLOT(.45,.75,-3)
       X = 0.5
       Y = 0.5
       XL = 0.10
       YL = 0.125
       iX = (1000. * X) + 0.5
       iY = (1000. * Y) + 0.5
       ixL = (100. * xL) + 0.5
       iyL = (100. * yL) + 0.5
C      ir = (1000. * r) + 0.5
       ir = 0
       encode (106,701,buff) iX,IY,IXL,IYL,IR,TITLE
701    format ('^IV',i5.5,'^IH',i5.5,'^M',2i3.3,i5.5,'^DL',9A8)
      CALL qUIC(BUFF,106)
```

```
      N = N1
      X1(N+1) = 0
      X1(N+2) = 0.5
      Y1(N+1) = 0
      Y1(N+2) = 0.05
C** DO 1st PLOT -- Coverage vs Exposure for: all, with & w/o repulsions
C**
c       CALL AXIS(0.,0.,'EXPOSURE',-8,.1*N/X1(N+2)+1.,0.,X1(N+1),X1(N+2))
C**
C** NOTE: previous line assumes 0.02*4.08 L per point
C**
c       CALL AXIS(0.,0.,'COVERAGE',8,12.,90.,Y1(N+1),Y1(N+2))
c       CALL PLOT(0.,0.,-999)
C** DO 2nd PLOT -- Sticking coeffient
C**
      CALL FACTOR(0.5)
      CALL PLOT(2.,2.,-3)
      X2(N2+1) = 0
      X2(N2+2) = 1./30.
      Y2(N2+1) = 0
      Y2(N2+2) = 0.1
      CALL AXIS(0.,0.,'ADSORPTION COEFFICIENT',22,10.,90.,
     1 Y2(N2+1),Y2(N2+2))
      CALL AXIS(0.,0.,'COVERAGE',-8,16.,0.,X2(N2+1),X2(N2+2))
      CALL SYMBOL(1.,18.,.15,TITLE,0.,+72)
        call newpen(5)
      CALL LINE(X2,Y2,N2,1,-1,0)
C       CALL CURVE(X2,Y2,-N2,-0.05)
C** Now plot known - Sticking coeffient
        open (unit=9,status='OLD',form='formatted',err=929)
      n1 = 0
        call newpen(5)
        DO 600 I=1,20
        read (9,605,err=610) C(I),X2(I),S(I),Y2(I)
        n1 = n1 + 1
 605    format(7x,4f7.4)
600     CONTINUE
 610    close (9)
        c(N1+1) = 0
        c(N1+2) = 1./30.
        s(N1+1) = 0
        s(N1+2) = 0.1
c       CALL LINE(C,S,N1,1,-1,4)
        x1(3) = 0
        x1(4) = 1./30.
        y1(3) = 0
        y1(4) = 0.1
        DO 620 I=1,n1
        X1(1) = c(i)
        X1(2) = c(i)
        Y1(1) = s(i) - y2(i)/2.
        Y1(2) = s(i) + y2(i)/2.
        CALL LINE(x1,y1,2,1,0,4)
        X1(1) = c(i) - x2(i)/2.
        X1(2) = c(i) + x2(i)/2.
        Y1(1) = s(i)
        Y1(2) = s(i)
        CALL LINE(x1,y1,2,1,0,4)
620     CONTINUE
C!*********************************************************************
C Now Plot TDS files
C*********************************************************************
C*********************************************************************
  929 LUNM = 20
      LUN = LUNM
        call newpen(3)
        ISO = 0
        TYPE *,'ENTER ISOTOPE TO BE PLOTTED (0=BOTH)'
        read (5,*,end=333) ISO
333     TYPE *,'ISOTOPE =',ISO
```

```
      SUMSIZE = 0
      DO 410 J=1,10
      READ(LUN,121,END=959,err=959) SIZE,ED,EN,EA,ER,EM,SO,CHI,
     1 TS,DSBINT,IR,(TITLE(I),I=1,9),LCTP,E,EO,NAAVG,DT,BETA
      LUN = LUN + 1
      SIZA(J) = SIZE
      SUMSIZE = SUMSIZE + SIZA(J)**2
      IF (N1 .NE. 0 .and. J .EQ. 1) CALL PLOT(0.,0.,-999)
      TYPE 29,LUN,(TITLE(I),I=1,9),SIZE,SIZE,ED,EN,ER,EA,
     1 EN,SO,CHI,TS,IR
      LUN = LUN + 1
      WRITE (6,128) EO,DT,NUO,A,BETA
  128 FORMAT(' ISOLATED N2 ATTRACTION IS E = ',
     3  F6.3,' (Kcal)',/,' TEMPERATURE INCREMENT',F8.4,/,1X,
     4 'PREFACTOR:',1P1E9.2,' * EXP(',0PF5.2,
     5 ' * COV)',/,' BETA:',F5.1,//)
  410 CONTINUE
  959 IF (LUN .EQ. LUNM) GOTO 2999
      LUN = LUN - 1
C*************************************************************************
      call portr
        X = 0.5
        Y = 0.5
        XL = 0.07
        YL = 0.10
        iX = (1000. * X) + 0.5
        iY = (1000. * Y) + 0.5
        ixL = (100. * xL) + 0.5
        iyL = (100. * yL) + 0.5
C       ir = (1000. * r) + 0.5
        ir = 0.
        encode (106,701,buff) iX,IY,IXL,IYL,IR,TITLE
        ipol = 3
        ncnv = 5
!       type *,'TDS: polynomial size, convolute size'
!       read (5,*,end=224) ipol,ncnv
224     CALL qUIC(BUFF,106)
      CALL FACTOR(0.5)
      CALL PLOT(2.,2.,-3)
      CALL AXIS(0.,0.,'TEMPERATURE',-11,14.,0.,50.,10.)
      CALL SYMBOL(1.,16.,.2,'ISOTOPE = ',0.,+10)
        IF (iso .eq. 0) THEN
          CALL SYMBOL(999.,999.,.2,'BOTH',0.,+4)
        else
          CALL NUMBER(999.,999.,.2,1.*iso,0.,-1)
        endif
        call newpen(3)
C*************************************************************************
C**  NOW READ IN POINTS FROM FILE
      TINT = 0.0001      ! So that we don't divide by zero
      NPLT = -1
 1100 N2 = 0
      COVP = 0.0
      SUMSIZE = 0
      TP = 0.0
      DO 420 L=LUNM,LUN
C SKIP OVER FILE IF IT HAS ENDED ALREADY
      IF (SIZA(1+L-LUNM) .EQ. 0) GOTO 420
      READ (L,125,END=969) NP(1+L-LUNM),COVO
  125 FORMAT(I5,F8.4)
      N2 = max(N2,NP(1+L-LUNM))
      IF (L .NE. LUNM .AND. ABS(COVO-COVP) .GT. 0.02) THEN
        TYPE *,'ERROR WRONG COVERAGE',L,COVO,COVP
        STOP
      ELSE
        COVP = COVO
      ENDIF
      SUMSIZE = SUMSIZE + SIZA(1+L-LUNM)**2
      GOTO 420
C END OF FILE -- SKIP OVER FILE NEXT TIME
```

```
  969 SIZA(1+L-LUNM) = 0
      CLOSE(L)
  420 CONTINUE
C IF SUMSIZE IS ZERO THEN ALL FILES ARE NOW EMPTY
      IF (SUMSIZE .EQ. 0) goto 1999

      mdes = 0
      NADS1 = 0
      NADS2 = 0
      DO 300 K=1,N2
      NDSB1(K) = 0
      NDSB2(K) = 0
      if (k .gt. 3) temp(k) = temp(k-1) + tint
      DO 202 L=LUNM,LUN
C SKIP OVER FILE IF IT HAS ENDED ALREADY OR IF WE HAVE READ ALL
C       POINTS FROM THIS TDS SCAN
      IF (SIZA(1+L-LUNM) .EQ. 0 .or. K .GT. NP(1+L-LUNM)) GOTO 202
      READ (L,124,end=2999) TP
  124 FORMAT(F6.2)
c** Is this T < 0
      IF (tp .lt. 0.) THEN
        NP(1+L-LUNM) = 0        ! prevent reading more points from current file
        goto 202
      ENDIF
      IF (L .EQ. LUNM .AND. k .le. 3) TEMP(K) = TP
      IF (ABS(TEMP(K)-TP) .GT. 0.1) THEN
        TYPE *,'ERROR WRONG TEMPERATURE',K,L,TEMP(K),TP
        STOP
      ENDIF
  126 FORMAT(7I6,3x,7I6)
      READ (L,126,end=2999) (((NI(I,J,IK),I=1,7),IK=1,2),J=1,7)
      DO 202 I=1,7
      DO 202 J=1,7
      NDSB1(K) = NDSB1(K) + NI(I,J,1)
      NDSB2(K) = NDSB2(K) + NI(I,J,2)
  202 CONTINUE
      NADS1 = NADS1 + NDSB1(K)
      NADS2 = NADS2 + NDSB2(K)
      IF (K .EQ. 3) TINT = TEMP(3) - TEMP(2)
  300 CONTINUE
      NADS = 0
        IF (ISO .NE. 2) NADS = NADS + NADS1
        IF (ISO .NE. 1) NADS = NADS + NADS2
        NDSB = 0
      DO 305 K=1,N2
        IF (ISO .NE. 1) NDSB = NDSB + NDSB2(K)
        IF (ISO .NE. 2) NDSB = NDSB + NDSB1(K)
      y1(k) = NADS - NDSB
  305 CONTINUE
      DX = -0.5*(TINT*SUMSIZE) / sclfct
c**     pad coverage with zeros
        y1(n2+1) = 0
        y1(n2+2) = 0
        y1(n2+3) = 0
        y1(n2+4) = 0
        y1(n2+5) = 0
        type *,'Averaged coverage = ',(1.*nads)/sumsize,' Type 1 to omit'
        read (5,*,end=225) iomit
        if (iomit .eq. 1) goto 1100
225     NPLT = NPLT + 1
!      TYPE 449,(Y1(I),I=1,N2)
!      TYPE *,'DX = ',DX
        call SDRV(y1,y2,n2+5,ncnv,ndrop,ipol)
      DO 205 I=1,N2
      Y2(I) = Y2(I) / DX        ! dC/dE
  205 CONTINUE
      TEMP(N2+1) = 50.
      TEMP(N2+2) = 10.
      Y2(N2+1) = -0.008*(specspc * NPLT + 0.25)
```

```
      Y2(N2+2) =  0.008
!      TYPE 449,(TEMP(I),I=1,N2+2)
!      TYPE 449,(Y2(I),I=1,N2+2)
  449 FORMAT(1X,8F10.5)
      CALL LINE(TEMP,Y2,N2,1,1,NPLT)
!      CALL CURVE(TEMP,Y2,-N2,-0.05)
      CALL NUMBER(12.5,.1+1.*NPLT,.2,COVO,0.,+3)
      GOTO 1100
 1999 CALL SYMBOL(12.4,1.1+NPLT,.2,'COVERAGE',0.,+8)
 2999 CALL PLOT(0.,0.,+999)
      STOP
      END
```

[BHT.N2.LASER]DERIV.FOR

```
C!*****************************************************************************
C*****************************************************************************
C** Program to smooth data using method of Savitsky and Golay from
C** Analytical Chemistry, Vol 36, 1627-1639 (1964)
C**
C** Also see: Steinier, Tremonia & Deltour, Analytical Chemistry, Vol 44
C** 1906-1909 (1972)
C**
C**  Modified to compute derivatives
C*****************************************************************************
C************************   Brian Toby 11/85   *******************************
C*****************************************************************************
      Subroutine SDRV(y,yt,n,np,ncm1o2,ipol)
C  Parameters:
c       Y  (real, array, input)          -- data array to be smoothed
c       YT (real, array, output)         -- resultant smoothed data
c       N  (integer, input)              -- number of points in Y and YT
c       NP (integer, input)              -- number of points in smoothing
c                                        convolute, larger ==> more smoothing
c       NCM1O2 (integer, output)         -- number of unsmoothed points at
c                                        beginning and end of array YT
c                                        = (NC-1)/2 where NC is the actual
c                                        convolute size
C       IPOL                             -- order of smoothing polynomial
c                                        (3<= IPOL <= 5)
C
      real y(1),yt(1)
      integer coef(50),sum,s,n,nc,np
      data nc/-9999/
      save nc,coef,sum,ipolprev
      if (np .eq. nc .and. ipol .eq. ipolprev)
     1      goto 4  ! have we already read in this convolute?
      if (ipol .le. 3) then
        open(file='pub:quaddirv',unit=1,status='old',
     1      shared,readonly)
      elseif (ipol .eq. 4) then
        open(file='pub:cubdirv',unit=1,status='old',
     1      shared,readonly)
      else
        open(file='pub:quintdirv',unit=1,status='old',
     1      shared,readonly)
      endif
1     read (1,*,end=999) i
      read (1,*) (coef(j),j=1,i),sum
      if (i .eq. np) goto 3
      if (i .lt. np) goto 1
C** This is the largest or closest sized convolute we'll get
999   type *,'Size ',np,' not found on data file. Using',i
3     close(1)
      nc = i
      ipolprev = ipol
```

```
4       ncm1o2 = (nc-1)/2
        do 100 i=1,N
        if (i .gt. ncm1o2 .and. n-i .gt. ncm1o2) then
C** Go ahead and apply the convolute
        t = 0
          do 200 j=1,nc
            t = t + coef(j)*y(i+j-ncm1o2)
200       continue
          Yt(i) = t/sum
        else
C** Nope we're on the wings and can't smooth it, stick in "simple deriv"
          if (i .lt. n) then
             Yt(i) = Y(i+1) - Y(i)
          else
             Yt(i) = Y(i) - Y(i-1)
          endif
        endif
100     continue
        return
        end
```

[BHT.N2.LASER]QUADDIRV.DAT

```
5
-2,-1,0,1,2,10
7
-3,-2,-1,0,1,2,3,28
9
-4,-3,-2,-1,0,1,2,3,4,60
11
-5,-4,-3,-2,-1,0,1,2,3,4,5,110
```

3.5 Program FFTMAP

[BHT.N2.LASER]FFTMAP.FOR

```
C*************************************************************************
C*************************************************************************
C**
C**     PROGRAM TO COMPUTE DIFFRACTION PATTERNS FROM A HEXAGONAL SURFACE
C**
C**  This program computes a 2-D FFT using a 1-D real to complex FFT and then
C**  a 1-D complex to complex FFT.  This gives matrix INTEN which gives
C**  intensities for one half of reciprocal space.  All reciprocal space is
C**  then mapped into this matrix by subroutine ARR.  Subroutine LSTFIT uses
C**  a least-squares iteration to determine the width, height and center of
C**  the root 3 spot.
C**
C**              Brian H. Toby  12/84
C**
C*************************************************************************
C*************************************************************************
      COMMON /A/ INTEN,M,N
      COMMON /B/ MO2Pi,COV,COVT,IALL,NSCAT,RSCAT
      COMMON /pgplt/ MC,NC,K,GAM,ERRS,covS,exposS,timeS
      character*72 TITLE
      REAL INTEN(129,256),INTMP(129,256)
      REAL*8 SCAT(128,256)
      COMPLEX*16 DPAT(129,256)
      INTEGER SIZE,TSIZE,PRVSZ,NSCAT,RSCAT
      INTEGER NA(20),nsel(4),siza(10)
      REAL BETA,NU,NUO,E,T,NAAVG,LCTP,CHI,ERRS(4)
      REAL*8 DATSTR(2)
      REAL IMAX,MC,NC,K,GAM,R
      REAL XC(4),YC(4),YL1/0.0/,YL2/0.2/
      REAL ALIN(20),DLIN(20),XLIN(202),YLIN(202)
      REAL CDESPL(20),EDESPL(20),TDESPL(20)
      byte ch,ty(132)
      INTEGER fta,hofg,cnum,wofg,bhi,bwi,orient,NSEG/20/
      Data fta/9999/,orient/1/,nplt/0/,siza/10*0/
      DATA CDESPL/20*-1./,EDESPL/20*-1./,TDESPL/20*-1./
      DATA icd,ied,itd/3*1/
      D(I,J,MC,NC) = SQRT(((I-mc)/M)**2 + 3.*((j-nc)/N)**2)
      R3 = SQRT(3.)
c** ILOG   0 ==> linear intensity scaling
c** ILOG > 0 ==> log intensity scaling
c** ILOG < 0 ==> no versatec plot
      TYPE *,'Enter 0 for a linear intensity scale'
      TYPE *,'Enter n>0 logarithmic (10**n is the intensity range)'
      TYPE *,'Enter -1 for no diffraction map'
      ACCEPT *,ILOG
C
      TYPE *,'Enter Scattering power of N2, Ru'
      READ (5,*) NSCAT,RSCAT
      WRITE (6,913) NSCAT,RSCAT
  913 FORMAT(' N2 SCATTERING POWER IS',I3,/,
     1 ' Ru SCATTERING POWER IS',I3,/)
C
C
c       type *,'Enter  0 for unit weights'
c       type *,'Enter  1 for radial weighting'
c       type *,'Enter -1 for intensity weighting'
c       accept *,iweigh
c       IF (IWEIGH) 1,2,3
c1     type *,'Using intensity weighting'
c      goto 901
c2     type *,'Using unit weights'
c      goto 901
c3     type *,'Using radial weighting'
C*************************************************************************
```

```
901    type *,'Enter 0 to process all spectra, 1 to select by coverage'
       ACCEPT *,iall
C
       IPASS1 = 0
       IF (IALL .EQ. 0) THEN
           WRITE (6,914)
914        FORMAT(' PLOT ALL MAPS',/)
       ELSE
         write (6,*) 'Enter map coverages'
         READ (5,*,END=199) (CDESPL(I),I=1,20)
199      write (6,*) 'Enter map exposures'
         READ (5,*,END=299) (EDESPL(I),I=1,20)
299      write (6,*) 'Enter map times'
         READ (5,*,END=399) (TDESPL(I),I=1,20)
       ENDIF
399      continue
C
C*******************************************************************************
C** FILE DEFINITIONS
       LUNQ = 1            ! QUIC FILE
       LUNo = 9
       LUNM = 10
       LUN = LUNM
C*******************************************************************************
       DO 210 J=1,10
       CALL OPENIN(LUN,LUNo,NSCAT,RSCAT,TSIZE,TITLE)
       SIZA(J) = TSIZE
       IF (TSIZE .LE. 0) GOTO 919
C**  NOW REDUCE TSIZE SO THAT SIZE = 2*N
       SIZE = 2 * IFIX(TSIZE / 2.)
       IF (SIZE .NE. TSIZE) WRITE (6,902) TSIZE,SIZE
  902 FORMAT(' REDUCING LATTICE SIZE FROM',I3,' TO',I3,/)
       IF (J .EQ. 1) PRVSZ = size
       IF (PRVSZ .NE. size) then
         WRITE(6,903) PRVSZ,SIZE
903      FORMAT(' ***ERROR*** UNEQUAL LATTICE SIZES',I3,'<>',I3)
         goto 998
       endif
       LUN = LUN + 1
  210 CONTINUE
C*******************************************************************************
C*******************************************************************************
  919 IF (LUN .EQ. LUNM) GOTO 998
       LUN = LUN - 1
       M = SIZE
       N = 2 * SIZE
       NO2P1 = SIZE / 2 + 1
c** INITIALIZE MAP?
       IF (ILOG .LT. 0) GOTO 998
C YES ***********************************************************************
C** START Plot -- landscape mode
         call qini(0,LUNQ,orient,'leed.qms')
c** define the glyph heigth and width in terms of the number of sites
         hofg = 7. * 300. / (2*size + 1.)  ! Font size in dots (300 dots/inch)
c(7 inches ==> lattice from -size ... 0 ... size)
         wofg = hofg * 2. / r3 + 0.5      ! adjust font for scaling of n to m
         bhi = hofg       ! height of bit map (in dots)
         bwi = wofg       ! width of bit map (in dots)
C        type *,'font height:',hofg,'dots ',hofg/300.,' inches'
C        type *,'font width: ',wofg,'dots ',wofg/300.,' inches'
C        type *,'font ratio: ',wofg * 1./hofg,' (',2./r3,' perfect)'
C*******************************************************************************
C*NOW DEFINE THE FONT SET
         call qfnt(1,fta,orient,0,'bht1',hofg,0)
         nchar = 20
         do 212 i=0,nchar
           ch = 65 + i
           den = i / 20.
C* N.B. for landscape BWI and BHI are reversed
```

```
          call qfdef(0,ch,wofg,bwi,bhi,0,0)
          CALL font(LUNQ,bwi,bhi,den)
212     continue
c** End font definition
        call qfdef(-1)
c       CALL DATE(DATSTR)
C!*****************************************************************************
C** NOW READ IN MAPS
C*****************************************************************************
1000  SUMSIZE = 0
      WRITE (6,33)
   33 FORMAT('0',75('*'))
C** IADD = 0 ==> Zero INTEN array
      IADD = 0
      covS = 0.0
      exposS = 0.0
      timeS = 0.0
      IFLAG = 0
      DO 220 L=LUNM,LUN
C SKIP OVER FILE IF IT HAS ENDED ALREADY
      tsize = SIZA(1+L-LUNM)
      IF (tsize .EQ. 0) GOTO 220
      CALL READIN(L,tsize,cov0,expos,time)
      IF (cov0 .LE. 0) THEN
C**     END OF FILE -- SKIP OVER FILE NEXT TIME
        SIZA(1+L-LUNM) = 0
        CLOSE(L)
      else
        covS = covS + cov0*tsize*tsize
        exposS = exposS + expos*tsize*tsize
        timeS = timeS + time
C**   SHOULD WE DIFFRACT THIS MAP?
        IF (IALL .EQ. 0 .OR. Iflag .NE. 0) THEN
          IFLAG = 1
        ELSE
            IFLAG = 0
          IF (ABS(COV0 - CDESPL(ICD)) .le. 0.011) THEN
             IFLAG = 1
             ICD = ICD + 1
          endif
          IF (ABS(expos/eDESPL(IeD)-1) .le. 0.05) THEN
            IFLAG = 1
            IeD = IeD + 1
          endif
          IF (ABS(time/tDESPL(ItD)-1.) .le. 0.05) THEN
            IFLAG = 1
            ItD = ItD + 1
          endif
        endif
        IF (IFLAG .EQ. 1)
C**   Calculate the FFT
     1     CALL DIFFRACT(SCAT,DPAT,IADD)
C** IADD >= 1 ==> Add to INTEN array next time
        IADD = IADD + 1
        SUMSIZE = SUMSIZE + SIZA(1+L-LUNM)**2
        WRITE (6,34) LUN,COV0,expos,time,IFLAG
34      FORMAT(' File #',i3,' COVERAGE = ',F6.3,
     1.   ', EXPOS =',f6.2,', TIME =',f9.1,' Sec  (',I1,')')
      endif
  220 CONTINUE
C*****************************************************************************
C IF SUMSIZE IS ZERO THEN ALL FILES ARE NOW EMPTY
      IF (SUMSIZE .LE. 0) goto 999
      covS = covS/sumsize
      exposS = 4.08*exposS/sumsize
      timeS = timeS/iadd
      avgSIZE = SQRT(SUMSIZE)
      WRITE (6,35) covS,exposS,timeS
35    FORMAT(' Averages: COVERAGE = ',F6.3,
```

```
     1   ', EXPOS =',f6.2,', TIME =',f9.1,' Sec',/,' ',75('*'))
      IF (IFLAG .NE. 1) goto 1000
c** Adjust intensities to reflect number of averaged maps
      IF (IADD .gt. 1) THEN
        DO 205 I=1,MO2P1
        DO 205 J=1,N
          INTEN(I,J) = INTEN(I,J) / iadd
205     CONTINUE
      ENDIF
C*******************************************************************************
C*******************************************************************************
C** DRAW INTENSITY MAP?
      IMAX = 1.E-30
      DO 200 I=1,N
      DO 200 J=1,MO2P1
      IF (INTEN(J,I) .GT. IMAX) IMAX = INTEN(J,I)
  200 CONTINUE
C** START NEW PLOT IF THIS IS NOT THE FIRST PASS
      IF (IPASS1 .NE. 0) CALL qini(-1)
      IPASS1 = 1
      CALL QAPOS(7.8,1) ! Y COORDINATE
      IF (ED .GT. -1) then
      CALL QAPOS(1.5,2) ! X COORDINATE
        encode (58,731,ty) covS,exposS,timeS
731     format('ADSORBED TO',F5.2,', EXPOSURE =',F5.1,'L, TIME =',
        1       1PG10.3,' Sec' )
        call qlbl(0.15,0.15,0.,58,ty,1)
      ELSE
      CALL QAPOS(2.5,2) ! X COORDINATE
        encode (16,701,ty) 'DESORBED TO',covs
701     format(A,F5.2)
        call qlbl(0.15,0.15,0.,16,ty,1)
      ENDIF
        call qapos(0.25,1)      ! y coordinate
        call qapos(1.25,2)      ! x coordinate
        encode (72,711,ty) TITLE
711     format(A72)
        call qlbl(0.1,0.1,0.,72,TY,1)
C**  Now plot contents of intensity matrix
      NL = -M
      NH =  M
      NL = -N/2
      NH =  N/2
C*******************************************************************************
C**
        call qfnt(0,fta)
      ii = 0
      DO 120 J=NL,NH
      ii = ii + 1
      X = 0.25
      Y = II * hofg / 300.  + 0.5
        call qapos(x,2) ! x coordinate
        call qapos(y,1) ! y coordinate
      jj = 0
      DO 130 I=NL,NH
      If(jj .ge. 100) then
        CALL qbuff(jj,ty,0)
        jj = 1
      else
        jj = jj + 1
      endif
      IF (ILOG .EQ. 0) XINT = 20. * ARR(I,J) / IMAX + 0.5
      IF (ILOG .GT. 0) XINT = 20. * (1.+ ALOG10(ARR(I,J)/IMAX+1.E-20)
     1  /ilog)+ 0.5
      ty(jj) = 65 + JMAX0(0,JMIN0(JINT(XINT),20))
  130 CONTINUE
      CALL qbuff(jj,ty,0)
      CALL qbuff(2,'^-',0)
  120 CONTINUE
```

```
C*************************************************************************
C** now put squares of known density on page
      ii = 50./hofg     ! number of pixels per square
      DO 320 J=0,nchar
      DO 320 I=1,ii
      Y = I * hofg / 300.  +  0.25 * J + 1.0
        call qapos(8.5,2)       ! x coordinate
        call qapos(y,1) ! y coordinate
      DO 330 k=1,ii
      ty(k) = 65 + J
  330 CONTINUE
      CALL qbuff(ii,ty,0)
      CALL qbuff(2,'^-',0)
  320 CONTINUE
      DO 340 J=0,nchar
        call qapos(8.8,2)       ! x coordinate
      Y = hofg / 300.  +  0.25 * J + 1.05
        call qapos(y,1)         ! y coordinate
      IF(ILOG .EQ. 0) THEN
         XINT =  J / (1.*nchar)
        encode (5,702,ty) xint
702     format(f5.3)
        call qlbl(0.1,0.05,0.,5,ty,1)
      ELSE
         XINT = 10 ** ((J-NCHAR) * ilog/20.)
        encode (7,703,ty) xint
703     format(f7.5)
        call qlbl(0.15,0.12,0.,7,ty,1)
      ENDIF
  340 CONTINUE
      CALL qbuff(2,'^-',0)
C*************************************************************************
C**  Find the root 3 spot beam profile
      GOTO 1000
c* Delete font, close files
999   IF (ILOG .ge. 0) then
        call qfnt(-1,fta,orient)
        CALL qini(1)
      endif
  998 STOP
      END
C!*************************************************************************
      SUBROUTINE READIN(LUN,tsize,cov0,expos,time)
      COMMON /C/ SIZE,HEX
C**
      INTEGER HEX(128,128)
      INTEGER SIZE,TSIZE
C*************************************************************************
C** readin preface of map
      READ (LUN,912,END=999) imore,cov0,expos,time
912     FORMAT(1X,I5,f6.3,f11.3,f11.1)
      if (imore .eq. 0) goto 999
C*************************************************************************
C** NOW READ IN MAP (HEX MATRIX)
C*************************************************************************
 1000 ICOV = 0
      DO 1003 I = 1, TSIZE
      READ (lun,911,END=998) (HEX(I,J),J=1,TSIZE)
  911 FORMAT(1X,100I1)
C** now compute actual coverage on surface
c       DO 1003 J = 1, TSIZE
c       IF (HEX(I,J) .NE. 0) ICOV = ICOV + 1
 1003 CONTINUE
c       COV = ICOV / (1.*TSIZE **2)
C*************************************************************************
C** return to main program - readin successful
       RETURN
C** return to main program - no more maps on file
```

```
999   COVO =  0.0
      RETURN
C** return to main program - Unexpected end of file or other error
998   COVO =  -1.0
      RETURN
      END
C!*****************************************************************************
      SUBROUTINE DIFFRACT(SCAT,DPAT,IADD)
      COMMON /A/ INTEN,M,N
      COMMON /B/ MO2P1,COV,COVT,IALL,NSCAT,RSCAT
      COMMON /C/ SIZE,HEX
C**
      REAL*8 SCAT(M,N),WK(1486)
      COMPLEX*16 DPAT(MO2P1,N),CVEC(256)
      REAL INTEN(129,256)
      INTEGER HEX(128,128)
      INTEGER SIZE,TSIZE,NSCAT,RSCAT
C*****************************************************************************
C**  Lets start by expanding the "Quasi-rectangular" HEX matrix into the
C       "True Rectangular" matrix SCAT
      DO 1000 J = 1,N
      NJ = (J + 1)/2
      DO 1000 I = 1,M
      SCAT(I,J) = 0
      IF (MOD(I+J,2) .EQ. 0) GOTO 1000
      SCAT(I,J) = NSCAT * HEX(I,NJ) + RSCAT
 1000 CONTINUE
C*****************************************************************************
C**  Now compute the FFT of the matrix
C*****************************************************************************
C** COMPUTE THE FFT ALONG THE FIRST AXIS
      DO 240 J=1,N
      CALL FFTRC(SCAT(1,J),M,DPAT(1,J),WK,WK)
  240 CONTINUE
C** COMPUTE THE FFT ALONG THE SECOND AXIS
      DO 250 I=1,MO2P1
C** REMOVE ROW FROM MATRIX
      DO 251 J = 1,N
      CVEC(J) = DPAT(I,J)
  251 CONTINUE
C** NOW TRANSFORM THE VECTOR
      CALL FFTCC(CVEC,N,WK,WK)
C** PUT ROW BACK INTO MATRIX
      DO 252 J = 1,N
      DPAT(I,J) = CVEC(J)
  252 CONTINUE
  250 CONTINUE
C*****************************************************************************
C** Now calculate intensity (magnitude **2) from complex matrix
      IF (IADD .eq. 0) THEN
        DO 205 I=1,MO2P1
        DO 205 J=1,N
          INTEN(I,J) = 4.*(CDABS(DPAT(I,J)) / (M*N))**2
c** the 4 adjusts the intensities to reflect that the SCAT array is half zeros
205     CONTINUE
      ELSE
        DO 206 I=1,MO2P1
        DO 206 J=1,N
          INTEN(I,J) = INTEN(I,J) + 4.*(CDABS(DPAT(I,J)) / (M*N))**2
c** the 4 adjusts the intensities to reflect that the SCAT array is half zeros
206     CONTINUE
      ENDIF
C*****************************************************************************
      RETURN
      END
C!*****************************************************************************
      SUBROUTINE OPENIN(LUN,LUNo,NSCAT,RSCAT,TSIZE,TITLE)
      COMMON /pgplt/ MC,NC,K,GAM,ERRS,covS,exposS,timeS
      REAL ERRS(4)
      character*72 TITLE
```

```
      character*50 fnam
      INTEGER LUN,LUNo,NSCAT,RSCAT,TSIZE
      REAL BETA,NU,NUO,E,T,NAAVG,LCTP,CHI
C*************************************************************************
      WRITE (6,*) 'Enter filename'
      read (5,935,end=998) fnam
935   format(A50)
      open (unit=lun, file=fnam, status='old', err=998)
C*************************************************************************
      READ (LUN,21,ERR=998,END=998) TSIZE,ED,EN,EA,ER,EM,SO,CHI,TS,
     1 DSBINT,IR,TITLE,LCTP,E,EO,NAAVG,DT,A,NUO,BETA
   21 FORMAT(I5,6F10.6,/,3F10.3,I12,/,A72,/,F10.1,2F10.6,F6.2,
     1 F6.4,F6.2,E9.2,F6.1)
      RATIO = ER / EA
  211 WRITE(6,29) TITLE,TSIZE,TSIZE,ABS(ED),EN,ER,EA,
     1 RATIO,EM,SO,CHI,TS,IR
   29 FORMAT('0',72('*'),/,1X,A72,/,1X,72('*'),//' LATTICE IS',I4,
     1  ' BY',I4,/,' DESORPTION ENERGY: ',
     2 F5.3,/,' DESTABILIZATION ENERGY FOR FILLED SITE:',F7.3,/,
     3 ' REPULSIVE INTERACTION ENERGY:',F6.3,/,
     4 ' ATTRACTIVE INTERACTIVE ENERGY:',F6.3,/,
     5 ' ER / EA: ',F5.3,/,' MIGRATION ENERGY: ',F7.4,/,
     6 ' INITIAL STICKING COEFFICIENT: ',F6.4,/,' CHI = ',F12.5,
     7 /,' ADSORPTION TEMPERATURE:',F6.1,/,
     8 ' RANDOM STARTING POINT:',I10,//)
C*************************************************************************
      RETURN
C** return to main program - Unexpected end of file or other error
998   TSIZE  = -1
      RETURN
      END
C!*************************************************************************
      FUNCTION ARR(I,J)
      COMMON /A/ INTEN,M,N
      REAL INTEN(129,256)
      IP = MOD(I,M) + 1
      IF (IP .LE. 0) IP = IP + M
      JP = MOD(J,N) + 1
      IF (JP .LE. 0) JP = JP + N
      IF (IP .GT. M/2+1 .AND. JP .EQ. 1) THEN
        ARR = INTEN(M+2-IP,1)
      ELSE IF (IP .GT. M/2+1) THEN
        ARR = INTEN(M+2-IP,N+2-JP)
      ELSE
        ARR = INTEN(IP,JP)
      ENDIF
      RETURN
      END
C!*************************************************************************
      subroutine font(LUN,nr,nc,den)
C**** Program to create PIXEL Array for LASER PRINTER
C* nc is number of columns (bits per row);
C* nr is number of rows (bits per column);
        byte pixel(50),ca(16),lpixel(100,100)
        data ca/'0','1','2','3','4','5','6','7','8','9',
        1       'A','B','C','D','E','F'/
        data ir/1010101/
        ncp = (nc + 15.)/16.
        nch = 4*ncp
        ncp = 16*ncp
C* ncp is nc after padding to a multiple of 16
C* nch is number of characters per row
!       type *,nc,nr,ncp,nch
c** Now for the "rule" to determine the pattern
        if (den .ge. 0.5) then
          fill = 1
          over = 0
          idots = (1. - den) * nr * nc + 0.5    ! number of dots to set
        else
          fill = 0
```

```
          over = 1
          idots = den * nr * nc + 0.5   ! number of dots to set
        endif
        do 200 j=1,nr
        do 200 i=1,ncp
        if (i .gt. nc) then
          lpixel(i,j) = 0
        else
          lpixel(i,j) = fill
        endif
200     continue
        do 210 k=1,idots
211     i = nc * ran(ir) + 1
        j = nr * ran(ir) + 1
        if (lpixel(i,j) .eq. over) goto 211
          lpixel(i,j) = over
210     continue

        nm = 0
        do 100 j=1,nr
!       type 1,(lpixel(i,j),i=1,ncp)
1       format(1x,100i1)
        do 400 i=1,ncp,4
        num = 1 + lpixel(i,j)*8 + lpixel(i+1,j)*4 +
        1 lpixel(i+2,j)*2 + lpixel(i+3,j)
        nm = nm + lpixel(i,j) + lpixel(i+1,j) +
        1 lpixel(i+2,j) + lpixel(i+3,j)
        pixel((i-1)/4+1) = ca(num)
400     continue
      CALL qbuff(nch,pixel,0)
c       type 2,(pixel(i),i=1,nch)
2       format(1x,20a1)
100     continue
!       type *,'density:',den,nm/(1.*nr*nc),'(actual)'
        return
        end
```

Section II.

Reaction of Carboxylate and Ketone Ligands on Metal Surfaces

Chapter 4:

Introduction to Section II.

Reaction of Carboxylate and Ketone Ligands on Metal Surfaces.

The interactions of molecules with surfaces has been an important field of study since the pioneering work of Langmuir. With the advent of modern ultra-high vacuum techniques and continual improvements in sensitivity, reliability and decreased cost of solid-state electronic devices, new fields have opened. Detailed study of the bonding and reactions of molecules and metal surfaces is now possible.

Signal detection is a fundamental difficulty in these systems. Techniques used in surface science must measure a signal corresponding to a density on the order of 10^{13} to 10^{15} surface species per cm^2. Thus, the number of interactions that occur between a probe and surface species is limited by the physical size of the sample and experimental system. Techniques must also be able to distinguish surface properties from properties of the bulk material. The work described in the following section of this Thesis relies on two complementary techniques, high-resolution electron energy loss spectroscopy and thermal desorption mass spectrometry, techniques which are very well suited to the problem of determining adsorbate geometry and desorption/decomposition reaction kinetics.

Electron energy loss spectroscopy (EELS) allows measurement of the vibrational modes of adsorbed molecules. For the experimental results presented in this Thesis, a highly monochromatic beam of electrons (typically with an energy of 4 eV) is focused on a small area of the sample, which in the case of these studies is the [001] face of a Ru crystal. While most of the electrons incident on the sample are captured and conducted to ground, those electrons which are scattered from the surface (usually 1 to 10%) can be detected by an electron multiplier mounted in the energy analyzer, a second independent electron monochromator [**1**]. An EELS spectrum is measured by counting the number of scattered electrons while sweeping the energy of the analyzer.

While most of the electrons are scattered elastically, that is retaining their incident energy, a small number of electrons, (usually less than 1%) lose or gain

characteristic amounts of energy by coupling to vibrational modes of the surface or the adsorbate molecules. Two mechanisms have been have been determined for electron scattering, dipolar scattering and impact scattering.

In dipolar scattering, incident electrons couple to a time-dependent electronic (vibrational) dipole caused by instantaneous charge separation between two (or more) atoms. The metal surface can be modeled as a gas of free electrons which interacts with vibrational mode dipoles by creating an image dipole. This image dipole is parallel to the component of a vibrational mode dipole perpendicular to the surface and is antiparallel to the component of the vibrational mode dipole parallel to the surface. This effect cases the surface to enhance the dipole moment of vibrational modes with dipoles perpendicular to the surface and shield dipoles parallel to the surface. This results in the surface selection rule, which predicts that only modes with a perpendicular component to their dipole moment will have a high cross-section for dipolar scattering. The cross-section is highest for dipolar scattering the specular direction [**2**].

The mechanism of impact scattering involves short-range interaction between the incident electron and an electron potential function of an atom. There is no requirement for dipole orientation, but impact scattering is most commonly observed for modes of hydrogen atoms at the incident electron energies used for these experiments. The scattering is diffuse and, unlike dipole scattering, is not strongly peaked in the specular direction [**2**].

Thermal desorption mass spectrometry (TDMS) is performed by adsorbing molecules onto a surface and then heating the surface while monitoring the partial pressures of desorbing molecules with a mass spectrometer as a function of surface temperature. If the heating rate is slow and the rate of pumping is high, as is the case for the experiments described in this Thesis, the rate of desorption of a species can be well approximated by its partial pressure and the surface coverage can be determined by integrating the mass spectrometer intensity as a function of time. Analysis of thermal desorption lineshapes and

the variation of desorption temperatures with heating rate may be used to assign the Arrhenius prefactor and binding energy as well as the kinetic order of the desorption reaction, but such analysis is often inaccurate [**3**]. Nonetheless, TDMS is very useful technique for characterization of the gas phase products of decomposition reactions and for the estimation of kinetic parameters.

Thermal desorption of decomposition products or reaction products may occur directly following the formation of the product, or the product may remain adsorbed on the surface until its desorption temperature is reached. The former case is referred to as reaction-limited desorption, while the latter case is desorption-limited. Reaction-limited desorption yields direct information about the kinetics of the reaction, but other techniques, such as EELS must be used if product desorption is desorption limited.

The use of EELS and TDMS, and to a lesser extent, low energy electron diffraction, X-ray and ultra-violet photoelectron spectroscopies and infrared reflection-absorption spectroscopy has allowed surface scientists to approach the bonding of ligand molecules to metal surfaces using the traditional interpretive frameworks used by their colleagues who study organometallic and inorganic chemistry [**4,5**]. In particular, ligand bonding to Ru(001) has been an area of concentrated interest; a large number of small molecules including inorganics, oxygen-containing hydrocarbons and aromatics have been studied on this surface [**6**].

In Chapters 5, 6 and 7, EELS and TDMS are used to examine the bonding and decomposition of formic acid on the (001) surface of Ru. Formic acid is found to deprotonate upon adsorption at 80 K, forming monodentate and symmetrically bound bidentate formate species. Annealing the surface causes conversion of the monodentate formate to bidentate formate. Additional heating causes the formate species to decompose yielding CO, CO_2, H_2O, H_2 and O_2. Evidence for a surface hydroxyl intermediate, the first observed on Ru(001), is also presented.

In Chapter 8, Appendix D and Appendix E, the bonding and decomposition of acetone is studied on Ru(001) using EELS and TDMS. Molecular acetone is found to bond to the Ru(001) surface in two configurations, an η^1 species, bonded through the oxygen atom, and an η^2 species bonded side-on through the O-C bond. The η^2 species is bonded irreversibly and decomposes with heating, while the η^1 desorbs molecularly. The η^1 species is present in small concentrations on clean Ru(001), but preadsorption of an ordered p(2 $\times$ 2) O adatom overlayer increases the concentrations of the η^1 species with respect to the η^2 form. In Chapter 8, results for acetone adsorbed on the Pt(111) are also presented. On this surface only the η^1 species is observed and acetone does not decompose. From this work, a correlation can be made between surface Lewis acidity and bonding configurations of ketones.

References

[1] G. E. Thomas and W. H. Weinberg. Rev. Sci. Instrum. **50**, 497 (1979).

[2] H. Ibach and D. L. Mills, *Electron Energy Loss Spectroscopy and Surface Vibrations*, (Academic Press, New York, 1982).

[3] J. M. Soler and N. Garcia, Surface Sci. **124**, 563 (1983).

[4] N. D. S. Canning and R. J. Madix, J. Phys. Chem. **88**, 2437 (1984).

[5] N. R. Avery, J. Vac. Sci. Technol. A **3**, 1459 (1985).

[6] K. L. Shanahan and E. L. Muetterties, J. Phys. Chem. **88**, 1996 (1984).

Chapter 5:

Decomposition of Formic Acid on Ru(001): An EELS Search for a Formic Anhydride Intermediate

L574

Surface Science 122 (1982) L574–L578
North-Holland Publishing Company

SURFACE SCIENCE LETTERS

DECOMPOSITION OF FORMIC ACID ON Ru(001): AN EELS SEARCH FOR A FORMIC ANHYDRIDE INTERMEDIATE *

N.R. AVERY **, B.H. TOBY, A.B. ANTON and W.H. WEINBERG

Division of Chemistry and Chemical Engineering, California Institute of Technology, Pasadena, California 91125, USA

Received 21 June 1982

High resolution electron energy loss spectroscopy has demonstrated the existence of a symmetrical bidentate bridging formate as a stable intermediate in the decomposition of formic acid on the Ru(001) surface. This formate decomposes with two pathways – via C–H bond cleavage to give CO_2 and adsorbed hydrogen, and via C–O bond cleavage to give adsorbed hydrogen, oxygen and CO. Thermal desorption demonstrates the evolution of H_2, H_2O, CO and CO_2. The observation of this product distribution from Ru(100), Ni(100) and Ni(110) had prompted the proposal of a formic anhydride intermediate. The spectroscopic results reported here bring the presence of this postulated, normally unstable species into question.

Thermal desorption mass spectrometry (TDMS) studies of the decomposition of formic acid on clean, well characterized (110) and (100) surfaces of nickel have shown that an initial low temperature dehydration is followed by the evolution of CO_2, H_2 and CO at higher temperatures [1–3]. The CO_2 and H_2 appear in a common reaction-limited step between 350 and 370 K, whereas CO is evolved from the surface in a desorption-limited step at approximately 440 K. The ratio of CO_2 to CO evolved has been reported to be close to unity, and these results have been rationalized as a bimolecular dehydration to an adsorbed intermediate with the stoichiometry [HCOO · HCO], which subsequently decomposes in a single autocatalytic step to the observed products, viz. gaseous CO_2 and H_2, and adsorbed CO. In a comparable study of the decomposition of formic acid on the prismatic (100) surface of ruthenium, a similar dehydration, followed by the evolution of CO_2, H_2 and CO has been reported and similarly associated with a decomposition intermediate of stoichiometry [HCOO · HCO] [4]. In each of these cases, the investigators have postulated that the metal surface has stabilized the dehydration of formic acid to formic anhydride, normally an unstable species.

* Supported by the National Science Foundation under Grant No. CHE82-06487.

** Permanent address: Division of Materials Science, CSIRO, University of Melbourne, Parkville, Victoria, Australia 3052.

0039-6028/82/0000–0000/$02.75

By contrast, the decomposition of formic acid on Cu(100) [5], Ag(110) [6] and Pt(111) [7] yields only CO_2 and H_2 in a simple unimolecular dehydrogenation of an adsorbed formate intermediate. In each of these instances, Brönsted deprotonation of the adsorbed formic acid to the adsorbed formate intermediate has been *confirmed* spectroscopically by electron energy loss spectroscopy (EELS).

In this Letter we report some pertinent aspects of a TDMS and EELS study of the decomposition of formic acid on the close-packed (001) surface of ruthenium [8]. Although this is not the same surface of ruthenium for which TDMS has *implied* the existence of a formic anhydride intermediate [4], we expect that the fundamental chemistry of the two ruthenium surfaces will be quite similar, as is the case for the (100) and (110) surfaces of nickel [3]. The aim of this study is to determine unequivocally, via EELS, the structure of the

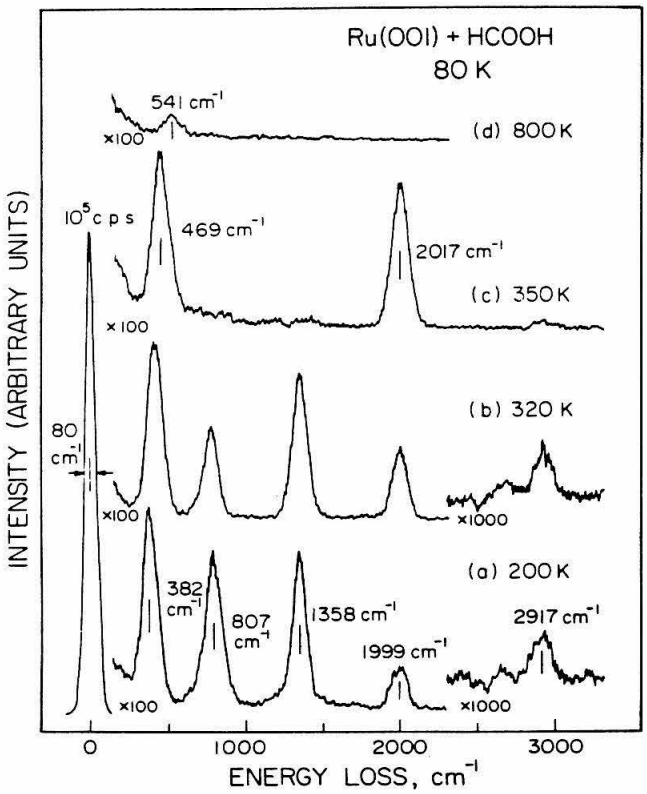

Fig. 1. EEL spectra obtained after adsorption of formic acid on a clean Ru(001) surface at 80 K followed by annealing to the indicated temperatures.

prominent adsorbed intermediate formed by decomposition of formic acid on Ru(001) and to reevaluate the feasibility of a decomposition scheme which proceeds through formation of a normally unstable formic anhydride intermediate. The electron energy loss spectrometer used in this work and the ultrahigh vacuum apparatus in which it is housed have been described in detail previously [9].

Fig. 1 shows a sequence of EEL spectra which were obtained after the adsorption at 80 K of slightly in excess of one monolayer of formic acid on a clean Ru(001) surface, followed by annealing to the indicated temperatures. Annealing to 200 K causes molecularly adsorbed (multilayer) formic acid to desorb, and the resulting EEL spectrum (fig. 1a) shows four conspicuous bands at 382, 807, 1358 and 2917 cm^{-1} which are easily assigned to the ν(Ru–O), δ(OCO), ν_s(OCO) and ν(CH) modes of an adsorbed formate, respectively [5–7]. Note also the absence of vibrational bands at 1040–1175 and 1700–1775 cm^{-1} in this spectrum, as would be seen for the ν_s(COC) and ν_s(CO) modes of an adsorbed anhydride, respectively [10]. The inherently strong ν_s(OCO) mode, expected at 1600 cm^{-1} for an adsorbed formate, has B_1 symmetry and could not be detected. This indicates, according to the surface selection rule for dipole excitations, an equivalence of the two oxygen atoms. Furthermore, the similarity between the frequencies of the ν_s(OCO) mode for the adsorbed formate (1358 cm^{-1}) and the free formate ion (1366 cm^{-1}) suggests a symmetric bidentate bridging configuration, as shown below [7,11]:

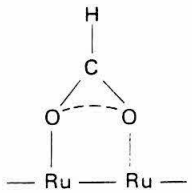

The only other surface species which could be detected is a weak band at 1999 cm^{-1} (fig. 1a) due to adsorbed CO [12]. This CO, representing less than 0.05 monolayer, is due to the onset of decomposition of the adsorbed formate and correlates with the evolution of H_2O below 200 K. Further annealing to 320 K (fig. 1b) causes the intensities of the bands due to the adsorbed formate to decrease and those due to adsorbed CO to increase, At 350 K (fig. 1c), the decomposition of the adsorbed formate is complete. Annealing to 800 K (fig. 1d) resulted in the desorption of CO, revealing a weak band at 541 cm^{-1} which could be removed by further annealing to 1630 K. This band is due to a small residual concentration of oxygen adatoms [13].

TDMS results demonstrate the evolution of HCOOH, H_2O, H_2, CO_2 and CO from the Ru(001) surface and reveal a complicated mechanism of decomposition. For initial coverages in excess of one monolayer, molecular formic

acid from condensed multilayers desorbs with a peak temperature of 195 K. A second molecular formic acid desorption feature is seen at 350 K for low coverages, shifting to 375 K and saturating for all initial coverages of a monolayer or greater. No molecular formic acid is detected by EELS above 200 K, suggesting that the desorption of formic acid at 350–375 K is due to recombination of adsorbed hydrogen and formate. For submonolayer initial coverages, H_2O desorbs in two peaks with maxima at 160 and 275 K. As mentioned earlier, this H_2O results from decomposition of the adsorbed formate and correlates with the appearance of CO in the EEL spectra. Carbon dioxide is evolved in a single reaction-limited step with a peak temperature of 300 K for low initial coverages, shifting to 365 K for saturation coverage. This temperature shift results from increased stability of the adsorbed formate at higher coverage [8]. Hydrogen is evolved in a single desorption-limited step with a peak temperature of 455 K for low initial coverages, shifting to 375 K at saturation. In this case the temperature shift probably results from repulsive interactions among hydrogen adatoms and other adsorbed species, the net effect of which increases with total surface coverage [14]. Carbon monoxide is evolved in a single desorption-limited step with a peak temperature of 480 K, and a trace of adsorbed oxygen remains to approximately 1600 K.

Since the probability of CO oxidation to CO_2 on Ru(001) under the conditions prevailing in these experiments is on the order of 0.1% of the probability of CO desorption [15], the appearance of both CO_2 and CO in TDMS results indicates that formic acid decomposes by two competing mechanisms on Ru(001). Initial dehydrogenation of formic acid to an adsorbed formate intermediate is followed by decomposition of the formate through dehydrogenation *or* through C–O bond cleavage. The integrated intensities of the CO_2 and CO desorption peaks, corrected for the relative sensitivity of the quadrupole mass spectrometer to each species, yield a ratio of CO to CO_2 evolution of approximately three to one, indicating that formate decomposition through C–O bond cleavage is more rapid than by simple dehydrogenation. An overall reaction scheme consistent with all EELS and TDMS results for formic acid decomposition on Ru(001) can be written as follows ((a) denotes an adsorbed species, (g) denotes a gaseous species):

Following adsorption of formic acid in excess of one monolayer, molecules in multilayers desorb intact near 195 K, while those in contact with the surface decompose to yield an adsorbed formate. Some recombination occurs on the surface to yield molecular formic acid near 375 K;

$$\mathrm{HCOOH(g)} \rightleftharpoons \mathrm{HCOOH(a)}, \quad \mathrm{HCOOH(a)} \rightleftharpoons \mathrm{HCOO(a)} + \mathrm{H(a)}.$$

The formate species decomposes by two competing mechanisms to yield adsorbed CO over a broad temperature range (150–400 K) and gaseous CO_2 between 300 and 365 K Mechanism (1) is more rapid than mechanism (2):

$$\mathrm{HCOO(a)} \begin{cases} \nearrow \mathrm{H(a) + CO(a) + O(a)}, & (1) \\ \searrow \mathrm{H(a) + CO_2(g)}. & (2) \end{cases}$$

Hydrogen adatoms and oxygen adatoms from formate decomposition recombine to yield water at 160 and 275 K:

$$\mathrm{H(a) + O(a) \rightarrow OH(a), \quad OH(a) + H(a) \rightarrow H_2O(g).}$$

Hydrogen and CO are evolved in desorption-limited steps at 375–455 K and 480 K, respectively. The oxygen adatoms, present in low concentration, are dissolved into the bulk of the Ru at approximately 1600 K,

$$\mathrm{2\,H(a) \rightarrow H_2(g), \quad CO(a) \rightarrow CO(g), \quad O(a) \rightarrow O(dissolved).}$$

In conclusion, the products of the decomposition of formic acid on Ru(001) are the same as those observed on Ru(100), Ni(100) and Ni(110), yet only a *formate intermediate* is present on Ru(001) as *verified* by EELS. The adsorbed formate intermediate present on Ru(001) does not decompose exclusively by dehydrogenation, as observed for formate intermediates on Cu(100) [5], Ag(110) [6] and Pt(111) [7], but also by C–O bond cleavage. These results bring into question earlier *speculation* of the presence of a formic anhydride intermediate on Ru(100), Ni(100) and Ni(110) which was *inferred* from the distribution of desorbing products of the decomposition reaction [1–4].

References

[1] R.J. Madix and J.L. Falconer, Surface Sci. 51 (1975) 546.
[2] J.B. Benzinger and R.J. Madix, Surface Sci. 79 (1979) 394.
[3] R.J. Madix, Advan. Catalysis 29 (1980) 1.
[4] L.A. Larsen and J.T. Dickinson, Surface Sci. 84 (1979) 17.
[5] B.A. Sexton, Surface Sci. 88 (1979) 319.
[6] B.A. Sexton and R.J. Madix, Surface Sci. 105 (1981) 177.
[7] N.R. Avery, Appl. Surface Sci. 11/12 (1982) 774.
[8] B.H. Toby, N.R. Avery, A.B. Anton and W.H. Weinberg, in preparation; also, B.H. Toby, N.R. Avery, A.B. Anton and W.H. Weinberg, in: Proc. 3rd Intern. Conf. on Vibrations at Surfaces, Asilomar, CA, 1982, to be published.
[9] G.E. Thomas and W.H. Weinberg, Rev. Sci. Instr. 50 (1979) 497.
[10] N.B. Colthup, J. Opt. Soc. Am. 40 (1950) 397.
[11] K. Nakamoto, Infrared and Raman Spectra of Inorganic and Coordination Compounds (Wiley, New York, 1978) p. 232.
[12] G.E. Thomas and W.H. Weinberg, J. Chem. Phys. 70 (1979) 1437.
[13] G.E. Thomas and W.H. Weinberg, J. Chem. Phys. 69 (1978) 3611.
[14] This effect has been demonstrated for the coadsorption of H_2 and CO on Ru(001). See: D.E. Peebles, J.A. Schreifels and J.M. White, Surface Sci. 116 (1982) 117.
[15] H.I. Lee, G. Praline and J.M. White, Surface Sci. 91 (1980) 581.

Chapter 6:

Electron Energy Loss Spectroscopy of the Decomposition of Formic Acid on Ru(001)

Journal of Electron Spectroscopy and Related Phenomena, 29 (1983) 317—321
Elsevier Scientific Publishing Company, Amsterdam — Printed in The Netherlands

ELECTRON ENERGY LOSS SPECTROSCOPY OF THE DECOMPOSITION OF FORMIC ACID ON Ru(001)*

B.H. TOBY[1], N.R. AVERY[2], A.B. ANTON[1] and W.H. WEINBERG[1]

[1]Division of Chemistry and Chemical Engineering, California Institutue of Technology, Pasadena, California 91125 U.S.A.

[2]Division of Materials Science, C.S.I.R.O., University of Melbourne, Parkville, Victoria, Australia 3052.

ABSTRACT

Electron energy loss spectroscopy has demonstrated the existence of both a monodentate and a symmetric bidentate bridging formate as stable intermediates in the decomposition of formic acid on the Ru(001) surface. The monodentate formate converts upon heating to the bidentate formate which decomposes via two pathways: C-H bond cleavage to yield CO_2 and adsorbed hydrogen; and C-O bond cleavage to yield adsorbed hydrogen, oxygen and CO. Thermal desorption spectra demonstrate the evolution of H_2, H_2O, CO and CO_2 as gaseous products of the decomposition reaction. The observation of this product distribution from Ru(100), Ni(100) and Ni(110) had prompted the proposal of a formic anhydride intermediate, the existence of which is rendered questionable by the spectroscopic results reported here.

INTRODUCTION

Recently, electron energy loss spectroscopy (EELS) has shown clearly that a formate is the stable surface intermediate in the decomposition of formic acid on (100)Cu (ref.1,2), Ag(110) (ref.3) and Pt(111) (ref.4) surfaces. However, based on *indirect* evidence, namely the product distribution in thermal desorption spectra, formic anhydride has been postulated to be a stable intermediate in the decomposition of formic acid on Ni(100) and (110)(ref.5-7) and Ru(100) (ref.8) surfaces. The present work was undertaken in order to decide whether a formic anhydride species exists on the (001) surface of Ru under any circumstances.

EXPERIMENTAL PROCEDURES

All relevant experimental details including a description of the EEL spectrometer (ref.9), the preparation of the clean Ru(001) surface (ref.10) and the handling of formic acid in the UHV system (ref.11) have been described previously.

*Supported by the National Science Foundation under Grant No. CHE82-06487.

318

RESULTS AND DISCUSSION

Electron energy loss spectra corresponding to exposures of formic acid greater than 4L at 80 K show bands characteristic of the molecular species, indicating multilayer condensation. Annealing to 200 K causes the multilayers of formic acid to desorb, and the resulting EEL spectrum [Fig. 1(a)] shows four bands at 382, 807, 1358 and 2917 cm^{-1} which are assigned easily to the ν_s(Ru-O), δ(OCO), ν_s(OCO) and ν_s(CH) modes of an adsorbed formate, respectively (ref.1-4,11). The inherently strong ν_a(OCO) mode, expected near 1600 cm^{-1} for an adsorbed formate, has B_1 symmetry and could not be detected. This indicates, according to the surface selection rule for dipolar excitations, an equivalence of the two oxygen atoms. Furthermore, the similarity between the frequencies of the ν_s(OCO) mode for the adsorbed formate (1358 cm^{-1}) and the free formate ion (1366 cm^{-1}) suggests a symmetric bidentate bridging configuration of C_{2v} symmetry, as shown schematically in (a) below (ref.12).

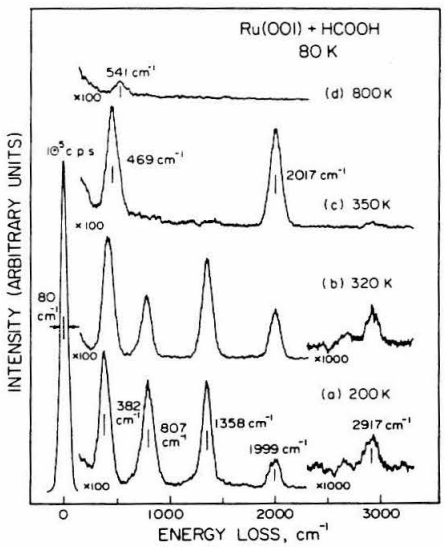

Fig. 1. EEL spectra obtained after the adsorption at 80 K of slightly in excess of one monolayer of formic acid on a clean Ru(001) surface, followed by annealing to the indicated temperatures.

The weak band at 1999 cm^{-1} in Fig. 1(a) is due to adsorbed CO (ref.13). This CO, representing less than 0.05 monolayer, is due to the onset of decomposition of the adsorbed formate and correlates with the evolution of H_2O below 200 K. Further annealing to 320 K [Fig. 1(b)] causes the intensities of the bands due to the adsorbed formate to decrease and those due to adsorbed CO to increase. At 350 K [Fig. 1(c)], the decomposition of the adsorbed formate is complete. Annealing to 800 K [Fig. 1(d)] results in the desorption of CO, revealing a weak band at 541 cm^{-1} which could be removed by further annealing to 1630 K. This band is due to a small residual concentration of oxygen adatoms (ref. 10).

An EEL spectrum corresponding to a submonolayer coverage of dissociatively adsorbed formic acid at 80 K is shown in Fig. 2. In addition to those modes observed in Fig. 1(a), there are additional bands at 1158, 1681, and 2357 cm^{-1}. The latter are assigned to the π(CH), the ν_a(OCO), and a "softened" ν_s(CH) mode [verified with DCOOD (ref.14)], respectively, for a monodentate formate, shown schematically in (b) above. Since both the π(CH) mode of B_2 symmetry and the ν_a(OCO) mode of B_1 symmetry are dipolar allowed, the formate is of C_1 symmetry, i.e. tilted with respect to the page in (b) above. The "softening" of the ν_s(CH) mode, which is manifest by a decrease of its frequency by over 500 cm^{-1}, indicates an H-Ru interaction in the chemisorbed monodentate formate. Below 200 K, both the monodentate and bidentate formates coexist on the Ru surface. Annealing the surface with both types of formate present to 200 K causes the bands corresponding to the monodentate species to disappear, and those

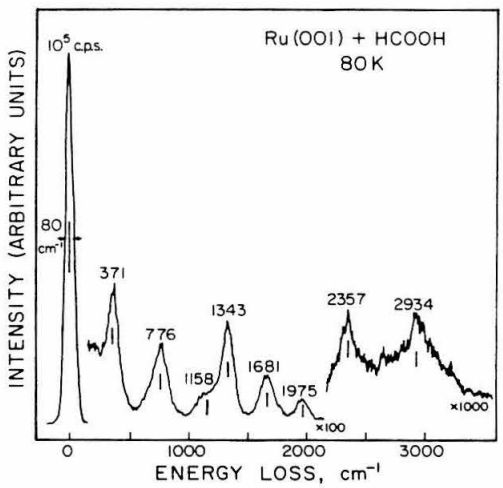

Fig. 2. EEL spectrum obtained after the adsorption at 80 K of a submonolayer amount of formic acid on a clean Ru(001) surface.

320

corresponding to the bidentate species to increase in intensity. This is clear evidence of the *irreverible* conversion of a monodentate to a bidentate bridging formate on the Ru(001) surface.

Thermal desorption results demonstrate the evolution of HCOOH, H_2O, H_2, CO_2 and CO from the Ru(001) surface and reveal a complicated mechanism of decomposition. For initial coverages in excess of one monolayer, molecular formic acid from condensed multilayers desorbs with a peak temperature of 195 K. A second molecular formic acid desorption feature is seen at 350 K for low coverages, shifting to 375 K and saturating for all initial coverages of a monolayer or greater. No molecular formic acid is detected by EELS above 200 K, suggesting that the desorption of formic acid at 350-375 K is due to recombination of adsorbed hydrogen and formate. For submonolayer initial coverages, H_2O desorbs in two peaks with maxima at 160 and 275 K. As mentioned earlier, this H_2O results from decomposition of the adsorbed formate and correlates with the appearance of CO in the EEL spectra. Carbon dioxide is evolved in a single reaction-limited step with a peak temperature of 300 K for low initial coverages, shifting to 365 K for saturation coverage. This temperature shift results from an increased stability of the adsorbed formate at higher coverage (ref.11,14). Hydrogen is evolved in a single desorption-limited step with a peak temperature of 455 K for low initial coverages, shifting to 375 K at saturation. Carbon monoxide is evolved in a single desorption-limited step with a peak temperature of 480 K.

Since the probability of CO oxidation to CO_2 on Ru(001) under the conditions prevailing in these experiments is on the order of 0.1 percent of the probability of CO desorption (ref.15), the appearance of both CO_2 and CO in the thermal desorption spectra indicates that formic acid decomposes by two competing mechanisms on Ru(001). Initial dehydrogenation of formic acid to an adsorbed formate intermediate is followed by decomposition of the formate *either* through dehydrogenation *or* through C-O bond cleavage with the latter favored somewhat, as judged by relative areas of thermal desorption peaks, i.e.,

$$HCOO(a) \xrightarrow{①} H(a) + CO(a) + O(a)$$
$$HCOO(a) \xrightarrow{②} H(a) + CO_2(g)$$

Reaction ① is not only slightly favored kinetically over reaction ②, it is also (marginally) favored thermodynamically, by approximately 6 kcal/mol (ref.16).

Formic acid dehydrogenates upon adsorption on Cu(100)(ref.1,2), Ag(110)(ref.3), and Pt(111)(ref.4) to yield a chemisorbed formate intermediate which decomposes via C-H bond cleavage exclusively. However, on Ni(110), Ni(100)(ref.5-7) and Ru(100)(ref.8), the same distribution of the products of decomposition was observed as that reported here. On these surfaces, a formic anhydride intermediate was postulated to explain the observed product distribution. The fact that the formic anhydride intermediate does not exist on Ru(001) under any

circumstances brings into considerable doubt its existence on Ni(110), Ni(100), and Ru(100).

REFERENCES

1 B.A. Sexton, Surface Sci. 88, 319 (1979).
2 B.E. Hayden and A.M. Bradshaw (private communication).
3 B.A. Sexton and R.J. Madix, Surface Sci. 105, 177 (1981).
4 N.R. Avery, Appl. Surface Sci. 11/12, 774 (1982).
5 R.J. Madix and J.L. Falconer, Surface Sci. 51, 546 (1975).
6 J.B. Benzinger and R.J. Madix, Surface Sci. 79, 394 (1979).
7 R.J. Madix, Advan. Catal. 29, 1 (1980).
8 L.A. Larsen and J.T. Dickinson, Surface Sci. 84, 17 (1979).
9 G.E. Thomas and W.H. Weinberg, Rev. Sci. Instrum. 50, 497 (1979).
10 G.E. Thomas and W.H. Weinberg, J. Chem. Phys. 69, 3611 (1978); 70, 954 (1979).
11 N.R. Avery, B.H. Toby, A.B. Anton and W.H. Weinberg, Surface Sci. (in press).
12 K. Nakamoto, *Infrared and Raman Spectra of Inorganic and Coordination Compounds*, Wiley, New York, 1978.
13 G.E. Thomas and W.H. Weinberg, J. Chem. Phys. 70, 1437 (1979).
14 B.H. Toby, N.R. Avery, A.B. Anton and W.H. Weinberg (in preparation).
15 H.I. Lee, G. Praline and J.M. White, Surface Sci. 91, 581 (1980).
16 W.H. Weinberg, unpublished results.

Chapter 7:

The Adsorption of Formic Acid and the Decomposition of the Formate Intermediate on the (001) Surface of Ruthenium

ABSTRACT

The adsorption of formic acid on the clean Ru(001) surface has been studied by electron energy loss vibrational spectroscopy and thermal desorption mass spectrometry. Large exposures of formic acid produce a molecular multilayer species with vibrational frequencies similar to those of crystalline formic acid. Two different formate species (a monodentate and a bidentate formate) and a surface hydroxyl have been identified as stable intermediates in the decomposition of formic acid on the Ru(001) surface. The monodentate formate species has a ν(C=O) mode at 1345 cm^{-1} and a softened C-H stretching mode, characteristic of a surface-hydrogen interaction. The monodentate formate species is completely converted to the bidentate species by heating to 200 K. The bidentate formate species is believed to bridge two adjacent binding sites. The formic acid decomposition products are CO_2, CO, H_2, H_2O and oxygen adatoms. The ratio of desorbed CO with respect to desorbed CO_2 increases both with slower heating rate and with lower formate coverages.

1. INTRODUCTION

Among the goals of surface science are the identification and characterization of adsorbed intermediates which serve to delimit the number of possible reaction mechanisms in catalytic reactions. The study of adsorbate structure and bonding provides a basis for understanding the role of the catalytic surface in heterogeneous catalysis. Of particular interest are reactions of molecules containing carbon-oxygen bonds, since numerous catalytic reactions involve the formation or cleavage of C-O bonds or the activation of carbon centers bonded to oxygen atoms in elimination, addition or reduction reactions. For this reason, there has been considerable interest in the interactions of formic acid with metal and metal oxide surfaces as model systems for carboxylate catalysis [**1**]. A goal of this work has been determining reaction mechanisms and the factors that influence catalytic specificity for different decomposition products.

Single crystalline surfaces offer the advantage of having well defined geometrical structures to which a wide array of surface sensitive spectroscopies may be applied. Using a number of these techniques, a large data base has been developed concerning the mechanism and the kinetics of the decomposition of formic acid. Most metal surfaces fall into two distinct classes with respect to the product selectivity of formic acid decomposition. On the majority of single crystalline surfaces that have been studied, including Fe(100) [**2**], Ni(111) [**3**], Ni(110) [**4**], Ni(100) [**5**], Ru(001) [**6**] and Ru(100) [**7**], the decomposition products are CO_2, CO, H_2O and H_2. On Pt(111) [**8**], Cu(100) [**9**] and Cu(110) [**10**], however, the decomposition products are CO_2 and H_2. Coadsorbates have been found to affect both the reactivity and selectivity. For example, on the clean Ag(110) surface, formic acid adsorbs molecularly and desorbs reversibly; but on a surface with presaturated oxygen adatoms ($\theta \approx 0.33$), dissociative adsorption occurs with CO_2, H_2O and H_2 desorption [**11**]. The preadsorption of an ordered $(\sqrt{5} \times \sqrt{5})$O adatom on Mo(100) causes formic acid to decompose to CO_2, CO, H_2O, CH_4 and H_2, as compared to the clean Mo(100) surface on which the

decomposition products are CO, H_2O and H_2 [**12**]. The formation of CO on the Ni(110) surface can be completely inhibited by a ordered (4 × 5) carbide overlayer [**13**].

Vibrational spectroscopy of surfaces on which formic acid is adsorbed has been employed on the Ag(110) [**11**], Al(110) [**14**], Au(110) [**15**], Au(111) [**15**], Cu(110) [**16**], Cu(100) [**9**], Mo(100) [**12**], Ni(110) [**13**], Pt(111) [**8**], Pt(110) [**17**] and Ru(001) [**6**] surfaces using either electron energy loss spectroscopy (EELS) or infrared reflection-absorption spectroscopy (IRAS). Formate intermediates, usually symmetrically bound (*i.e.*, bidentate with equivalent oxygen atoms), have been identified on all these surfaces. These symmetric formates are characterized by four strong vibrational modes, ν(M-O), δ(OCO), ν_s(OCO) and ν(CH). On the Cu(100) [**9**], Mo(100) [**12**], Pt(110) [**17**], Ru(001) [**6**], oxygen-saturated Ag(110) [**11**], and Ni(110)-(4 × 5)C [**13**] surfaces, the presence of additional dipolar enhanced vibrational modes, in particular the ν_a(OCO) mode which is forbidden by the surface selection rule for a symmetric formate [**18**], indicates the presence of an asymmetrically bound formate, which may be either an asymmetric, bidentate formate or a monodentate formate. The ν(C-O) and ν(C=O) modes of monodentate formates are located at similar frequencies to the ν_s(OCO) and ν_a(OCO) modes of bidentate formates. These asymmetric formates are observed at low temperatures (usually below 200 K) and heating causes an irreversible change in orientation to a symmetric formate. Two exceptions to this pattern are Cu(100) where the intensity of the ν_a(OCO) mode on the annealed surface increases if the surface is held at 100 K for 10 to 20 minutes, suggesting a reversible change in orientation [**9,19**], and Ni(110) where only the symmetric formate is observed on the clean surface and only the asymmetric formate is observed on the Ni(110)-(4 × 5)C surface [**13**]. On Pt(110), the bonding configuration has been assigned as an asymmetric bidentate formate where a vector through the oxygen atoms is at an angle of approximately 10° with respect to the plane of the surface [**17**]. All of the other asymmetric

formates appear to be monodentate [**8,12**].

Determinations of the bonding geometry of the symmetric formate intermediate on the Cu(110) [**20**] and Cu(100) [**21**] surfaces have been made using extended X-ray absorption fine structure (EXAFS) measurements. Different bonding geometries have been found for this formate on the two different surfaces. On Cu(100) each formate oxygen resides at a site between four copper surface atoms [**21**], while on Cu(110) each oxygen bonds in an "on-top" arrangement above adjacent Cu atoms, with the plane of the formate parallel to the $[1\bar{1}0]$ lattice vector and perpendicular to the surface [**20**]. *Ab initio* geometrical optimization calculations for a model of formate on a Ni(001) surface yield a similar geometry to that determined by EXAFS for the Cu(100) surface [**22**]. Vibrational spectroscopic comparisons of the two different geometrical bonding configurations on the Cu(100) and Cu(110) surfaces, as measured by EELS and IRAS, respectively, are limited by the restricted frequency bandwidth of the latter technique. Thus only two modes may be contrasted. The ν_s(OCO) mode at 1330 cm^{-1} on Cu(100) is found at 1350-1360 cm^{-1} on Cu(110) and the ν(CH) modes at 2840 and 2910 cm^{-1} on Cu(100) occur at 2900-2980 cm^{-1} on Cu(110) [**9,16**].

In this extension of our previous studies of the adsorption of formic acid on the Ru(001) surface [**6**], we present EEL spectral assignments for condensed (molecular) formic acid, bidentate and monodentate formate species and the first direct spectroscopic evidence for a surface hydroxyl species on Ru(001). Thermal desorption mass spectrometry (TDMS) results demonstrate two decomposition pathways leading either to CO desorption or to CO_2 desorption. This study is part of our ongoing investigations into the interactions of organic carbonyl ligands with the Ru(001) surface. Other reactants that have been investigated include acetone [**23**] and formaldehyde [**24**].

2. EXPERIMENTAL PROCEDURES

The ultrahigh vacuum system and the EEL spectrometer used for these studies have been described previously [**25**]. EEL spectra were recorded with a beam energy of approximately 5 eV. Count rates were typically 1 to 3 $\times$ 10^5 counts per second for the specularly scattered elastic beam, while maintaining a resolution equal to or better than 80 cm^{-1} (full-width at half-maximum intensity of the elastically scattered beam). Changes in EEL spectra as a function of temperature were observed by heating the crystal to various temperatures, followed by immediate cooling before recording the spectrum. All EELS measurements were made with the surface at a temperature of approximately 80 K.

Thermal desorption spectra were recorded in a second ultrahigh vacuum system equipped with Varian low-energy electron diffraction (LEED) optics, a Varian single pass cylindrical mirror Auger electron spectrometer, and a UTI 100C quadrupole mass spectrometer. A Digital Equipment Corp. LSI-11 computer was used to collect TDMS data, and the smoothing procedure of Savitzky and Golay was used to improve the signal-to-noise ratio [**26**]. Since no ordered superstructures were observed, no LEED results are presented.

The Ru(001) surfaces were cleaned chemically by exposure to O_2 at pressure of 5 $\times$ 10^-8 torr while cycling the surface temperature between 300 and 800 K, followed by annealing in vacuum at 1650 K to remove adsorbed oxygen, and with occasional Ar^+ sputtering cycles [**27**]. Surface cleanliness was confirmed with Auger spectroscopy, EELS or by thermal desorption of H_2 and CO. Formic acid samples, HCOOH (MCB spectroscopic grade), DCOOD (Stohler spectroscopic grade, nominal 99% D_2), HCOOD and DCOOH (Merck spectroscopic grade, nominal 99% D), were given a minimum of three freeze-thaw-pump cycles for additional purification before use, and gas handling lines were exposed numerous times to the deuterated formic acid to reduce isotopic exchange. Despite these precautions there appeared to be significant isotopic exchange of the hydroxyl

deuterium with hydrogen prior to the adsorption of formic acid on the surface.

The Ru(001) surfaces were exposed to formic acid by backfilling the bell jars. Exposures quoted are not corrected for ionization gauge sensitivities. The mass spectrometer sensitivity was calibrated by integrating TDMS from saturation coverages of CO and H_2. Mass spectrometer sensitivities for other species, relative to CO, were estimated using information provided by the manufacturer.

3. EELS IDENTIFICATION OF ADSORBED SPECIES

Formic acid adsorption on the Ru(001) surface gives rise to several adspecies which can be identified by their characteristic EEL features. The species are described below, along with their spectral assignments.

3.1 Molecular Formic Acid

Molecular formic acid is observed by EELS on the Ru(001) surface following exposures greater than 6 L at 80 K. EELS spectra following greater exposures are similar, but spectra at exposures above 10 L are less well resolved. The HCOOH spectrum shown in Fig. 1(a) is characterized by intense bands at 720, 940, 1235, 1370 and 1690 cm^{-1}, which are assigned as the δ(OCO), π(OH), ν(C-O), δ(CH), and ν(C=O) modes, respectively, of condensed multilayer formic acid. Also present are weaker, broader bands at 2640 and 2960 cm^{-1} which can be assigned as ν(OH) and ν(CH) modes, respectively. The significantly lowered frequency of the ν(OH) mode compared to that in the HCOOH monomer, 3570 cm^{-1}, is a consequence of the extensive hydrogen bonding in crystalline formic acid [**28**]. These assignments are confirmed by comparison to the DCOOD spectrum in Fig. 1b, where the bands observed at 970, 1260, and 1680 cm^{-1}, are assigned as the δ(CD), ν(C-O) and ν(C=O) modes, respectively. The most intense band at 690 cm^{-1} is the unresolved sum of the δ(OCO) and π(OD) modes. The ν(OD) and ν(CD) modes shift to 2020 and 2260 cm^{-1}, respectively. The small band at 2960 cm^{-1} is assigned as a ν(CH) mode from an HCOOH or HCOOD impurity. Evidence is also seen for a broad ν(OH) mode from a DCOOH or HCOOH impurity at approximately 2600 cm^{-1}. These energies agree well with those of crystalline formic acid and less well with those of liquid (dimerized) formic acid (cf. Table 1). The mode at 230 (220) cm^{-1} in the HCOOH (DCOOD) spectrum is assigned as a frustrated translational mode of molecules within the condensed lattice. A band at similar frequencies is observed for crystalline formic acid [**28**], as well as condensed formic acid on other metal surfaces [**9,11**].

3.2 Monodentate Formate

A monodentate formate species is observed on the Ru(001) surface following submonolayer exposures at 80 K as well as following the desorption of a formic acid multilayer at 170 K. Spectra of submonolayer exposures of HCOOH and DCOOD are shown in Fig. 2. The intense band at 1680 cm^{-1} in Fig. 2(a) is assigned to the ν(C=O) mode; this band cannot be the ν_a(OCO) mode which occurs at a similar frequency for symmetrical bidentate formates [**8,9,11-17,29**], since this mode would have a dipole parallel to the surface and thus is forbidden by the surface selection rule [**18**]. The band observed at 2355 cm^{-1} is the ν(CH) mode. The downward shift of this mode by over 500 cm^{-1} from its usual frequency implies that the hydrogen atom strongly interacts with the Ru(001) surface [**18**]. The assignment of this mode is confirmed by the deutero-formate spectrum, where this mode shifts to approximately 1700 cm^{-1} and is obscured by the 1650 cm^{-1} ν(C=O) mode. The observation of this "softened" CH mode has not been reported for any other monodentate surface formate species. These two modes allow the monodentate formate geometry to be assigned:

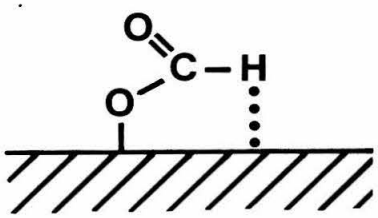

The EELS spectra exhibit bands at 370 (365), 775 (775), and 1345 (1315) cm^{-1} which are assigned as the ν(Ru-O), δ_s(OCO) and ν_s(OCO) modes for the monodentate HCOO (DCOO) species, respectively. The 1160 cm^{-1} band in the monodentate HCOO spectrum is assigned as a π(CH) mode. This mode is is obscured in the DCOO spectrum by the δ_s(OCO) mode. The upward shift of this mode may be indicative of a hydrogen interaction with the surface. The 1015 cm^{-1} band in the monodentate DCOO spectrum, is assigned as a δ(CD) mode and is obscured in the HCOO spectrum by the ν_s(OCO) mode.

The high frequency ν(CH) mode at 2935 cm^{-1} is best explained by the presence of a bidentate formate, discussed further in Section 3.3. The assignment of the 610 cm^{-1} peak observed in the monodentate DCOO spectrum will be discussed further in Section 3.4. Table 2 contains assignments for both Ru(001)-formate species, along with those for analogous metal-formate complexes and for formates adsorbed on other single crystalline metal surfaces.

3.3 Bidentate Formate

Annealing of the surface on the monodentate formate is present to temperatures above 200 K leaves a formate species with only four bands at 380, 805, 1360 and 2915 cm^{-1}, which are assigned as the ν(Ru-O), δ_s(OCO), ν_s(OCO) and ν(CH) modes, respectively, of a symmetrically bonded bidentate formate species [cf. Figs. 3(a) and 4(a)]. As the surface is heated from 80 K to 200 K, the vibrational bands due to the monodentate formate disappear with little increase in the intensity of the CO vibrational modes and no CO_2 production. This indicates that most, if not all, of the monodentate formate converts to the bidentate formate, rather than decomposes directly.

Metal complexes of carboxylic acids, particularly acetate complexes, have been studied extensively [**29**]. Two different bonding configurations of symmetrical bidentate formates are known: the bidentate bridging species, shown below as (a), and the bidentate chelating species, (b).

(a) (b)

While the difference in frequency between the ν_a(OCO) and the ν_s(OCO) modes provides the most conclusive diagnostic for discriminating between these two

bonding geometries, the ν_a(OCO) mode should not be observed in a symmetric bidentate formate because it does not have a dynamic dipole perpendicular to the surface. However, by comparison to the ν_s(OCO) mode in transition metal formate and acetate species, the bonding geometry can be assigned as bridging bidentate. In group VIII transition metal acetate complexes, the ν_s(OCO) mode has been reported in the range 1450-1465 cm^{-1} for the chelating configurations contrasting the range of 1410-1440 cm^{-1} for the bridging configurations [**29**]. However, the ν_s(OCO) mode of the the "free" (solvated) acetate ion at 1416 cm^{-1} is very close to that of the bridging configuration acetate ligand. By analogy to the acetate results, the ν_s(OCO) mode at 1360 cm^{-1} in the bidentate surface formate closely correlates with the same mode in transition metal bridging formate complexes at approximately 1370 cm^{-1} and in the "free" formate ion at 1351 cm^{-1} (cf. Table 2).

3.4 Surface Hydroxyl

The weak band observed in the both the monodentate and the bidentate formate EEL spectra from DCOOD at 610 cm^{-1} [cf. Figs. 2(b) and 4] cannot be assigned to either of these two species because no normal vibrational mode of either of these species corresponds to this frequency, and because its intensity correlates with neither species. It is observed in all DCOOD EELS spectra taken at temperatures up to 250 K, well above the conversion temperature for the monodentate formate, but it disappears by 300 K, while the bidentate formate modes remain strong. While water has been observed to desorb following formic acid exposures with a desorption maximum at 275 K [**6**], this mode cannot be due to adsorbed D_2O, which has been observed to have a frustrated rotational (librational) mode at 520 cm^{-1} at low coverages, increasing to 620 cm^{-1} at monolayer coverage, because submonolayer coverages of water desorb completely from the Ru(001) surface by 220 K [**30**]. This mode at 610 cm^{-1} is assigned as a δ(Ru-OD) mode from a small concentration of surface-hydroxyl (OD) groups which are produced along with CO by low temperature formate

decomposition. The presence of this hydroxyl species has not been observed spectroscopically heretofore on the Ru(001) surface, but it has been reported on the Pd(100)[**31,32**], Ag(110)[**33**] and Pt(111)[**34**] surfaces with δ(M-OH) frequencies in the range between 670 and 1015 cm^{-1} [490 and 750 cm^{-1} for δ(M-OD)]. This assignment cannot be confirmed by comparison to HCOOH spectra, because the δ(Ru-OH) mode is obscured by the strong δ_s(OCO) mode at 775-805 cm^{-1}. The intensity of the ν(OH) mode for surface hydroxyl, which has been reported between 3200 and 3500 cm^{-1} [ν(OD), between 2400 and 2600 cm^{-1}], is considerably less intense than the δ(M-OH) mode and would not be expected to be observed in these spectra, where the fractional coverage of surface OH is estimated to be on the order of 5%. The frustrated translational mode, ν(M-OH), which has been reported between 280 and 460 cm^{-1}, is obscured by the strong ν(Ru-O) formate mode at 380 cm^{-1}.

3.5 Formate Decomposition Products

As may been seen in Figs. 2-4, there is spectroscopic conformation of two other adsorbed products of formate decomposition, CO and oxygen adatoms. Loss features from low concentrations of CO, ν(Ru-CO) at approximately 460 cm^{-1} and ν(CO) at approximately 2000 cm^{-1}, appear in all spectra measured immediately following adsorption, and increase in intensity as the surface is annealed. There is some formate decomposition below 200 K, as judged by the small increase in the intensity of the ν(CO) mode of CO, and the δ(Ru-OD) of surface-hydroxyl (OD), prompting speculation that the small amount of low temperature decomposition of formate to CO and OH takes place at defect sites. The weak Ru-O stretching mode at 540 cm^{-1} from oxygen adatoms produced by formate decomposition is obscured by the ν(Ru-CO) mode of adsorbed CO, but it can be seen clearly at temperatures above those where CO desorbs [cf. Fig. 3(d)].

At temperatures above 300 K, formate continues to decompose yielding CO, as evidenced by the increased intensity of the CO modes, yet no surface hydroxyl

is observed by EELS above 300 K nor is water observed as a decomposition product. Thus, at temperatures above 300 K either the hydroxyl species quickly decomposes to O and H adatoms, or above 300 K another mechanism allows formate to decompose forming the CO, O and H adspecies directly, without the hydroxyl intermediate. These two mechanisms cannot be discerned on the basis of evidence presented in this study.

4. THERMAL DESORPTION MASS SPECTROMETRY RESULTS

Six species, molecular formic acid, CO_2, CO, H_2O, O_2 and H_2, desorb from the Ru(001) surface following formic acid adsorption and heating of the surface. The thermal desorption spectra of molecular formic acid, CO_2, CO, isotopes of hydrogen, and water are presented in Figs. 5, 6, 7, 9, and 10, respectively. Interpretations of these thermal desorption spectra are discussed in Sections 4.1 through 4.5. The oxygen adatoms observed by EELS desorb as O_2 at approximately 1500 K. No attempt was made to record TDMS in this temperature range.

4.1 Formic Acid Desorption

Figure 5 exhibits desorption of molecular formic acid for several formic acid exposures. At an exposure of 5 L [cf. Fig. 5(c)], formic acid desorbs molecularly with a peak at approximately 200 K. With exposures in excess of 10 L, an additional lower temperature peak develops at 170 K which does not saturate, due to multilayer (condensed) formic acid, as shown in Fig. 5(d). The 200 K feature is attributed to adsorption of a nondissociated layer of formic acid above the first layer of formate adsorbed on the Ru surface. This second layer comprised of molecular formic acid has a higher binding energy than condensed formic acid multilayers. The 200 K feature cannot be attributed to adsorbed formate recombining with surface hydrogen to yield formic acid. The peak does not shift with temperature as would accompany second-order desorption. There is no evidence for the recombination of surface formate with hydrogen adatoms; if a surface with adsorbed formate is heated to 200 K to desorb all molecular formic acid and then is cooled and exposed to H_2, no further molecular formic acid desorption is observed.

There is no molecular desorption of formic acid above 200 K. The tentative suggestion of formic acid desorption between 300 and 350 K [**6**] has been shown to be due to an overlap with significant desorption of CO_2 for the mass spectrometric resolution employed previously.

4.2 CO_2 Desorption

There is a negligible amount of CO_2 desorption following a formic acid exposure of 0.4 L, which corresponds to a formate coverage of 10% of the saturation formate coverage [cf. 6(a)], as estimated from the TDMS of CO and CO_2. At higher formate coverages, a CO_2 desorption feature appears at 310 K and the desorption peak shifts to higher temperatures with increasing coverage, reaching 365 K for a saturation formate coverage (cf. Fig. 6). This desorption of CO_2 is "reaction-limited" since it has been demonstrated that CO_2 does not adsorb on Ru(001) at temperatures above 77 K [**35**].

The presence of both CO and CO_2 as decomposition products from surface formate demonstrates the existence of two decomposition pathways since the probability of the reaction $CO(a) + O(a) \rightarrow CO_2$ is less than 10^{-3} at temperatures below 400 K [**35-37**].

4.3 CO Desorption

The decomposition of the surface formate also yields adsorbed CO and hydroxyl fragments or hydrogen and oxygen adatoms, as discussed previously. While the onset of formate decomposition to CO is observed by EELS at temperatures below 200 K, all CO extrusion from the surface is "desorption-limited" (cf. Fig. 7) [**38**]. Thus, no kinetic information concerning the decomposition of formate to CO may be derived from these thermal desorption spectra.

Integration of the thermal desorption peaks of CO and CO_2 establishes the saturation formate coverage to be 0.28 ± 0.04 monolayer (0.28 formate adspecies per surface Ru adatom). Two interesting effects are noted in the branching ratio, the relative amounts of desorbing CO and CO_2. Figure 8(a) shows the amounts of formate that decompose to yield CO and CO_2, relative to the saturation formate coverage, as well as the ratio of desorbed CO to CO_2. As noted previously, the onset of CO_2 desorption is at approximately 10% of saturation coverage. The CO desorption feature saturates well before the CO_2 desorption feature saturates. In contrast, for formic acid decomposition on Ru(100), the

branching ratio is independent of coverage [7]. The branching ratio on Ru(001) is also influenced by the heating rate. Figure 8(b) shows the ratio of CO to CO_2 as a function of heating rate for a formate surface at approximately 40% of saturation coverage. The relative amount of CO_2 is minimized by reducing the heating rate. If the Ru surface is precovered with formate at 40% of the saturation coverage and is then annealed at 240 K for 5 minutes prior to the commencement of TDMS, the amount of CO_2 is decreased by a factor of five.

The change in branching ratio with coverage is explained by an increase in the activation barrier for the the CO decomposition reaction due to accumulation of product oxygen adatoms. Precoverage of the surface with oxygen adatoms also lowers the ratio of CO to CO_2 [**39**]. The change in branching ratio is consistent with the CO reaction having a lower preexponential factor than the CO_2 decomposition reaction.

4.4 Hydrogen Desorption

Hydrogen adatoms may be produced from three different reactions:

$$\mathrm{HCOOH(a)} \rightarrow \mathrm{HCOO(a)} + \mathrm{H(a)}, \qquad (A)$$

$$\mathrm{HCOO(a)} \rightarrow \mathrm{CO(a)} + \mathrm{H(a)} + \mathrm{O(a)}, \qquad (B)$$

and

$$\mathrm{HCOO(a)} \rightarrow \mathrm{CO_2(g)} + \mathrm{H(a)}. \qquad (C).$$

Deuterium-labeled formic acid, DCOOH, was used in the thermal desorption measurements so that "hydrogen" from the dehydrogenation reaction (A) could be distinguished from that resulting from the formate decomposition reactions (B) and (C).

Thermal desorption spectra of H_2, HD and D_2 from DCOOH are shown in Figs. 9(A), 9(B) and 9(C), respectively. The poor signal-to-noise ratio seen for the D_2 thermal desorption spectra compared to the H_2 and HD spectra results because the the mass spectrometer has a sensitivity of approximately 25% for D_2 with respect to H_2.

As demonstrated by the EELS results presented in Section 3.2, all adsorbed DCOOH decomposes below 200 K via reaction (A) to form adsorbed formate and H adatoms. These H adatoms combine to produce desorption-limited H_2 [cf. Fig 9(A)]. At formate coverages of approximately 10% of saturation, the peak for H_2 desorption is at 410 K, but shifts to lower temperature with increasing formate coverage. At saturation formate coverage, the desorption-limited peak shifts to 310 K and a second, reaction-limited peak is seen at 350 K, as the desorption-limited peak shifts to lower temperatures. The reaction-limited peak is 10 to 20 K below the CO_2 desorption peak temperature. The second peak correlates with the CO_2 desorption peak and is a result of a shift in the thermal desorption peak to lower temperatures due to the higher coverage of hydrogen adatoms.

Reaction (B), the decomposition of formate to produce CO, hydrogen, hydroxyl and O adspecies, is evidenced by the increased intensity of modes attributed to adsorbed CO in the EELS spectra, as discussed previously in Section 3.5. This reaction begins below the temperature for hydrogen desorption. The D adatoms from reaction (B) combine with the H adatoms from reaction (A) producing desorption-limited HD at the same temperatures as H_2 desorption [cf. Fig. 9(B)]. Reaction (C), the decomposition of formate to yield D adatoms and CO_2, has been discussed in Section 4.2. At low formate coverages, all decomposition occurs below the desorption temperature for hydrogen and all evolution of HD from the surface is desorption-limited. At saturation formate coverage, there are two peaks, a desorption-limited peak at 310 K and a reaction-limited peak at 350 K, similar to H_2 TDMS.

Desorption of D_2 is qualitatively similar to HD desorption. At low formate coverages, all decomposition occurs below the hydrogen desorption temperature and all evolution of D_2 from the surface is desorption-limited [cf. Fig. 9(C)]. At higher formate coverages, desorption-limited hydrogen evolution shifts to lower temperatures. Consequently, the H adatom coverage is lower when reaction (C)

is active and this reaction produces increased amounts of D_2 with respect to HD. This is also reflected by a shift of the reaction-limited D_2 peak 10 to 20 K higher than the H_2 and HD peaks.

The peak temperatures for desorption-limited hydrogen evolution have shifted to lower temperatures with respect to H_2 on clean Ru(001), where hydrogen desorbs at 440 K at low coverage and 340 K at saturation coverage [**40**]. Similar shifts have been seen for the coadsorption of CO and hydrogen [**41**].

4.5 Water Desorption

Water has been reported as a major decomposition product from formic acid on the (100) surface of Ru [**7**], but only very small amounts of water are a product on Ru(001), desorbing at 275 K [cf. Fig. 10]. The reaction of hydrogen and oxygen adatoms to give H_2O does not occur on the Ru(001) surface at temperatures below that at which hydrogen adatoms recombine and desorb thermally as H_2 [**42**]. Thus this small amount of desorbed water must be produced by the recombination of hydroxyl fragments and surface hydrogen from formic acid dehydrogenation. Integration of CO, CO_2 and H_2 TDMS from HCOOH, with heating rates of approximately 15 K/s, yields an estimate for the total H_2O production as 0.02 ± 0.01 molecule per surface Ru atom. Slow heating rates increase the amount of water and the slow annealing cycles used for EELS measurements would be expected to increase the hydroxyl coverage in those experiments.

5. CONCLUSIONS

This study has demonstrated the existence of two formate intermediates to formic acid decomposition on the Ru(001) surface, a monodentate formate and a bidentate formate. The bidentate formate bonds in a bridging configuration. The formate molecules decompose to produce CO, CO_2, water, O adatoms and hydrogen. Two forms of molecular formic acid are observed, a first-layer state which desorbs at 200 K and a multilayer state which desorbs at 170 K. Small exposures of formic acid dehydrogenate upon adsorption to produce a monodentate formate. The formate species do not recombine with H adatoms.

On the basis of EELS and TDMS results, the following reaction scheme can be constructed for formic acid decomposition of the Ru(001) surface.

$$\mathrm{HCOOH(g)} \xrightarrow{<80\mathrm{K}} \text{monodentate-HCOO(a)} + \mathrm{H(a)}$$

$$\text{monodentate-HCOO(a)} \xrightarrow{80-200\mathrm{K}} \text{bidentate-HCOO(a)}$$

$$\text{bidentate-HCOO(a)} \xrightarrow{<300\mathrm{K}} \mathrm{OH(a)} + \mathrm{CO(a)}$$

$$\text{bidentate-HCOO(a)} \xrightarrow{200-350\mathrm{K}} \mathrm{O(a)} + \mathrm{H(a)} + \mathrm{CO(a)}$$

$$\text{bidentate-HCOO(a)} \xrightarrow{300-350\mathrm{K}} \mathrm{H(a)} + \mathrm{CO_2(g)}$$

$$\mathrm{OH(a)} + \mathrm{H(a)} \xrightarrow{\sim 275\mathrm{K}} \mathrm{H_2O(g)}$$

$$2\,\mathrm{H(a)} \xrightarrow{300-400\mathrm{K}} \mathrm{H_2(g)}$$

$$\mathrm{CO(a)} \xrightarrow{450-500\mathrm{K}} \mathrm{CO(g)}$$

The ratio of products is influenced by two factors, the formate coverage and the heating rate. At a formate coverage of 10% of saturation, almost all decomposition yields CO. The amounts of both CO and CO_2 increase with formate coverage, but the CO decomposition channel saturates before the CO_2 channel. Slower heating rates are found to increase the relative amounts to water and CO. This is explained by deactivation of the surface by O adatoms and by a lower prefactor for HCOO decomposition to CO than to CO_2.

Two interesting features of this study are: the first spectroscopic evidence for a surface hydroxyl species on Ru(001) and the first reported observation of a softened ν(CH) mode for a surface formate species. While monodentate formate species have been proposed for other metal surfaces, this argument has been advanced solely on the assignment of a band at approximately 1660 cm^{-1} as the ν(C=O) mode in a monodentate formate, rather than the ν_a(OCO) mode of a bidentate formate, which would be dipolar allowed for an asymmetric bidentate bonding configuration. The observation of a softened ν(CH) mode provides additional evidence for the existence of a surface monodentate formate and indicates an interaction between the hydrogen atom and the surface, indicative of a short H-surface distance.

ACKNOWLEDGMENTS

The authors wish to thank Dr. Theodore E. Madey, John Parmeter and Dr. Udo Schwalke for extremely useful discussions. This research was supported by the National Science Foundation under Grant No. CHE82-06487.

Table 1

Assignments of vibrational modes observed using EELS for molecular HCOOH and DCOOD on Ru(001) from this work. The fundamental mode assignments for formic acid monomers, dimers and crystalline formic acid are listed also [**28**]. All frequencies are in cm^{-1}.

Mode	HCOOH			DCOOD		HCOOH	DCOOD
	Monomer	Dimer	Solid	Dimer	Solid	Ru(001)	
ν(OH)	3570	3110	2532	2323	2041	2640	2020
ν(CH)	2943	2957	2958	2226	2272	2960	2260
					2247		
ν(C=O)	1770	1754	1703	1720	1671	1690	1680
			1609		1590		
ν(C-O)	1105	1218	1255	1246	1270	1235	1260
			1224		1253		
δ(CH)	1387	1365	1380[a]	987	993	1370	970
				976			
δ(OH)	1229	1450	1560	1055	1090		
					1075		
π(CH)	1033	1050	1083	890	899		
δ(OCO)	636	397	720	642	662	720	[b]
π(OH)	636	917	974	678	708	940	[b]

(*a*) composed of three bands at closely spaced frequencies.

(*b*) a band with intensity due to both these modes appears at 690 cm^{-1}. The exact positions of the two modes can not be determined.

Table 2

Assignments and frequencies (in cm^{-1}) of vibrational modes for various formate species. Numbers in parentheses are for the equivalent deuterated formate species.

Mode		Inorganic Formate Complexes (IR)						Surface Formate Species (EELS)					
bidentate	monodentate	Solution	Monodentate			Bidentate		Monodentate			Bidentate		
			Cr	Fe	Pt	Cr	Fe	Ag(110)-O	Mo(110)	Ru(001)	Pt(110)	Ni(110)	Ru(001)
		(Free)						(tilted)		this	(tilted)		this
		[29,43]	[44]	[45]	[46]	[44]	[44]	[11]	[12]	work	[17]	[13]	work
	ν(CH)	2803				2975	2975	2900	2910	2355	2950	2950	2915
						2898	2953	(2150)			(2185)		(2200)
ν_s(OCO)	ν(C-O)	1351	1310	1293	1310	1374	1369	1340	1320	1345	1340	1370	1360
								(1310)		(1315)	(1320)		(1340)
	δ_s(OCO)	760	770[a]			771	760[b]	770	750	775	785	780	805
						761		(770)		(775)	(785)		(800)
ν_a(OCO)	ν(C=O)	1585	1574	1620	1620	1644	1635	1640	1650	1680	1560		
							1625	(1640)		(1660)	(1560)		
	δ_s(CH)	1385				1391	1385	(1010)		(1015)	(1010)		
	π(CH)	1069	1050			1040	1052	1050		1160	1050		
	ν(M-O)							280	380	370	355	430	380
								(260)		(365)			(410)

(*a*) Raman frequency.

(*b*) Composed of three closely spaced bands.

Figure Captions

Figure 1: Electron energy loss spectra of molecular formic acid multilayers on Ru(001) at 80 K following exposures of 10 L of HCOOH, (a), and 10 L of DCOOD, (b).

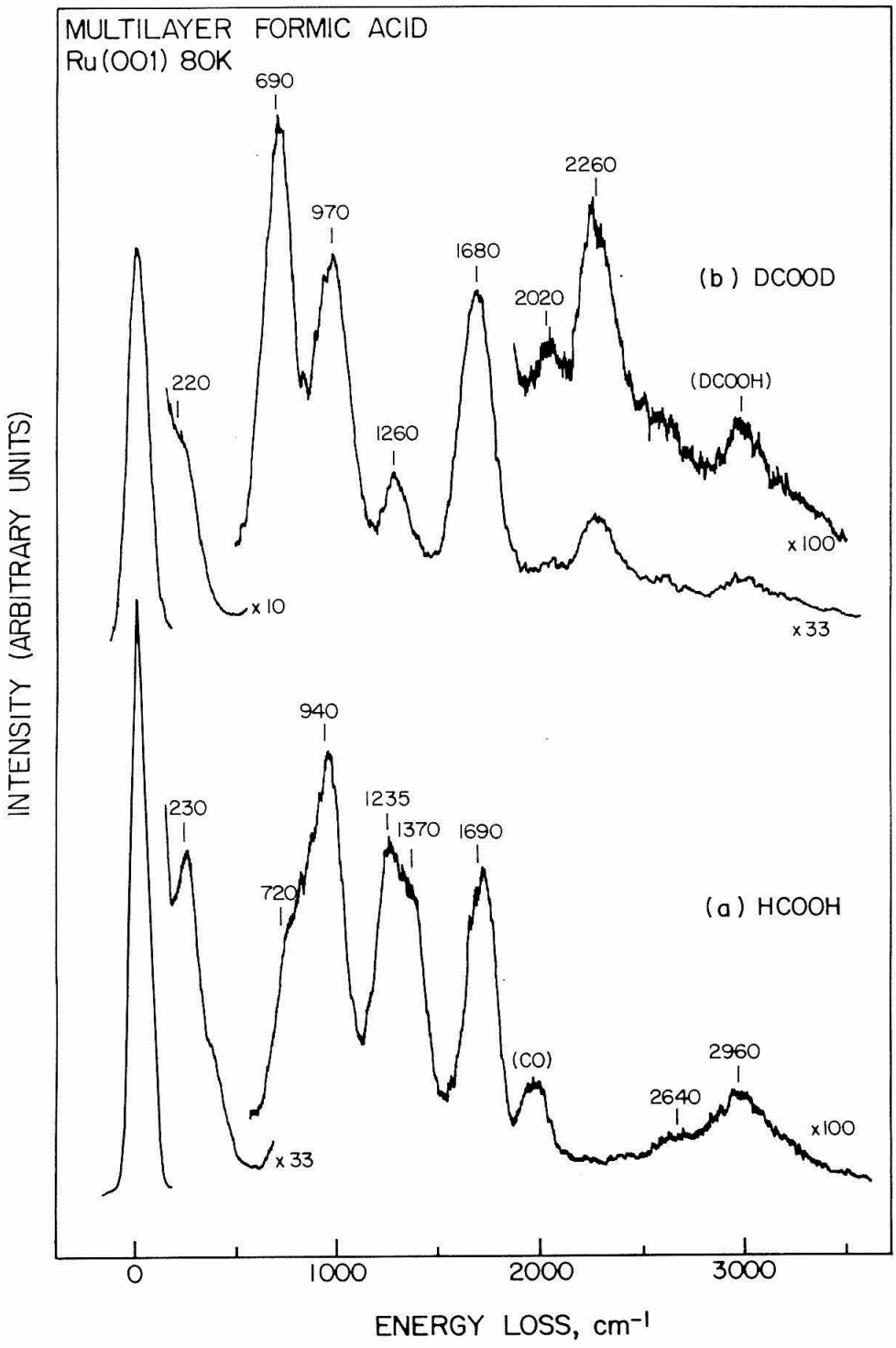
MULTILAYER FORMIC ACID
Ru(001) 80K
690
970
1680
2260
2020
(b) DCOOD
220
1260
(DCOOH)
x 100
x 10
x 33
940
230
1235
1370
1690
720
(a) HCOOH
(CO)
2960
2640
x100
x 33
0
1000
2000
3000
ENERGY LOSS, cm-1
INTENSITY (ARBITRARY UNITS)

Figure 2: Electron energy loss spectra of monodentate formate on Ru(001) at 80 K following exposures of 4 L of HCOOH, (a), and 2 L of DCOOD, (b).

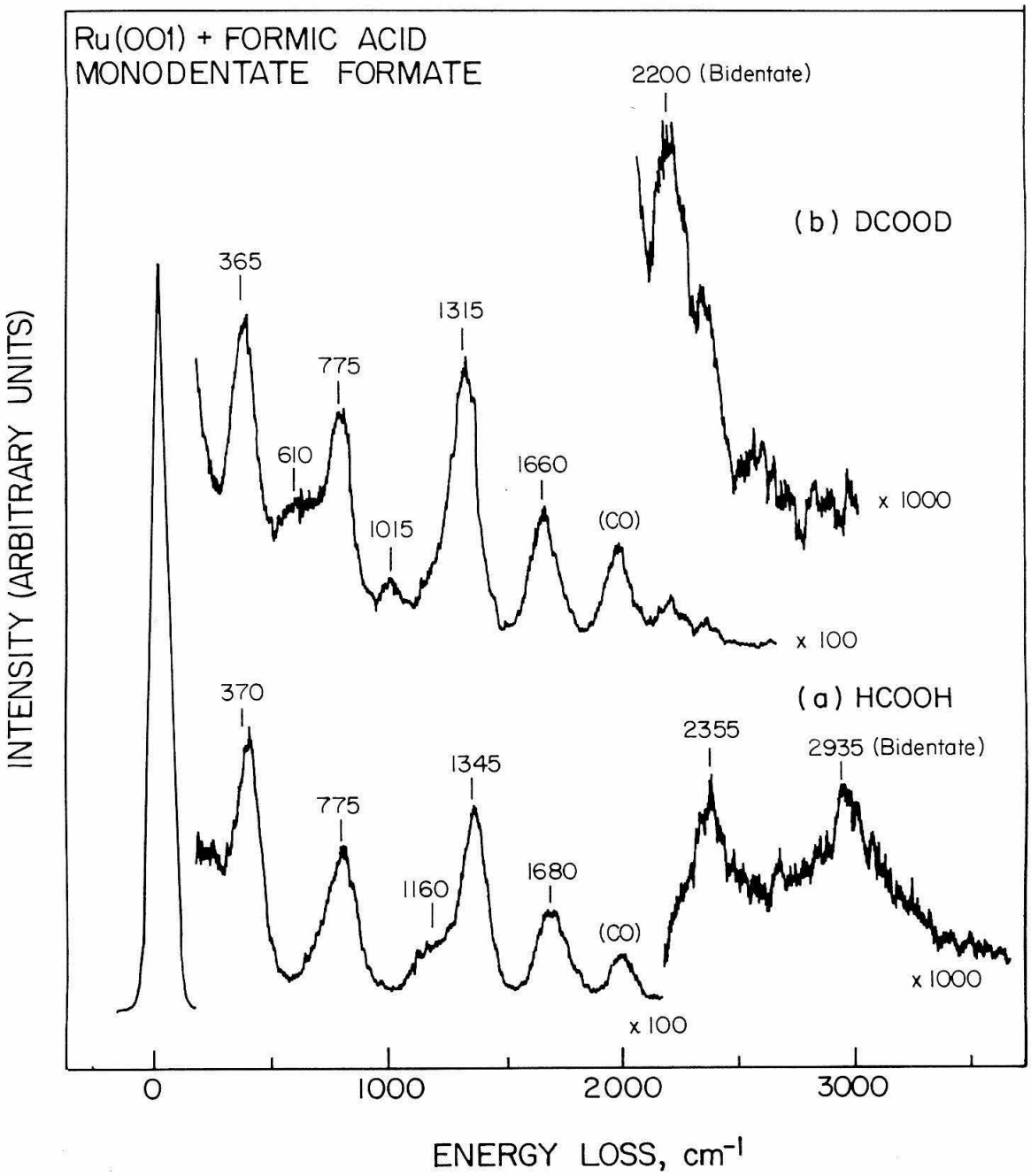
Ru(001) + FORMIC ACID
MONODENTATE FORMATE
2200 (Bidentate)
(b) DCOOD
365
775
610
1315
1660
1015
(CO)
x 1000
x 100
370
(a) HCOOH
2355
2935 (Bidentate)
1345
775
1160
1680
(CO)
x 1000
x 100
INTENSITY (ARBITRARY UNITS)
0
1000
2000
3000
ENERGY LOSS, cm-1

Figure 3: Electron energy loss spectra showing bidentate formate decomposition on Ru(001) following a 10 L exposure of HCOOH at 80 K and annealing to the indicated temperatures.

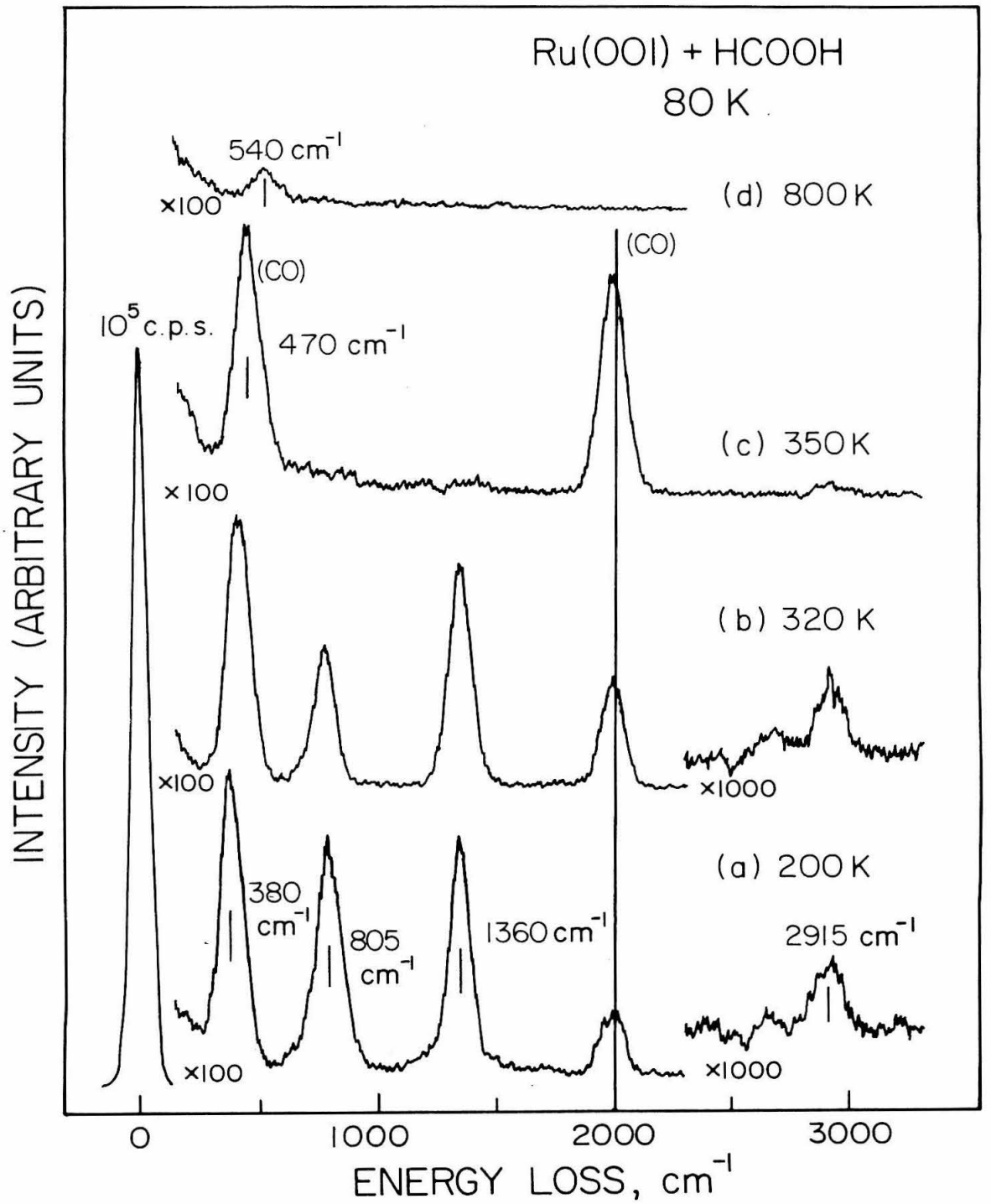
Ru(001) + HCOOH
80 K
540 cm⁻¹
×100
(d) 800 K
(CO)
(CO)
10⁵ c.p.s.
470 cm⁻¹
(c) 350 K
×100
(b) 320 K
×100
×1000
(a) 200 K
380 cm⁻¹
805 cm⁻¹
1360 cm⁻¹
2915 cm⁻¹
×100
×1000
INTENSITY (ARBITRARY UNITS)
0
1000
2000
3000
ENERGY LOSS, cm⁻¹

Figure 4: Electron energy loss spectra showing bidentate formate on Ru(001) following a 4 L exposure of DCOOD at 80 K and annealing to the indicated temperatures. Note that the intensity of the 610 cm^{-1} band due to a surface deuteroxyl does not correlate with the other spectral features.

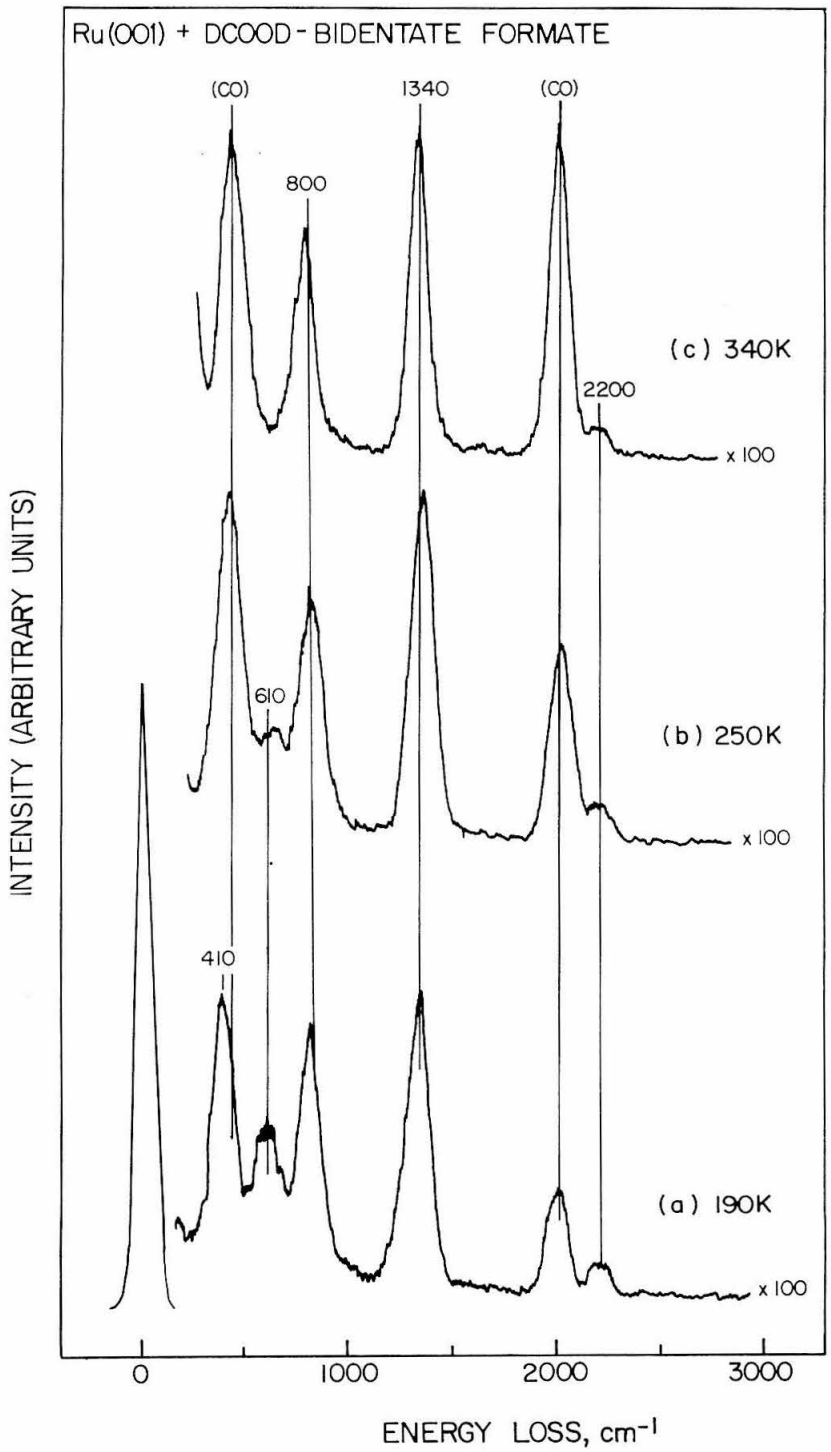
Ru(001) + DCOOD - BIDENTATE FORMATE
(CO)
1340
(CO)
800
2200
(c) 340K
x 100
610
(b) 250K
x 100
410
(a) 190K
x 100
INTENSITY (ARBITRARY UNITS)
0
1000
2000
3000
ENERGY LOSS, cm⁻¹

Figure 5: Thermal desorption mass spectra of molecular formic acid desorption from Ru(001) following exposures of (a) 3 L, (b) 5 L, (c) 10 L and (d) 20 L of DCOOH.

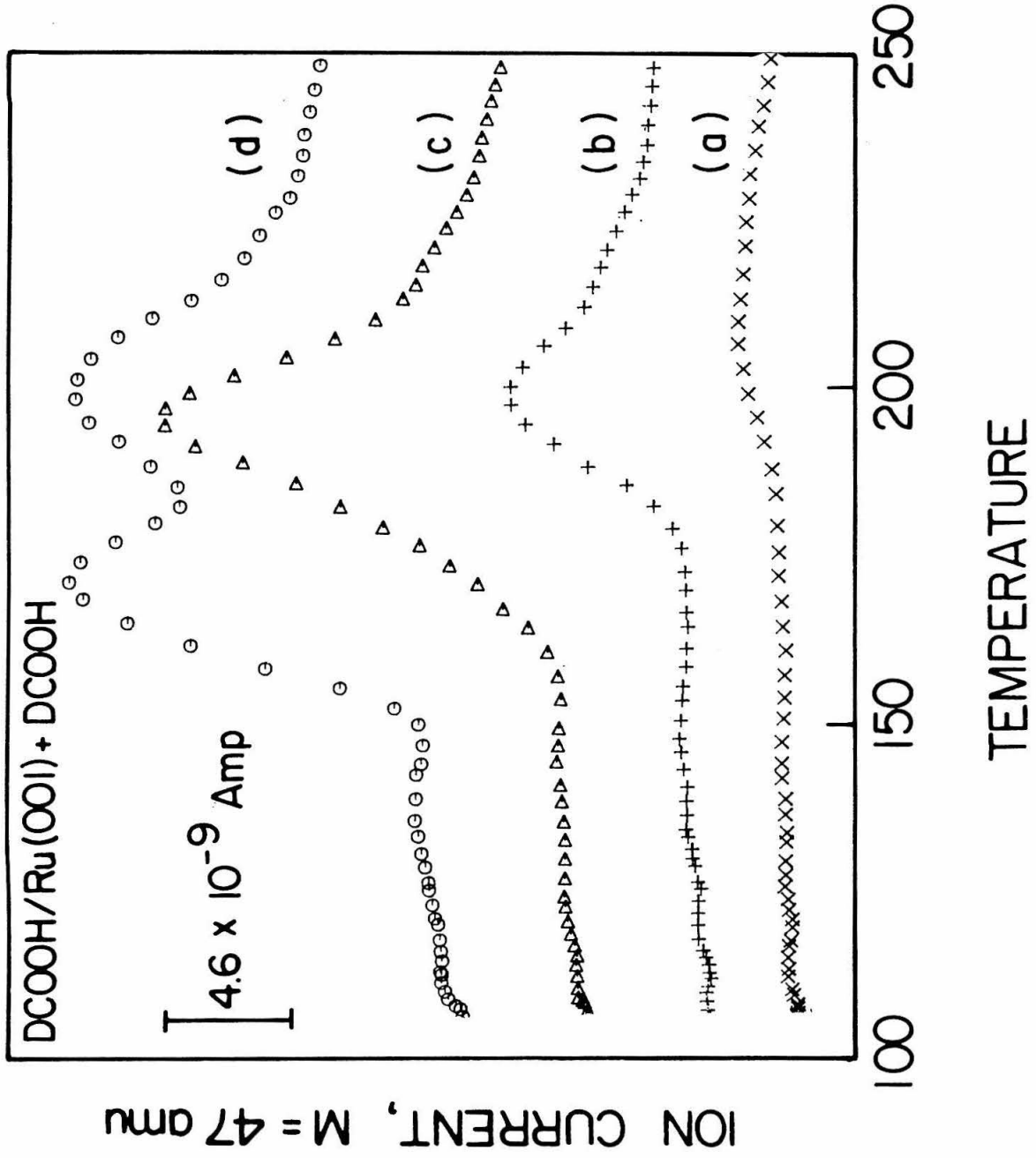
DCOOH/Ru(001) + DCOOH
4.6 x 10⁻⁹ Amp
(d)
(c)
(b)
(a)
100
150
200
250
TEMPERATURE
ION CURRENT, M = 47 amu

Figure 6: Thermal desorption mass spectra of CO_2 desorption from Ru(001) following exposures of (a) 0.4 L, (b) 0.6 L, (c) 1 L, (d) 3 L, (e) 5 L and (f) 10 L of DCOOH.

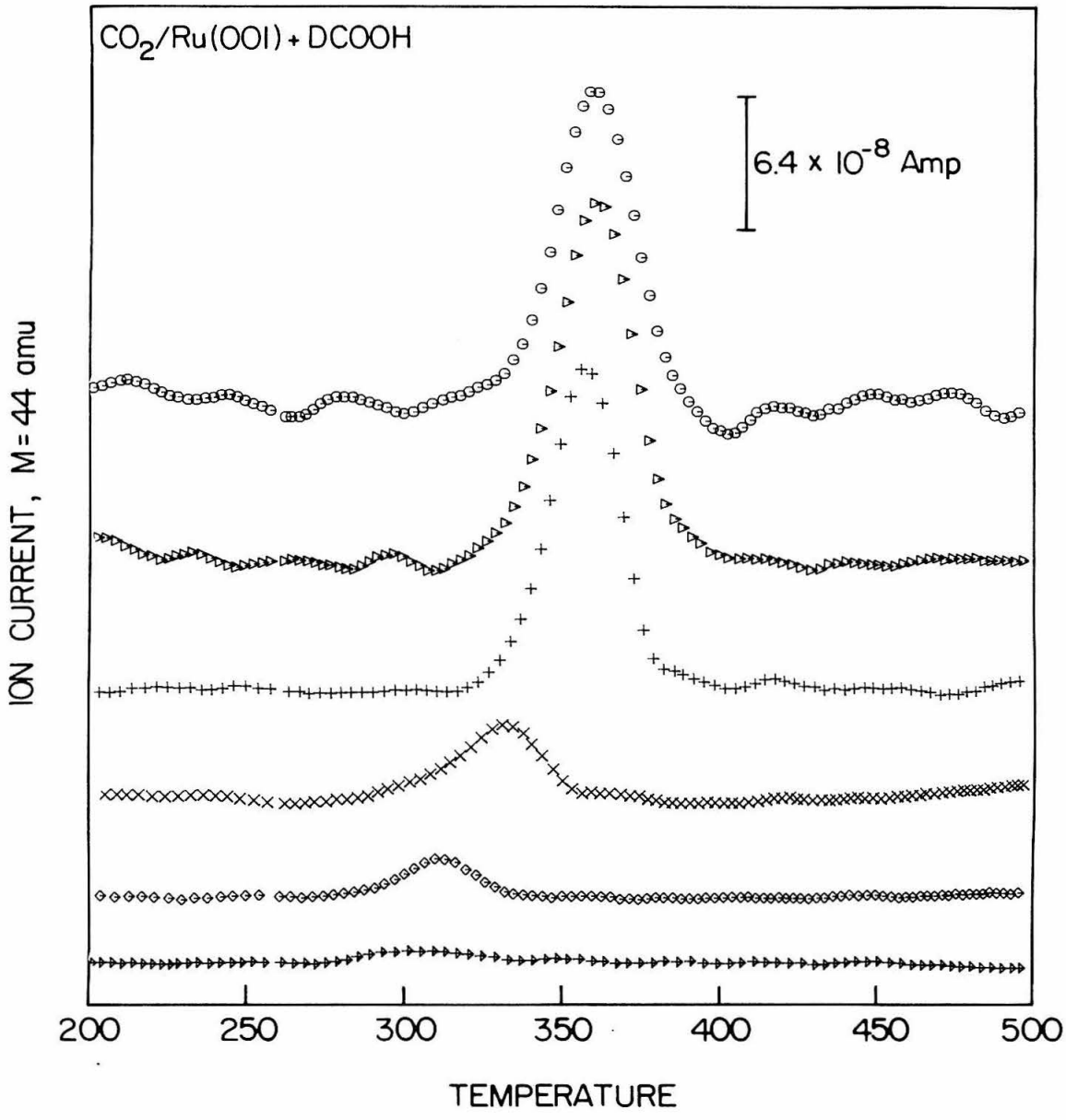
CO_2/Ru(001) + DCOOH
6.4 x 10^{-8} Amp
ION CURRENT, M = 44 amu
200
250
300
350
400
450
500
TEMPERATURE

Figure 7: Thermal desorption mass spectra of CO desorption from Ru(001) following exposures of (a) 0.4 L, (b) 0.6 L, (c) 1 L, (d) 3 L, (e) 5 L and (f) 10 L of DCOOH.

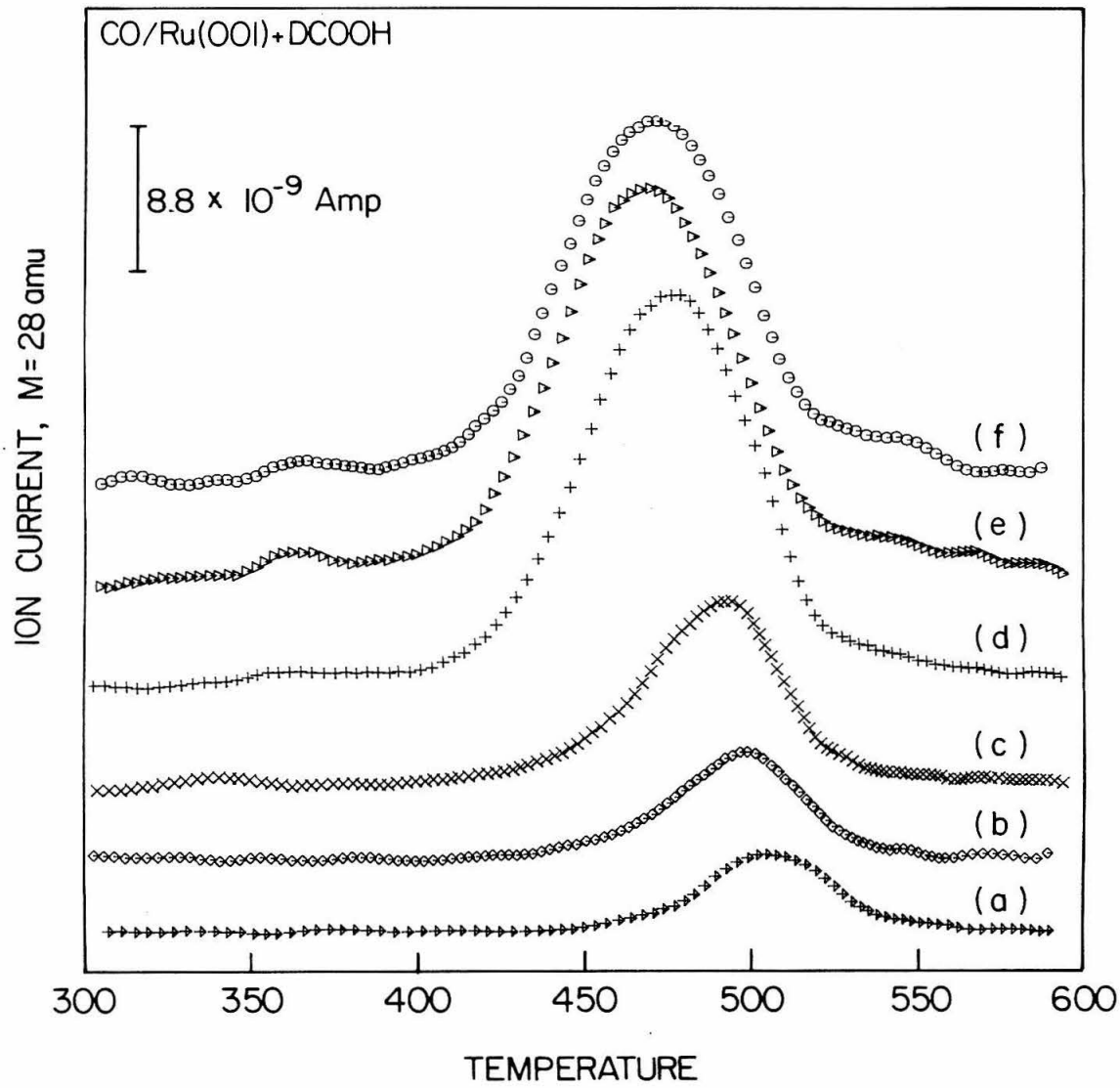
CO/Ru(001)+DCOOH
8.8 x 10^-9 Amp
ION CURRENT, M=28 amu
(f)
(e)
(d)
(c)
(b)
(a)
300
350
400
450
500
550
600
TEMPERATURE

Figure 8: Formic acid decomposition products on Ru(001) as a function of reaction conditions: (A) the amounts of CO and CO_2 evolved relative to a saturation coverage of formate and the ratio of CO_2 to CO versus the formic acid exposure (in L) for a heating rate of approximately 15 K/s; (B) the ratio of CO_2 to CO versus the heating rate (in K/s) for a 1 L exposure (approximately 40% of saturation). The ratio of products from a surface annealed at 240 K for 300 s and then ramped at 13 K/s was used as the zero heating rate extrapolation.

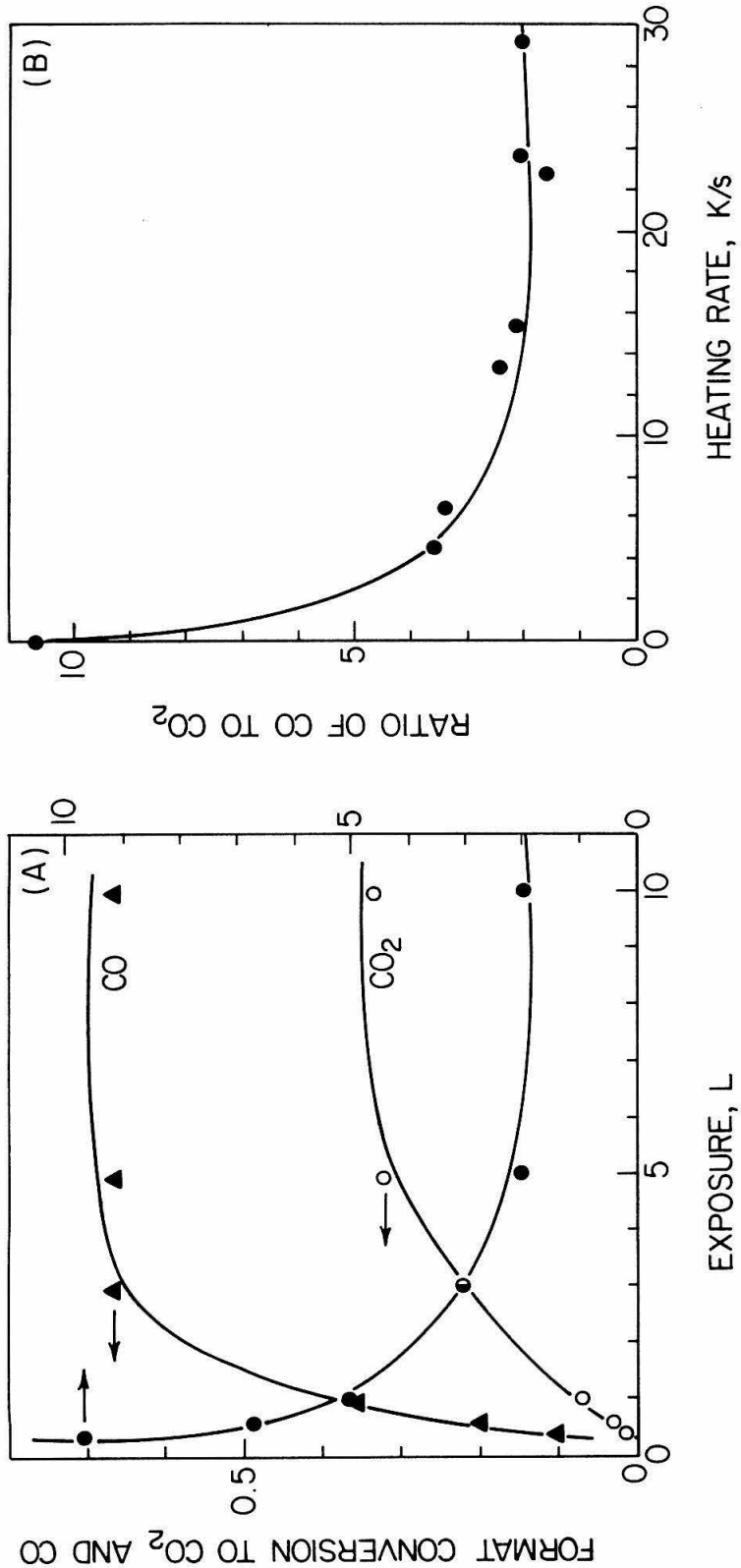
(A)
CO
CO_2
FORMAT CONVERSION TO CO_2 AND CO
0.5
0
5
10
EXPOSURE, L
(B)
RATIO OF CO TO CO_2
0
5
10
0
10
20
30
HEATING RATE, K/s

Figure 9: Thermal desorption mass spectra of (A) H_2, (B) HD and (C) D_2 desorption from Ru(001) following exposures of (a) 0.4 L, (b) 0.6 L, (c) 1 L, (d) 3 L, (e) 5 L and (f) 10 L of DCOOH.

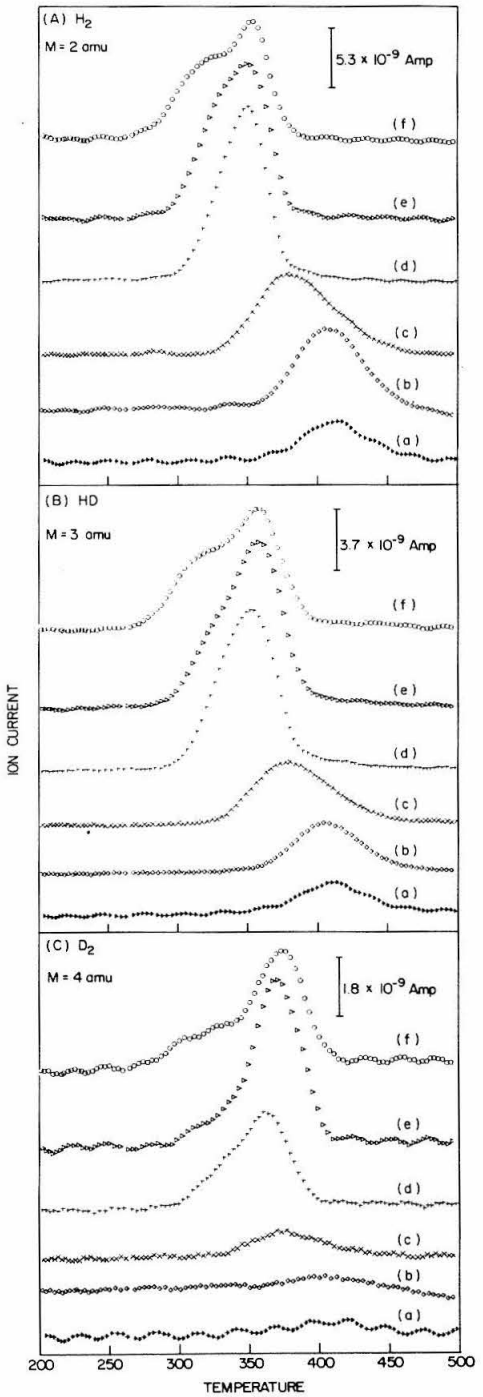
(A) H_2
M = 2 amu
5.3 x 10^{-9} Amp
(f)
(e)
(d)
(c)
(b)
(a)
(B) HD
M = 3 amu
3.7 x 10^{-9} Amp
(f)
(e)
(d)
(c)
(b)
(a)
(C) D_2
M = 4 amu
1.8 x 10^{-9} Amp
(f)
(e)
(d)
(c)
(b)
(a)
ION CURRENT
200
250
300
350
400
450
500
TEMPERATURE

Figure 10: Thermal desorption mass spectra of H_2O desorption from Ru(001) following an exposure of 5 L of DCOOH.

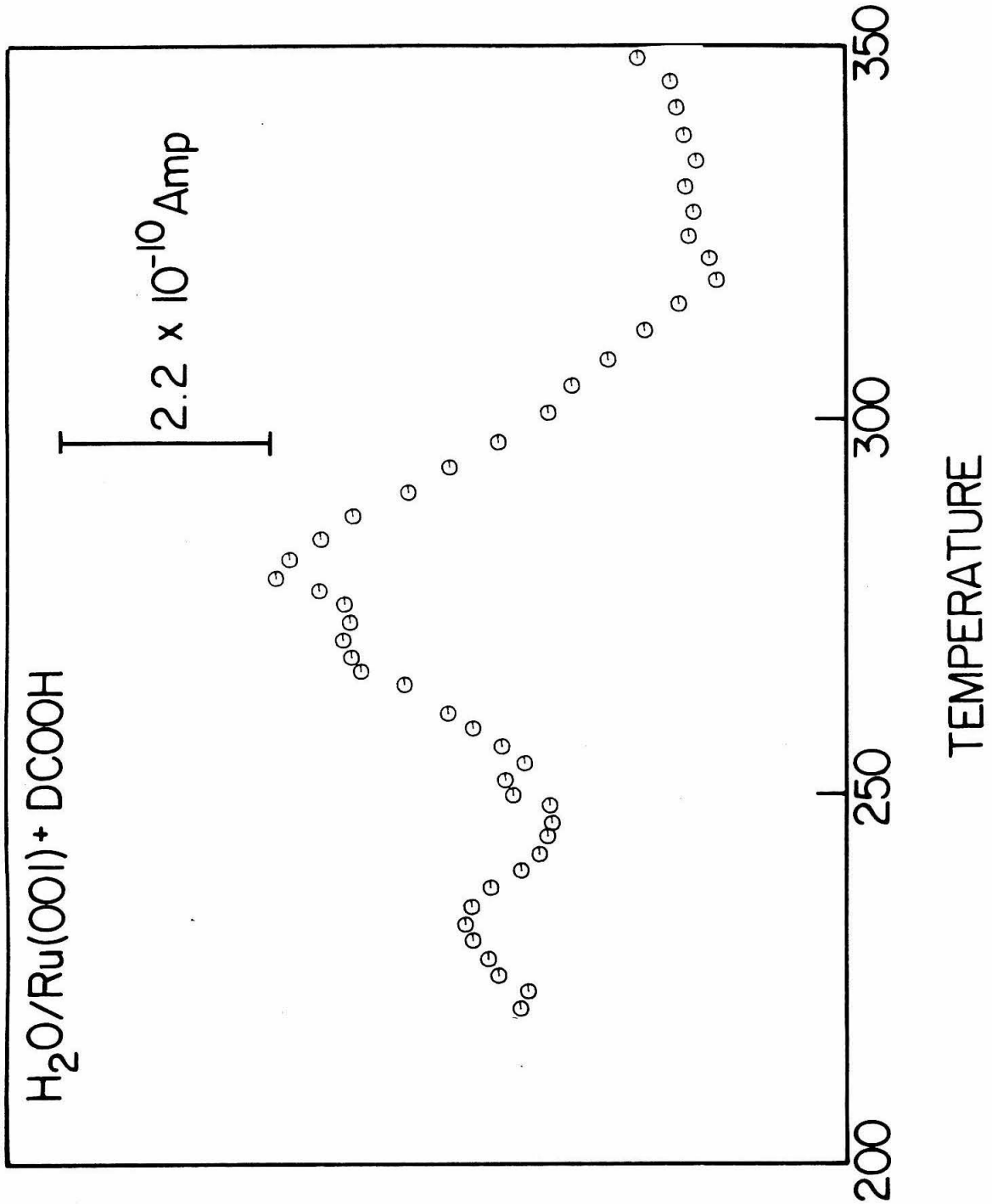
H2O/Ru(001)+ DCOOH
2.2 x 10-10 Amp
200
250
300
350
TEMPERATURE

References

[1] See for example, R. J. Madix, Advan. Catal. **29**, 1 (1980); E. Iglesia and M. Boudart, J. Catal. **81**, 224 (1983); and N. D. S. Canning and R. J. Madix, J. Phys. Chem. **88**, 2437 (1984).

[2] J. B. Benziger and R. J. Madix, J. Catal. **65**, 49 (1980).

[3] J. B. Benziger and G. R. Schoofs, J. Phys. Chem. **88**, 4439 (1984).

[4] See J. L. Falconer and R. J. Madix, J. Catal. **31**, 47 (1978) and references cited therein.

[5] J. B. Benziger and R. J. Madix, Surface Sci. **79**, 394 (1979).

[6] N. R. Avery, B. H. Toby, A. B. Anton and W. H. Weinberg, Surface Sci. **122**, L574 (1982); and B. H. Toby, N. R. Avery, A. B. Anton and W. H. Weinberg, J. Electron Spect. **29**, 233 (1983).

[7] L. A. Larson and J. T. Dickinson, Surface Sci. **84**, 17 (1979).

[8] N. R. Avery, Appl. Surface Sci. **11/12**, 774 (1982).

[9] B. A. Sexton, Surface Sci. **88**, 319 (1979).

[10] D. H. S. Ying and R. J. Madix, J. Catal. **61**, 48 (1980).

[11] B. A. Sexton and R. J. Madix, Surface Sci. **105**, 177 (1981).

[12] S. L. Miles, S. L. Bernasek and J. L. Gland, Surface Sci. **127**, 271 (1983).

[13] R. J. Madix, J. L. Gland, G. E. Mitchell and B. A. Sexton, Surface Sci. **125**, 481 (1983).

[14] M. Liehr, P. A. Thirty, J. J. Pireaux and R. Caudano, Phys. Rev. B **31**, 42 (1985).

[15] M. Chtaib, P. A. Thirty, J. P. Delrue, J. J. Pireaux and R. Caudano, J. Electron Spect. **29**, 293 (1983).

[16] B. E. Hayden, K. Prince, D. P. Woodruff and A. M. Bradshaw, Surface Sci. **133**, 589 (1983).

[17] P. Hofmann, S. R. Bare, N. V. Richardson and D. A. King, Surface Sci. **133**, L459 (1981).

[18] H. Ibach and D. L. Mills, *Electron Energy Loss Spectroscopy and Surface Vibrations,* Academic Press, New York, 1982.

[19] Other workers have suggested that the reappearance of the band assigned as the ν_A(OCO) mode is due to adsorption of molecular formic acid desorbing from other surfaces within the belljar **(I4)**.

[20] A. Puschmann and J. Haase, M. D. Crapper, C. E. Riley and D. P. Woodruff, Phys. Rev. Letters **54**, 2250 (1985).

[21] J. Stöhr, D. A. Outka, R. J. Madix and U. Döbler, Phys. Rev. Letters **54**, 1256 (1985).

[22] T. H. Upton, J. Chem. Phys. **83**, 5084 (1985).

[23] N. R. Avery, W. H. Weinberg, A. B. Anton and B. H. Toby, Phys. Rev. Letters **51**, 682 (1983); A. B. Anton, N. R. Avery, B. H. Toby and W. H. Weinberg, J. Am. Chem. Soc., **108**, 684 (1986).

[24] A. B. Anton, J. E. Parmeter and W. H. Weinberg, J. Am. Chem. Soc., in press.

[25] G. E. Thomas and W. H. Weinberg, Rev. Sci. Instrum. **50**, 497 (1979).

[26] A. Savitzky and M. J. E. Golay, Anal. Chem **36**, 1627 (1964); and J. Steinier, Y. Termonia and J. Deltour, Anal. Chem **44**, 1906 (1972).

[27] G. E. Thomas and W. H. Weinberg, J. Chem. Phys. **70**, 954 (1979).

[28] R. C. Millikan and K. S. Pitzer, J. Am. Chem. Soc. **80**, 3515 (1958).

[29] K. Nakamoto, *Infrared and Raman Spectra of Inorganic and Coordination Compounds,* Wiley, New York, 1978.

[30] P. A. Thiel, F. M. Hoffmann and W. H. Weinberg, J. Chem. Phys. **75**, 5556 (1981).

[31] E. M. Stuve, S. W. Jorgensen and R. J. Madix, Surface Sci. **146**, 179 (1984).

[32] C. Nyberg and C. G. Tengstål, J. Chem. Phys. **80**, 3463 (1984).

[33] E. M. Stuve, R. J. Madix and B. A. Sexton, Surface Sci. **111**, 11 (1981).

[34] G. B. Fisher and B. A. Sexton, Phys. Rev. Letters **44**, 683 (1980).

[35] N. R. Avery and A. B. Anton, unpublished results.

[36] H. I. Lee, G. Praline and J. M. White, Surface Sci. **91**, 581 (1980).

[37] T. E. Madey, H. A. Engelhardt and D. Menzel, Surface Sci. **48**, 304 (1975).

[38] T. E. Madey and D. Menzel, Japan. J. Appl. Phys., Suppl. **2**, Pt. 2, 229 (1974).

[39] B. H. Toby, M. M. Hills and W. H. Weinberg, unpublished results.

[40] H. Shimizu, K. Christmann and G. Ertl, J. Catal. **61**, 412 (1980).

[41] D. E. Peebles, J. A. Schreifels and J. M. White, Surface Sci. **116**, 117 (1982).

[42] S. K. Shi, J. A. Schreifels and J. M. White, Surface Sci. **105**, 1 (1981).

[43] K. Ito and H. J. Bernstein, Can. J. Chem. **34**, 170 (1956).

[44] M. K. Johnson, D. B. Powell and R. D. Cannon, Spectrochim. Acta **37A**, 995 (1981).

[45] D. J. Darensbourg, M. B. Fischer, R. E. Schmidt, Jr. and B. J. Baldwin, J. Am. Chem. Soc. **103**, 1297 (1981).

[46] A. Immirzi and A. Musco, Inorg. Chim. Acta **22**, L35 (1977).

Chapter 8:

Contrasting Bonding Configurations of Acetone on Pt(111) and Ru(001) Surfaces

Journal of Electron Spectroscopy and Related Phenomena, 29 (1983) 233—237
Elsevier Scientific Publishing Company, Amsterdam — Printed in The Netherlands

CONTRASTING BONDING CONFIGURATIONS OF ACETONE ON Pt(111) AND Ru(001) SURFACES.

N.R. AVERY,[1] A.B. ANTON,[2] B.H. TOBY[2] and W.H. WEINBERG[2]

[1]CSIRO Division of Materials Science, University of Melbourne, Parkville, 3052, Victoria, Australia.

[2]Division of Chemistry and Chemical Engineering, California Institute of Technology, Pasadena, CA 91125, USA.

ABSTRACT

The comparative chemistry of acetone adsorption on Pt(111) and Ru(001) has been studied by EELS. On the more easily oxidized Ru(001) surface, acetone bonded in a side-on, η^2(O,C) configuration, whereas on the well-defined, close-packed regions of the Pt(111) surface acetone adopted a weak adduct-like, end-on, η^1(O) configuration. On Pt(111), some η^2(O,C) was also observed and associated with adsorption at low coordination accidental step sites.

INTRODUCTION

As part of a continuing study of the organometallic chemistry of weak donor ligands on metal surfaces, we have studied the interaction of acetone with two single crystal metal surfaces viz. Pt(111) and Ru(001). In this way, it has been shown that acetone bonds either through the oxygen in an end-on or η^1(O) configuration or through the oxygen and ketonic carbon atoms in a lying-down or η^2(O,C) configuration.

EXPERIMENTAL

Descriptions of the EEL spectrometers used for the Pt(111) (ref.1) and Ru(001) (ref.2) work have been given previously. All spectra were taken in the specularly reflected beam. Clean surfaces were prepared by well-established Ar^+ sputtering and oxidation techniques. Thoroughly degassed acetone was adsorbed either by back-filling the vacuum chamber in the Ru(001) work or with a movable doser located in front of the Pt(111) crystal. Base pressures of $<10^{-10}$ torr were routinely obtained with both systems.

RESULTS AND INTERPRETATION

Multilayer acetone. The EEL spectrum from multilayer acetone on Pt(111) at 130 K (Fig. 1) may be assigned according to Dellepiane and Overend (ref.3). Acetone (C_{2v} point group) has 24 normal modes which may be divided into 18 internal methyl modes and 6 modes involving the Me_2CO (Me ≡ methyl) skeleton. The skeletal modes involve dynamic dipole moments along the two-fold axis (A_1)

0368-2048/83/0000—0000/$03.00

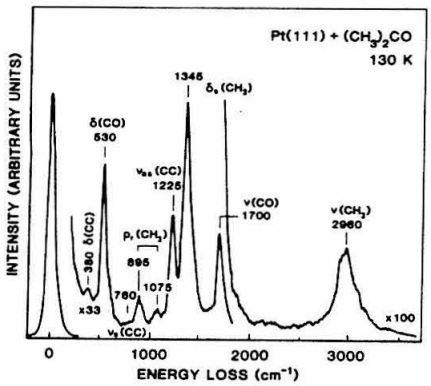

Fig. 1. EEL spectrum from multilayer acetone on Pt(111) at 130 K.

or perpendicular to the two-fold axis but either in the molecular plane (B_1) or perpendicular to it (B_2). There are three A_1 modes viz. ν(C=O), ν_s(MeCMe) and δ(MeCMe), two strong B_1 modes viz. ν_{as}(MeCMe) and δ(CO) and a single weak B_2 mode viz π(CO) which could not be resolved from the δ(CO) in the present spectrum.

Monolayer acetone on Ru(001).

Heating the Ru(001) surface, which had previously been covered with multilayer acetone, to 190 K desorbed the excess adsorbate and revealed the spectrum of monolayer acetone (Fig. 2a). This spectrum showed a systematic absence of the intrinsically strong A_1 and B_1 modes, indicating, according to the surface selection rule for dipole excitations, that the CO bond is parallel, or almost so, to the surface. Instead, conspicuous bands at 3000 cm^{-1}, 1385 cm^{-1} and 990 cm^{-1} are seen and assigned to methyl stretching, deformation and rocking modes, respectively. The 675 cm^{-1} band is assigned to a skeletal angle deformation mode.

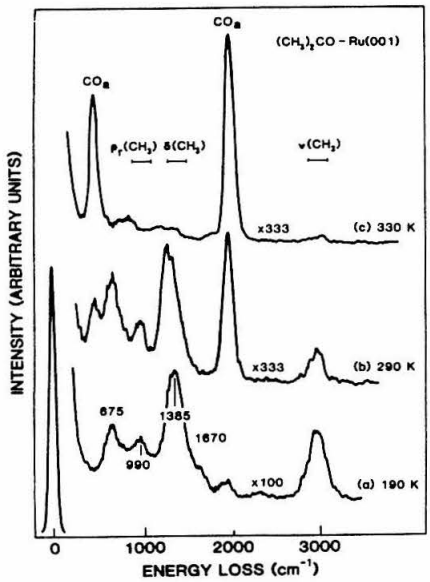

Fig. 2. EEL spectra from (a) monolayer acetone on Ru(001) at 190 K and after heating to (b) 290 K and (c) 330 K.

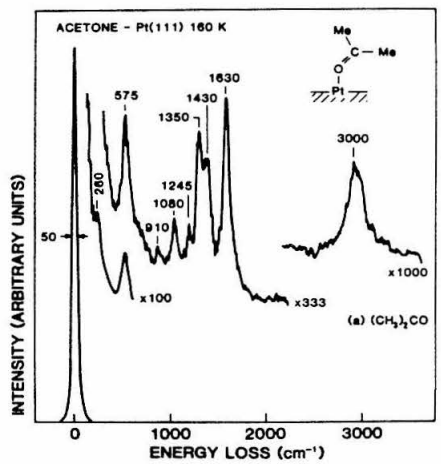

Fig. 3. EEL spectrum from monolayer acetone on Pt(111) at 160 K.

In the absence of a clearly detectable ν(CO) mode or the ability to measure the C-O bond length, it is not possible to estimate the bond-order and with it the extent of rehybridization of the ketonic carbon atom. Conceivable bonding configurations include I, II and III. In I it is envisaged that the

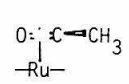

I

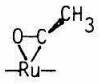

II

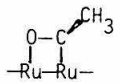

III

ketonic carbon atom retains its sp^2 character whereas in II and III substantial rehybridization to sp^3 occurs. The real structure of adsorbed acetone on Ru(001) probably lies between these extremes. The resulting species is designated η^2(O,C) acetone to signify the involvement of both the oxygen and carbon atoms in bonding to the metal atom.

With further heating to 290 K (Fig. 2c), EEL bands due to adsorbed CO appear and dominate the spectrum after a further flash to 330 K (Fig. 2d). Molecular acetone does not desorb in this temperature regime suggesting that instead, η^2(O,C) acetone decomposes to adsorbed CO and by inference adsorbed H and C thus:

$$\eta^2(O,C) \text{ acetone} \xrightarrow{300\ K} CO_a + C_a + H_a \qquad (1)$$

Monolayer acetone on Pt(111). An EEL spectrum of acetone adsorbed on Pt(111) at 160 K is shown in Fig. 3. This spectrum shows the presence of methyl stretching, deformation and rocking modes which are essentially unperturbed from their free acetone frequencies indicating that the methyl groups are inert and play no role in the bonding to the surface. Of greater diagnostic significance is the presence of the two B_1 modes viz. δ(CO) (575 cm^{-1}) and ν_{as}(CC) (1245 cm^{-1}) both slightly blue-shifted from their free acetone frequencies and a ν(CO) band (A_1 symmetry) which is similarly red-shifted by 80 cm^{-1}. This indicates that the adsorbed species on Pt(111) is bonded through the oxygen atom and from the surface selection rule for dipole excitations, that the Pt-O-C bond must be bent significantly from 180°, as in IV. The bands in this spectrum are attenuated, in unison, after heating to 180-190 K corresponding to a thermal desorption pulse of molecular acetone seen in the same temperature range. When regions of crystal closer to the edge were probed by the EELS beam weak residual methyl stretching, deformation and rocking bands were seen after the η_1(O) species was desorbed at 190 K. No adsorbed CO bands arising from acetone decomposition were seen. These bands are attributed to a small concentration of η^2(O,C) acetone, analogous to that which forms the majority species on Ru(001), confined to the accidental step sites which inevitably contribute to a real

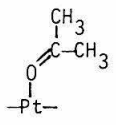

IV

crystal surface, particularly near the edges. The $\eta^2(O,C)$ species on Pt(111) is a minority state and its properties will be discussed more fully elsewhere (ref.1b). By inference, the $\eta_1(O)$ species is associated with adsorption on the well-defined, close-packed regions of the Pt(111) surface and is the majority species.

DISCUSSION

In summary, EELS has identified two basically different forms of adsorbed acetone which have been designated $\eta^1(O)$ and $\eta^2(O,C)$ for end-on and side-on bonding configurations, respectively. On Ru(001), the $\eta^2(O,C)$ form is the majority species. On Pt(111), the $\eta^1(O)$ form has been identified as the majority species on the well-defined, close-packed regions of the surface whereas a small contribution from the $\eta^2(O,C)$ form has been associated with accidental step sites.

In inorganic coordination compounds, acetone bonded in an end-on $\eta^1(O)$ configuration are well known. Labile donor ligands of this kind are easily exchanged for other ligands and consequently are widely exploited in synthesis reactions. In X-ray structure analysis of two ruthenium complexes, the Ru-O-C bond has been shown to be bent at angles of 153^o (ref.5) and 138^o (ref.6) in, or close to, the molecular acetone plane. A bonding scheme for both these complexes and $\eta^1(O)$ adsorbed acetone may be devised by reference to the frontier orbitals of acetone (ref.7). The highest filled orbital is a non-bonding atomic p-like orbital located on the oxygen atom and oriented in the molecular plane. If one lobe of this orbital is regarded as a Lewis base and interacts with an empty Pt orbital, the desired bent Pt-O-C bond is formed. Clearly, there is a strong similarity between $\eta^1(O)$ acetone and these inorganic acetone complexes.

Inorganic compounds with acetone bonded in an $\eta^2(O,C)$ configuration have not been isolated. However, comparable compounds with the more electrophillic $(CF_3)_2CO$ are well known in both three (ref.8) and four (ref.9) membered heterocyclic ring configurations analogous to the surface structure II and III. In these compounds, almost complete rehybridization of the ketonic carbon to sp^3 has occurred, whereas in a nickel $(CF_3)_2CO$ complex (ref.10) only partial rehybridization occurs and bonding must be regarded as being more π-like. In the latter case, the $(CF_3)_2CO$ skeleton is much less distorted from the plannar free $(CF_3)_2CO$ configuration than in the ruthenium complexes. The nickel complex is the organic analog of I whereas the ruthenium complexes correspond to II and III.

The ability of the Ru(001) surface to adsorb acetone in the $\eta^2(O,C)$ configuration would indicate that the solid surface is more easily able to raise its oxidation state than the isolated atoms in the inorganic compounds. Similarly, the close-packed regions of the Pt(111) surface will be less easily oxidized

and therefore failed to form a comparable species but instead adsorb acetone in a weak donor ligand, or adduct configuration. The minority component of η^2(O,C) acetone on the Pt(111) surface is confined to the low coordination and therefore more easily oxidized step sites.

REFERENCES

1 N.R. Avery, (a) Appl Surface Sci. 13 (1982) 171; and (b) Surface Sci. (submitted).
2 G.E. Thomas and W.H. Weinberg, Rev. Sci. Instrum. 50 (1979) 497.
3 G. Dellepiane and J. Overend, Spectrochimica Acta 22 (1966) 593.
4 Introduction to Infrared and Raman Spectroscopy, 2nd Edition (Academic Press) 1975.
5 R.D. Gould, W.J. Sime and T.A. Stephenson, J.C.S. Dalton (1978) 76.
6 M.A. Bennett, T.W. Matheson, G.B. Robertson, W.L. Steffen and T.W. Turney, J.C.S. Chem. Comm. (1979) 32.
7 W.L. Jorgensen and C. Salem, The Organic Chemist's Book of Orbitals (Academic Press) 1973.
8 B. Clarke, M. Green, R.B.L. Osburn, F.G.A. Stone, J. Chem. Soc. (A) (1969) 20.
9 M. Green, J.A.K. Howard, A. Laguna, L.E. Smart, J.L. Spencer and F.G.A. Stone, J. Chem. Soc. (Dalton)(1977) 278.
10 R. Countryman and B.R. Penfold, J. Crys. Molec. Structure 2 (1972) 281.

Appendix D:

End-On and Side-On Bonding of Ketones to Surfaces: Acetone on the Ru(001) and Pt(111) Surfaces

VOLUME 51, NUMBER 8 PHYSICAL REVIEW LETTERS 22 AUGUST 1983

End-On and Side-On Bonding of Ketones to Surfaces: Acetone on the Ru(001) and Pt(111) Surfaces

N. R. Avery,[a] W. H. Weinberg, A. B. Anton, and B. H. Toby
Division of Chemistry and Chemical Engineering, California Institute of Technology, Pasadena, California 91125

(Received 10 February 1983)

High-resolution electron-energy-loss spectroscopy has verified the existence of two fundamentally different types of adsorbed acetone, η^1-bonded acetone on Pt(111) and η^2-bonded acetone on Ru(001). On a Ru(001) surface, the Lewis acidity of which has been increased by the presence of oxygen adatoms, the η^1 and η^2 forms of acetone coexist. The η^1-bonded acetone desorbs molecularly, whereas η^2-bonded acetone is a precursor to dissociation on the surface.

PACS numbers: 68.30.+z, 61.14.-x, 68.20.+t, 82.65.Jv

Previous investigations[1-15] concerning the bonding of prototypical ketones to metal centers in organometallic complexes have provided a qualitatively consistent picture of the effect of the Lewis acidity of a metal on its selectivity toward various possible configurations for the bonding of the ketonic ligands. The advent of high-resolution electron-energy-loss spectroscopy (EELS) for the vibrational analysis of adsorbed overlayers on solid surfaces has rendered feasible incisive studies of the organometallic chemistry of macroscopic, well-defined single-crystalline surfaces[16] and a rigorous comparison to the chemistry of analogous homogeneous complexes. In this Letter, new and unprecedented results are reported concerning the interaction of acetone (a weak donor ligand) with the close-packed Pt(111) and Ru(001) surfaces, as well as the Ru(001) surface on which an ordered $p(2\times 2)$ overlayer[17] of atomic oxygen is present.[18-20] The contrasting bonding configurations and the possible decomposition of acetone observed on these surfaces systematize the chemical effects of relative Lewis acidities of metals,[21] while clarifying the comparative chemistry of these surfaces and their relationship to analogous coordination complexes.

Descriptions of the EEL spectrometers (and the UHV chambers in which they are contained) used for the Ru (Ref. 22) and Pt (Ref. 23) studies have been published previously. A typical resolution in both spectrometers (for a disordered overlayer of low electron reflectivity) is 80 cm^{-1} (full width at half maximum of the elastically scattered electron beam), and optimum resolutions are below 40 cm^{-1}. Atomically clean single-crystalline surfaces were prepared by Ar^+ sputtering and chemical cleaning with oxygen followed by high-temperature reductive annealing.[24] The ordered $p(2\times 2)$ overlayer of atomic oxygen on Ru(001) was prepared by exposing the clean surface to 0.8 L of oxygen (1 L = 1 langmuir $\equiv 10^{-6}$ Torr s) at 95 K, followed by thermal ordering at a temperature of approximately 350 K.[18-20] The Pt crystal was exposed to acetone with a directional beam doser consisting of a multichannel array of microcapillaries, whereas the Ru crystal was exposed to acetone by backfilling the UHV chamber. The acetone was degassed with multiple freeze-pump-thaw cycles before use, and its purity was verified *in situ* mass spectrometrically.

EEL spectra for acetone adsorbed on the three surfaces are shown in Fig. 1, and a summary of the surface structures, the measured vibrational frequencies, and the mode assignments is presented in Table I. Spectra obtained for adsorption of $(CD_3)_2CO$ rather than $(CH_3)_2CO$ are shown in Figs. 1(b) and 1(c), since they afford better clarity and resolution of the signature modes critical to the identification of the adsorbed species.

On the Pt(111) surface, the EEL spectrum of adsorbed acetone, shown in Fig. 1(a), exhibits (dipolar enhanced) modes of both A_1 and B_1 symmetry and a down-shifted carbonyl stretching frequency (relative to liquid acetone or acetone multilayers condensed on the Pt and Ru surfaces). Consequently, on Pt(111) acetone is bonded in an η^1 (end on) fashion through the oxygen atom with C_s symmetry (a mirror plane through the plane of the molecule, perpendicular to the surface), and a Pt–O=C bond angle that is less than 180°, as shown in Fig. 2(a). The bonding of the acetone to the Pt(111) surface is typical of a weak donor ligand since the temperature corresponding to the maximum rate of desorption of molecular ace-

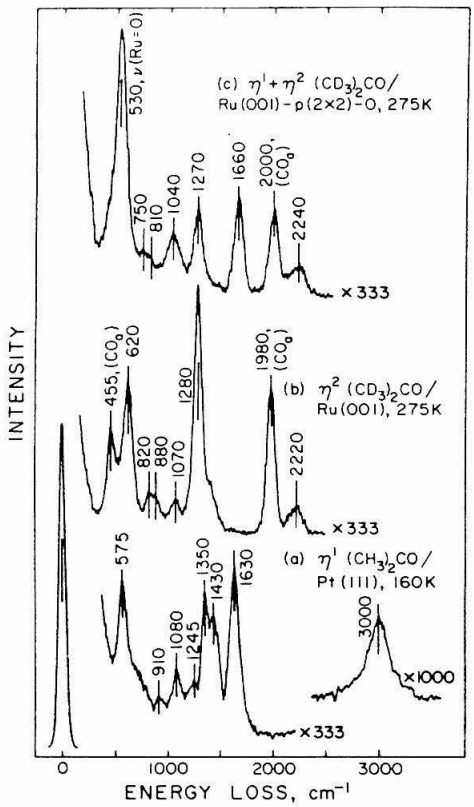

FIG. 1. EEL spectra for (a) a monolayer of $(CH_3)_2CO$ on the Pt(111) surface; (b) a monolayer of $(CD_3)_2CO$ on the Ru(001) surface; and (c) a monolayer of $(CD_3)_2CO$ on the Ru(001) surface with an ordered $p(2\times2)$ overlayer of oxygen adatoms present. Features at 455 and 1980–2000 cm^{-1} in spectra (b) and (c) are due to adsorbed CO from the onset of decompsotion of the η^2 acetone. All spectra were recorded in the specular direction where dipolar scattering dominates the inelastic electron scattering cross section (Ref. 16).

tone is 185 K, suggesting a binding energy of approximately 11.5 kcal/mol.

It has been recognized for a number of years that acetone can bond coordinately in an η^1 configuration in various organometallic complexes.[1-8] The frequencies observed for η^1 acetone on the Pt surface are in good agreement with those reported previously for homogeneous (monometallic) complexes of η^1-bonded acetone.[1,7,8]. In x-ray diffraction crystallographic structural determinations of Ru complexes of η^1-bonded acetone, the Ru–O=C bond angle ranges from 135° to 153°, and the Ru–O=C–C_2 torsional angles are within

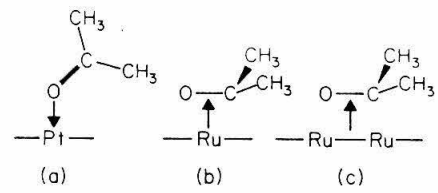

FIG. 2. Schematic bonding configurations for (a) η^1 acetone on Pt(111) and Ru(001) on which a $p(2\times2)$ oxygen adatom superstructure exists; (b), (c) η^2 acetone on Ru(001).

7° of planarity.[7,8] The frequency of the carbonyl stretching mode shifts from 1710 cm^{-1} in liquid acetone to approximately 1630 cm^{-1} on the Pt surface and is down shifted similarly in the organometallic complexes of Ru.[7,8] Consequently, especially since the acetone is adsorbed with C_s symmetry, quite similar bonding occurs in η^1-bonded acetone complexes and on the extended, close-packed surface of Pt.

At 275 K on the Ru(001) surface, a temperature at which all the acetone has desorbed reversibly from Pt, the acetone is bonded in an η^2 (side on) configuration as indicated schematically in Figs. 2(b) and 2(c).[27] This form of adsorbed acetone is identified by a substantially down-shifted carbonyl stretching mode at 1280 cm^{-1}, isopropyl-like rocking modes at 990 and 1170 cm^{-1}, and a skeletal mode at 670 cm^{-1} [at 1280, 820, and 880, and 620 cm^{-1} for $(CD_3)_2CO$, respectively; see Table I and Fig. 1(b)]. The feature at 670 cm^{-1} is due to the π(CO) mode of acetone which is transformed from B_2 to A' symmetry as the symmetry of the acetone skeleton is lowered from C_{2v} to C_s (a mirror plane through the C=O bond, perpendicular to the surface) with the rehybridization of the ketonic carbon atom from sp^2 to nearly sp^3 upon adsorption. This η^2 form of acetone on Ru is a stable intermediate in the decomposition of the acetone. The rapid decomposition of η^2 acetone to adsorbed CO, CH_x fragments ($x \leq 3$), and hydrogen adatoms occurs at temperatures slightly above 275 K.

A number of side-on bonded ketonic and related homogeneous complexes which resemble the η^2-bonded acetone on the Ru(001) surface have been reported.[9-15] In particular, the analogy with two zero-valent complexes of nickel are noteworthy, namely, (hexafluoroacetone)*bis*(triphenylphosphine) nickel(0),[9] and (benzophenone)*bis*(triethylphosphine) nickel(0).[13] An extension of the carbonyl bond length by approximately 0.1 Å in both

TABLE I. Vibrational frequencies (in inverse centimeters) observed with high-resolution electron-energy-loss spectroscopy of η^1 acetone on Pt(111), η^2 acetone on Ru(001), and a mixture of η^1 and η^2 acetone on Ru(001)$p(2\times2)$-O. [Corresponding frequencies for deuterated acetone, $(CD_3)_2CO$, are given in brackets. The mode assignments, their symmetry types, and the ir and Raman frequencies of liquid acetone are listed as well.]

Mode	Symmetry C_{2v}	Symmetry C_s	ir and Raman of liquid[a]	EELS on Pt(111) η^1	EELS on Ru(001) η^2	EELS on Ru(001)$p(2\times2)$-O η^1	EELS on Ru(001)$p(2\times2)$-O η^2
			3004[2255] (*s*)				
$\nu(CH_3)$			2964[2222] (*s*)	3000[2250]	2970[2220]	2970[2240]	2970[2240]
			2924[2111] (*s*)				
ν_s (CO)	A_1	A'	1710[1701] (*vs*)	1630[1630]	1280[1280]	1660[1660]	1280[1270]
			1430[1085] (*s*)	1430		1420[1040]	
$\delta(CH_3)$			1361[1037] (*vs*)	1350[1030]	1370[1070]		1370[1040]
			1356[1036] (*w*)				
ν_a (Me-C-Me)	B_1	A''	1220[1245] (*vs*)	1245[1290]			
			1092 (*m*)		1170[880]	1090	
$\omega(CH_3)$			1066[890] (*m*)	1080	990[820]		960[810]
			902 (*m*)	910		890[750]	
ν_s (Me-C-Me)	A_1	A'	786[695] (*w*)				
δ(CO)	B_1	A''	530[478] (*s*)	575[530]		[b]	
π(CO)	B_2	A'	393[331] (*w*)[c]		670[620]		[b]
δ(Me-C-Me)	A_1	A'	493[410] (*w*)[c]				

[a] Ref. 25.

[b] Obscured by the very strong ν_s (Ru=O) mode at 530 cm^{-1}.

[c] The original assignments of these modes (Ref. 25) have been reversed by Raman polarization measurements (Ref. 26).

complexes is strong evidence of π bonding to the nickel (i.e., π donation and π^* back-donation). If the bonding is thought of in terms of the Dewar-Chatt-Duncanson model,[28,29] then in view of the importance of back-bonding, side-on (π-bonded) ligands are stabilized by electronegative substituents on the ligand which serve to lower the energy of the π^* orbital. There is a concomitant need for "electron rich" metals, i.e., those in low formal oxidation states, to facilitate this type of bonding. This is the reason why only rather recently has η^2-bonded acetone been observed in a low-valent homogeneous Ta complex[15] compared to the earlier observation of an η^2-bonded hexafluoroacetone complex with Ni.[9] This is also the reason why the more "electron rich" Ru surface binds acetone in an η^2 configuration, whereas a geometrically identical surface of Pt does not. The degree of rehybridization of the ketonic carbon atom is similar in the $Ta(\eta^5\text{-}C_5Me_5)(\eta^2\text{-acetone})Me_2$ complex (Me = CH_3)[15] compared to η^2 acetone on the Ru surface as judged by the carbonyl stretching frequencies, 1200 cm^{-1} in the former and 1280 cm^{-1} in the latter.

If the Lewis acidity of the Ru surface is increased by the adsorption of an ordered $p(2\times2)$ overlayer of oxygen adatoms (corresponding to a quarter-monolayer surface coverage), the behavior of the (subsequently) chemisorbed acetone is *qualitatively different* from that of acetone on reduced Ru, as is evident from the EEL spectrum in Fig. 1(c). In the presence of the oxygen overlayer, a significant fraction of the adsorbed acetone exists as an η^1 ligand which desorbs *molecularly* near 300 K. This is a consequence of a through-metal depletion of the electron density on the surface Ru atoms due to the presence of the electronegative oxygen adatoms. On this modified Ru surface of greater Lewis acidity, the acetone adsorbs as a donor ligand with a binding energy considerably greater than on the reduced Pt surface. Consequently, the modified surface of Ru behaves similarly, but not identically, to the Pt surface. This fact is also apparent from the coexistence of η^1 and η^2 acetone on the Ru(001)$p(2\times2)$-O surface [cf. Table I and Fig. 1(c)], whereas the η^2 form of acetone does not exist on reduced Pt.

To summarize, high-resolution EELS measurements have verified the existence of two fundamentally different types of adsorbed acetone, η^1-bonded acetone on Pt(111) and η^2-bonded acetone on Ru(001). On a Ru(001) surface, the Lewis acidity of which has been increased by the pres-

ence of oxygen adatoms, the η^1 and η^2 forms of acetone coexist. The η^1-bonded acetone desorbs molecularly, whereas η^2-bonded acetone is a precursor to dissociation to chemisorbed CO, CH_x fragments, and hydrogen. These results systematize the nature of the bonding of (ketonic) organometallic ligands to metal clusters and to metal surfaces, i.e., they provide a quantification of the so-called "metal-cluster, metal-surface analogy." More detailed descriptions and discussions of the results reported here are in preparation.[30,31]

This research was supported by the National Science Foundation under Grant No. CHE82-06487.

---

[a]Permanent address: Division of Materials Science, CSIRO, Catalysis and Surface Science Laboratory, University of Melbourne, Parkville 3052 Victoria, Australia.

[1]W. L. Driessen and W. L. Groeneveld, Recl. Trav. Chim. Pays-Bas 88, 977–988 (1969).

[2]W. L. Driessen and W. L. Groeneveld, Recl. Trav. Chim. Pays-Bas 90, 258–264 (1971).

[3]K. Jackowski and Z. Kecki, J. Inorg. Nucl. Chem. 39, 1073–1078 (1977).

[4]C. White, S. J. Thompson, and P. M. Maitlis, J. Chem. Soc. Dalton Trans. 1977, 1654–1661.

[5]C. White, S. J. Thompson, and P. M. Maitlis, J. Organomet. Chem. 134, 319–325 (1977).

[6]S. J. Thompson, C. White, and P. M. Maitlis, J. Organomet. Chem. 136, 87–93 (1977).

[7]R. O. Gould, W. J. Sime, and T. A. Stephenson, J. Chem. Soc. Dalton Trans. 1978, 76–79.

[8]M. A. Bennett, T. W. Matheson, G. B. Robertson, W. L. Steffen, and T. W. Turney, J. Chem. Soc. Chem. Commun. 1979, 32–33.

[9]R. Countryman and B. R. Penfold, J. Cryst. Mol. Struct. 2, 281–290 (1972).

[10]D. Walther, Z. Chem. 15, 490–491 (1975).

[11]S. D. Ittel, J. Organomet. Chem. 137, 223–228 (1977).

[12]S. D. Ittel, Inorg. Chem. 16, 2589–2597 (1977).

[13]T. T. Tsou, J. C. Huffman, and J. K. Kochi, Inorg. Chem. 18, 2311–2317 (1979).

[14]W. R. Roper, G. E. Taylor, J. M. Waters, and L. J. Wright, J. Organomet. Chem. 182, C46–C48 (1979).

[15]C. D. Wood and R. R. Schrock, J. Am. Chem. Soc. 101, 5421–5422 (1979).

[16]See, for example, H. Ibach and D. L. Mills, *Electron Energy Loss Spectroscopy and Surface Vibrations* (Academic, New York, 1982); W. H. Weinberg, in *Experimental Methods of Surface Physics*, edited by R. L. Park and M. G. Lagally (Academic, New York, 1983).

[17]In a $p(2\times 2)$ overlayer, both edges of the primitive unit cell of the adsorbate lattice are twice the magnitude of those of the primitive unit cell of the substrate, i.e., the area of the former is four times that of the latter, and the fractional surface coverage is 0.25. For a detailed discussion of surface crystallography, see M. A. Van Hove, W. H. Weinberg, and C.-M. Chan, *Low-Energy Electron Diffraction* (Elsevier, Amsterdam, 1983).

[18]T. E. Madey, H. A. Englehardt, and D. Menzel, Surf. Sci. 48, 304–328 (1975).

[19]G. E. Thomas and W. H. Weinberg, J. Chem. Phys. 69, 3611–3613 (1978).

[20]T. S. Rahman, A. B. Anton, N. R. Avery, and W. H. Weinberg, to be published.

[21]P. C. Stair, J. Am. Chem. Soc. 104, 4044 (1982).

[22]G. E. Thomas and W. H. Weinberg, Rev. Sci. Instrum. 50, 497–501 (1979).

[23]N. R. Avery, Appl. Surf. Sci. 13, 171–179 (1982).

[24]G. E. Thomas and W. H. Weinberg, J. Chem. Phys. 70, 954–961 (1979).

[25]G. Dellepiane and J. Overend, Spectrochim. Acta 22, 593–614 (1966).

[26]J. R. Allkins and E. R. Lippincott, Spectrochim. Acta, Part A 25, 761–764 (1968).

[27]Whether the acetone is bound to a single ruthenium atom as in Fig. 1(b) or is bridging two (or three) ruthenium atoms as in Fig. 1(c) cannot be determined from the high-resolution EELS data.

[28]M. J. S. Dewar, Bull. Soc. Chim. Fr. 18, C74–C79 (1951).

[29]J. Chatt and L. A. Duncanson, J. Chem. Soc. 1953, 2939–2947.

[30]N. R. Avery, to be published.

[31]B. H. Toby, A. B. Anton, N. R. Avery, and W. H. Weinberg, to be published.

Appendix E:

Adsorption of Acetone both on the Clean Ru(001) Surface and on the Ru(001) Surface Modified Chemically by the Presence of an Ordered Oxygen Adatom Overlayer

Reprinted from the Journal of the American Chemical Society, 1986, *108*, 684.

Adsorption of Acetone Both on the Clean Ru(001) Surface and on the Ru(001) Surface Modified Chemically by the Presence of an Ordered Oxygen Adatom Overlayer

A. B. Anton, N. R. Avery,† B. H. Toby, and W. H. Weinberg*

Contribution from the Division of Chemistry and Chemical Engineering, California Institute of Technology, Pasadena, California 91125. *Received August 23, 1985*

Abstract: The adsorption of acetone on the clean Ru(001) surface and the Ru(001) surface on which an ordered p(2 × 2) overlayer of oxygen adatoms is present has been investigated via electron energy loss vibrational spectroscopy and thermal desorption mass spectrometry. On both surfaces, two fundamentally different forms of adsorbed acetone coexist at temperatures below approximately 200 K—an η^1 species, bonded end-on through the oxygen atom, and an η^2 species, bonded side-on through both the oxygen atom and the acyl carbon atom. Both of these types of bonding have been identified previously in homogeneous organometallic complexes. On the clean Ru(001) surface, the η^2 species is dominant, with the η^1 species present only in low concentrations. Addition of the p(2 × 2)O overlayer increases the Lewis acidity of the Ru(001) surface, stabilizing η^1-acetone with respect to η^2-acetone. The η^1 species desorbs molecularly upon heating of the surface, whereas the more strongly bound η^2 species is an intermediate to dissociation. The results are compared with acetone adsorption on the Pt(111) surface and to the chemistry of analogous organometallic coordination complexes. The nature of the bonding on the two Ru(001) surfaces is interpreted in terms of the electronic structures of both the ketonic ligand and the metallic substrate.

I. Introduction

One of the principal aims of organometallic chemistry is to provide an interpretive framework in which the mechanistic details of metal-catalyzed reactions can be understood.[1] Reactions are conducted under carefully controlled conditions, and all reactants and products are thoroughly characterized with regard to their structural and chemical properties, both by spectroscopic techniques and by comparison to theoretical descriptions of the metal–ligand bonding interactions which govern their behavior. The stable coordination geometries for reactants, intermediates, and products represent local minima on the potential energy surface which describes all the possible metal–ligand interactions for the particular system investigated, and both transition-state structures and microscopic reaction mechanisms can often be inferred without ambiguity by this procedure. Our present understanding of metal-assisted chemical reactions in solution is a tribute to, and a direct result of, the success of this type of analysis.

One of the obvious goals of modern surface science research is to extend these results to the understanding of analogous reactions which occur under heterogeneous conditions, catalyzed by (extended) metal surfaces. A similar procedure must be followed, including careful control of reaction conditions and thorough characterization of the metal surface on which the reactions occur. Again, the structures of adsorbed (i.e., coordinated) intermediates can be used to delimit the transition-state structure(s) and microscopic mechanism(s) which describe the surface reaction(s) observed. Within this context, it is clear that heterogeneous catalysis is in fact the organometallic chemistry of extended metal surfaces, and as one might expect, results obtained for metal–ligand interactions in homogeneous systems prove to be very valuable in the interpretation of results obtained on metal surfaces.

The success of this approach for both homogeneous and heterogeneous systems relies on the ability to determine experimentally the structures of coordinated reaction intermediates. In homogeneous studies, stable products can often be separated, purified, and crystallized, allowing detailed deduction of chemical bond lengths and bond angles via X-ray crystallography.[2] The surface-sensitive analogue, low-energy electron diffraction (LEED),[3] can be applied most easily to systems where a single reaction intermediate is formed in a translationally periodic, two-dimensional lattice on a single-crystalline metal surface.[4] Even on single-crystalline metal surfaces, more than one intermediate is frequently formed with no long-range order to facilitate a LEED analysis. Thus, other approaches must be taken to identify surface structures. Of the various spectroscopic techniques available presently for the identification of reaction intermediates on surfaces, both the sensitivity and the wide spectral range of high-resolution electron energy loss vibrational spectroscopy (EELS) make it arguably the most powerful tool for chemical analysis of adsorbed species on well-characterized surfaces of low area.[5] Although the structural information provided by vibrational spectroscopy does not directly measure bond lengths and bond angles, it does identify both the nature of the bond and the bond order, and through application of the selection rules appropriate to EELS on metal surfaces,[6] the chemical identity and orientation of adsorbed species can be determined. With this type of information at hand, a rigorous comparison of the chemistry of extended metal surfaces to that of corresponding organometallic complexes can be made.

This paper reports results obtained via EELS and thermal desorption mass spectrometry for the interaction of acetone with the clean Ru(001) surface and the Ru(001) surface on which there is an ordered p(2 × 2) overlayer of oxygen adatoms.[7] The results help to quantify the relationship between the Lewis acidity of a metal surface and its selectivity toward both reactive and nonreactive bonding configurations of adsorbed acetone, providing an enlightening comparison of the chemistry of these surfaces to the chemistry of analogous organometallic complexes.[8]

The interaction of acetone and similar substituted ketones, R_1R_2CO, with metal centers in homogeneous systems has been

† Current address: Division of Materials Science, C.S.I.R.O., Catalysis and Surface Science Laboratory, University of Melbourne, Parkville 3052, Victoria, Australia.

(1) See, for example: Collman, J. P.; Hegedus, L. S. "Principles and Applications of Organotransition Metal Chemistry"; University Science: Mill Valley, 1980.
(2) Wells, A. F. "Structural Inorganic Chemistry", 4th ed., Clarendon Press: Oxford, 1975.
(3) Pendry, J. P. "Low Energy Electron Diffraction"; Academic Press: London, 1974.
(4) One notable example is the successful determination via LEED of the structure of the ethylidyne species which ethylene and acetylene form upon reaction with the Pt(111) surface. See: Kesmodel, L. L.; Dubois, L. H.; Somorjai, G. A. *J. Chem. Phys.* **1979**, *70*, 2180. Steininger, H.; Ibach, H.; Lehwald, S. *Surface Sci.* **1982**, *117*, 685.
(5) Ibach, H.; Mills, D. L. "Electron Energy Loss Spectroscopy and Surface Vibrations"; Academic Press: New York, 1982; Chapter 6.
(6) Reference 5, Chapter 3.
(7) Rahman, T. S.; Anton, A. B.; Avery, N. R.; Weinberg, W. H. *Phys. Rev. Lett.* **1983**, *51*, 1979.
(8) Avery, N. R.; Weinberg, W. H.; Anton, A. B.; Toby, B. H. *Phys. Rev. Lett.* **1983**, *51*, 682.

0002-7863/86/1508-0684$01.50/0

the subject of a number of investigations. Two general classes of bonding configurations have been identified, characterized structurally, and correlated with the electronic properties of both of the (R_1 and R_2) substituents of the ketonic ligands and the metal centers to which they bond. Electron-deficient metals (those in high formal oxidation states, for example) and weakly electronegative substituents (such as the CH_3 groups of acetone) generally facilitate bonding via σ donation from the ligand to the metal to produce an η^1(O) configuration (bonded end-on to the metal through the oxygen atom and hereafter referred to as η^1).[9-12] In this case, the metal serves as a weak Lewis acid and accepts an electron pair from the ketonic ligand. For metals weakly basic in the Lewis sense, i.e., those in a low formal oxidation state, or for ketonic ligands with more electronegative substituents (R_1 and R_2 = H, CF_3, and Ph), an η^2(O,C) configuration (bonded side-on to the metal through both the carbon and oxygen atoms and hereafter referred to as η^2) occurs.[13-20] This type of interaction, first described by Dewar and by Chatt and Duncanson,[21] results from simultaneous donation of electrons from the π orbital of the ligand to the d orbitals of the metal and backdonation of metal d electrons to the π^*-antibonding orbital of the ligand. This is a general feature of the interaction of many unsaturated ligands with metals.[22-24] The understanding of conditions prevailing at metal surfaces which yield selectively these two types of coordination interactions is an important and worthwhile pursuit. For example, η^1-carbonyl ligands are quite labile and nonreactive, exchanging easily in solution with other more tightly bound ligands,[10] whereas η^2 bonding is postulated to be important in the formation of reactive intermediates in heterogeneously catalyzed reactions such as the Fischer–Tropsch synthesis.[25]

Although several investigations of acetone adsorption on metal surfaces have appeared in the literature,[26,27] only one report has presented an unequivocal determination of the binding configurations of acetone on a single-crystalline metal surface.[27] In this case of acetone adsorption on the clean Pt(111) surface, EELS and thermal desorption mass spectrometry were used to identify an η^1 species which desorbed reversibly and a small concentration of an η^2 species, some of which decomposed upon heating the crystal. These results provide a particularly useful contrast and comparison to the results reported here for the adsorption of acetone on the Ru(001) and Ru(001)-p(2 × 2)O surfaces.

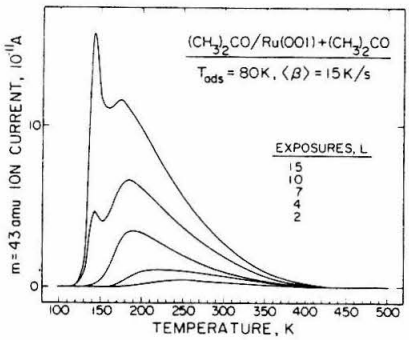

Figure 1. Thermal desorption spectra for increasing exposures of $(CH_3)_2CO$ on the clean Ru(001) surface at 80 K. The most abundant cracking fragment of $(CH_3)_2CO$, m = 43 amu, was monitored, and the average heating rate ⟨β⟩ was 15 K/s.

II. Experimental Procedures

A description of the EEL spectrometer and the ultrahigh vacuum (UHV) system in which it is contained has been published previously.[28] EEL spectra were recorded at a resolution of approximately 80 cm^{-1} (full-width at half-maximum) with a maximum count rate of 10^5 Hz in the specularly reflected, elastically scattered electron beam. Beam kinetic energies at the sample were between approximately 5 and 6 eV.

The Ru(001) surface was cleaned by thermal cycling between 400 and 1100 K in 10^{-7} torr of oxygen to remove surface impurities, followed by reductive annealing in vacuum at 1750 K.[29] Occasional Ar^+ sputtering was also used to clean the surface. Surface cleanliness was monitored via EELS and thermal desorption mass spectrometry, the surface was judged clean when the EEL spectrum was featureless, and the peak positions and intensities in thermal desorption spectra for various coverages of CO were reproduced. The ordered p(2 × 2) overlayer of oxygen adatoms, with an ideal surface coverage of 0.25 monolayer, was prepared by exposing the clean surface to 0.8 L of oxygen (1 L = 10^{-6} torr-s) at 95 K, followed by thermal ordering at a temperature of approximately 350 K.[7,30]

The $(CH_3)_2CO$ and $(CD_3)_2CO$ used in the experiments were degassed with multiple freeze–pump–thaw cycles, and their purities were verified in situ via mass spectrometry. The isotopically labeled compounds, $^{18}O_2$ and $(CD_3)_2CO$, were >99% purity in their specified isotopes. The crystal was exposed to all gases by backfilling the UHV chamber through leak valves, and exposures quoted in the text were measured with a Bayard-Alpert ionization gauge uncorrected for relative ionization cross sections.

Thermal desorption measurements were made in a line-of-sight mode with a UTI 100C quadrupole mass spectrometer, oriented approximately 40° from the surface normal. Surface coverages of hydrogen and CO reported for the (reaction product) thermal desorption measurements were obtained by comparing the time-integrated ion current for the desorption spectra to those obtained for desorption of known coverages of hydrogen[31] and CO.[32] The accuracy in this comparison is approximately ±10%.

Since the adsorbed overlayers were prepared by backfilling the UHV chamber, exposing uniformly all cold surfaces in the chamber to the particular adsorbate, and since the mass spectrometer had no provision for selective sampling of the single-crystalline surface, the features in the thermal desorption spectra associated with desorption from the crystal surface were superposed on a broad background signal due to desorption from all other chilled surfaces which are warmed during the collection of a thermal desorption trace. This is a particularly important consideration for a species such as acetone which condenses in UHV at liquid nitrogen temperatures. In the apparatus used for the experiments reported here, the Ru(001) sample was supported by two 0.020 in. diameter tantalum wires which were spot-welded to its rear face and clamped by two 0.109 in. diameter copper wires to form an electrical current path through the sample. The copper wires were in contact with a liquid nitrogen reservoir to provide conductive cooling of the sample, and

(9) Driessen, W. L.; Groeneveld, L. *Recl. Trav. Chim. Phys-Bas* **1969**, *88*, 977.
(10) Thompson, S. J.; White, C.; Maitlis, P. M. *J. Organomet. Chem.* **1977**, *136*, 87.
(11) Gould, R. O.; Sime, W. J.; Stephenson, T. A. *J. Chem. Soc. Dalton Trans.* **1978**, 76.
(12) Bennett, M. A.; Matheson, T. W.; Robertson, G. B.; Steffen, W. L.; Turney, T. W. *J. Chem. Soc., Chem. Commun.* **1979**, 32.
(13) Brown, K. L.; Clark, G. R.; Headford, C. E. L.; Marsden, K.; Roper, W. R. *J. Am. Chem. Soc.* **1979**, *101*, 503.
(14) Berke, H.; Bankhardt, W.; Huttner, G.; Seyerl, J. V.; Zsolnai, L. *Chem. Ber.* **1981**, *114*, 2754.
(15) Clarke, B.; Green, M.; Osborn, R. B. L.; Stone, F. G. A. *J. Chem. Soc. A* **1968**, 167.
(16) Browning, J.; Cundy, C. S.; Green, M.; Stone, F. G. A. *J. Chem. Soc. A* **1969**, 20.
(17) Countryman, R.; Penfold, B. R. *J. Cryst. Mol. Struct.* **1972**, *2*, 281.
(18) Wood, C. D.; Schrock, R. R. *J. Am. Chem. Soc.* **1979**, *101*, 5421.
(19) Green, M.; Howard, J. A. K.; Laguna, A.; Smart, L. E.; Spencer, J. L.; Stone, F. G. A. *J. Chem. Soc. Dalton Trans.* **1977**, 278.
(20) Adams, H.; Bailey, N. A.; Gauntlett, J. T.; Winter, M. J. *J. Chem. Soc., Chem. Commun.* **1984**, 1360.
(21) Dewar, M. J. S. *Bull. Soc. Chim. Fr.* **1951**, *18*, C79. Chatt, J.; Duncanson, L. A. *J. Chem. Soc.* **1953**, 2939.
(22) Greaves, E. O.; Lock, C. J. L.; Maitlis, P. M. *Can. J. Chem.* **1968**, *46*, 3879.
(23) Chisholm, M. H.; Clark, H. C. *Acc. Chem. Res.* **1973**, *6*, 202.
(24) Ittel, S. D. *Inorg. Chem.* **1977**, *16*, 2589.
(25) Henrici-Olivé, G.; Olivé, S. *Angew. Chem., Int. Ed. Engl.* **1976**, *15*, 136 and references therein.
(26) Blyholder, G.; Neff, L. D. *J. Phys. Chem.* **1966**, *70*, 893. Young, R. P.; Sheppard, N. *J. Catal.* **1967**, *7*, 223. Blyholder, G.; Shihabi, D. *J. Catal.* **1977**, *46*, 91. Lüth, H.; Rubloff, G. W.; Grobman, W. D. *Surface Sci.* **1977**, *63*, 325.
(27) Avery, N. R. *Surface Sci.* **1983**, *125*, 771.
(28) Thomas, G. E.; Weinberg, W. H. *Rev. Sci. Instrum.* **1979**, *50*, 497.
(29) Thomas, G. E.; Weinberg, W. H. *J. Chem. Phys.* **1979**, *70*, 954.
(30) Madey, T. E.; Engelhardt, H. A.; Menzel, D. *Surface Sci.* **1975**, *48*, 304.
(31) Shimizu, H.; Christmann, K.; Ertl, G. *J. Catal.* **1980**, *61*, 412.
(32) Williams, E. D.; Weinberg, W. H. *Surface Sci.* **1979**, *82*, 93.

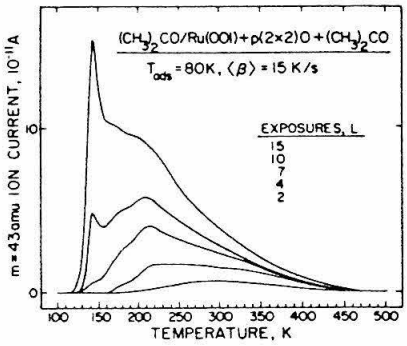

Figure 2. Thermal desorption spectra recorded under conditions identical with those of Figure 1 except for adsorption on the Ru(001)–p(2 × 2)O surface.

heating was accomplished by conduction of the heat generated almost totally by the tantalum wires to the sample as an electric current was passed through the sample via the copper and tantalum support leads. The heavy copper leads were also warmed by conduction of heat from the tantalum support wires, but their temperature lagged well behind that of the Ru(001) sample. The net result of these effects, then, for a thermal desorption spectrum of the mass spectrometer signal intensity vs. sample temperature for acetone desorption was to yield first a small, narrow signal burst at the beginning of the temperature ramp due to desorption from the rapidly heated tantalum leads and then features at their characteristic temperatures for desorption from the Ru(001) surface, superposed on a broad, slowly varying background due to desorption of condensed acetone from the slowly warming copper leads. For rather sharp desorption features, as were observed in the thermal desorption spectra for the H_2 and CO decomposition products, the background base lines in the spectra can be identified unambiguously, and the contribution due to desorption from the Ru(001) surface can be separated clearly. For broad features, however, as were observed for the desorption of molecular acetone from both the clean Ru(001) and the Ru(001)–p(2 × 2)O surfaces, the base lines were less certain. In all thermal desorption spectra presented below, the sharp burst at low temperatures and best estimates of the base lines due to background desorption have been subtracted for a more useful illustration of the experimental results. For the molecular acetone desorption spectra of Figures 1 and 2, however, the uncertainty in the amplitudes of the broad feature which extends from approximately 200–450 K prevents a quantitative determination of the total amounts of acetone desorption in the spectra. The qualitative differences in the spectra, to be discussed later, namely the increased amount of molecular desorption from the Ru(001)–p(2 × 2)O surface for a given acetone exposure as compared to the clean surface, are reliable and are the most noteworthy results evident in Figures 1 and 2.

III. Results

A. Thermal Desorption Spectra of Acetone from the Clean Ru(001) and the Ru(001)–p(2 × 2)O Surfaces. Thermal desorption spectra recorded after the indicated exposures of the clean Ru(001) surface to $(CH_3)_2CO$ at 80 K are shown in Figure 1. For exposures below 4 L, almost no molecular acetone desorption is observed. For exposures of 4 L and above, however, a broad feature with a desorption rate maximum near 220 K, shifting with increasing exposure to 180 K for a monolayer saturation exposure, is observed. A peak due to the formation of a condensed multilayer appears at 140–150 K for exposures greater than 7 L. This multilayer state first appears at exposures below that necessary to saturate the monolayer state, suggesting that some "clustering" may occur, as has been observed in the thermal desorption spectra of H_2O from the Ru(001) surface.[33] No evidence for a "second layer" desorption state, like that observed for acetone adsorption on Pt(111),[27] can be extracted unambiguously from the thermal desorption spectra of Figure 1, although some evidence for such a state is observed in the EELS results to be presented below.

Noteworthy is the "tailing" of the monolayer desorption feature from its desorption rate maximum near 200 K to approximately

(33) Thiel, P. A.; Hoffmann, F. M.; Weinberg, W. H. *J. Chem. Phys.* **1981**, *75*, 5556.

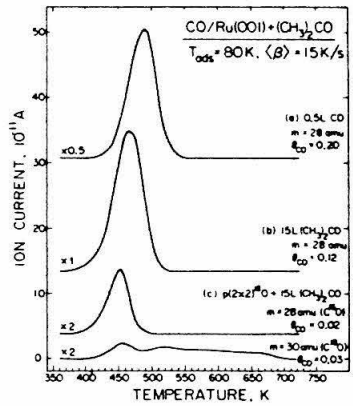

Figure 3. Thermal desorption spectra for the CO decomposition product from 15-L exposures of the clean Ru(001) and the Ru(001)–p(2 × 2)^{18}O surfaces to $(CH_3)_2CO$. The top spectrum shows CO desorption following exposure of the clean surface to 0.5 L of CO for comparison.

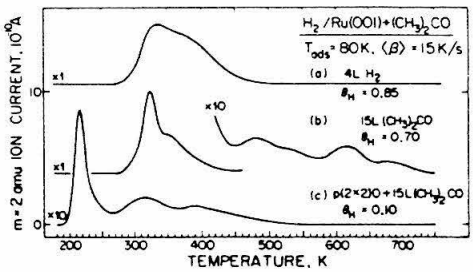

Figure 4. Thermal desorption spectra for the H_2 decomposition products from 15-L exposures of the clean Ru(001) and the Ru(001)–p(2 × 2)O surfaces to $(CH_3)_2CO$. The top spectrum shows H_2 desorption following exposure of the clean surface to 4 L of H_2 for comparison.

400 K. This indicates a broad range of binding energies for the monolayer molecular species, due perhaps to repulsive interactions which lower its binding energy at high coverages and are relieved as desorption progresses, or to attractive interactions of acetone with surface species present at higher temperatures (and lower surface coverages).

A series of thermal desorption spectra for exposures equal to those of Figure 1, but instead on the Ru(001)–p(2 × 2)O surface, are shown in Figure 2. Although qualitatively similar, several quantitative differences are apparent: more molecular acetone is evolved in the temperature range between 200 and 450 K for all exposures; two rate maxima for monolayer desorption, near 180 and 200 K, are observed; and the multilayer feature is clearly evident for lower exposures, appearing first at 7 L.

B. Thermal Desorption Spectra of the Decomposition Products, CO and H_2, from the Clean Ru(001) and the Ru(001)–p(2 × 2)O Surfaces. Hydrogen and CO are the only products of the decomposition of $(CH_3)_2CO$ on the clean and the Ru(001)–p(2 × 2)O surfaces, as detected by thermal desorption spectra. The desorption spectra recorded for these products are shown in Figures 3 and 4 following multilayer exposures (15 L) of both surfaces to $(CH_3)_2CO$ at 80 K. For comparison, spectrum a of Figure 3 shows desorption of CO from the clean Ru(001) surface following exposure to 0.5 L of CO (θ_{CO} adsorbed CO molecules per ruthenium surface atom = 0.20), and spectrum a of Figure 4 shows desorption of H_2 from the clean Ru(001) surface following exposure to 4 L of H_2 ($\theta_H = 0.85$). For spectra c of both Figures 3 and 4, p(2 × 2)O overlayers were produced via adsorption of $^{18}O_2$ to allow separate detection of the CO produced by the decomposition of adsorbed $(CH_3)_2CO$, appearing at $m = 28$ amu, and that produced by reaction of adsorbed carbon from CH_3 decomposition, with the ^{18}O of the p(2 × 2)O overlayer appearing

at $m = 30$ amu. Furthermore, this increases the sensitivity of the thermal desorption measurement to H_2O ($m = 20$ amu), which might be expected to be a product of the reaction of $(CH_3)_2CO$ with the Ru(001)–p(2 × 2)O surface. However, no $H_2{}^{18}O$ was detected under any circumstances.

The CO evolution from a saturated monolayer of $(CH_3)_2CO$ on the clean Ru(001) surface, shown in Figure 3b, yields $\theta_{CO} = 0.12$, and since no CO_2, H_2O, or other oxygen-containing desorption products were observed, this demonstrates that the clean surface is active for the decomposition of approximately one-eighth of a monolayer of adsorbed acetone. This is to be compared with the $m = 28$ amu spectrum below it for the same exposure on the Ru(001)–p(2 × 2)O surface, Figure 3c, where $\theta_{CO} = 0.02$. Obviously, the presence of the ordered oxygen overlayer decreases the decomposition activity of the Ru(001) surface by a factor of approximately 6.

Proper stoichiometry in the overall surface decomposition reaction,

$$(CH_3)_2CO + 2{}^{18}O \rightarrow CO + 3H_2 + 2C{}^{18}O$$

would suggest that $\theta_{C^{18}O}$ for the $m = 30$ amu desorption spectrum of Figure 3d should be equal to 0.04 rather than 0.03. This discrepancy may be a result of an inaccurate base-line determination in the spectra, or more likely is due to slight ($\theta_{CO} = 0.05$) adsorption of background CO ($m = 28$ amu) from the chamber ambient during exposure to $(CH_3)_2CO$, making θ_{CO} for the associated $m = 28$ amu spectrum (Figure 3c) larger than the value of 0.015 necessary by stoichiometry to match the $\theta_{C^{18}O} = 0.03$ of the $m = 30$ amu spectrum.

The $m = 30$ amu desorption spectrum of Figure 3d identifies the temperature range over which adsorbed carbon and oxygen react to form and evolve CO, i.e., between approximately 400 and 700 K. The absence of CO desorption in this temperature range for the $m = 28$ amu spectra confirms that no carbon–oxygen bond cleavage occurs in the decomposition of adsorbed acetone.

The $m = 28$ amu desorption spectra of Figure 3b and c for the clean Ru(001) and the Ru(001)–p(2 × 2)O surfaces have the temperatures corresponding to their maximum desorption rates downshifted from 490 K, shown in the clean surface CO desorption spectrum of Figure 3a, to 470 and 455 K, respectively. This can be attributed to interactions between the adsorbed CO molecules and adsorbed hydrocarbon fragments[34] and the oxygen adatoms of the p(2 × 2)O overlayer.[35]

Comparison of the thermal desorption spectrum b of Figure 4, which shows H_2 evolution from a saturated monolayer of $(CH_3)_2CO$ on the clean Ru(001) surface, to that of Figure 4c for the same exposure on the Ru(001)–p(2 × 2)O surface shows an approximate sevenfold decrease in the amount of acetone decomposition upon the addition of the oxygen overlayer to the Ru(001) surface, a value that is consistent, within experimental uncertainties, with the results shown previously in Figure 3. Furthermore, the hydrogen coverages, obtained by comparison to the spectrum of Figure 4a for desorption from a saturation exposure of the clean surface to H_2, compare well with the values expected on the basis of the corresponding observed CO coverages and the stoichiometry expected from the aforementioned surface decomposition reaction, i.e., $\theta_H = 6\theta_{CO} = 0.72$ and 0.12, respectively.

The peak shapes of the thermal desorption spectra shown in Figure 4b and c are of particular interest. Comparison to results of thermal desorption measurements for coadsorbed overlayers of CO and hydrogen on Ru(001)[36] indicates that the H_2 desorption features appearing in Figure 4b between 280 and 450 K are due solely to the recombination of hydrogen adatoms on the Ru(001) surface in the presence of coadsorbed CO. The series of weak features between approximately 450 and 750 K are due to the decomposition of adsorbed hydrocarbon fragments which result from the decomposition of adsorbed acetone. In Figure 4c, the sharp feature at 220 K is due to hydrogen adatoms recombining in the presence of adsorbed oxygen, its shape and peak temperature depending sensitively on the presence of the p(2 × 2)O overlayer.[37] Features above 250 K in this spectrum, representing slightly more than half of the total yield of hydrogen from the surface, are due to the decomposition of adsorbed hydrocarbon fragments from acetone decomposition in this temperature range.

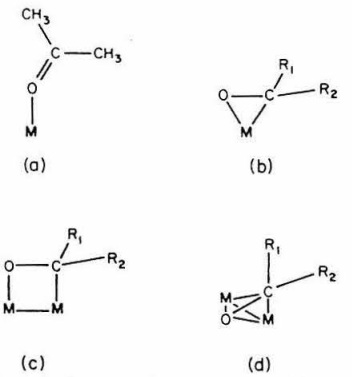

Figure 5. Schematic η^1 (a) and η^2 (b, c, and d) bonding configurations for ketonic ligands observed in homogeneous complexes.

Also noteworthy is the absence of H_2O production from the decomposition of $(CH_3)_2CO$ in the presence of the p(2 × 2)O overlayer. Although evidence for the reaction of disordered, adsorbed oxygen with hydrogen on Ru(001) to evolve H_2O has been obtained in the thermal decomposition of adsorbed HCOOH,[38] thermal desorption measurements recorded following hydrogen adsorption on the Ru(001)–p(2 × 2)O surface produce no H_2O, only desorption of H_2.[37] Thus, the relative probability of H_2O production vs. H_2 desorption depends sensitively on the long-range order of the oxygen overlayer. This can be explained by consideration of two important effects of the oxygen order on these reactions, both of which act to make hydrogen adatom recombination and desorption more likely. First, the formation of the ordered p(2 × 2)O overlayer upon the annealing of a disordered overlayer of adsorbed oxygen[7,30] indicates that attractive interactions which increase the Ru=O binding energy are maximized in the p(2 × 2) configuration, increasing the energy barrier to the abstraction of adsorbed oxygen by reaction with hydrogen. Second, the p(2 × 2)O overlayer destabilizes adsorbed hydrogen into a new binding state with an activation energy of desorption below 9 kcal/mol, desorbing near 220 K, as compared with the clean surface state, desorbing near 400 K with an activation energy of desorption of approximately 17 kcal/mol.[31]

C. EELS of Acetone on the Clean Ru(001) Surface. Exposures of the Ru(001) surface to 15 L or more of acetone at 95 K produces EEL spectra typical of the condensed species and virtually identical with the multilayer spectra reported for acetone adsorption on Pt(111).[27] The modes observed for multilayer $(CH_3)_2CO$ and their assignments based on a comparison with the IR and Raman spectra of liquid acetone[39] are listed in Table I.

The EEL spectra for the monolayer states of acetone both on the clean Ru(001) and the Ru(001)–p(2 × 2)O surfaces show evidence for species coordinated both in η^1 and η^2 configurations. Before attempting to assign the spectra, however, a review of the vibrational structure expected for both of these species will be helpful.

Consideration of the σ-bonding interaction which leads to coordination in an η^1 configuration, to be discussed later, indicates

(34) Hills, M. M.; Weinberg, W. H., unpublished results.
(35) Lee, H.-I.; Praline, G.; White, J. M. *Surface Sci.* **1980**, *91*, 581.
(36) Peebles, D. E.; Schreifels, J. A.; White, J. M. *Surface Sci.* **1982**, *116*, 117.
(37) Anton, A. B.; Weinberg, W. H., unpublished results.
(38) Avery, N. R.; Toby, B. H.; Anton, A. B.; Weinberg, W. H. *Surface Sci.* **1982**, *122*, L574. Toby, B. H.; Avery, N. R.; Anton, A. B.; Weinberg, W. H. *J. Electron Spectrosc.* **1983**, *29*, 233.
(39) Dellepiane, G.; Overend, J. *Spectrochim. Acta* **1966**, *22*, 593. Allkins, J. R.; Lippincott, E. R. *Spectrochim. Acta* **1968**, *25A*, 761.

Table I. Assignments of Vibrational Bands (in cm^{-1}) Observed with High-Resolution Electron Energy Loss Spectroscopy of $(CH_3)_2CO$ and $(CD_3)_2CO$ on Ru(001) and Ru(001)-p(2 × 2)O. Also Listed Are the Raman and IR Bands of Liquid Acetone and Their Symmetry Types for the Free Acetone Molecule

				EELS—acetone on Ru(001)				
	liquid acetone[39]			$(CH_3)CO$			$(CD_3)_2CO$	
mode	symmetry (C_{2v})	$(CH_3)_2CO$	$(CD_3)_2CO$	multilayer	η^1 (95 K)	η^2 (275 K)	η^1 (95 K)	η^2 (275 K)
ν(CO)	A_1	1711 (vs)	1701 (vs)	1720	1690	1300	1665–1675	1275
ν_a(C–C–C)	B_1	1221 (vs)	1249 (vs)	1240			1260	
ν_s(C–C–C)	A_1	787 (w)	696 (m)		780–825		715–720	
δ(CO)	B_1	530 (m)	478 (s)	535	515–540[a]		495–505[a]	
δ(C–C–C)	A_1	493 (w)	410 (w)					
π(CO)	B_2	393 (w)	331 (w)			655		610
		3006 (s)	2257 (s)				2210–2240	
$\nu(CH_3)$		2967 (s)	2222 (s)	3030	2950–2995	2955		2220
		2922 (s)	2109 (s)				2070–2090	
		1430 (s)	1088 (s)					
$\delta(CH_3)$		1361 (vs)	1037 (vs)	1380	1395–1440	1370	1030–1045	1075
		1356 (w)	1006 (w)					
		1092 (m)			1050–1110	1170		880
$\omega(CH_3)$		1066 (m)	889 (m)	905		980	920	
		902 (m)			890–905			820

[a] Not resolved from the mode at 530 cm^{-1} due to oxygen adatoms of the p(2 × 2)O overlayer.

that little perturbation of the structure of the acetone skeleton from that of the free molecule is expected in the η^1 configuration, depicted in Figure 5a. This is manifest in the vibrational spectra of η^1-acetone complexes by a preservation of the polarizations and only a weak perturbation of the frequencies of the methyl and nearly all of the skeletal vibrations of free acetone.[27] The only strongly affected mode is the ν(CO), which is red-shifted from its free acetone value of 1711 cm^{-1} to near 1650 cm^{-1} in a range of organometallic complexes of the type $\{[(CH_3)_2CO]_6M\}^{2+}$,[9] to 1661[11] and 1665 cm^{-1} [12] in two η^1-acetone complexes of ruthenium, and to 1630 cm^{-1} for η^1-$(CH_3)_2CO$ adsorbed on the Pt(111) surface.[27] The presence of a carbonyl band in this frequency range and methyl vibrations at frequencies characteristic of free acetone in the EEL spectra identify unambiguously the presence of η^1-acetone. The appearance in the spectra of other unperturbed skeletal vibrations with polarizations well-defined with respect to the symmetry properties of the acetone skeleton—ν_a(CCC), ν_s(CCC), δ(CO), δ(CCC), and π(CO)—will depend on the orientation of the adsorbed acetone skeleton with respect to the surface plane through consideration of the "dipolar selection rules" for adsorbate vibrations.[40] Such considerations can be used to determine the symmetry of the η^1-surface complex.[27]

The vibrational spectrum expected for acetone coordinated in an η^2 configuration is not so well-defined. Several η^2 configurations have been identified in the homogeneous chemistry of ketonic-like ligands with the general formula R_1R_2CO, including rigid three-membered rings with single metal centers, as in Figure 5b (e.g., $R_1 = R_2 = H$, M = Os,[13] M = Fe;[14] $R_1 = R_2 = CF_3$, M = Pt,[15] M = Ni;[16,17] and $R_1 = R_2 = CH_3$, M = Ta[18]), a rigid four-membered ring with two metal centers, as in Figure 5c ($R_1 = R_2 = CF_3$ and $M_1 = M_2 = Pt$[19]), and a perpendicular bridge (μ-η^2) configuration where the carbon–oxygen bond of the ligand bisects the bond between the two metal atoms, as in Figure 5d (e.g., $R_1 = CH_3$, $R_2 = H$, and $M_1 = M_2 = Mo$[20]). Any of these configurations must be considered a possible product of the interaction of acetone with the Ru(001) surface. Those complexes which have been characterized by vibrational spectroscopy show bands ascribed to ν(CO) in the range 1017–1220 cm^{-1},[13,14,18] signifying in all cases a substantial lowering of the carbon–oxygen bond order of the free ligand from two to nearly one upon coordination and rehybridization of the ketonic carbon from sp^2 to nearly sp^3. Those complexes characterized by an X-ray structural analysis show C–O bond lengths between 1.32 and 1.59 Å and significant deviation of the R_1–C–R_2 plane and the C–O bond from the coplanar configurations of the free ligands.[13,17,19,20] This is indicative of the rehybridization of the ketonic carbon which occurs as a result of electron donation to the π^*_{CO}-antibonding orbital of the ligand in all these configurations. Consequently, an adsorbed η^2-acetone should display a C–O vibration that is red-shifted by several hundred wavenumbers from that of the η^1 species and skeletal vibrations that are consistent with the rehybridization of the ketonic carbon to nearly sp^3.

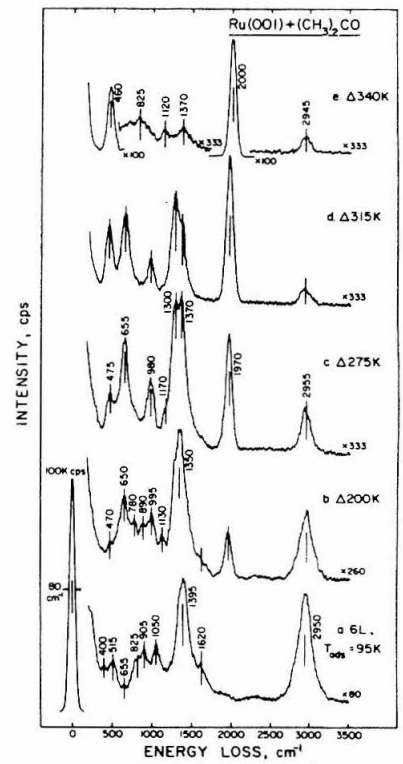

Figure 6. EEL spectra recorded after exposure of the clean Ru(001) surface to 6 L of $(CH_3)_2CO$ at 95 K. The symbol "Δ" signifies momentary heating to the indicated temperatures, followed by cooling to 95 K to record the spectra.

With this framework established, the results of the EELS experiments can now be interpreted. Figures 6 and 7 show EEL spectra recorded after exposure of the clean Ru(001) surface at 95 K to 6 L of $(CH_3)_2CO$ and 6 L of $(CD_3)_2CO$, respectively, followed by momentary annealing at the indicated temperatures and recooling to 95 K to record the spectra. Assignments of the

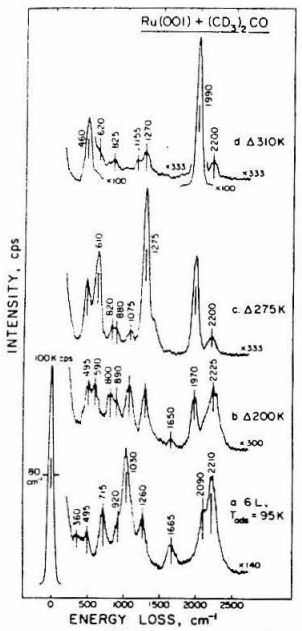

Figure 7. EEL spectra recorded after exposure of the clean Ru(001) surface to 6 L of $(CD_3)_2CO$ at 95 K, heating to the indicated temperatures, and recooling to 95 K.

surface species that are identified are listed in Table I.

Spectrum a of Figure 6, recorded immediately after adsorption at 95 K, shows strong modes at 2950, 1395, 1050, and 905 cm^{-1} due to the ν, δ, and ω modes of the CH_3 groups of adsorbed $(CH_3)_2CO$. The shoulder at 1620 cm^{-1}, its apparent position red-shifted somewhat from its true position by overlap with the tail of the strong $\delta(CH_3)$ band, signifies the existence of some $(CH_3)_2CO$ adsorbed in an η^1 configuration. The ν, δ, and ω modes of CH_3 appear with an intensity too great to be attributed solely to the η^1 species identified by $\nu(CO)$ at 1620 cm^{-1}, however, and must therefore result from the presence of another adsorbed species which coexists with η^1-$(CH_3)_2CO$ at this temperature and exposure. The appearance of clustering in the monolayer, as evidenced by the thermal desorption results discussed previously, and the identification of a "second-layer" state in the thermal desorption spectra for acetone adsorption on Pt(111)[27] suggest that the "extra" intensity in these features may be due to the onset of adsorption into the multilayer (or alternatively, a second layer) state at this exposure. A correspondingly strong feature due to the $\nu(CO)$ mode of A_1 symmetry of the multilayer species, expected at 1720 cm^{-1} (cf. Table I), is conspicuously absent, indicating via the dipolar selection rule that the molecules in this state are oriented with their molecular planes nearly parallel to the surface. This interpretation is substantiated by the presence of a weak mode at 400 cm^{-1}, which can be assigned most readily to the B_2 $\pi(CO)$ vibration of the same second or multilayer species. The mode at 515 cm^{-1} and the poorly resolved feature labeled at 825 cm^{-1} are due to the B_1 $\delta(CO)$ and A_1 $\nu_s(CCC)$ vibrations of η^1-$(CH_3)_2CO$, respectively, and the feature at 655 cm^{-1} is the first indication of the presence of an η^2 species.

Annealing the surface to 200 K produces spectrum b of Figure 6. Substantial desorption has occurred (note the change of scale between spectra a and b), but a small amount of η^1-$(CH_3)_2CO$ remains, as evidenced by the presence of $\nu(CO)$ near 1620 cm^{-1}, $\omega(CH_3)$ at 890 cm^{-1}, and $\nu_s(CCC)$ at 780 cm^{-1}. New bands associated with η^2-$(CH_3)_2CO$ appear near 995 and 1130 cm^{-1}, the feature near 650 cm^{-1} gains intensity relative to the other modes in the spectra, and the broad band associated with $\delta(CH_3)$ shifts noticeably from 1395 to 1350 cm^{-1}. Some decomposition is evidenced by bands near 470 and 2000 cm^{-1} due to ν(RuC) and $\nu(CO)$ of the adsorbed CO.[29]

Before proceeding further with the $(CH_3)_2CO$ spectra, the corresponding behavior in the $(CD_3)_2CO$ spectra of Figure 7 should be addressed. The presence of η^1-$(CD_3)_2CO$ in spectrum a at 95 K is revealed by the $\nu(CO)$ mode at 1665 cm^{-1} and the A_1 $\nu_s(CCC)$ mode at 715 cm^{-1}. Again, the methyl vibrations—$\nu(CD_3)$ at 2210 and 2090 cm^{-1}, $\delta(CD_3)$ at 1030 cm^{-1}, and $\omega(CD_3)$ near 920 cm^{-1}—appear with anomalously high intensity compared to the $\nu(CO)$ mode at 1665 cm^{-1}, suggesting the presence of a second layer species, and the B_2 $\pi(CO)$ of the latter is visible at 360 cm^{-1}. Other modes at 1260 and 495 cm^{-1} can be assigned to the B_1 $\nu_s(CCC)$ and B_1 $\delta(CO)$ modes of η^1-$(CD_3)_2CO$, respectively. Heating the surface to 200 K initiates decomposition, desorbs most of the η^1-$(CD_3)_2CO$, and reveals features due to η^2-$(CD_3)_2CO$ near 1260, 890, 800, and 590 cm^{-1}.

The EEL spectra of η^2-$(CH_3)_2CO$ and η^2-$(CD_3)_2CO$ are developed fully after annealing the surface to 275 K and are shown in Figures 6c and 7c, respectively, with assignments of these spectra listed in Table I. The band at 1300 cm^{-1} in the $(CH_3)_2CO$ spectrum, which is barely resolved from the $\delta(CH_3)$ band at 1370 cm^{-1}, and the band at 1275 cm^{-1} in the $(CD_3)_2CO$ spectrum are assigned to the $\nu(CO)$ mode of η^2-acetone, red-shifted by over 400 cm^{-1} from $\nu(CO)$ for free acetone and implying considerable skeletal reorganization in this bonding configuration. This significant rehybridization of the ketonic carbon atom from sp^2 toward sp^3, analogous to that observed in the η^2 complexes of related ligands described earlier, reduces the C–C–C bond angle of acetone toward a tetrahedral configuration, which is manifest in two other features of the η^2-acetone spectra. First, the $\omega(CH_3)$ modes typical of free and η^1-$(CH_3)_2CO$, expected near 900 and 1100 cm^{-1} (cf., Table I), are replaced by a strong band at 980 cm^{-1} and a weaker band at 1170 cm^{-1} in the spectrum of η^2-$(CH_3)_2CO$. This is a result of strong coupling between the methyl rocking modes and the C–C stretching mode of a CH_3 group bonded to an sp^3 carbon atom and is typical of isopropyl and *tert*-butyl configurations.[41] In isopropyl alcohol, for example, similar coupling leads to a strong band at 950 cm^{-1} and a weaker band at 1140 cm^{-1}.[42] As a result of this coupling, CH_3 rocking modes often do not yield good group frequencies, and the disparity between the frequencies of the coupled rocking modes in isopropyl alcohol and in η^2-$(CH_3)_2CO$ is of lesser significance than the fact that a strong band in the 900–1000 cm^{-1} region is expected for this type of structural configuration. In the spectrum of η^2-$(CD_3)_2CO$, the difference in frequency between the $\omega(CD_3)$ modes and the C–C stretching vibrations precludes strong coupling, and the $\omega(CD_3)$ modes appear with low intensity at 820 and 880 cm^{-1}, close to the values obtained for the corresponding vibrations of free $(CD_3)_2CO$. The second manifestation of the skeletal reorganization in η^2-acetone is the appearance of the band at 655 cm^{-1} for η^2-$(CH_3)_2CO$ and at 610 cm^{-1} for η^2-$(CD_3)_2CO$, which develops concomitantly with the other features ascribed to the η^2 species. This band is assigned to an O–C–C_2 angle bending vibration, which may be regarded as being derived from the weak $\pi(CO)$ mode of free acetone at 393 cm^{-1} for $(CH_3)_2CO$ and 331 cm^{-1} for $(CD_3)_2CO$, respectively. With both the oxygen and carbon atoms of the carbonyl function bonded to the ruthenium surface in the η^2 configuration, this mode corresponds to the motion of the two methyls in unison up-and-down against the surface.

Further evidence justifying the assignment of bands near 655 and 1300 cm^{-1} in the η^2-acetone spectra to the signature skeletal vibrations can be obtained by consideration of the spectra shown in Figure 8. The bottom spectrum, recorded in the specular direction where dipolar inelastic scattering is dominant, is identical with that shown in Figure 6c. The top spectrum, recorded with the EELS analyzer rotated 6° toward the surface normal from the specular direction, is expected to show enhancement of features

(40) Reference 39, Chapter 4.
(41) Coltup, N. B.; Daly, L. H.; Wiberley, S. E. "Introduction to Infrared and Raman Spectroscopy"; Academic Press: New York, 1975; Chapter 5.
(42) Reference 41, p 458.

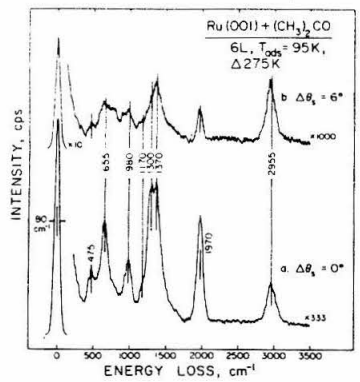

Figure 8. EEL spectra recorded in the specular direction (a) and 6° out of the specular direction (b), after exposure of the clean Ru(001) surface to 6 L of $(CH_3)_2CO$ at 95 K, heating to 275 K, and recooling to 95 K.

which include a significant contribution from (short-range) impact inelastic scattering relative to the (long-range) dipolar scattering. As has been shown previously, impact scattering is significant only for vibrational modes dominated by hydrogen or deuterium motion at the electron beam kinetic energy employed in these measurements.[6] Thus, the top spectrum of Figure 8 should show enhancement of the CH_3 modes relative to the skeletal modes. As may be seen, the ν(CO) and π(CO) modes at 1300 and 655 cm^{-1}, respectively, as well as the dipolar modes due to chemisorbed CO at 475 and 1970 cm^{-1}, have lost intensity relative to $\nu(CH_3)$ at 2955 cm^{-1}, $\delta(CH_3)$ at 1370 cm^{-1}, and $\omega(CH_3)$ at 1170 and 980 cm^{-1}, confirming the previous assignments and the correspondence indicated between the spectra for η^2-$(CH_3)_2CO$ and η^2-$(CD_3)_2CO$.

The dipolar selection rule for adsorbate vibrations indicates that only those vibrations which involve a component of motion perpendicular to the surface plane, i.e., only those modes which belong to the totally symmetric representation of the point symmetry group of the adsorbate–substrate complex, should couple to the incident EELS beam to produce inelastic scattering via the dipolar mechanism.[6] One might then ask why such a strong loss feature is observed for the ν(CO) mode of η^2-acetone, which for all possible η^2 configurations depicted in Figure 5 is polarized nearly parallel to the surface. First, the highest point group symmetry attainable by each of the possible η^2-acetone configurations is C_s, which results when a mirror symmetry plane exists through the carbon–oxygen bond perpendicular to the surface. In this case, the A_1 ν(CO) mode of free acetone (point group C_{2v}) transforms to the A' representation of the C_s adsorbate complex and is dipolar-active by symmetry considerations alone. Furthermore, the population of the π^*_{CO} orbital of η^2-acetone varies with the carbon–oxygen bond length, causing charge flow to and from the surface as the carbon–oxygen bond vibrates, producing the strong dynamic dipole which leads to the intense inelastic scattering observed for this mode. Comparable effects have been observed for similar parallel modes of C_2H_2 and C_2H_4 [ν(CC)] on Pt(111),[43] $(CH_3)CN$ [ν(CN)] on Pt(111),[44] and O_2 [ν(OO)] on Pt(111),[45] and Ag(110).[46]

No distinction between configurations such as b, c, or d of Figure 5 for η^2-acetone on Ru(001) can be made on the basis of the EELS results. Each would be expected to give methyl and skeletal vibrations similar to those observed and would differ only in the low-frequency vibrations which represent motion of the bonds which coordinate the acetone molecule to the ruthenium surface atoms. These modes are not resolved in the EEL spectra, and no vibrational data in this frequency range for model complexes are available to allow a useful diagnostic comparison. The details of the η^2-coordination geometry are, of course, far less significant than the fact that η^2 coordination occurs.

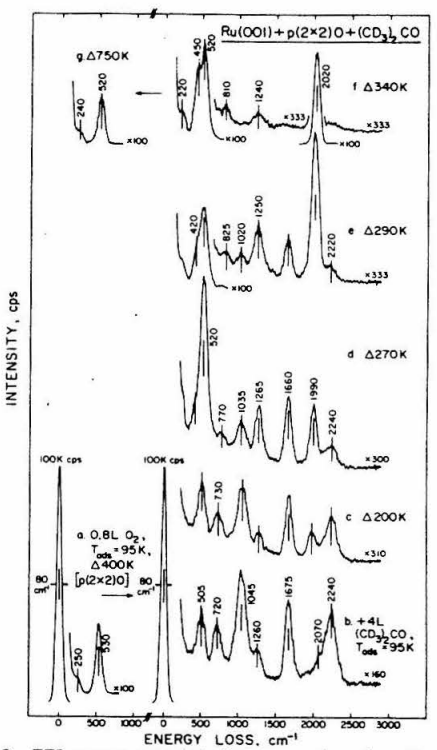

Figure 9. EEL spectra recorded after preparation of a p(2 × 2)O overlayer on the Ru(001) surface (a), followed by exposure to 4 L of $(CD_3)_2CO$ at 95 K, heating to the indicated temperatures, and recooling to 95 K.

Further heating of the Ru(001) surface to 310–315 K results in an attenuation of the features due to η^2-acetone and an increase in the intensities of the features due to adsorbed CO, resulting from decomposition of η^2-acetone (cf. Figure 6d and 7d). Finally, after heating to 340 K, the EEL spectrum of the decomposition products of η^2-$(CH_3)_2CO$, shown in Figure 6e, displays broad, weak bands at 825, 1120, 1370, and 2945 cm^{-1} due to CH_x ($x \leq 3$) hydrocarbon fragments.

D. EELS of Acetone on the Ru(001)–p(2 × 2)O Surface. Exposure of the clean Ru(001) surface to 0.8 L of O_2 at 95 K, followed by annealing to 400 K, produces the EEL spectrum of the p(2 × 2)O overlayer shown in Figure 9a. In addition to the feature at 530 cm^{-1} due to motion of the oxygen adatoms in threefold sites perpendicular to the surface, a mode appears at 250 cm^{-1} which results from coupling of the overlayer to a ruthenium surface phonon.[7] Addition of the p(2 × 2)O overlayer, with an ideal fractional surface coverage of 0.25, changes the work function of the Ru(001) surface by +0.20 eV.[30] When a Ru=O bond length of 2.05 Å[7] is employed and depolarization effects are ignored, this change in work function can be shown[47] to be equivalent to the transfer of 0.02 electron from the ruthenium surface to each oxygen adatom of the p(2 × 2)O overlayer, producing a quantifiable increase in the Lewis acidity of the surface ruthenium atoms.

The effects of the addition of the p(2 × 2)O overlayer on the properties of the acetone adsorbed on the Ru(001) surface are demonstrated dramatically in the EEL spectra of Figures 9 and 10, recorded after exposure of the Ru(001)–p(2 × 2)O surface to 4 L of $(CD_3)_2CO$ and 6 L of $(CH_3)_2CO$ at 95 K, respectively,

(43) Ibach, H.; Hopster, H.; Sexton, B. *Appl. Surface Sci.* **1977**, *1*, 1.
(44) Sexton, B. A.; Avery, N. R. *Surface Sci.* **1983**, *129*, 21.
(45) Gland, J. L.; Sexton, B. A.; Fisher, G. B. *Surface Sci.* **1980**, *95*, 587.
(46) Backx, C.; DeGroot, C. P. M.; Biloen, P. *Surface Sci.* **1981**, *104*, 300.
(47) Topping, J. *Proc. R. Soc. London Ser. A* **1927**, *114*, 67.

Table II. Point Groups and Symmetry Types of Acetone Skeletal Vibrations for Free Acetone and the Adsorbed Configurations Shown in Figure 11

		skeletal mode					
configuration	point group	ν(CO)	ν_s(CCC)	δ(CCC)	ν_a(CCC)	δ(CO)	π(CO)
free	C_{2v}	A_1	A_1	A_1	B_1	B_1	B_2
(a) η^1	C_{2v}	A_1	A_1	A_1	B_1	B_1	B_2
(b) η^1	C_s	A'	A'	A'	A'	A'	A''
(c) η^1	C_s	A'	A'	A'	A''	A''	A'
(d) η^1	C_1	A	A	A	A	A	A
(e) η^2	C_s	A'	A'	A'	A''	A''	A'

followed again by momentary annealing to the indicated temperatures.

The 95 K spectra, Figures 9b and 10a, are dominated by modes due to η^1-acetone and permit rather straightforward assignments (Table I) and interpretation. In the $(CD_3)_2CO$ spectrum, modes at 1675 and 720 cm^{-1} are due to the A_1 ν(CO) and ν_s(CCC) modes of η^1-$(CD_3)_2CO$, while those at 2070 and 2240 cm^{-1} are due primarily to the $\nu(CD_3)$ modes of η^1-$(CD_3)_2CO$ and partly to similar modes of a small amount of η^2-$(CD_3)_2CO$. The feature at 1260 cm^{-1} contains contributions both from the B_1 ν_a(CCC) vibration of η^1-$(CD_3)_2CO$ and the ν(CO) mode of η^2-$(CD_3)_2CO$. The $\delta(CD_3)$ modes from both species are evident at 1045 cm^{-1}, and the broadened band at 505 cm^{-1} results from both the ν-(Ru=O) mode of chemisorbed oxygen and the B_1 δ(CO) mode of η^1-$(CD_3)_2CO$. Although the strong $\omega(CH_3)$ and $\nu(CH_3)$ modes in the corresponding $(CH_3)_2CO$ spectrum may indicate the presence of some multilayer or second layer acetone from the slightly larger initial exposure in this spectrum, the observed features can be assigned confidently to η^1-$(CH_3)_2CO$ as follows: $\nu(CH_3)$ at 2995 cm^{-1}, A_1 ν(CO) at 1690 cm^{-1}, $\delta(CH_3)$ at 1440 cm^{-1}, $\omega(CH_3)$ at 1110 and 900 cm^{-1}, and B_1 δ(CO) unresolved from the mode due to adsorbed oxygen at 540 cm^{-1}.

Annealing to progressively higher temperatures attenuates the bands due to η^1-$(CH_3)_2CO$ and η^1-$(CD_3)_2CO$ concomitantly (cf., Figure 9c–e and Figure 10b–d) and reveals bands due to low concentrations of η^2-$(CH_3)_2CO$ and η^2-$(CD_3)_2CO$, the assignments of which parallel those given earlier for the clean surface spectra. The most significant aspect of these annealing sequences is the presence of η^1-acetone at temperatures approaching 300 K, correlating well with the increased stability of molecularly adsorbed acetone at higher temperatures evident in the thermal desorption spectra from the p(2 × 2)O overlayer in comparison to the clean Ru(001) surface. On the clean Ru(001) surface, η^1-acetone was barely detectable by EELS at 200 K, and it was not detected at 275 K. On the Pt(111) surface, η^1-acetone desorbs at 185 K. Consequently, the presence of the p(2 × 2)O overlayer serves to stabilize η^1-acetone compared to η^2-acetone, not only increasing the concentration of the η^1 bonded species, but also increasing its binding energy to the Ru(001) surface, as evidenced by the increased temperature of desorption.

Further heating attenuates the remaining bands due to η^2-acetone as it decomposes. Finally, heating to 750 K retrieves the spectrum of atomic oxygen (cf., Figure 9g), the intensity of which is diminished due to depletion of the oxygen adatoms via reaction with the surface carbon from the decomposition of η^2-acetone.

E. EELS and the Orientations of the Adsorbed Species. The vibrational spectrum of free acetone contains 24 fundamental normal modes, six of which are due to the motion of the C_2CO skeleton, and the remainder of which are due to the internal motion of the methyl groups. The symmetry types of the six skeletal vibrations of free acetone (point group C_{2v}), as well as their frequencies for liquid $(CH_3)_2CO$ and $(CD_3)_2CO$,[39] are listed in Table I.

As was mentioned earlier, the polarizations of the acetone skeletal vibrations (i.e., the orientation of the transition dipole moment of each mode with respect to the symmetry elements of the acetone skeleton) are preserved when acetone is coordinated in an η^1 configuration. For simplicity in the analysis that follows, the surface is assumed to be a structureless flat plane. Inclusion of the effects of the surface structure on the symmetry of the adsorbed species is necessary only when the atoms of the adsorbate

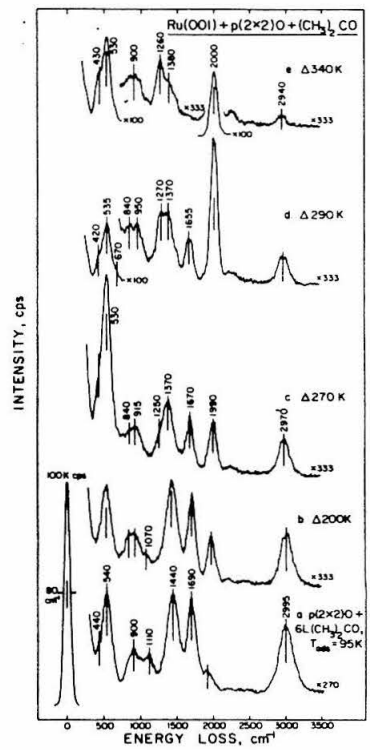

Figure 10. EEL spectra recorded after exposure of the Ru(001)–p(2 × 2)O surface to 6 L of $(CH_3)_2CO$ at 95 K, heating to the indicated temperatures, and recooling to 95 K.

interact strongly with surface atoms other than those to which the adsorbate is coordinated and is therefore superfluous in this analysis for adsorbed acetone. The dipolar activity of each of the acetone skeletal modes as a function of the orientation of the acetone skeleton with respect to the surface plane can be deduced by consideration of the possible coordination geometries shown schematically in Figure 11. The results of this analysis are listed in Table II.

Figure 11a shows the acetone skeleton coordinated to the surface plane in the η^1 configuration of highest possible symmetry (C_{2v}), preserving the C_2 rotational axis and both mirror planes of the free acetone molecule. The A_1 modes of the free acetone skeleton—ν(CO), ν_s(CCC), and δ(CCC)—are polarized parallel to the C_2 axis and strictly perpendicular to the surface plane in this configuration and are therefore dipolar-active. The B_1 modes—ν_a(CCC) and δ(CO)—are polarized in the σ_1 mirror plane strictly parallel to the surface and are dipolar-inactive. The B_2 mode—π(CO)—is polarized in the σ_2 plane, parallel to the surface, and is also dipolar-inactive. Tilting the molecule in the σ_1 plane, as in Figure 11b, reduces the symmetry of the adsorbate complex from C_{2v} to C_s, transforming the A_1 and B_1 modes of C_{2v} to A' of C_s and the B_2 mode to A''. Only the A' modes are dipolar-active.

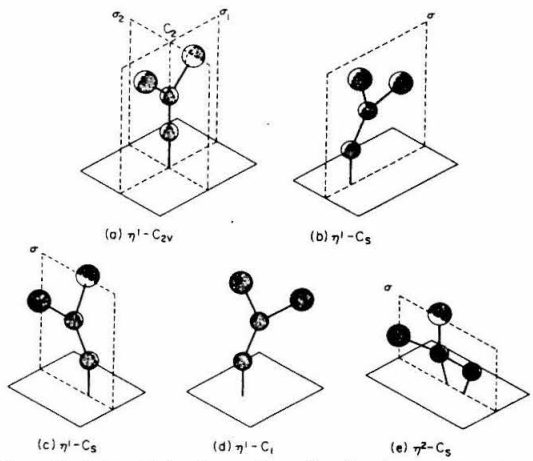

Figure 11. Schematic bonding configurations for η^1-acetone on a structureless flat surface (a–d), illustrating the symmetry elements preserved in each configuration. The η^2 configuration (e) is shown for comparison. In each case, the larger circles represent methyl groups, and the smaller circles represent the carbon and oxygen atoms.

Tilting the molecule in the σ_2 plane produces the C_s configuration shown in Figure 11c, with the A_1 and B_2 modes transforming to A' and the B_1 modes to A''. In Figure 11d, the molecule has been tilted away from both mirror planes, reducing the symmetry to C_1. All modes transform to A of C_1 and are dipolar-active. By the same reasoning as was applied in these examples, an acetone molecule lying flat on the surface could have symmetry no higher than C_s, as is shown for the η^2 configuration in Figure 11e. Note that in terms of symmetry arguments, this configuration is formally equivalent to Figure 11c, and the differences in their vibrational spectra would depend on the effects of the skeletal rehybridization which accompanies the η^2 interaction depicted in Figure 11e.

Returning to the results listed in Table I, obtained from the most clearly resolved spectra of the monolayer η^1 and η^2 species, only modes of A_1 and B_1 symmetry are observed for η^1-acetone on Ru(001), confirming as correct the configuration shown in Figure 11b. This is also the configuration that would be expected to result from the interaction of a single lobe of the oxygen lone pair orbital, a p-type orbital in the plane of the molecule,[48] with a single metal atom of the surface, and agrees with the results obtained for acetone adsorption on Pt(111)[27] and two structurally characterized η^1 complexes of ruthenium, where Ru–O–C bond angles of 153°[11] and 135°[12] have been reported. For the η^2 species, modes derived from the A_1 ν(CO) and ν_s(CCC) and the B_2 π(CO) are observed, confirming e of Figure 11 as the appropriate configuration.

IV. Discussion

The dramatic effect of oxygen preadsorption on the selectivity of the Ru(001) surface toward the nonreactive (η^1) and reactive (η^2) coordination geometries for adsorbed acetone has important implications in the understanding of more complex catalytic reactions. Two possibilities come immediately to mind. The ability to identify and modify selectively those properties of a heterogeneous catalyst which produce the adsorbed intermediate structures which ultimately lead to the desired products could be used to increase the rate and especially the yield for the catalytic reaction. Furthermore, these results may lead directly to a better understanding of how otherwise "inert" coadsorbed species can act as promoters or poisons to affect the product distribution in a heterogeneously catalyzed reaction. To appreciate these possibilities more fully, an understanding of the acetone–ruthenium bonding interaction with and without the effects of coadsorbed oxygen will be developed.

Three factors can be identified which control the type and strength of bonding which coordinate a ligand to a metal center or surface.[22] First, orbitals of the same symmetry must exist on both the ligand and the metal to allow their mixing; second, the spatial extent of the orbitals must be sufficient to facilitate significant overlap; and third, the energies of the interacting orbitals must be similar. Changes in the relative importance of these three factors make one coordination geometry favored over another for a particular ligand–metal system.

Let us first consider the η^1- and η^2-coordination geometries observed for acetone in terms of the "frontier" orbitals of the free acetone ligand.[48] The lowest unfilled orbital is the π^*_{CO}-antibonding orbital, which lies at +4.4 eV with respect to the vacuum level and has its amplitude more strongly localized on the acyl carbon atom than on the oxygen atom. The highest filled molecular orbital is the nonbonding oxygen lone pair, resembling an atomic p-like orbital with lobes localized strongly on the oxygen atom and in the skeletal plane. Its energy lies at 11.2 eV below the vacuum level. The next highest filled level is the π_{CO}-bonding orbital at −12.9 eV, the amplitude of which is slightly greater on the oxygen than on the acyl carbon atom.

An η^1-coordination geometry for organometallic complexes of acetone results from overlap of a single lobe of the nonbonding oxygen lone pair orbital of acetone with a d_σ acceptor orbital of the metal, resulting in a net transfer of electron density from the ligand to the metal. The bent M–O–C bond, identified for the two η^1-acetone complexes of ruthenium mentioned earlier[11,12] and for the orientation of η^1-acetone on both Pt(111)[27] and Ru(001), is a consequence of the spatial distribution of this lone pair donor orbital on acetone. Presumably due to the low amplitude of the π^*_{CO}-antibonding orbital on the oxygen atom, little backdonation from the metal d_π levels to this ligand orbital occurs, as evidenced by the rather small (less than 100 cm^{-1}) red-shifts of the ν(CO) mode observed for homogeneous complexes[9-12] and metal surfaces[27] which bind acetone in this configuration. The role of the metal in this type of interaction is that of a weak Lewis acid, and the purely dative metal–acetone bond which results is correspondingly weak. In many cases, depending on the metal and the properties of other ligands coordinated to it which affect its electronic structure, η^1-acetone complexes are too unstable to be isolated and characterized structurally.[9,10] Thermal desorption results suggest a binding energy of 11.6 kcal/mol for η^1-acetone on the Pt(111) surface,[27] and a similar analysis[49] of the thermal desorption data for Ru(001) suggests binding energies in the range of 10–15 kcal/mol on the clean surface and 10–19 kcal/mol on the Ru(001)–p(2 × 2)O surface.

An η^2-coordination geometry for organometallic complexes of acetone results from overlap of the π_{CO}-bonding orbital of acetone with a d_σ or sp hybrid acceptor level of the metal, along with backdonation from metal d_π levels into the π_{CO}-antibonding orbital of the acetone ligand.[21] The strength of this interaction, and therefore the probability of its occurrence relative to the η^1 interaction, depends critically on the ability of the ligand–metal bond to facilitate backdonation, since in the absence of backdonation the remaining π-donor bond is particularly weak and unstable.[22] Indeed, each of the organometallic complexes isolated and characterized structurally which shows η^2 coordination of ligands similar to acetone[13-20] and the η^2-acetone identified on Ru(001) in this work display substantial rehybridization of the acyl carbon from sp^2 to nearly sp^3, giving clear evidence of efficient backdonation. The fact that backdonation dominates the η^2 interaction has been concluded in similar studies of olefin[50] and acetylene[22,23] bonding to transition metals and illustrates the function of the metal as a Lewis base in these cases.[50] Since transition-metal atoms provide both orbitals of π symmetry to match the symmetry of the π^*_{CO}-antibonding orbital and spatial extent to afford efficient overlap,[22] it is the energy match of the interacting orbitals

(48) Hess, B.; Bruna, P. J.; Buenker, R. J.; Peyerimhoff, S. D. *Chem. Phys.* **1980**, *18*, 267.

(49) Redhead, P. A. *Vacuum* **1962**, *12*, 203.
(50) Ugo, R. *Coord. Chem. Rev.* **1968**, *3*, 319.

which most strongly affects this backbonding interaction.

The effect of d_π and π^*_{CO}-orbital energies on η^2 bonding is illustrated in the properties of the complexes with acetone-like ligands in η^2-coordination geometries. Recall that coordination of acetone to a number of transition metals, including rhodium and iridium[10] and ruthenium,[11,12] produces η^1 complexes. Substitution of hydrogen for CH_3 in acetone, however, lowers the energy of the π^*_{CO}-antibonding orbital from +4.4 to +3.1 eV,[48] decreasing the energy gap between the π^*_{CO} and d_π levels. This enhances d_π to π^*_{CO} backdonation, and η^2-formaldehyde complexes with a number of metals, including osmium[13] and iron,[14] result. Substitution of the more electronegative CF_3 for CH_3 depolarizes the carbon–oxygen bond of hexafluoroacetone relative to acetone, lowering its π^*_{CO}-orbital energy dramatically and yielding η^2 complexes with electronegative metals such as platinum[15,19] and nickel.[16,17] Of particular significance with respect to these arguments is that the only unsubstituted η^2-acetone complex isolated to date is formed with a low valent and electropositive tantalum center.[18] The lower d-level occupancy of tantalum ($5d^36s^2$) relative to rhodium ($4d^85s^1$), iridium ($5d^76s^2$), and ruthenium ($4d^75s^1$) ensures that its d levels have higher energy and therefore can more easily populate the π^*_{CO} level of acetone to facilitate η^2 bonding.

On the basis of these arguments, the formation of η^2-acetone on the Ru(001) surface can be understood. Interactions among metal atoms at a surface broaden the d levels to form bands which extend to higher energies than the d levels of isolated metal atoms (i.e., the Fermi level of a bulk metal is at a higher energy than the highest occupied level of an isolated metal center),[51] causing the atoms of the surface to behave as isolated metal atoms of lower net d-level occupancy. In effect, metal atoms at a surface are more electron rich than isolated atoms in a complex and can therefore raise their formal oxidation state more easily to yield backdonor bonding. The π^*_{CO} orbital of acetone is apparently at the appropriate energy to allow a dramatic distinction between the behavior of the Ru(001) surface, where the Fermi level is at −5.4 eV[52] and where substantial η^2 bonding of acetone occurs, and the Pt(111) surface, the increased d-level occupancy of which ($5d^96s^1$) lowers its Fermi level to −5.9 eV[53] and thus favors η^1 bonding.

It remains to explain in these same terms the effect of coadsorbed oxygen on the bonding of acetone on Ru(001). As was discussed previously, the p(2 × 2)O overlayer increases substantially both the concentration and the stability of η^1-acetone on the Ru(001) surface. We attribute this to a "short-range" through-metal electron deficiency at neighboring ruthenium surface sites, due to the presence of the electronegative oxygen adatoms, increasing the Lewis acidity of the former. The stability of other surface species coordinated to the Ru(001) surface via σ-donor bonds shows a similar enhancement in the presence of coadsorbed oxygen, including N_2,[54] N_2O,[55] and bridge-bonded formate.[56]

Addition of the p(2 × 2)O overlayer increases the work function of the Ru(001) surface by 0.20 eV (i.e., lowers the Fermi level by 0.20 to −5.6 eV),[30] increasing the disparity between the energy of the occupied d band of the metal and that of the π^*_{CO} acceptor level of acetone. This renders backdonation more difficult and causes Ru(001) to behave more like Pt(111). The implications of this for the effects of catalyst poisons and promoters are interesting: adsorption of electronegative substituents such as sulfur would produce an increase in the surface work function similar to oxygen and should therefore inhibit reactions which proceed through backbonded intermediates, whereas the adsorption of "cationic" species such as potassium would decrease the surface work function and should promote the formation of backbonded intermediates (based solely on the shift in energy difference between the donor and acceptor levels caused by each). The net effects of these bonding interactions on the surface chemistry of acetone adsorbed on both the clean Ru(001) and the Ru(001)–p(2 × 2)O surfaces may be illustrated by overall reaction schemes for the monolayer species adsorbed on both surfaces, which result from consideration of both the EELS and thermal desorption results discussed previously.

On the clean Ru(001) surface, both η^1- and η^2-acetone are produced upon adsorption of a saturated first layer of acetone at 95 K

$$(CH_3)_2CO(g) \rightarrow \eta^1\text{-}(CH_3)_2CO$$

and

$$(CH_3)_2CO(g) \rightarrow \eta^2\text{-}(CH_3)_2CO$$

Heating the surface causes η^1-acetone to desorb molecularly in the temperature range between approximately 150 and 250 K,

$$\eta^1\text{-}(CH_3)_2CO \rightarrow (CH_3)_2CO(g)$$

whereas η^2-acetone decomposes between approximately 200 and 320 K to adsorbed CO and CH_3 fragments:

$$\eta^2\text{-}(CH_3)_2CO \rightarrow CO(a) + 2CH_3(a)$$

Decomposition of the CH_3 fragments follows rapidly through CH_x ($x < 3$) intermediates

$$CH_3(a) \rightarrow CH_2(a) + H(a) \rightarrow CH(a) + 2H(a) \rightarrow C(a) + 3H(a)$$

Adsorbed CO is evolved from the surface in a desorption rate-limited reaction near 470 K,

$$CO(a) \rightarrow CO(g)$$

and hydrogen adatoms from CH_x decomposition recombine on the surface to evolve H_2 in a desorption rate-limited reaction near 330 K and a series of reactions between 400 and 750 K which have their desorption rates limited by the rates of decomposition of the CH_x fragments on the surface in this temperature range:

$$2H(a) \rightarrow H_2(g)$$

Adsorbed carbon from the methyl groups remains on the surface. The total amount of CO and H_2 evolution from the surface indicates that approximately one-eighth of the monolayer of η^2-acetone adsorbs and decomposes on the clean Ru(001) surface under these conditions.

On the Ru(001)–p(2 × 2)^{18}O surface, substantially more η^1-acetone and less η^2-acetone are formed upon adsorption at 95 K compared to the clean surface. Heating of the surface causes η^1-acetone to desorb molecularly in the temperature range between approximately 150 and 320 K, and the remaining η^2-acetone decomposes to adsorbed CO and CH_3 fragments in the temperature range between 200 and 350 K. The p(2 × 2) oxygen overlayer not only increases the yield of η^1-acetone and stabilizes it to higher desorption temperatures, but it also retards the rate of decomposition of η^2-acetone, as evidenced by its persistence in EEL spectra of higher temperatures on the Ru(001)–p(2 × 2)O surface than on the clean surface. Decomposition of the CH_3 fragments follows rapidly after their formation, producing H_2 in desorption rate-limited reactions near 220 K and a series of reactions between 250 and 550 K, the desorption rates of which are limited by the rates of decomposition of the adsorbed CH_x fragments. The CO produced from the decomposition of η^2-acetone (m = 28 amu) is evolved in a desorption rate-limited reaction at 450 K, and C^{18}O produced by the reaction of adsorbed carbon from CH_3 decomposition with the oxygen adatoms (^{18}O) of the p(2 × 2) overlayer (m = 30 amu) is evolved between 400 and 700 K. The total amounts of CO (m = 28 amu), H_2, and C^{18}O (m = 30 amu) evolution from the surface indicate that

(51) Saillard, J.-Y.; Hoffmann, R. *J. Am. Chem. Soc.* **1984**, *106*, 2006.
(52) Himpsel, F. J.; Christmann, K.; Heinmann, P.; Eastman, D. E. *Phys. Rev. B* **1981**, *23*, 2546.
(53) Nieuwenhuys, B. E.; Sachtler, W. H. M. *Surface Sci.* **1973**, *34*, 317.
(54) Anton, A. B.; Avery, N. R.; Madey, T. E.; Weinberg, W. H., in preparation.
(55) Madey, T. E.; Anton, A. B.; Avery, N. R.; Weinberg, W. H., in preparation.
(56) Toby, B. H.; Avery, N. R.; Anton, A. B.; Weinberg, W. H., in preparation.

approximately 0.02 monolayer of η^2-acetone adsorbs and decomposes on the Ru(001)-p(2 × 2)O surface under these conditions.

Two pathways can be postulated for the decomposition of η^2-acetone on the Ru(001) surface. In one case, the acetone skeleton would decompose initially through C–C bond cleavage to produce CO and methyl groups on the surface. Since molecular dissociation in general proceeds through population of an antibonding molecular orbital,[51,57] the difference in reactivity of the Ru(001) surface toward η^1- and η^2-acetone would be a clear and obvious manifestation of the bonding interactions which lead to the formation of each species if C–C bond cleavage were the dominant dissociation channel. The reaction coordinate for this mechanism would be the ν(CO) vibration of η^2-acetone, since its amplitude controls most directly the population of the π^*_{CO}-antibonding orbital, and this orbital in turn controls the integrity of the acetone skeleton. A second possible mechanism invokes first C–H bond cleavage, with decomposition of the destabilized acetone skeleton following rapidly thereafter. In this case, η^2-acetone, with its methyl groups in closer proximity to the ruthenium surface atoms than the η^1 species, would again be expected to be more reactive. Decomposition would proceed via population of the $\pi^*_{CH_3}$-anitbonding orbital of acetone, and either the π(CO) vibration of η^2-acetone near 600 cm^{-1}, the motion of which controls the approach of the methyl groups to the surface, or the ν(CH) vibration would represent the reaction coordinate. A distinction between these possibilities could only be made if the experimental results showed clear evidence of a kinetic isotope effect. For example, if the decomposition of η^2-$(CD_3)_2CO$ occurred at higher temperatures than η^2-$(CH_3)_2CO$, this would identify ν(CH) as the reaction coordinate and C–H bond cleavage as the rate-limiting step in η^2-acetone decomposition. Such a kinetic isotope effect was not observed, however. Since the π^*_{CO} orbital of acetone is already partially populated in the stable η^2 configuration, and since the $\pi^*_{CH_3}$ orbital is at significantly higher energy than the π^*_{CO} orbital (16.5 vs. 8.2 eV for free acetone[48]), decomposition of η^2-acetone via C–C bond cleavage would appear to be the favored mechanism.

(57) Sung, S.-S.; Hoffmann, R. *J. Am. Chem. Soc.* **1985**, *107*, 578.

V. Summary

The important conclusions of this work may be summarized as follows:

(1) Acetone bonds molecularly to the Ru(001) surface at 95 K in two different configurations: an η^1 (end-on) configuration which desorbs reversibly and an η^2 (side-on) configuration which dissociates upon heating of the surface.

(2) The η^2 configuration is the majority species on the clean Ru(001) surface. The appearance of a red-shifted ν(CO) vibration near 1300 cm^{-1} indicates significant rehybridization of the acyl carbon in this configuration, to that found for homogeneous organometallic complexes with η^2-ketonic ligands.

(3) The η^1 configuration is adsorbed with C_s symmetry and a nonlinear Ru–O–C bond, as has been observed in analogous organometallic η^1 complexes of acetone.

(4) Addition of an ordered p(2 × 2) overlayer of oxygen adatoms to the Ru(001) surface stabilizes the η^1 configuration of adsorbed acetone, rendering it the majority surface species and increasing its binding energy relative to the clean surface.

(5) The selectivity of the Ru(001) and the Ru(001)-p(2 × 2)O surfaces toward the η^1- and η^2-acetone bonding configurations can be explained in terms of the electronic properties of these surfaces and their effects on the bonding interactions which dictate the two coordination geometries.

Acknowledgment. We thank Profs. R. H. Grubbs and J. E. Bercaw for valuable discussions during the preparation of this manuscript. This research was supported by the National Science Foundation under Grant CHE82-06487.